Modellering van de persoonlijke blootstelling in ruimte en tijd
aan verkeersgerelateerd fijn stof met behulp van geluid als een proxy

Spatiotemporal Modelling of Personal Exposure to
Traffic Related Particulate Matter Using Noise as a Proxy

Luc Dekoninck

Promotoren: prof. dr. ir. D. Botteldooren, prof. dr. L. Int Panis
Proefschrift ingediend tot het behalen van de graad van
Doctor in de Ingenieurswetenschappen: Toegepaste Natuurkunde

Vakgroep Informatietechnologie
Voorzitter: prof. dr. ir. D. De Zutter
Faculteit Ingenieurswetenschappen en Architectuur
Academiejaar 2015 - 2016

UNIVERSITEIT
GENT

ISBN 978-90-8578-837-9
NUR 973, 943
Wettelijk depot: D/2015/10.500/81

Promotoren:

Prof. Dr. Ir. Dick Botteldooren
Prof. Dr. Luc Int Panis

Examencommissie

Prof. Dr. Ir. Patrick de Baets (voorzitter)	Universiteit Gent
Prof. Dr. Ir. Timothy Van Renterghem (secretaris)	Universiteit Gent
Prof. Dr. Ir. Dick Botteldooren (promotor)	Universiteit Gent
Prof. Dr. Luc Int Panis (promotor)	VITO / Universiteit Hasselt
Prof. Dr. Ir. Herman Van Langenhove	Universiteit Gent
Prof. Dr. Ir. Aonghus McNabola	Trinity College Dublin
Dr. Evi Dons	VITO / Universiteit Hasselt

Universiteit Gent
Faculteit Ingenieurswetenschappen en Architectuur

Vakgroep informatietechnologie
Sint-Pietersnieuwstraat 41, B-9000 Gent, België

Tel: +32 9 264.99.95
Tel: +32 9 264.99.69

Dankwoord

Een doctoraat is een proces dat niet alleen veel cijfers en informatie omvat maar ook veel interacties met mensen die invloed hebben op het gehele gebeuren. Het basisidee van dit werk is boven komen drijven toen ik samen werkte met Dominique Gillis in het Steunpunt Mobiliteit over verkeersleefbaarheid. Deze interessante samenwerking werpt vier jaar later nog vruchten af. Het is ook naar aanleiding van dit karwei dat de eerste contacten met het VITO zijn gelegd om het idee af te toetsen op de haalbaarheid en het potentieel van de hypotheses in dit werk. Luc Int Panis, mijn copromotor en Evi Dons, op dat ogenblik nog een doctoraatskandidaat, zijn vanaf dat moment fantastische aanspreekpunten geworden. Het idee om de meetcampagne van Evi te gebruiken als externe validatie voor mijn werk is cruciaal. Zonder deze openheid en hun antwoorden op mijn soms domme vragen zou dit niet mogelijk zijn geweest. Ook de vele andere contacten met jullie collega's waren inspirerend. Dick, bedankt voor de al vele jaren in de groep akoestiek en de kans om ook tussen de andere opdrachten door aan dit doctoraat te werken. Ik moet me ook verontschuldigen voor mijn belabberde schrijfcapaciteiten maar het lijkt er nu toch op dat ik mijn gedachten op papier heb kunnen krijgen. Ik hoop dat dit doctoraat nog tot interessante nieuwe projecten zal leiden.

Luc Int Panis opende met zijn contacten ook een nieuwe wereld voor mij. Eén van de mooiste episodes is de fantastische samenwerking met Steve Hankey en Julian Marshall uit Minnesota, US. Een eerste handdruk met de valiezen in aanslag aan het einde van een conferentie en drie maand later ging de mobiele meetcampagne in Bangalore, India van start. Karthik S en Grishma Jain hebben daar op de fiets hun leven geriskeerd voor de wetenschap. Ik ben het gehele team heel erg dankbaar.

Ik moet ook de mensen danken die aan de andere meetcampagnes hebben meegewerkt. Marijke, Pieter, Peter, Angela, Iris, Sara, Veerle en Marc hebben de mobiele metingen in de auto uitgevoerd. Kurt heeft de meetcampagne in de Tolhuislaan mogelijk gemaakt. Bedankt dat ik jullie op de meest onmogelijke uren en dagen mocht komen lastig vallen voor filtertjes en netwerkproblemen. Er zijn ook veel contacten geweest met andere mensen waar de mobiele metingen zijn gebruikt voor bewustwording en educatie. De meeste van die projectjes

komen uit de kast van Trage Wegen, inclusief de 'mobiele ezel' metingen. Dries, Steven en collega's, bedankt voor de zeer enthousiaste samenwerking en we klinken op een vervolg.

Ik kom dichter bij mijn eigen bureau. Bram en Tom, jullie zijn al een tijdje weg bij de groep akoestiek, maar openden de wereld van Python voor mij. Jullie tools zijn nog altijd een deel van de gepresenteerde oplossingen. Annelies, ik heb je dikwijls lastig gevallen voor R en om mijn statistiek wat op te vijzelen. R is ondertussen de tweede technische poot van mijn doctoraat geworden. Samuel, de samenwerking in het IDEA project heeft me de meetopstelling opgeleverd die het vervelende werk (bijna) eenvoudig maakte en ik moet ook dringend wat meer Linux leren. Arnaud, bedankt voor de samenwerking rond de mobiele metingen. Annelies, Arnaud, Samuel, Damiano, Bert, Karlo, Pieter, Peter, Weigang, Mirjana, Gemma, Vincent, Timothy, Lei, Laurent, Michiel, Kang, bedankt voor de sfeer en de vele grote en kleine dagdagelijkse dingen.

Ma, bedankt voor de kans om 'naar den unief' te gaan. Het was niet evident, dat weet ik heel goed, maar alles wat er uit gevolgd is, is een belangrijk deel geworden van mijn leven, werk, vrienden, vrouw en kinderen incluis. Broer en zus, het doet me deugd dat het ook met jullie goed gaat. Ik kom dus stilletjes aan thuis. Marijke, bedankt dat ik (aardig) wat van mijn (en onze) vrije tijd heb mogen opofferen aan een oude en bijna vergeten droom. Ik heb me eigenlijk wel geamuseerd en heel veel bijgeleerd, ook over mezelf. Ewoud, Warre en Roel, sorry dat ik s' avonds soms met mijn gedachten ergens ver weg zat en maar met een half oor luisterde. Ik weet het, dat gebeurt ook als ik gewoon de Humo aan het lezen ben, maar vergeet niet, ook ouders hebben (nog) passies en dat is niet slecht. Plezier hebben thuis, bij vrienden en op het werk maakt je gelukkig.

Bedankt,
Luc

Whatever discipline you are in:
don't model the average, model the distribution.[1]

[1] Robert Cailliau, co-developer of the world wide web at CERN (final sentence of his speech at the 12th FEA PhD Symposium, organized by the Faculty of Engineering and Architecture of Ghent University, December 7, 2011, Aula, Ghent, Belgium).

Summary

Improving the quality of life (QoL) of individuals and the population as a whole is the driving force behind many, if not all scientific fields. The scope of this work is the exposure assessments of traffic related environmental burdens. Exposure to those burdens varies strongly in space and time and people move throughout the day in this changing environment. Combining the changing environment and the individual time-activity pattern is commonly referred to as 'personal exposure'. This work focusses on improving personal exposure assessments.

In an initial phase, a broad person centred Traffic Liveability model (TL) gathers spatial data to calculate sixteen predefined traffic and mobility related indicators. The aim is to predict the response of individuals to the quality of life question (QoL): *"How satisfied are you generally on the quality of life (safety, child friendliness, environment …) in your neighbourhood?".* Not only negative aspects of traffic are evaluated, also the positive effects such as reachability are included. The TL model evaluates the personal time-activity pattern at the dwelling, along the trips and at the destinations. The personal time-activity pattern is simulated for a virtual population and the resulting set of indicators is spatially aggregated to a 'Traffic Liveability Index' (TLI). The TLI is an indicator of the local environment, including the spatial features of the personal time-activity patterns. The calculated TLI correlates well with the individual responses for the QoL question of the participants living in that area. Noise exposure is within the set of indicators the strongest component. In addition, a spatial analysis of the noise levels along the roads near the dwellings detects additional effects of traffic on the perception of the surroundings of the dwelling. High-density roads near the dwelling reduce the reported satisfaction. Summarized, the perception of the quality of life includes a spatial evaluation of the amount of traffic on the roads near his dwelling and this can be detected with a noise evaluation along the roads. Noise exposure acts as a proxy for traffic in the personal perception of the local environment.

Indicators can only be evaluated at the spatial resolution of the available external data. The TL model provides a methodology to assess personal time activity patterns with a spatial resolution of meters but the underlying air pollution maps have a spatial resolution of kilometres. Consequently, the air pollution evaluation path in the TL model is not as sensitive to the personal behaviour as for the noise evaluations. Since traffic emits simultaneously noise and air pollution, traffic related air pollution can express a similar spatial behaviour. The following question emerges and captures the main theme in this PhD:

> *Can we use noise exposure to predict the air pollution exposure and by doing so; increase the spatial resolution of the air pollution personal exposure assessments?*

Air pollution concentration is a combination of gases and particulate matter, with complex physical and chemical interactions and highly influenced by meteorological conditions. The environmental exposures to several toxic components (acid rain, lead, benzene, CO…) were largely reduced in the last decades, while particulate matter (PM) is still a major issue. PM is related to incomplete combustion and other sources. PM_{10}, the particles with diameter smaller than 10µm, is chemically divers and does not express the variability of traffic related pollutants. Black Carbon (BC) and Ultra-Fine Particles (UFP), both fractions of PM_{10} are directly combustion related and express the traffic related exposure much stronger compared to PM_{10}. The first epidemiological evaluations detect stronger health effects for BC compared to PM_{10} due to the improved spatial detail. The WHO supports further investigations of BC. This PhD therefore focusses on BC.

The use of noise as a proxy for BC is first evaluated for bicyclists. Simultaneous measurements of noise and BC are performed over the course of a year, capturing the local variability of noise and BC in all meteorological conditions. Particulate emission of the vehicles is known to be highly sensitive to the local traffic dynamics and noise emission shows similar features as well. Vehicles emit engine noise (low frequencies) and tyre related rolling noise (high frequencies). Spectral evaluation of the noise exposure can distinguish between engine throttle and vehicle speed and add value to the prediction model. The bicyclists' BC exposure is however influenced by the changing background concentrations (higher during winter, lower at high wind speeds). Adjusting the measurements for the background concentration results in a noise based model capable of estimating the instantaneous exposure to BC with a temporal resolution of 10 seconds. BC exposure can be defined as the sum of a background component and a local traffic related component, referred to as "the additive approach" throughout the PhD. In a similar but shorter measurement campaign in Bangalore, India, this additive background adjusted approach was successful applied for both BC and UFP. The fundamental feature of this modelling approach is the capability to disentangle the variation in the BC/UFP exposure into a highly dynamic local traffic related component and the slow varying but sometimes large meteorological influence.

From an epidemiological point of view and for the investigation of long-term health effects in general, annual averaged exposures are required. The bicyclist's instantaneous exposure model sampled the roads and meteorological conditions sparsely but can now be extrapolated to a full year of meteorological conditions. This results in a yearly averaged exposure map with a spatial resolution of 50 m along the road network where all meteorological variability is accounted for. A sensitivity analysis proved that during rush hour, a valid annual average BC exposure is reached with as little as four bicycle passages at a specific road segment. A methodology is presented using on-bicycle noise measurements as a fast and cheap way to provide a city-wide map for the bicyclists' BC exposure.

The spatial properties of noise maps can also act as a spatial layer in air pollution exposure models. Instantaneous noise based land-use regression models are developed for in-

vehicle and indoor exposure at home. External validation is achieved through a large personal BC exposure experiment available at VITO. In that campaign, thirty-one households were sampled during a week in summer and winter of 2010-2011. Successful prediction of these external measurements provides in a fully independent validation in this work.

The in-vehicle model is based on a participatory campaign with nine volunteers, gathering 230 hours of data over the course of a year (2013). The measurements are attributed in a ten seconds temporal resolution with traffic data, vehicle speed, background concentrations, spatial and meteorological parameters. The L_{DEN} noise map is included as an alternative for the traffic counts. L_{DEN} is a standardized noise mapping deliverable within the EU Noise directive; compatible L_{DEN} maps are available for all agglomerations in Europe. A six parameter model including the L_{DEN} noise map successfully fits the measurements. The external validation results in a good correlation (Spearman correlation of 0.8) but fails to estimate the absolute exposure levels. About 40% of the exposure could not be explained. However, in the long-term measurements of the Flemish Environmental Agency (VMM), a similar reduction of the BC background concentrations is recorded over that period. The implementation of the Euro5 emission standard in 2009 reduced the PM emission limit from 0.025 to 0.005 g/km for diesel-powered vehicles and is a plausible cause of the discrepancy in the validation. The in-vehicle model is valid but requires an emission correction to adjust for the fast evolving vehicle fleet.

In the indoor model, a bold hypothesis is tested. The instantaneous bicyclist model, valid for rush hours only, is evaluated using the L_{DEN} noise map instead of the actual noise measurements. It converts the noise map to a Black Carbon map but is still including sensitivity to the instantaneous meteorology and background concentrations. This approach assumes that the spatial variability of the L_{DEN} noise map is similar to the BC exposure. A single L_{Aeq} based noise diurnal pattern adjusts for the hour of the day for all dwellings to extrapolate the rush hour model to the full day. The indoor exposure is defined as the sum of a background concentration and a local component estimate based on the estimated $L_{Aeq,hour}$ noise level at the dwelling. An outdoor-to-indoor correction from literature converts the outdoor estimate to an indoor exposure level. The model is extended with additional corrections to account for changing ventilation settings for different seasons. In the indoor model, no details for the traffic near the dwellings are available and the L_{DEN} map is not sensitive to the local traffic dynamics, which proved highly significant for the bicyclists. Despite this missing information, the indoor model reaches a correlation of 0.65. The main limitation is the origin of the underlying exposure data: the combination of a noise map and the bicycle exposure data as an estimate of local variability of the BC concentration. The other limitation is related to the external validation dataset, no dwellings were available close to major roads or highways. More indoor exposure measurements near major roads and highways are required to extend this approach to the highest exposed dwellings.

To test if noise based traffic assessment at a dwelling has the potential to further improve the indoor model, six weeks of simultaneous noise and BC measurements were performed at the facade of highly exposed dwelling. Again, the additive background adjusted approach and spectral evaluation of the noise is used. Since 2014, more background measurement stations are available at the Flemish Environmental Institute (VMM) and the sensitivity of the facade model towards the choice of the background measurement station is evaluated. The default closest measurement station appears not to be the best option. Background stations with a distinctive diurnal traffic pattern reduce the capability of the noise evaluation to detect the diurnal traffic related variation of BC. With a well-founded choice of the background measurement locations, noise measurements at the dwelling facades will add relevant data in future air pollution measurement campaigns and promise further improvement of the indoor model. Strong benefits emerge if these measurements include indoor air pollution to resolve the outdoor-indoor ratios as a function of traffic near the dwelling.

The validation of the total daily personal exposure is achieved by applying the in-vehicle model and the indoor model to the full personal behaviour of the participants of the external participatory sensing campaign. The daily personal exposure estimates reaches a correlation of 0.65 with the external measurements. Similar strength is achieved for all indoor and all-in-traffic activities. The exposure during active transportation modes (walking and biking) is underestimated. This can be contributed to the lack of traffic data at the low density roads. We can conclude that noise assessments are a valid proxy for exposure to traffic and the resulting noise based activity specific models can predict the instantaneous personal exposure to Black Carbon. This required microscopic land-use regression models (µLUR) with the following properties:

- Instantaneous traffic evaluation (using noise as a proxy)
- High spatiotemporal resolution in both traffic and BC exposure measurements
- Coverage of the full range of meteorological and traffic conditions
- Non-linear modelling with generalized additive models (gams)

This result was not possible without an extended software development. The exposure modelling software (MEX) is therefore presented as an independent result. It combines all functionality to process simulated populations and participatory sensing campaigns, attributes the personal behaviour in space and time to any external dataset and enables the extrapolation of the models to custom populations. The workflow is person centred, activity based and route sensitive. The most fundamental components in the workflow are the activity specific models which are in this application, the µLURs. The MEX implementation includes many of the requirements of a full ‘exposome’ solution (= sum of all environmental exposures), an important topic in the epidemiological field. MEX allows extensive policy support and has huge potential to attribute epidemiological datasets. Evaluating personal exposure indicators for both noise and air pollution on an epidemiological cohort is the most important application of this work in the near future. The issue of potential mutual confound-

ing of noise and air pollution exposure in the traffic related health evaluations can now be investigated in an unprecedented resolution. The multidisciplinary approach cumulates at this point in important synergies: detailed noise evaluations not only provide the relevant data to evaluate the health effects of noise and quality of life, but improve the personal exposure estimates to traffic related particulate matter exposure as well.

Samenvatting

De leefkwaliteit van individuen en de bevolking in zijn geheel is een drijvende kracht in veel, zo niet alle wetenschappelijke onderzoek. De blootstelling aan verkeer gerelateerde omgevingsparameters varieert sterk in ruimte en tijd en de mensen bewegen gedurende de dag door deze continu wijzigende omgeving. Het combineren van de wijzigingen in de omgevingsparameters en het individuele activiteitenpatroon wordt omschreven als de 'persoonlijke blootstelling'. Dit werk focust op de verbetering van de rekenmethodes voor deze persoonlijke blootstelling.

In een eerste fase is een model opgesteld voor het evalueren van de verkeersleefbaarheid. Het persoonlijk verplaatsingsgedrag wordt geëvalueerd voor zestien verkeer en mobiliteit gerelateerde indicatoren. Het doel is het antwoord op de vraag: *"Hoe tevreden bent u in het algemeen over de leefkwaliteit (veiligheid, kindvriendelijkheid, leefmilieu, …) in uw buurt?"* te voorspellen op basis van geografische informatie. Zowel de positieve als de negatieve aspecten van verkeer worden in rekening gebracht. De indicatoren worden berekend op de woonplaats en op de bestemming en indien van toepassing, ook tijdens de verplaatsingen. Het persoonlijk verplaatsingsgedrag wordt gesimuleerd voor een virtuele bevolking. De verzamelde indicatoren worden geaggregeerd tot een verkeersleefbaarheidsindex (VLI). De VLI is een indicator voor de perceptie van de leefkwaliteit gebaseerd op de ruimtelijke eigenschappen van het persoonlijk verplaatsingsgedrag. De berekende VLI voor de gesimuleerde personen voorspelt de respons van personen die in die omgeving wonen zeer goed. De geluidsblootstelling is de sterkste component in deze voorspelling. In een gedetailleerde analyse blijkt de evaluatie van het geluid langs de wegen in de directe omgeving van de woning de perceptie van de leefkwaliteit mee te verklaren. In woningen met lage geluidsblootstelling, maar hoge blootstelling langs de wegen in de omgeving wordt de levenskwaliteit lager geschat en ook de omgekeerde relatie wordt waargenomen. De persoonlijke beoordeling van de leefkwaliteit verbetert door gebruik te maken van evaluatie van geluid langs de trajecten.

De kaarten voor luchtverontreiniging hebben niet dezelfde ruimtelijke resolutie als de geluidskaarten en kunnen de effecten van luchtverontreiniging niet in het gewenste detail in het model inbrengen. Aangezien verkeer tegelijkertijd geluid en luchtverontreiniging uitstoot, kan verondersteld worden dat de blootstelling in verkeer voor de luchtverontreiniging een vergelijkbare ruimtelijk patroon zal vertonen als de blootstelling aan geluid. Dit wordt het centrale thema in dit doctoraat:

Kunnen we de blootstelling aan geluid gebruiken als een voorspellende factor voor de blootstelling in verkeer en bij uitbreiding ook voor de woningen en de bestemmingen?

Luchtverontreiniging is een complexe combinatie van chemische, fysische en meteorologische condities. We worden blootgesteld aan een combinatie van gassen en fijn stof. De omgevingsconcentraties zijn al decennia sterk aan het dalen, maar vooral fijn stof is nog steeds een belangrijke zorg. De meest gebruikte parameter is PM_{10}, deeltjes met een diameter van minder dan 10 micrometer. PM_{10} is chemisch heel erg divers en de ruimtelijke verspreiding is niet erg gevoelig voor de lokaal verkeer gerelateerde uitstoot. Black Carbon (BC), de roetfractie in het fijn stof, en Ultrafijn stof, de allerkleinste deeltjes in het fijn stof worden geproduceerd tijdens verbrandingsprocessen. Ze zijn dan ook belangrijker voor de blootstelling aan verkeer dan PM_{10} maar andere bronnen van verbranding zoals verwarming van gebouwen en industriële activiteiten hebben ook een relevante bijdrage. Black Carbon trekt recent meer en meer de aandacht bij de evaluatie van de gezondheidseffecten. De gezondheidseffecten geëvalueerd op basis van blootstelling aan Black Carbon worden tot 10 maal hoger geschat als in een vergelijkbare evaluatie voor PM_{10}, alleen door rekening te houden met de grotere ruimtelijke variatie van BC. In deze evaluaties wordt alleen rekening gehouden met de blootstelling aan de woning. Er is een ruime consensus in de epidemiologie dat het inbrengen van het persoonlijk gedrag in de blootstellingsevaluaties de gezondheidseffecten beter zal kunnen begroten.

Aangezien de blootstelling aan geluid in een groot detail kan worden gemeten en berekend voor het dagelijks persoonlijk verplaatsingspatroon, bied dit een mogelijkheid om de hogere resolutie in ruimte en tijd ook toe te passen in de persoonlijke blootstelling aan verkeer gerelateerde luchtverontreiniging. De blootstelling aan Black Carbon kan worden gemeten met een draagbaar toestel in een hoge resolutie in de tijd. Dit maakt het mogelijk de blootstelling aan verkeer gerelateerde blootstelling in een verbeterende resolutie te bepalen. De blootstelling is sterk afhankelijk van de aard van de activiteit en wordt sterk beïnvloed door de aard van de omgeving en modale keuze (fiets, auto, trein, thuis, op kantoor, open lucht enz.). Specifieke modellen voor elk van deze micro-omgevingen zullen de blootstelling over het gehele activiteitenpatroon verbeteren.

De relatie tussen geluid en Black Carbon wordt eerst onderzocht voor fietsers. Gedurende een jaar werden gelijktijdige metingen uitgevoerd van de blootstelling aan geluid en Black Carbon tijdens woon-werk verplaatsingen, in alle weersomstandigheden en met veel aandacht voor alternatieve routes en lokale variatie aan verkeer. Hoge blootstelling aan geluid is een maat voor meer verkeer in de directe omgeving. Uit de spectrale analyse van de geluidsmetingen kunnen gegevens over de dynamiek van de verkeersstroom worden afgeleid. Verkeersgeluid bestaat uit twee belangrijke componenten, motorgeluid en rolgeluid. Het motorgeluid is laagfrequent en varieert sterk met het motorregime. Versnellende voertuigen produceren beduidend meer motorgeluid. Voertuigen produceren bij hoge snelheid meer hoogfrequent rolgeluid en minder motorgeluid. Het regime van de motor is ook een belang-

rijke factor in de emissie van fijn stof. Meer dynamisch verkeer stoot meer deeltjes uit. De meetresultaten worden geanalyseerd met een tijdsresolutie van 10 seconden en vertonen een goede correlatie met de verkeerdynamiek waargenomen via de geluidsmetingen. Er zijn echter grote verstoringen door de wijzigende meteorologische condities en achtergrondconcentraties. Vooral in de winter is de achtergrondconcentratie hoger door woningverwarming en door lagere verdunning door de stabielere atmosfeer. Een correctie van de metingen op basis van de achtergrondblootstelling blijkt nodig om een correcte voorspelling te maken op basis van de lokale verkeersdynamiek. De blootstelling van een fietser kan worden berekend als de som van een achtergrondconcentratie en een lokale blootstelling. De lokale blootstelling is functie van het motorgeluid, de windsnelheid, een rolgeluid gerelateerde geluidscomponent en de dichtheid van de bebouwing langs de straat ("street canyon"). De gemiddelde blootstelling over een verplaatsing tijdens de spits kan worden voorspeld met een correlatie van 0.86. De methode is met een geautomatiseerde meetopstelling getest in Bangalore, India. De metingen zijn in die campagne uitgebreid met Ultrafijn stof (UFP). Voor zowel Black Carbon als UFP is de methode geldig, ondanks de hogere achtergrondblootstelling. Het succes van de modellen wordt bepaald door de mogelijkheid om de variatie in de blootstelling uit te splitsen in een lokale component van sterk wijzigend lokaal verkeer en een grootschaligere component door de traag variërende achtergrondblootstelling.

Aangezien de geluidsmetingen minder gevoelig zijn voor meteorologische omstandigheden zijn er veel minder mobiele metingen nodig om het lokale verkeer te bepalen in vergelijking met luchtverontreinigingsmetingen. Voor veel epidemiologische evaluaties worden jaargemiddelde blootstellingen gebruikt. Het ogenblikkelijk model maakt het mogelijk om de gemiddelde jaarlijkse blootstelling langs een bepaald traject te berekenen met een gewogen gemiddelde over alle meteorologische omstandigheden. Uit de analyses blijkt dat slechts vier passages langs een bepaald straatsegment bij een typische verkeerssituatie de jaarlijkse blootstelling correct voorspellen. Er wordt een methodologie voorgesteld waarbij voor een stad en zijn directe omgeving een mobiele geluidsmeetcampagne wordt uitgevoerd om het verkeer en de dynamiek van het verkeer te meten. De werkelijke verkeerssituatie kan ook worden bepaald op wegen waar geen verkeersgegevens beschikbaar zijn, inclusief de lokale dynamiek van het verkeer. Op basis van een korte parallelle meetcampagne met Black Carbon en/UFP kan een aangepast voorspellend model worden gemaakt die rekening houdt met de lokale samenstelling van het wagenpark. Internationale vergelijkingen kunnen dan nieuwe informatie bieden over de samenstelling en evoluties van de voertuigvloot. De resulterende gemeten geluidskaart kan worden gebruikt in routeplanners om fietsers betere alternatieve routes aan te bieden. Een alternatieve route kan de blootstelling met 30 tot 70 % verlagen in functie van het seizoen en de beschikbaarheid van alternatieven voor het specifieke traject.

De mogelijkheden om de ruimtelijke resolutie van de geluidskaarten te gebruiken voor persoonlijke blootstelling in de auto en in gebouwen worden verder onderzocht. In dit deel

van het werk wordt een externe validatie uitgevoerd op basis van een persoonlijke blootstellingscampagne uitgevoerd door het VITO in 2010-2011. De tijdsresolutie van de externe meetcampagne is vijf minuten. Om een ogenblikkelijk model op te bouwen voor de blootstelling in personenwagens is in 2013 230 uur metingen verzameld met een resolutie van 10 seconden (positie via GPS en Black Carbon blootstelling in de auto). De metingen worden aangevuld met de 'virtuele' blootstelling van de auto op de geluidskaart, externe verkeersgegevens en de meteorologische informatie. Er kan een geldig model worden opgesteld voor de blootstelling in de auto op basis van een geluidskaart, uur van de dag en de meteorologische gegevens. De resultaten worden vergeleken met de externe gegevens van VITO en de externe validatie blijkt wel een goede correlatie te vertonen, maar onderschat de blootstelling met ongeveer 40%. De verschillen tussen de persoonlijke gedragspatronen en de meteorologische omstandigheden in beide meetcampagnes zijn klein en kunnen de afwijking niet verklaren. In de continue Black Carbon metingen van de VMM (Vlaamse Milieu Maatschappij) is echter een sterk dalende trend te zien over de periode 2010–2013 met dalingen tot 40 % tijdens de spits en tussen 20 en 30% tijdens de daluren. De daling is met grote waarschijnlijkheid het gevolg van de Europese wetgeving voor uitstoot van de dieselvoertuigen waarbij de norm in 2009 met 80% daalt. Door de grote aandeel diesel in de voertuigvloot en de snelle vernieuwing van de bedrijfsvoertuigen is een daling van de emissie van de vloot van 40 % realistisch. De effectiviteit van de Europese regelgeving is de belangrijkste oorzaak voor de verschillen tussen beide meetcampagnes. Het in-verkeersmodel is geldig maar moet gecorrigeerd worden voor de snel wijzigende emissie van het wagenpark.

Voor de blootstelling in de woningen is geen bijkomende meetcampagne uitgevoerd maar wordt een alternatieve hypothese geformuleerd en getest. De fietsmetingen kunnen gemodelleerd worden op basis van de geluidskaart in plaat van op basis van de oorspronkelijke simultane geluidsmetingen. Dit betekent dat een belangrijk deel van de informatie (echt verkeer, inclusief verkeersdynamiek) vervangen wordt door een geluidskaart op basis van de beschikbare verkeersgegevens. De toegevoegde waarde ten opzichte van de huidige modeleringen binnen de discipline geluid op basis van de verkeersgegevens op de dichtstbijzijnde weg bestaat nu vooral uit de meer gedetailleerde resultaten voor de positie van de geluidsbronnen en de woningen. Het model op basis van fietsgegevens geeft een voorspellende waarde voor de blootstelling buitenshuis. Op basis van externe gegevens wordt een correctie toegepast voor de blootstelling binnenshuis. De correctie is afhankelijk van de gemiddelde dagtemperatuur en vertoont een duidelijk seizoenseffect. In de zomer is de correctie kleiner dan in de winter door wijzigende ventilatie. Er wordt een correlatie van 0.65 bereikt voor de gemiddelde blootstelling per activiteit voor alle huishoudens in de externe gegevens. De externe gegevens van VITO bevatten geen woningen op korte afstand van snelwegen en primaire wegen. Bijkomende metingen van geluid en luchtverontreiniging aan en in hoog blootgestelde woningen zijn nodig om deze methode verder te valideren en ruimtelijk uit te breiden.

De laatste stap is het testen van de voorspelling van de volledige persoonlijke blootstelling voor iedere individuele persoon-dag uit de externe meetcampagne van het VITO. Het model voor de blootstelling in de auto wordt ook toegepast voor de blootstelling in de bus. Het model voor de blootstelling thuis wordt ook gebruikt voor de blootstelling op de bestemmingen. Voor fietsers, spoorverkeer, wandelen en andere buitenactiviteiten wordt het model voor de woningen toegepast zonder de correctie voor de blootstelling binnenshuis. Een correlatie van 0.65 wordt bereikt ondanks de vele benaderingen en beperkingen van zowel de externe gegevens als de eigen modellen. Een vergelijkbaar resultaat wordt bereikt voor alle activiteiten binnen en alle in-verkeersactiviteiten. De blootstelling voor de actieve modi (wandelen en fietsen) wordt sterk onderschat en dat kan worden toegewezen aan ontbrekende verkeersgegevens op de lokale wegen. Er kan gesteld worden dat de ruimtelijke resolutie van de geluidskaarten en de ogenblikkelijke evaluaties een grote toegevoegde waarde hebben voor het voorspellen van de persoonlijke blootstelling aan verkeer gerelateerde blootstelling voor fijn stof.

De metingen, simulaties en analyses worden verwerkt op basis van een veralgemeende methodologie om algemene indicatoren te berekenen voor een volledig persoonlijk activiteitenpatroon. De modellen en meetgegevens worden met een ongeëvenaarde resolutie in ruimte en tijd uitgewerkt. De modellen zelf zijn niet-lineaire modellen die betere resultaten opleveren voor de extrapolaties van de resultaten dan de meer gebruikelijke lineaire regressie technieken. De veralgemeende methodologie is persoon specifiek, activiteit specifiek en routegevoelig. De technische uitvoering maakt het mogelijk om de modellen toe te passen op andere mobiele populaties waarbij het gedrag ofwel gesimuleerd of opgemeten is. Simulaties van gedragswijzigingen en hun effecten op de blootstelling kunnen het beleid van de lokale overheden evalueren en ondersteunen. De modellen kunnen in alle detail worden toegepast op epidemiologische cohorten en zo het gezondheidsonderzoek versterken.

Preface

This PhD is in several ways unconventional, including this preface. First there is my age. I decided to start this PhD when I was 42 years old. Secondly, it is a personal initiative performed in parallel with my daily tasks. Of course there are huge synergies with my work and projects at the Acoustics Group at INTEC-UGent. Thirdly, I am an acoustician working on a subject in an adjacent scientific discipline: traffic related air pollution. All things considered, the scope of this PhD can be conceived as highly ambitious.

All of the outcomes are the result of a slow and steadily growing insight, gradually emerging from a simple idea in combination with results from prior work. Scientific reporting does not allow me to present these gradual growing insights in the actual text. The preface explains the path to the outcomes of this PhD. It frames the results in the flow of growing insights and will make this document a more gentle reading experience.

The goal behind the horizon is a fundamental issue of health effects due to traffic exposure. Both the air pollution and noise pollution communities detect adverse effects of their actors. For decades, the potential interactions and potential confounding due to the correlating exposures has been a subject of debate. Improving the current knowledge in this debate is the driving force behind the work. The basic idea is found at the other end of the spectrum. When a bicyclist is in traffic, he/she is simultaneously exposed to traffic related air pollution and noise, both in a direct way, with no physical barriers. This so-called bicycle 'micro-environment' is the best place to put the physical link of noise and air pollution to the test.

In previous work, the high resolution of noise assessments along the roads proved already relevant to predict the subjective response to a Quality of Life questionnaire. This was a scientific outcome of a Traffic Liveability project funded by the Flemish Government, performed in cooperation with IDM, a mobility expert group at the University of Ghent in 2009-2010. The acquired knowledge in this project was the actual trigger of this PhD. The model and scientific results of that project are (briefly) summarized in this PhD as well. These sections might look in disjoint with the main part of the work but they are not. The relevance of the increased spatial resolution and route sensitivity was already proven in the Traffic Liveability project. The basic concept is the same: use noise as an intermediate proxy for exposure to traffic and traffic related effects. The only difference is the outcome: personal perception of the neighborhood versus traffic related air pollution exposure.

The first experiment measures Black Carbon and noise simultaneously on the bicycle. I took the equipment while commuting to the office with me and started to include various alternative trajectories to capture more variation in local traffic and traffic dynamics. This dataset is the basis of everything I learned about air pollution exposure and everything that

will follow in this PhD. The first logical step was to build a classical land-use regression model on the bicycle data, using the noise as a traffic proxy. I gathered data over a full year and had three to four times more data than any other bicycle based campaign before. We expected this was enough to use this data for a yearly exposure LUR. This resulted in a draft paper, ready to submit. It was my promotor who prohibited the submission with the phrase: “Let’s first test plan B, see if you can build an instantaneous model.” The instantaneous model proved much stronger, the classical approach would not even have fitted in the final conclusions of this PhD.

This was a crucial moment. Despite the very large dataset, the data was still strongly biased due to the combination of sparse sampling of meteorology, traffic and traffic dynamics all influencing the exposure simultaneously. A high resolution instantaneous model including the traffic dynamics was the only way to understand the exposure of the bicyclist. From this moment on, the path was (almost) clear. I had to do something similar for in-vehicle exposure and see what was possible for the indoor exposure.

Here occurs a very strong synergy with the IWT funded IDEA-project at our office. Colleagues of INTEC and VITO were building a fixed monitoring network to monitor noise and air pollution with cheap equipment. Based on the successful bicycle model, I joined the project and a mobile version of the technology was added in the IDEA setup. This made it possible to perform the in-vehicle measurement campaign efficiently. The equipment was sent to Bangalore in India to test the bicycle model in extreme traffic conditions. A variant of the equipment was used to perform long-term measurements at a dwelling facade.

In the meantime, I redeveloped the software of the Traffic Liveability model to be able to include mobile measurements and to support all technology necessary to apply the instantaneous models to any mobile population, tracked or simulated. In 2013 I came across the Vision and Strategy document for Epidemiology of Lioy and Smith. It is a wish list with required functionalities of the epidemiologists. The data workflow that I was testing was capable of resolving several items on that wish list. This triggered me to present the data workflow in this perspective. All dots were in place now and ‘only’ needed to be connected.

To summarize, I see this PhD as the explicit result of not having a research plan and only little budget. I was free to do what I seemed fit and it is that freedom that has led to this result. Is the outcome ambitious? Yes. Was this the plan? No. I did a large experiment on the bicycle. I followed the breadcrumbs in the data and this lead me to this outcome. Have a nice reading experience.

List of Abbreviations

Air pollution

TRAP	Traffic Related Air Pollution.
BC	Black Carbon
PM	Particulate Matter
PM_{10}	Particles in the aerosol with an aerodynamic diameter smaller than 10µm
$PM_{2.5}$	Particles in the aerosol with an aerodynamic diameter smaller than 2.5µm
UFP	Ultra-Fine Particles (mostly expressed as the number of particles <100nm)
EC	Elemental Carbon, alternative (pyrolysis based) measurement methodology for Carbon content of the air pollution (WHO, 2012).
OC	Organic Carbon, other alternative measurement methodology for Carbon content of the air pollution (WHO, 2012).
CO	Carbon Monoxide
NO_2	Nitrogen dioxide, combustion related gaseous exhaust.
NO_X	Nitrogen oxides, nitrogen based exhaust in all variants.
O_3	Ozone, highly reactive air pollutant formed in high polluted air in sunny condition.
PAH	Polycyclic aromatic hydrocarbons, divers set of carcinogenic components, emitted as the result of incomplete combustion (Benzene, Toluene …).

Noise

L_{Aeq}	A-weighted equivalent noise level, expressed in dBA.
L_{AX}	A-weighted statistical noise level, noise level exceeded in X % of the time in a preselected time window, expressed in dBA.
L_{OLF}	Spectral noise evaluation, quantifying the engine related exposure. Energetic sum of third octave bands of 100 Hz to 200 Hz (in dBA) on a (10 seconds) running smoothed data series with a 1 second temporal resolution. In most cases, L_{OLF} is aggregated to a 10 second interval for modelling (see Appendix B8).
L_{OHF}	Spectral noise evaluation, quantifying the rolling noise related exposure. Similar definition as L_{OLF} but with third octave bands of 1000 Hz to 2000 Hz (in dBA).
L_{HFmLF}	Spectral noise evaluation, difference between L_{OHF} and L_{OLF}, an indicator for the speed of the traffic flow.

Model related

QoL	Quality of Life, general terminology for Well-being of an individual or population towards the targeted subdomain.
LUR	Land-Use Regression, modelling technique to use external spatial data sources to estimate the targeted indicator.
µLUR	Newly introduce terminology to indicate an instantaneous spatiotemporal and micro-environment specific LUR.
ASM	Activity Specific Model, general reference to a model to describe the behaviour of an indicator for a specific indicator.
ASF	Activity Specific Function, the actual function or statistical model providing the actual indicator calculation.DPSIR Generalized environmental methodology: Drivers, Pressure, State, Impact, Response
DALY	Disability Adjusted Life Year, generalize methodology for multidisciplinary comparison of the magnitude of health effects, expressed in year of lower quality due to the targeted indicator.

BC_{raw}	Acronym for models based on unadjusted, instantaneous BC concentrations.
BC_{loc}	Acronym for models based on background adjusted, instantaneous BC levels, representing the local traffic contribution in the BC concentration.

List of terminology

Concentration	amount of an air pollutant at a given location at a specific time
Immission level	common terminology for the noise level
Exposure	Concentration of a pollutant near a person
Dose	Integrated exposure over a certain time potentially adjusted for personal and activity specific characteristics (inhalation rate, in-body correction, internal transport to specific organs).
Personal exposure	Evaluation of the exposure of a person including his personal time-activity pattern. In other contexts, personal exposure is sometimes presented including dose corrections. Application specific information is required to interpret dose in that context. In this work no dose corrections are included in the personal exposure models.
Dose-effect	Quantification of a (health) effect matching a specific dose
Indicator	a parameter or a value derived from parameters that points to, provides information about and/or describes the state of the environment, and has a significance extending beyond that directly associated with any given parametric value. The term may encompass indicators of environmental pressures, conditions and responses (OECD definition).
Black Carbon	a reflectance based measure for the soot fraction of airborne particulate matter
Black Smoke	Old methodology for combustion related air pollution, other alternative measurement methodology for Carbon content of the air (WHO, 2012).
Exposome	General concept to investigate the sum of all external environmental exposures affecting health (in contrast to the genome, the genetic component of the health status).

Table of Contents

Chapter 1 Introduction

Improving the quality of life of individuals and the population as a whole is the driving force behind many, if not all scientific fields. The scope of this work is to study the effect of traffic related environmental burdens on the quality of life in a broad, and at the same time, detailed perspective. Existing indicators related to quality of life and traffic related health effects lack spatial and temporal resolution to evaluate the sometimes subtle but most of the time highly complex exposure dynamics. This PhD zooms in on the exposure evaluations of both air and noise pollution. It incorporates the diurnal time-activity patterns of individuals in the evaluation. The path from the source to exposure, dose and health effects crosses many different disciplines. The first part of this chapter introduces these disciplines and emphasizes on the most important topics influencing the research on the traffic related health effects. The second part will set the detailed goals of this PhD. The third part gives the outline of the PhD as guidance for the reader.

1.1 State of the art

The state of the art is addressed in four sections. The quality of life and the use of indicators are introduced in general. Three detailed sections introduce the state of the art in the epidemiological field in general; the physical features of particulate matter and the current approaches to assess personal exposure.

1.1.1 Quality of Life

1.1.1.1 Indicators in general

Indicators are quantifiable characteristics of a population or society, which researchers, policy makers and governments use to support their decisions and actions. The UN defines an environmental indicator as: *"a parameter or a value derived from parameters that points to,*

provides information about and/or describes the state of the environment, and has a significance extending beyond that directly associated with any given parametric value. The term may encompass indicators of environmental pressures, conditions and responses." (United Nations, 1997). The OECD defines more complex 'composite indicators' as *"formed when individual indicators are compiled into a single index, on the basis of an underlying model of the multi-dimensional concept that is being measured"* (OECD, 2004). Typically, researchers use survey methodologies to gather information and statistics to generalize the collected information for the entire population. Evaluating composite indicators has the potential to investigate interactions between the underlying indicators (WHO, 2000). Most indicator schemes focus on macroscopic evaluations of populations (Albino et al., 2012, Bradshaw et al., 2010, Bruggeman et al., 2010). Recently, methodologies aggregating multiple aspects on an individual level emerge. Brereton investigated the rural change on the well-being in Ireland on that personal level (Brereton et al., 2011). In health sciences, typical examples are the personal 'self-reported health' surveys, linking environmental burdens to the quality of life on an individual level (Daniau et al., 2013, Schimmack et al., 2008, Shen et al., 2013, Sirgy et al., 2010, Smyth et al., 2011, Distaso et al., 2007). In Denmark, this approach is extended to a "Strategic Environmental Assessment" in spatial planning (Kornov et al., 2009). Interacting indicators on a personal level reveal secondary and/or combined effects of the driving forces of the individual indicators into composite indicator.

Summarizing: indicators are widely used to reduce the complexity of life and society into standardized frameworks with the aim to provide relevant policy support. Combining the benefits of composite and multi-level indicators with evaluations at a personal level add value in the fields of 'Quality of Life' and environmental exposure.

1.1.1.2 Quality of Life, well-being, environment and traffic

In societies where basic needs are largely fulfilled, attention for mental well-being is growing. The quality of the living environment is one of the main determinants for this well-being (Kovac et al., 2001, Guite et al., 2006, Leslie et al., 2008, Moro et al., 2008). Therefore, there is a growing interest in how the quality of a neighbourhood is to be assessed and monitored. The overall appreciation of the living quality of a neighbourhood depends on various factors, which can be grouped into personal attributes, attributes of the dwelling and the characteristics of the neighbourhood (Parks et al., 2002). One of the specific domains is the so-called 'traffic liveability' and 'walkability': how does local traffic affect the local inhabitants? The topic was introduced by Appleyard in the early seventies and used by many others since (Appleyard, 1972, Leslie et al., 2005). Recent research has attempted to quantify the walkability in route specific ways (Dills et al., 2012, Gallimore et al., 2011). Rundle introduced the use of Google Street View as a novel approach to audit neighbourhood environments (Rundle et al., 2011). Walkability was related to air pollution (Marshall et al., 2009, Hankey et al.,

2012). This brief overview gives an impression of the vast and growing field of quantifying well-being and traffic related environmental features of the living environment.

1.1.1.3 Quality of Life and noise exposure

Noise annoyance due to traffic related sources is a large field of investigation, but it focuses mostly on specific sources like airports, freight traffic and railways. When aspects of the quality of life are assessed, noise exposure was largely neglected. Recently several authors started to include noise exposure and noise annoyance in general approaches for quality of life evaluations (Brink et al., 2011, Shepherd at al., 2010, Dratva et al., 2010, Moser et al., 2006, Welch et al., 2013). An emerging field is the research of quiet areas as a driving force in improving the quality of life (Shepherd et al., 2013, Roswall et al., 2015).

1.1.2 Exposure science, epidemiology and the eco-exposome

Epidemiology is the science that studies of the patterns, causes, and effects of health and disease conditions in populations. Environmental epidemiology is the branch of epidemiology concerned with discovery of health effects of the environmental exposures. Exposure science is a scientific field that delivers the relevant exposure information to the environmental epidemiologists and other stakeholders. Since these fields are strongly connected, several efforts have been made to integrate all aspects of the pathway from the pollution source to the health effect. In the NRC committee recommendations for exposure research: "A Discussion of Exposure Science in the 21st Century: A Vision and a Strategy" such a pathway is proposed for health effects due to external stressors. It starts at the pollution sources and works through the environmental concentration, the personal external exposure and the internal dose to the actual in-body target of the pollutant (Lioy and Smith, 2013). Other authors try to expand the scope of integrated approaches to include policy responses. The general DPSIR framework is very popular. In a recent review "Integrating health and environmental impact" (Reis et al., 2013), a modified ecosystem enriched Drivers, Pressures, State, Exposure, Effects and Actions or 'eDPSEEA' model is proposed, addressing similar concerns due to the *"continuing failure to truly integrate human health and environmental impact analysis..."*. They explicitly express the need to extend the conceptual models to include "an effective and robust science-policy interface". In the dissemination of the European funded AIRNET project, a set of key points for the research requirements and the implications towards policy were added as a strategic necessity (Janssen et al., 2003, Janssen et al., 2005, Totlandsdal et al., 2007). They include the investigation of causal agents of air pollution, the intake fraction models, harmonized monitoring techniques, source attribution, personal exposure, micro-environmental characteristics, socio-economic factors and the need

for new exposure modelling approaches. The most important features in the cross section of exposure, epidemiology, exposome and policy are addressed in detail in the next sections.

1.1.2.1 Exposure at the dwelling

In current practice, epidemiological evaluations for environmental burden map the exposure of a person to the exposure at his dwelling. It is well established that for many pollutants and especially for traffic related air pollution, the contribution of the in-traffic exposure is an important component of the total diurnal exposure (Oglesby et al, 2000, Ducret-Stick et al, 2008, Lioy and Smith, 2013, Dons et al., 2011, Dons et al., 2012). Health evaluation of air pollution exposure suffers strongly from the misclassification of the persons due to the discrepancy between the actual personal exposure and yearly averaged exposure based on the home address and due to the uncertainty of the spatial exposure models (Molitor et al., 2007, Suh and Zanobetti, 2006, Suh and Zanobetti, 2010, Hoek et al., 2008). The at-home exposure assessment does not result in a statistically significant traffic related health risk. The first epidemiological studies including personal exposure are available in literature (Jerrett et al., 2008, Hannam et al., 2013). Adjusting the exposure of the person to include the in-traffic and the activity related contributions is a rapidly expanding research field and crucial to resolve the traffic related health effects.

1.1.2.2 Activity specific exposure

The activity specific nature of exposure is tackled from different points of view. Some authors refer to activities as the main components in the personal exposure, other focus on the different exposure dynamics in the so-called microenvironments (in-vehicle, biking, indoor etc.). The activity based methods are referred to as ‘activity based models’, ‘daily mobility’, ‘time-activity patterns’ or ‘dynamic populations’. All refer to the behavioural characteristics of individuals. Individuals move and travel and are exposed to different environmental conditions at different times of the day (Lin et al., 2007, Beckx et al, 2009a, Beckx et al, 2009b, Beckx et al, 2009c, Lin et al., 2009, Beckx et al, 2010, Hatzopoulou and Miller, 2010, Dons et al., 2011, Dons et al., 2012, Setton et al., 2011, Dhondt et al., 2012, Steinle et al., 2013, Buonanno et al., 2014). Some authors focus on commuting, a subset of transport activities (Knibbs et al., 2011, Hansson et al., 2011, Zuurbier et al., 2009, Zuurbier et al., 2011). The different points of view are valid but interact frequently. People perform activities and that results in time spent in a specific microenvironment. The personal activities are the driving force; the microenvironment is an attribute of the activity. The exposure dynamics in a microenvironment can be studied as such and are applicable to different types of activities.

The activity based approach itself is crucial since it is an important driving force in the integrated approaches for personal exposure (Lioy and Smith, 2013, Reis et al., 2013). The personal activity pattern is a specific target of the policy makers. Policy actions will attempt to modify the personal behaviour and by doing so affect the personal exposure (Reis et al.,

2013). Policy actions can affect both the activities and the properties of the micro-environments simultaneously. Fuel pricing policy will simultaneously modify the personal behaviour and fleet composition (Dhondt et al., 2012). The more detailed aspects of in-transport exposure dynamics will be addressed in sections 1.1.5.2 and 1.1.5.3.

1.1.2.3 Dose corrections and dose-effect relationships

The physical or chemical exposure of the individual is not necessarily equal to the actual intake of the pollutant by the individual. Corrections are needed which are typically referred to as dose corrections. They express the difference between external exposure and internal exposure (Lioy and Smith, 2013). Several physical barriers have to be crossed and several correction factors are necessary to quantify the 'internal dose'. This is the point where exposure science touches the toxicology. Each pollutant has its own internal exposure path related to its physical and chemical properties. For a single pollutant, different internal dose corrections might be needed to assess the different health pathways (Lioy and Smith, 2013). Many of the dose corrections in the air pollution field are related to the level of physical activity and account for changing lung ventilation. Several authors address this feature to compare the potential effects of active travel modes (biking, walking) with motorized transportation modes (car, public transport) (Steerenberg et al., 2005, De Kok, 2006, Marshall et al., 2006, Int Panis et al., 2010, Zuurbier et al., 2010, Rojas-Rueda et al., 2011, De Hartog et al., 2010). Buonanno found associations between personal dose and respiratory health effects in children (Buonanno et al., 2013). Complex models are available including size-fraction sensitive deposition in the lungs and are applied in air pollution science as well (ICRP, 1994; Oberdörster, 2000, Rothen-Rutishauser et al., 2005).

In the noise exposure field a dose correction can account for the quality of the insulation of the dwelling and adjusts the maximum noise event levels inside the bedroom. The advanced noise exposure research in soundscapes, attention modelling and annoyance models can be regarded as dose corrections for the physical noise exposure as well. They can adjust for the different responses of the subjects due to activity specific vulnerabilities (Kurra et al., 1999, Ohrstrom, 2004, Bjork et al., 2006, Michaud et al., 2008). Noise evaluations can also include the personal sensitivity of the subject (Nivison et al., 1993, Kjellberg et al., 1996, Fyhri et al., 2009, Shepherd et al., 2010, Schreckenberg et al., 2010).

A second type of dose correction is the dose-effect relationship, converting the physical property to an effect indicator. In the toxicology field they differentiate towards different compounds in the air pollution (Gerlofs-Nijland et al., 2007, Xia et al., 2004, Schlesinger et al., 2003, Staniswalis et al., 2005). In the noise exposure field, different annoyance functions are available for different noise sources which can be used to differentiate the potential health impact to the source type (Miedema and Oudshoorn, 2001).

1.1.2.4 Combined exposure

Another fundamental issue in health research is the difficulty to estimate health effects of combined exposures. One of the strongest driving forces of the integrated health approaches is the necessity to investigate of the effects of multiple pollutants (Lioy and Smith, 2013). Effects can be falsely identified as a health effect of the pollutant under investigation while an underlying correlating parameter is causing the effect. This issue, known as 'confounding', is a fundamental problem in epidemiological research. It is impossible to cover the vast number of epidemiological techniques to investigate confounding and adjust for potential confounding. Combined exposure can however superimpose if synergistic effects exist.

Combustion based engines in vehicles simultaneously emit air pollutants and noise. The co-exposure is an intrinsic property of the traffic related pollution. Independent air pollution studies and noise studies detect adverse health effects related to the distance to the major roads and highways (Laumbach et al., 2012, Gan et al., 2011, Gan et al, 2012, Bauer et al., 2010, Kaelsch et al, 2014). Distinguishing the health effects of traffic related noise and air pollution exposure has not been resolved at full. For traffic related health effects the co-exposure to noise and air pollution is established and the potential confounding of the health effects is a popular and important research debate (Klaeboe et al., 2000, Heimann et al., 2010, Clark et al., 2012, Beelen et al., 2008, Davies et al., 2009, Davies et al., 2013, Foraster et al., 2011, Foraster et al., 2013, Tétreault et al., 2013, de Kluizenaar et al., 2013). Tétreault summarized existing literature in a recent review and compared the approaches of the studies investigating the potential mutual confounding of noise and air pollution. He found no evidence of confounding in the current data. The final remark of Tétreault is intriguing: *"Results from this review suggest that confounding of cardiovascular effects by noise or air pollutants is low, though with further improvements in exposure assessment, the situation may change."* All studies use air pollution assessments at the dwelling. The author suggests that including the personal exposure into air pollution assessments might resolve the classification errors for the air pollution and that this improvement might reveal the mutual confounding in the future.

1.1.2.5 Policy for local and global challenges now and in the future

The purpose of improving knowledge about the complicated relation between driving forces, the environment and human health, is to disseminate results to the stakeholders, the community and the policy makers. In "Integrating health and environmental impact assessment" (Reis et al., 2013), the core idea is that: *"human activity with all its social, economic and cultural aspects must be seen as integral to, and in dynamic interaction with, the ecosystems on whose functionality humans depend"*. The need to provide relevant information for the policy maker is crucial: *"Future health and well-being can only be built on ecological principles and must move fast from the periphery to the heart of the public policy discourse"*.

At this point the indicator based “Quality of Life” research and the environmental health sciences meet in the societal and policy driven questions on sustainable development and growth. Human health, quality of life, preservation of the environment and global change are all components of the same societal goals: improve our living environment now and in the future.

1.1.3 Noise, the basics

Most readers of this document will have little experience with noise evaluations. A short introduction is therefore necessary. These basic concepts, including some specific traffic specific methodologies (noise emission functions and noise mapping legislation) are enough to understand the noise specific components in this work. The required knowledge is limited to environmental evaluations. Details on wave propagation and the linked wave specific features of sound propagation (interference, intensity, noise cancelation etc.) are not required.

1.1.3.1 Noise, a physical exposure

Sound is the propagation of a vibration through matter. In the environmental noise segment the propagation occurs through the air and the interaction with humans occurs through our auditory system. A basic noise measurement captures the energy in the sound. The instantaneous noise level L_p at a certain place and moment in time is a measure of the pressure changes in the sound wave and it is represented in a logarithmic quantity (dB, decibel). The measure is calculated relative to a reference value of 20 µPa. It is a relative measure with a reference level matching the absolute threshold of the human auditory system. The sound waves are a combination of waves with different frequencies. Capturing the frequency information is crucial for this work but only the basic techniques are relevant for the reader of this thesis. The most common methods to present the frequency information in the noise are the fast fourrier transform (FFT) and third-octave band spectra. In this work, the spectral evaluation will be performed in third-octave bands.

The human auditory system is not equally sensitive for all frequencies. The absolute physical pressure is therefore in many cases presented including the sensitivity of the human auditory system, known as the A-weighting. This is also the case for environmental evaluations of noise. Therefore, all noise measurements in this work will include A-weighting by default. Most of the standard noise level meters will be able to provide the measurement data as used for the noise based models: $L_{Aeq,1sec}$ and the third-octave band levels with the evaluation time of 1 second.

1.1.3.2 EU noise directive and noise mapping standardization

The Environmental Noise Directive (END), published by the European Commission, describes the legal obligations of the member states towards several aspects of noise exposure. An important part of the obligations is to provide noise maps for the main noise sources. This includes detailed traffic noise maps in cities and agglomerations with more than 50,000 inhabitants. The EU Joint Research Center published a reference document for the member states on how to implement the standardized CNOSSOS-EU methodology (Kephalopoulos et al, 2012). This will improve the quality and comparability of the noise maps provided to the EU commission in the framework of the END. In the Commission Directive (EU) 2015/996 document, published on May, 19, 2015, the common noise assessment methods according to the Directive 2002/49/EC are compiled. This method has to be used from December, 31, 2018 onwards (EU commission, 2015). Below is a brief description of these methods.

Traffic noise is a complex combination of multiple sources of noise in a car: engine noise, exhaust noise, aerodynamic noise, gearbox noise, tyre noise. Each of these noise sources has its specific spectrum and evolution in time, each with different functions of the speed and acceleration and can include complex interactions between the road surface and the tyres. In the noise emission standard the total emission of a vehicle is simulated as the combination of two main components, the engine related noise and the rolling noise. Engine is mainly low frequency noise; tyre noise is mainly high frequency noise. Engine noise is mainly sensitive to the speed and acceleration, rolling noise is mainly sensitive to the speed of the vehicle. These features of vehicle noise emissions will become a fundamental part of this PhD.

Noise exposure of individuals is assessed as the noise level at the dwelling facade and is reported in L_{DEN}. L_{DEN} is a weighted average of the L_{Aeq} over the day, evening and night period where penalties of respectively 5 and 10 dB are included for the evening and night. The definition of the day, evening and night periods can vary by noise source (road, rail, aviation) and by country to match specific features of the diurnal pattern of the noise source and local life-style. To summarize, noise mapping is moving forward quickly; standardization is improving and ongoing and noise maps are abundantly available.

1.1.4 Particulate matter

In this section, the focus will be on air pollution and very specifically on the particulate matter component of the air pollution. Particulate matter is a very broad concept and includes next to the anthropogenic particles (transport, energy, agriculture etc.), also a large variety of natural compounds (sea salt, pollen, viruses, volcanic ashes, etc.). Particulate matter is a globally acting air pollution parameter influencing cloud formation and precipitation. The heterogeneity of the chemical and physical composition of particulate matter results in a complex research field. In Figure 1.1.1 an overview of the type of particles and their typical

size is shown. PM_{10} and $PM_{2.5}$ is limited by size only (< 10 µm or < 2.5 µm), not restricted by the origin of the particles.

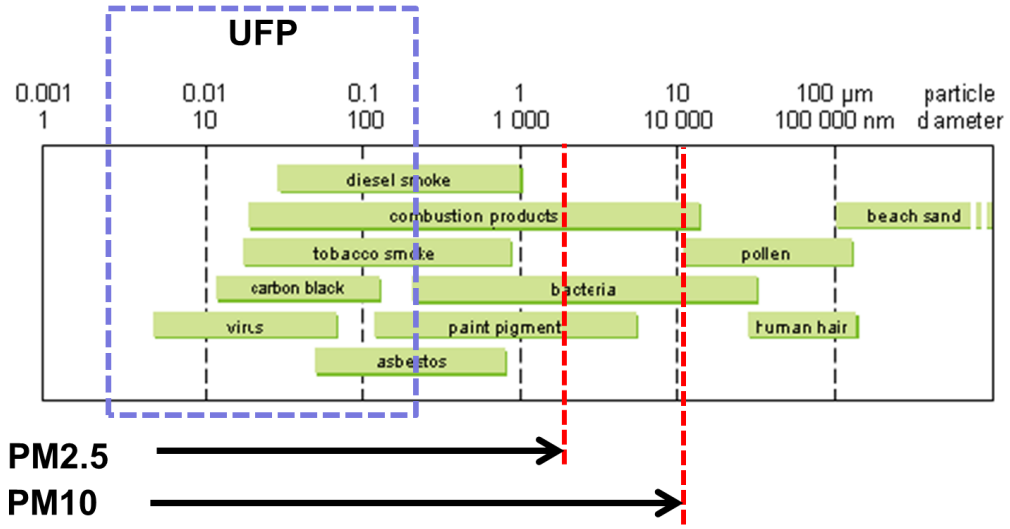

Figure 1.1.1: Particle size, traffic and natural contribution and standard measures PM_{10}, $PM_{2.5}$ and UFP.

Recently more effort is made in evaluating the smaller fractions: $PM_{2.5}$ and ultrafine particles (UFP, particles < 100 nm). Also Black Carbon (BC), the carbonaceous component of the combustion related part of particulate matter, is gaining focus. It is a measure for the soot resulting from the incomplete combustion processes. Black Carbon is more source specific and correlates more with traffic compared to the more general and chemically more heterogeneous size fraction based particulate matter $PM_{2.5}$ and PM_{10} (Karner et al., 2010).

Black Carbon is also an important theme in the global climate change debate, since it is next to CO_2, a relevant factor in the heat balances on a global scale. Health effects are expected due to global change due to combustion related human activities (McMichael et al., 2006, Haines et al., 2006, Costello et al., 2009). This PhD will not elaborate on the large scale and global effects of Black Carbon. At a personal level, exposure to traffic related air pollution is relevant for health on a local scale. Local actions to reduce personal exposure to traffic related air pollution will however align with the required reduction of traffic related combustion emission in the global context.

In the next paragraphs, different features of Black Carbon will be introduced in more detail. First the relation between UFP and Black Carbon is addressed.

1.1.4.1 Ultrafine particles and Black Carbon

Traffic emission is a mixture of volatile components and particulate matter with a wide range of particle sizes. Black Carbon and UFP are two different particulate measures with a large overlap. Many of the features of UFP are relevant for Black Carbon as well. The formation of UFP is complex and is summarized in this section and for a large part applicable to Black Carbon. Most of the information in this section is retrieved from the review paper “Ambient nano- and ultrafine particles from motor vehicle emissions: Characteristics, ambient pro-

cessing and implications on human exposure" (Morawska et al., 2008). Additional references are added if relevant.

Combustion generates particulate matter in different ways. The primary combustion derived particles are generated directly from the engine and measure from 30 to 500 nm which is referred to as the 'accumulation mode'. Particles of this size have a short life span and coagulate to larger sizes. Secondary particles are formed by condensation of gaseous components in the engine exhaust. They are volatile and consist mainly of hydrocarbons and hydrated sulphuric acid. They are smaller than 30 nm and form the 'nucleation mode' (Morawska et al., 2008). Important interactions between the size fractions exist, strongly influencing the lifetime of the different fractions. When large amounts of particles in the accumulation mode are present, the nucleation mode is scavenged by the larger particles. When few particles are available in the accumulation mode, the nucleation mode has a longer lifetime. The particulate size distribution can change fast due to these mechanisms. The formation and scavenging mechanisms are influenced by temperature and humidity resulting in complex emission dynamics. The number of small particles increases in warmer periods which are also visible in the diurnal patterns of the size fraction below 100 nm. In the early morning strong increases of particles between 11-30 nm are observed. Size distributions also reveal the 'age' of the particles. Different size distributions are found for background concentrations and for near road concentrations. The size distribution of emitted particles is influenced by the source, fuel type, engine mode and vehicle technology. To illustrate the complexity of the fine particle emission dynamics three out of sixteen engine regimes for an engine operating on ultra-low sulphur diesel are presented in Figure 1.1.2 (reconstruction of the figures in Chuepeng et al., 2011).

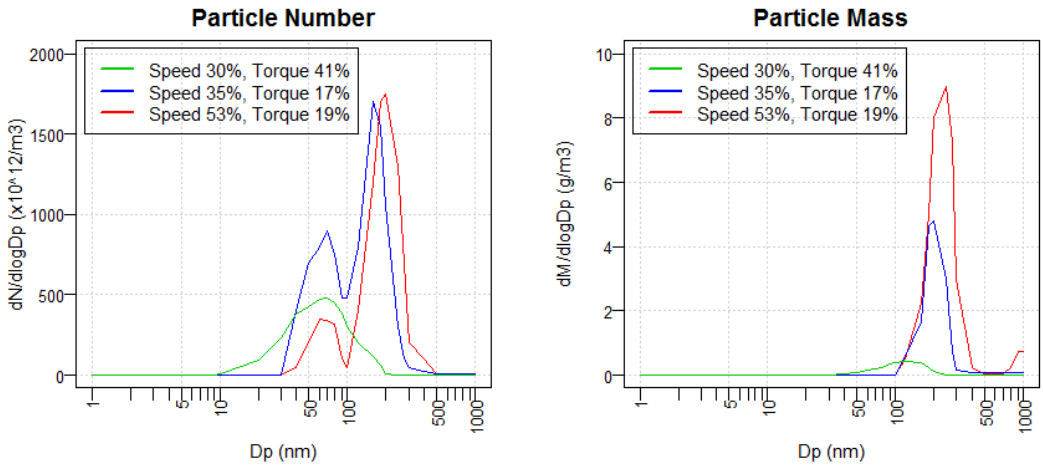

Figure 1.1.2: Particle number and mass concentration distributions for three engine-operating modes for a modern diesel engine (adjusted from Chuepeng et al, 2011). Speed and torque in % of maximum of the engine specifications.

The difference between the distributions of particle number (left) and resulting particle mass (right) illustrates the importance of the measurement technique. Large amounts of small particle are produced at high torque of the engine but this feature is not well identified

in the mass based measurements. Black Carbon measurements are mass-based; UFP is mostly measured in particle number. Evaluation of traffic exposure to Black Carbon will therefore be less sensitive to the particle number compared to UFP.

Meteorological effects influence the formation and propagation of UFP, wind speed influences the dilution of the exhaust plumes, precipitation has a washout effect. Temperature inversion is a meteorological condition that prevents the vertical mixing and results in high background concentrations in winter. The diurnal variation shows a bi-model distribution indicating the traffic rush hours with a higher peak for the morning rush hour compared to the evening rush hour. Strong seasonal variation exist as well (Mishra et al., 2012).

Diesel fuel results in higher amount of BC and UFP while alternative fuels (LPG/CNG) produce less BC. The European emission standards and especially the Euro5 standard are stringent. Euro5 diesel engines emit 98% less PM compared to Euro0. Also for particle numbers, the progress is impressive (reduction of 95% for diesel between Euro3 and Euro5) (Hausberger et al., 2010). The differences between the emissions of diesel and gasoline are reduced by the latest standards. The transition of the fleets to cleaner vehicles is not yet completed, but the first exposure changes due to fleet composition are already reported (Sabaliauskas et al., 2012, Fontaras et al., 2014, Dardiotis et al., 2015).

Summarizing, traffic related UFP and BC is a highly variable and complex matter with fast changing chemical and physical properties. The properties change within seconds after emission and the emission fleet characteristics change continuously.

1.1.4.2 Particle size, internal dose and toxicology

Particulate matter has complex and highly variable particle size distributions and this also affects the intake of the particles. Toxicologists attempt to estimate the actual amount of pollutants that reach the different organs and rely on this information to evaluate the actual toxicological effects on the in-body biochemical processes.

In Figure 1.1.3, the deposition of particles in the lung by size is visualized. Large particles are deposited in the outer airways, smaller particles reach into the narrower parts of the respiratory system and are deposited deeper matching their size. This knowledge is not new, but the relevance is now put into a new perspective. The mobility of people has increased impressively. The average kilometre travelled by day is multiplied by a factor five in four decades (1960-2000) (Holden, 2007). More people are exposed to more traffic emission at home and on an individual level they are more mobile than ever before. The personal exposure to the small fraction of in-traffic related air pollution has increased. This illustrates the complexity of the health effects research and indicates the necessity to quantify the personal exposure in detail and adjust that personal exposure for particle size and toxicity.

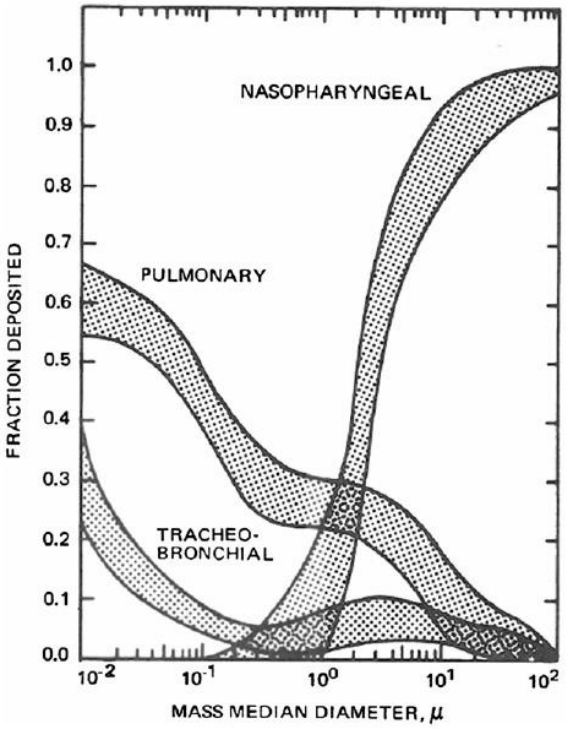

Figure 1.1.3: Fraction of particles deposited in the three respiratory tract compartments as a function of particle diameter. Source: U.S. Department of Health, Education and Welfare (1969).

1.1.4.3 Black Carbon exposure, a potential indicator for health effects

In a recent overview "Health effects of black carbon" by the WHO the current state of the art on the health effects of Black Carbon is summarized (WHO, 2012, Janssen et al., 2012). First the definition and measurement technology is addressed. Black Carbon is measured by light absorption of the airborne particles. The measurement technology for Black Carbon is not standardized yet. Consequently, research reports are sometimes difficult to compare. The few available health effect studies investigating both PM_{10} and BC exposure show stronger effects for BC than for PM_{10}. The studies detect BC related health effects up to 10 times the health effects of the PM_{10} for the same mass. The health effects of particulate matter and for BC specifically, seem to be stronger for the cardiovascular disease than the lung related health effects, showing opposite effects to other gaseous air pollution components (Mordukhovich et al. 2009, Janssen et al., 2011, Keuken et al., 2011). Diesel exhaust and UFP has been reported to pass through the lung lining, pass the lung-blood barrier and even deposits in the brains have been reported (Terzano et al., 2010, Campen et al., 2012). BC itself might be not the actual toxic component but it can carry other toxic components. BC is not established as the primary air pollution health component yet, but the evidence is accumulating. The WHO report supports further investigation in BC as a relevant component to investigate traffic related air pollution.

1.1.5 Personal exposure in detail

As shown in the previous sections, improving health evaluations implies the improvement of the estimation of the personal exposure. The methods to measure personal exposure are introduced and the current knowledge on exposure properties related to the microenvironment, modal choice, route choice and the local traffic conditions are summarized in this section.

1.1.5.1 Participatory sensing

The whereabouts of the subjects and their behaviour related exposure are mainly investigated through participatory sensing campaigns. New technology has enabled measuring the actual personal exposure for some pollutants. The campaigns include measurements of GPS coordinates, exposure, micro-environments, physical activity, biomarkers etc. (Dons et al., 2011, Dons et al., 2012, de Nazelle et al. 2011, Hankey et al., 2012). Recently, measurements of personal exposure to Black Carbon prove the importance of the in-traffic contribution to the total diurnal Black Carbon exposure. The in-traffic exposure accounts for 25 to 60% of the total diurnal exposure and is strongly related to the commuting behaviour (Dons et al., 2012). Several authors have discussed the requirements of participatory sensing campaigns. A state of the art overview of current practices in participatory sensing measurements is presented by Steinle (Steinle et al., 2013), evaluating numerous 'must-have' properties of research setups. The requirements are also part of the 'eco-exposome vision and strategy' (Lioy and Smith, 2013). Participatory sensing campaigns are expensive and require a lot of technical support, which makes it difficult to achieve representative population samples. The difficulty in extrapolating the exposure measurements to representative populations for epidemiological research and governmental policy is recognized as the most important issue to be solved in the exposome research (Lioy and Smith, 2013).

1.1.5.2 Micro-environments and personal exposure

Many of the participatory sensing campaigns focus on the differences between the different travel modes. The microenvironment is a generalisation of the different types of environments a person spends his activity in (car, rail, subway, dwelling, etc...). Each of these microenvironments has its specific exposure dynamics for different air pollutants and is therefore often investigated separately. The difference between indoor and outdoor exposure is frequently discussed in respect to the health evaluations for at home exposure (Raaschou-Nielsen et al., 2011, Kierney et al., 2011). Biking and walking have been investigated in high detail by many authors (Kaur et al., 2005, Wang et al., 2011, Berghmans et al., 2010). Several authors compared different micro-environments (Kaur et al., 2005, Briggs et al., 2007, Tsai et al., 2008, Asmi et al., 2009, Int Panis et al., 2010, Zuurbier et al., 2010, Apte et al., 2011, Dons et al., 2011).

1.1.5.3 Local traffic dynamics, route choice and personal exposure

The temporal variation of the exposure in a microenvironment is for a large part related to the local traffic conditions. Several authors addressed the effect of route choice on the exposure (Hertel et al., 2008, Pattinson, 2009, Strak et al., 2012, Ragetti et al., 2013). The in-vehicle environment is highly influenced by local traffic conditions and street characteristics (Fruin et al., 2004, Fruin et al., 2007, Hudda et al., 2012, Dons et al., 2013, Cattani et al., 2013). Many authors already indicated the strong effects of the ventilation settings and the influence of the age, make and quality of the vehicle (Zhu et al., 2007, Hudda et al., 2011, Knibbs et al., 2010, Fruin et al., 2011, Wu et al., 2013, Lee et al., 2014). Predicting the in-vehicle exposure is a daunting task. A first attempt was made by Li; investigating the modelling techniques for PAH, PN, $PM_{2.5}$ and NO_2 (Li et al., 2013). The authors concluded that the non-linear effects of the meteorological conditions hamper the prediction when using linear regression models. Non-linear approaches tend to result in better models. Short-term exposure assessment and health effects studies may require similar exposure estimates at a high temporal resolution (Li et al., 2013).

1.1.5.4 Physical activity and personal exposure

Physical activity is for many different reasons an important factor in the health evaluations. Being physical active is health in itself (Warburton et al., 2006, Tremblay et al., 2012). When physically active, both the respiration rate and the volume of inhaled air increase and affect the total intake of air pollution. This is an example of an activity related dose correction as mentioned before in 1.1.2.3. Many authors have addressed the balance between the positive effects of being physically active and the negative effects of the consequent higher intake when performing high demanding tasks in high exposed environments (de Hartog et al., 2010, Strak et al., 2013, Jacobs et al., 2010, Bos et al., 2013). Some investigators attempt to detect the short-term effects of traffic related air pollution. Jacobs et al., 2010 could not detect short term effects for bicyclists in real traffic compared to clean laboratory conditions. Short-term effects were detected when using facemasks to reduce the personal exposure and effects were detected in cardiovascular health in patients with coronary heart disease (Langrish et al., 2009, Langrish et al., 2012). McCreanor detected respiratory effects of exposure to diesel traffic in persons with asthma (McCreanor et al., 2007). The lung ventilation rate is acknowledged as one of the most important activity related dose corrections to evaluate the health effects.

Most authors agree that for mortality the positive health effects of physical activity outweigh the simultaneous negative health effects of active travel modes (de Hartog et al. 2010, Rojas-Rueda et al., 2011) but for morbidity, this is an unsolved issue (Int Panis, 2011). It is a popular topic in the media and it influences the public sentiment on biking in the city. Promoting cycling is a central theme in the policy towards low carbon cities (Creutzig et al.,

2012). It is important to quantify the positive and negative health aspects of cycling in the cities to support local policy.

1.1.6 Modelling techniques

1.1.6.1 Spatial variation and Land-use regression models

Capturing the spatial variation of traffic related air pollution is critical to provide quantitative data to the epidemiologists. Many types of models are used to estimate the gaseous air pollutants and the general PM fractions. Micro-meteorological models exist for many pollutants but these models cannot be extrapolated city or region-wide due the complexity of the methods (Hoek et al., 2008). Large scale models are implemented to assess air pollution exposure. The most common technique is the land-use regression model (LUR). Land-use attributes (mainly traffic and habitation related information) are regressed against concentration measurements in order to extrapolate the exposure over larger project areas. Overviews of methodologies and comparison of modelling techniques have been reported extensively (Hoek et al., 2008, Marshall et al., 2008, Hoek et al., 2009, Hankey et al., 2012).

More recently more detailed measurements in near road settings have shown large difference in the spatial variability for different pollutants. The ultrafine particles show decreases of over 50% within the first 150 m from the edge of the road. $PM_{2.5}$, PM_{10}, Benzene and NO_2 show lower or even no decay relative to the edge of the road (Karner et al., 2010). The strong distance to source effects of Black carbon and UFP were illustrated on a motorway flyover as well (Van Poppel et al, 2012.). Strong up-wind and downwind effect with similar distance effects are reported for UFP by Hu et al. (Hu et al., 2009). High contrasts from street to street in air pollution components have been reported by several authors (Boogaard et al., 2011, Hankey et al., 2014, Padro-Martinez et al, 2012). The available Land-use regression models mainly focus on PM_{10}, $PM_{2.5}$ and NO_2 have a much lower spatial variation compared to BC and UFP. To capture the exposure to the traffic related small particles adequately; the LUR models will be forced to improve their spatial resolution to match the spatial variation of UFP and BC. A first LUR for BC is published by Evi Dons (Dons et al. 2013, Dons et al. 2014).

1.1.6.2 Linear versus smooth modelling techniques

Land-use regression techniques commonly use linear regressions to fit the measurements to the spatial attributes. Many aspects of the personal exposure are known to express non-linear aspects. Traffic dynamics and traffic congestion are a highly non-linear function of the traffic counts and the properties of road infrastructure. Noise and air pollution emission are both complex functions of the traffic dynamics (see 1.1.4.1). This is relevant for the in-vehicle air pollution exposure since the distance to the exhaust of the preceding vehicle is

one of the driving forces of the in-vehicle exposure. Wind speed and street canyon configuration modify the dispersion of air pollution in a non-linear fashion (Jicha et al., 2000, Johansson et al., 2007). Extending the modelling with non-linear techniques is therefore relevant. The non-linear modelling techniques have benefits but also important drawbacks. The main drawback is the high risk to overfit the data.

Several techniques are available: random forest (Johns et al., 2012), neural networks (Moustris et al., 2010), support vector machines (Feng et al., 2011) and generalized additive models (GAM) are only a few of the options. The relevance of the GAM technique for time series analysis in the air pollution field and epidemiology was shown by Dominici in 2002 (Dominici et al., 2002). An on-road model for the concentration of air pollutants in California explicitly compared the performance of the GAM model with the linear regression techniques and reported significant better performance for the GAM model (Li. Et al., 2013). In this PhD, no explicit comparisons to distinguish the different non-linear techniques are included since this is out of the scope of this work. GAMs will be used throughout the work to include non-linear aspects into the models.

GAMs are specific cases of scatterplot smoothing functions and were introduced by Hastie and Tibshirani in 1986 (Hastie and Tibshirani, 1986). The behaviour of the parameters ('covariates' in the GAM terminology) is fitted with splines. A spline is a numeric function that is piecewise-defined by polynomial functions, and which possesses a high degree of smoothness at the places where the polynomial pieces connect. The strength of a model is mainly determined by the 'deviance explained' and 'Akaike Information Criterion' (AIC). Many technical implementations and improvements have become available over the years (Woods, 2004, Woods, 2006).

1.1.6.3 Managing overfitting in GAMs

Generalized additive models are sensitive to non-linear behaviour of the covariates but this implies high sensitivity to overfit the data. The GAM implementation in R (mgcv library) includes parameters to control the number of degrees of freedom in the data by means of a k-factor (Woods, 2006). Larger k gives more freedom to the fitted spline. More complex behaviour of the covariate can be captured, but the risk of overfitting the underlying data increases. In Figure 1.1.4 an example of the effect of the degrees of freedom in a GAM model is presented. The GAM model is explaining the background Black Carbon concentration in a fixed location with a set of meteorological parameters. Three versions of the model are shown with respectively k=3; k=4 and k=6 for all the covariates. The 'deviance explained' of the three variants are 21.0%, 24.9% and 29.8% respectively. Larger degrees of freedom result in larger 'deviance explained'.

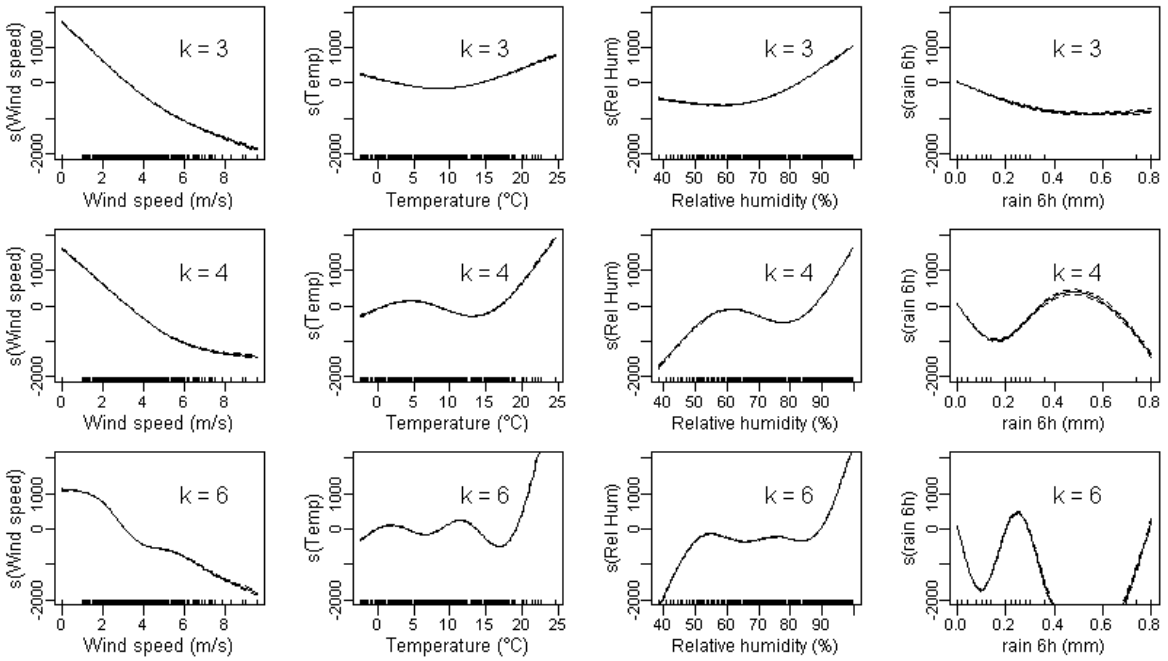

Figure 1.1.4: Example of the impact of the degrees of freedom in a GAM model. Three versions of the same GAM model predicting the BC concentration in a background measurement location are presented including the splines with different degrees of freedom for the four covariates (wind speed, temperature, relative humidity and rain during the past 6 hours). Higher degrees of freedom (k-factor) result in overfitting the data.

In the example, the last covariate (rain during the last six hours) is highly overfitting a few very low background values around values of 0.5 mm. This can be an artefact of the sampling. That specific meteorological condition might have been sampled only during high wind speed conditions. The decision to select a GAM model variant should not be based on the 'deviance explained' only. Covariates with expected complex behaviour can get higher k-factors, covariates with a more linear behaviour or basic saturations can have lower k-factors. In the example, the expected behaviour of the background BC concentration is explained better in the model with k=3. Higher wind speeds and more rain are related to lower background concentrations, relative humidity correlates with the background concentration and the temperature expresses a more complex behaviour. The splines of the GAM model visualize multiple dimensions of the behaviour of the data simultaneously. Understanding the underlying data becomes a question of being able to provide the relevant covariates in the required resolution and quality. The prediction function in the GAM implementations uses the splines to reconstruct the expected value for each relevant combination of covariates, even if that combination was not sampled in the underlying data. The most important technique to evaluate the quality of a model is external validation.

1.1.7 Summary

To assess the exposure to BC and UFP a higher spatial and temporal resolution is necessary due to the strong local variation. Instantaneous exposure to particulate matter is a function of the amount of local traffic, the local traffic conditions and the distance between the source and the subject. The particulate matter emission is a highly non-linear function of the local traffic flow conditions including fleet composition, congestion, speed etc. In most cases, little or no traffic information is available to include these features into the models. Each microenvironment has, on top of that, its own specific exposure dynamics in relation to the local traffic, background concentration and meteorological influences. The two most important requirements in the exposome research are the transition toward personal exposure and the capability to extrapolate more sensitive spatiotemporal models to larger populations. The most important requirement towards policy support is the quantification of the exposure and health effects due to changing behaviour for individuals in the population.

1.2 Concept and structure

1.2.1 The physical link between noise and PM emission

The basic concept of this PhD is the physical relation between the simultaneous exposure to noise and air pollution. In most noise evaluations assessing the health effects of noise on humans, the A-weighted equivalent noise L_{Aeq} or the more aggregated parameter L_{DEN} is used. The actual physical relation between noise and PM emissions is more complex and does not fit the L_{Aeq} or L_{DEN}. This is visually illustrated in Figure 1.2.1.

	Vehicle emissions			
	PM (BC/UFP)	Engine noise	Rolling noise	Total noise
Cruising (low speed)	=	=	=	=
Cruising (high speed)	+	+	+++	+++
Accelerating (low speed)	+++	+++	+	+++
Decelerating/Idle	-	-	=/-	=/-

Figure 1.2.1: Structure of chapter 4 and 5. The underlying data (noise measurement or noise maps) is related to the investigated micro-environments (ME). At the right side, the matching evaluation level of the sections is shown.

The different emissions (PM, engine related noise, tyre related rolling noise and the total noise levels) are related to different driving conditions in a qualitative way. The engine regime (throttle) has a stronger link with the instantaneous PM emissions compared to L_{Aeq}. It is important to understand that the evaluation of the noise related health effects use different noise indicators than the indicators that will be used in this work to predict the in-traffic air pollution exposure.

1.2.2 Goals

- Present a person centred approach for assessing the subjective perception based Quality of Life including evaluations at the dwelling, in traffic and at the destinations and evaluate the potential of the noise assessments as a proxy for the subjective perception of the traffic related quality of life.
- Develop a generalized activity based and person centred data flow framework to enable the calculation of any spatiotemporal indicator on any predefined mobile population.
- Use noise exposure as a proxy for local traffic assessment to model and predict Black Carbon exposure in different micro-environments. Instantaneous micro-environment specific land-use regression models will be evaluated for three micro-environments: bicycle, in-vehicle and indoor. These models will be referred to as µLUR ('microscopic' in time and space and micro-environment specific).
- Model and evaluate the instantaneous spatiotemporal personal exposure to Black Carbon for the full time-activity pattern, including a validation with external exposure measurements.

1.2.3 Outline

The PhD builds on prior work from the traffic related Quality of Life model. The first part of the second chapter describes the multi-indicator methodology of this model. In the second part of the second chapter a more generalized indicator workflow is presented. It extends the functionality of the Quality of Life model to activity specific models and adds functionality towards participatory sensing. The third chapter summarizes the results of the Quality of Life model. The focus in this chapter is on the power of the spatial information in noise maps to act as a proxy for the subjective perception of the traffic related quality of life, also referred to as 'Traffic Liveability'. Extended literature on this work and other outcomes can be found in the publication list (1.2.4).

The fourth chapter describes the noise based micro-environment specific Black Carbon exposure models. It is important to define 'exposure' in this context. Many authors and dis-

ciplines use similar nouns in different contexts (see also 1.1.2.3). In the presented models no dose corrections of any type (inhalation rate, deposition in lungs, etc.) are included, only the concentration at the position of the subject in space and time is modelled and evaluated. This is referred to as 'personal exposure' since the personal time-activity pattern is the main driving force. Dose corrections become only relevant when the personal exposure is linked to potential health effects. This work does not extend the results to health effects and includes therefor no activity related dose corrections. The general data workflow presented in 2.3 can include dose corrections. The dose corrections will be added in future applications through a multidisciplinary and project specific decision process (see section 6.1).

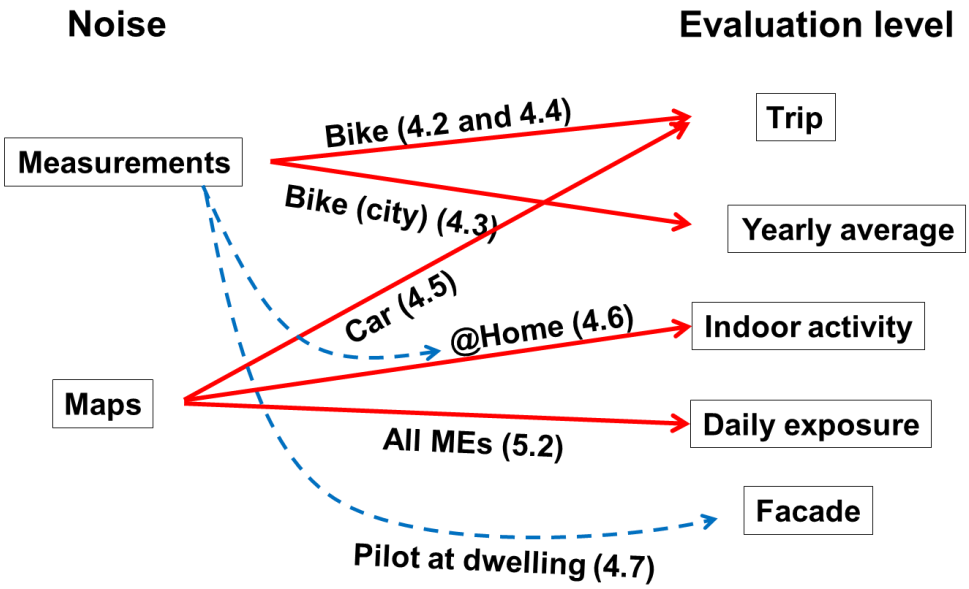

Figure 1.2.2: Structure of chapter 4 and 5. The underlying data (noise measurement or noise maps) is related to the investigated micro-environments (ME). At the right side, the matching evaluation level of the sections is shown.

In Figure 1.2.2, the relation and the evaluation levels of the different sections are presented. It starts with an instantaneous model for the BC exposure of bicyclists (4.2). A yearly meteorology adjusted exposure and a city wide mapping methodology is presented in section 4.3. In section 4.4, the technique is tested with an automated noise measurement setup in an international context and includes an extension from BC to UFP. In section 4.5, an instantaneous model for in-vehicle exposure is presented. The traffic assessment moves from noise measurements to noise maps. In section 4.6, the instantaneous model for bicyclists is merged with noise map data and is used to build an instantaneous exposure model for the indoor micro-environment. In section 4.7, the lessons learned throughout the chapter are tested in a pilot experiment using simultaneous noise and BC measurements at a dwelling facade. In the fifth chapter, the results of chapter four are combined to predict the personal daily exposure to Black Carbon (5.2). Section 4.2, 4.3 and 4.4 are published as independent research articles.

A general discussion is added, summarizing all features of the presented work (5.3). In chapter six, the future potential and applications are presented and the conclusions are summarized.

1.2.4 Publication list

Not all my publications are directly related to this PhD. The publications with a direct link to this work are indicated with an asterisk.

1.2.4.1 A1 peer reviewed papers

*Dekoninck, Luc, Dick Botteldooren, and Luc Int Panis. "Using city-wide mobile noise assessments to estimate annual exposure to Black Carbon.", *Environment international* 83 (2015): 192-201.

*Dekoninck, Luc, Dick Botteldooren, Luc Int Panis, Steve Hankey, Grishma Jain, Karthik S, Julian Marshall. "Applicability of a noise-based model to estimate in-traffic exposure to black carbon and particle number concentrations in different cultures" Environment International, Volume 74, January 2015, Pages 89–98.

*Dekoninck, Luc, Dick Botteldooren, and Luc Int Panis. "An Instantaneous Spatiotemporal Model to Predict a Bicyclist's Black Carbon Exposure Based on Mobile Noise Measurements." ATMOSPHERIC ENVIRONMENT 79 (2013): 623–631.

*Can, Arnaud, Luc Dekoninck, and Dick Botteldooren. "Measurement Network for Urban Noise Assessment: Comparison of Mobile Measurements and Spatial Interpolation Approaches." *APPLIED ACOUSTICS* 83 (2014): 32–39.

Van Renterghem, Timothy, Dick Botteldooren, and Luc Dekoninck. "Airborne Sound Propagation over Sea During Offshore Wind Farm Piling." JOURNAL OF THE ACOUSTICAL SOCIETY OF AMERICA 135.2 (2014): 599–609.

Bockstael, Annelies, Luc Dekoninck, Arnaud Can, et al. "Reduction of Wind Turbine Noise Annoyance: An Operational Approach." ACTA ACUSTICA UNITED WITH ACUSTICA 98.3 (2012): 392–401.
Impact factor: 0.714, category: ACOUSTICS, rank: 19/31.

Van Renterghem, Timothy, Dick Botteldooren, and Luc Dekoninck. "Evolution of Building Facade Road Traffic Noise Levels in Flanders." JOURNAL OF ENVIRONMENTAL MONITORING 14.2 (2012): 677–686.
Impact factor: 2.085, category: ENVIRONMENTAL SCIENCES, rank: 84/209.

*Botteldooren, Dick, Luc Dekoninck, and Dominique Gillis. "The Influence of Traffic Noise on Appreciation of the Living Quality of a Neighborhood." INTERNATIONAL JOURNAL OF ENVIRONMENTAL RESEARCH AND PUBLIC HEALTH 8.3 (2011): 777–798.

*Can, Arnaud, Luc Dekoninck, Michaël Rademaker, et al. "Noise Measurements as Proxies for Traffic Parameters in Monitoring Networks." SCIENCE OF THE TOTAL ENVIRONMENT 410 (2011): 198–204.
Impact factor: 3.286, category: ENVIRONMENTAL SCIENCES, rank: 29/203.

1.2.4.2 Conferences

*Dekoninck, Luc, Dick Botteldooren, and Luc Int Panis. "A spatiotemporal, route-enabled framework to disentangle personal exposure and dose indicators for noise and air pollution." ISEE 2014: Young Researchers Conference on Environmental Epidemiology, CREAL, Barcelona, October 20-21, 2014. 758–758.

*Dekoninck, Luc, Dick Botteldooren, and Luc Int Panis. "Noise exposure and its spectral components as a proxy for particulate matter exposure in different micro-environments." ISEE 2014: Young Re-

searchers Conference on Environmental Epidemiology, CREAL, Barcelona, October 20-21, 2014. 758–758.

Lercher, Peter, Alex Eisenmann, Luc Dekoninck, et al. “Noise Exposure and Health Effects in Children: Results from a Contextual Soundscape Perspective.” *AIA-DAGA 2013, International Conference on Acoustics, Merano*. Berlin, Germany: Deutsche Gesellschaft für Akustik (DEGA), 2013. 1465–1468.

Lercher, Peter, Alex Eisenmann, Luc Dekoninck, et al. “The Relation Between Disturbed Sleep in Children and Traffic Noise Exposure in Alpine Valleys.” *Proceedings of the 42nd International Congress and Exposition on Noise Control Engineering (Inter-Noise 2013)*. 2013.

*Dekoninck, Luc, Dick Botteldooren, Luc Int Panis, et al. “Traffic Noise and Particulate Matter Exposure: How Can We Distinguish Between Them in Effect Studies?” *Proceedings of the 42nd International Congress and Exposition on Noise Control Engineering (Inter-Noise 2013)*. 2013.

Lercher, Peter, Annelies Bockstael, Luc Dekoninck, et al. “Can Noise from a Main Road Be More Annoying Than from a Highway?: An Environmental Health and Soundscape Research.” *Proceedings of the 42nd International Congress and Exposition on Noise Control Engineering (Inter-Noise 2013)*. 2013.

*Dekoninck, Luc, Dick Botteldooren, and Luc Int Panis. “Mobile Noise Measurements as a Proxy for BC Exposure: Spatiotemporal and Spatial Analysis.” *Environment and Health : Bridging South, North, East and West*. 2013. 758–758.

Botteldooren, Dick, Timothy Van Renterghem, Damiano Oldoni, et al. “The Internet of Sound Observatories.” *Proceedings of Meetings on Acoustics*. Vol. 19. Melville, NY, USA: Acoustical Society of America, 2013.

*Gillis, Dominique, Dirk Lauwers, Luc Dekoninck, et al. “Modelling the Impact of Traffic on Quality of Life: Scenario Evaluation for the City of Ghent.” *2nd International Conference on Road and Rail Infrastructure, Proceedings*. Ed. Stjepan Lakusic. 2012. 757–764.

*Dekoninck, Luc, Dick Botteldooren, and Luc Int Panis. “Guidelines for Participatory Noise Sensing Based on Analysis of High Quality Mobile Noise Measurements.” *Proceedings of the 41st International Congress and Exposition on Noise Control Engineering (Inter-Noise 2012)*. Institute of Noise Control Engineering, 2012.

Lercher, Peter, Annelies Bockstael, Bert De Coensel, et al. “The Application of a Notice-event Model to Improve Classical Exposure-annoyance Estimation.” *Proceedings of the Acoustics 2012 Hong Kong Conference*. 2012.

*Dekoninck, Luc, Dick Botteldooren, and Luc Int Panis. “Bicyclist Black Carbon Exposure and the Impact of Routes Choice and Biking Facilities, a Spatial Analysis.” *International Society for Environmental Epidemiology, Abstracts*. 2011.

*Dekoninck, Luc, Dominique Gillis, and Dick Botteldooren. “Perceived Quality of the Living Environment and Noise.” *Proceedings of the Institute of Acoustics (cd-rom)*. Ed. Barbara Griefahn. Vol. 33 (Pt.3). Institute of Acoustics, 2011. 921–928.

Can, Arnaud, Luc Dekoninck, Michaël Rademaker, et al. “Noise Measurements as Proxies for Traffic Parameters in Monitoring Networks.” *Forum Acusticum*. European Accoustics Association (EAA), 2011. 653–658.

Bockstael, Annelies, Luc Dekoninck, Bert De Coensel, et al. “Wind Turbine Noise: Annoyance and Alternative Exposure Indicators.” *Forum Acusticum*. European Accoustics Association (EAA), 2011. 345–350.

*Dekoninck, L., Gillis, D., & Botteldooren, D. (2011). Perceived quality of the living environment and noise. In 10th International Congress on Noise as a Public Health Problem (ICBEN-2011) (Vol. 33, pp. 921-928). Institute of Acoustics.

*Gillis, Dominique, Luc Dekoninck, Dirk Lauwers, et al. “Modelling the Impact of Traffic on Quality of Life: Results from a Case-study for the City of Ghent.” *Proceedings of the BIVEC-GIBET Transport Research Day*. Ed. Eric Cornelis. BIVEC-GIBET, 2011.

*Gillis, Dominique, Dirk Lauwers, Dick Botteldooren, et al. “The Assessment of Traffic Livability, Including Local Effects at Home, During Trips and at the Destination, Based on the Individual Activity Pattern

and Trip Behaviour." *REAL CORP 2010, Proceedings*. Ed. Manfred Schrenk et al. Ghent, Belgium: Ghent University, Department of Civil engineering, 2010. 721–720.

De Coensel, Bert, Annelies Bockstael, Luc Dekoninck, et al. "Application of a Model for Auditory Attention to the Design of Urban Soundscapes." *Proceedings of the EAA Euregio 2010 Congress*. Ljubljana, Slovenia: Slovenian Acoustical Society (SDA), 2010. 1–6.

Thomas, Pieter, Timothy Van Renterghem, Luc Dekoninck, et al. "Sound-field Research of Urban Squares Used for Outdoor Rock Concerts." *Noise Control Engineering, 39th International Congress, Proceedings*. 2010.

De Coensel, Bert, Annelies Bockstael, Luc Dekoninck, et al. "The Soundscape Approach for Early Stage Urban Planning: a Case Study." *Noise Control Engineering, 39th International Congress, Proceedings*. 2010.

Thomas, Pieter, Timothy Van Renterghem, Luc Dekoninck, et al. "Urban Square Sound Fields During Rock Concerts." *Proceedings of the Institute of Acoustics*. Vol. 32. Institute of Acoustics, 2010. 292–297.

*Botteldooren, Dick, Luc Dekoninck, Dominique Gillis, et al. "The Influence of Trip Behavior on Assessment of the Quality of the Living Environment." *Proceedings of the Institute of Acoustics*. Vol. 32. Institute of Acoustics, 2010. 126–131.

*Dekoninck, Luc, Dominique Gillis, and Dick Botteldooren. "Environmental Quality of Living Environment Assessment Including On-road and On-site Exposure to Noise and Air Pollution." *European Conference on Noise Control, 8th, Proceedings*. 2009.

Thomas, Pieter, Timothy Van Renterghem, Luc Dekoninck, et al. "Acoustic Evaluation of Public Squares Used for Outdoor Concerts." *European Conference on Noise Control, 8th, Proceedings*. 2009.

Lercher, P., Bram de Greve, Dick Botteldooren, et al. "Health Effects and Major Co-determinants Associated with Rail and Road Noise Exposure Along Transalpine Traffic Corridors." *Proceedings of the 9th Congress of the International Commission on the Biological Effects of Noise (ICBEN 2008)*. 2008. 322–332.

De Coensel, Bert, Dick Botteldooren, Luc Dekoninck, et al. "Noise Emissions at Intersections: Comparing Microscopic and Macroscopic Traffic Simulation Approaches." *Acoustics '08 Paris*. Paris, France: Société Francaise d'Acoustique (SFA), 2008.

Botteldooren, Dick, Luc Dekoninck, Bram de Greve, et al. "Annoyance by Combined Exposure to Noise from Road Traffic and Rail Traffic Discussed in the Framework of the Noticing Model (invited Paper)." *Proceedings of the 19th International Congress on Acoustics*. 2007.

LERCHER, P, Dick Botteldooren, Bram de Greve, et al. "The Effects of Noise from Combined Traffic Sources on Annoyance: The Case of Interactions Between Rail and Road Noise (invited Paper)." *Proceedings of the 36th International Congress and Exhibition on Noise Control Engineering (Inter-Noise 2007)*. 2007.

Botteldooren, Dick, and Luc Dekoninck. "Standardized Crumpling Noise Measurement." *Proceedings of the Thirteenth International Congress on Sound and Vibration (ICSV 2006)*. 2006.

LERCHER, P, C PFEIFER, Dick Botteldooren, et al. "Traffic Noise Exposure, Education and Annoyance: Longitudinal Experience from Crosssectional Surveys over Time (1989-2004)." *Proceedings of Forum Acusticum 2005*. 2005. 1795–1799.

Dekoninck, Luc, and Dick Botteldooren. "Prediction of Noise Annoyance Due to Local Traffic Using Geographic Information and Traffic Modeling." *Proceedings (on Cd-rom) of the 31th International Congress on Noise Control Engineering (Internoise) 2002, Vol., August 19-21, 2002, Dearborn, Michigan, USA, Paper 295 (6 Pages)*. 2002.

VAN WALSUM, E, Dick Botteldooren, Luc Dekoninck, et al. "Scenarios for the Acoustic Environment in Flanders in 2010." *URBAN TRANSPORT VII: URBAN TRANSPORT AND THE ENVIRONMENT IN THE 21ST CENTURY* 8 (2001): 555–564.

Dekoninck, Luc, Dick Botteldooren, G VINDEVOGEL, et al. "An Indicator for Road Traffic Noise: Monitoring and Prediction Model INTERNOISE 2000." *29th Int. Congress on Noise Control Engineering*. 2000.

1.2.4.3 Reports

*Gillis, Dominique, Luc Dekoninck, Thomas Verbeek, et al. “De Aanpak Van Verkeersleefbaarheid in Vlaanderen.” *De Sociale Staat Van Vlaanderen 2013*. Ed. Marc Callens, Jo Noppe, & Lieve Vanderleyden. Brussel: Vlaamse overheid. Studiedienst van de Vlaamse Regering, 2013. 273–312.

*Botteldooren, D., Dekoninck, L., & Gillis, D. (2008). Zwarte punten voor geluidshinder door straatverkeer in Vlaanderen : analyse van conflicten tussen verkeer en leefbaarheid. Diepenbeek: Steunpunt Mobiliteit en Openbare Werken.

*Botteldooren, D., De Coensel, B., Van Renterghem, T., Dekoninck, L., & Gillis, D. (2008). The urban soundscape : a different perspective. In G. Allaert & F. Witlox (Eds.), *Duurzame mobiliteit Vlaanderen : de leefbare stad* (pp. 177–204). Presented at the Duurzame mobiliteit Vlaanderen : de leefbare stad, Gent, België: Universiteit Gent. Instituut voor Duurzame Mobiliteit.

*Dekoninck, L., Gillis, D., Botteldooren, D., & Lauwers, D. (2010). Methodologie voor het objectief meten van het effect van verkeer op de leefbaarheid : een aggregatietechniek om de lokale effecten van verkeer (veiligheid, gezondheid en kwaliteit van de omgeving) , thuis, onderweg en op de bestemming te evalueren op basis van het individueel tijdsgebruik en verplaatsingsgedrag : theoretisch kader. Steunpunt Mobiliteit & Openbare Werken.

*Dekoninck, L., Gillis, D., Botteldooren, D., & Lauwers, D. (2011). Indicatoren voor verkeersleefbaarheid: uitwerking en toepassing van een model voor het meten van verkeersleefbaarheid. Steunpunt Mobiliteit & Openbare Werken.

*Dekoninck, L., Gillis, D., Botteldooren, D., & Lauwers, D. (2012). Ruimtelijke ontwikkeling, verkeer, geluidshinder en impact op leefbaarheid. Steunpunt Mobiliteit & Openbare Werken.

Botteldooren, Dick, Luc Dekoninck, Tom De Muer, et al. “Thema 2.7: Hinder.” *Milieu- En Natuurrapport Vlaanderen : Thema’s MIRA-T 2004*. Leuven: Lannoo Campus, 2004. 219–229.

Botteldooren, Dick, Luc Dekoninck, J THOEN, et al. “Lawaai.” MIRA-S 2000 Milieu- En Natuurrapport Vlaanderen : Scenario’s / Van Steertegem M. (Ed.). - Leuven-Apeldoorn : Garant, 2000. - ISBN 90-441-1048-9. 2000. 309–322.

1.3 References

Albino V, Dangelico RM. Green Economy Principles Applied to Cities: an Analysis of Best Performers and the Proposal of a Set of Indicators. Ifkad - Kcws 2012: 7th International Forum on Knowledge Asset Dynamics, 5th Knowledge Cities World Summit: Knowledge, Innovation and Sustainability: Integrating Micro & Macro Perspectives 2012: 2665-2689.

Albino V, Dangelico RM. Green Economy Principles Applied to Cities: an Analysis of Best Performers and the Proposal of a Set of Indicators. Ifkad - Kcws 2012: 7th International Forum on Knowledge Asset Dynamics, 5th Knowledge Cities World Summit: Knowledge, Innovation and Sustainability: Integrating Micro & Macro Perspectives 2012: 2665-2689.

Anenberg SC, Schwartz J, Shindell D, Amann M, Faluvegi G, Klimont Z, et al. Global Air Quality and Health Co-benefits of Mitigating Near-Term Climate Change through Methane and Black Carbon Emission Controls. Environmental Health Perspectives 2012; 120: 831-839.

Appleyard.D, Lintell M. ENVIRONMENTAL QUALITY OF CITY STREETS - RESIDENTS VIEWPOINT. Journal of the American Institute of Planners 1972; 38: 84-101.

Bauer M, Moebus S, Moehlenkamp S, Dragano N, Nonnemacher M, Fuchsluger M, et al. Urban Particulate Matter Air Pollution Is Associated With Subclinical Atherosclerosis Results From the HNR (Heinz Nixdorf Recall) Study. Journal of the American College of Cardiology 2010; 56: 1803-1808.

Beckx C, Panis LI, Arentze T, Janssens D, Torfs R, Broekx S, et al. A dynamic activity-based population modelling approach to evaluate exposure to air pollution: Methods and application to a Dutch urban area. Environmental Impact Assessment Review 2009a; 29: 179-185.

Beckx C, Panis LI, Janssens D, Wets G. Applying activity-travel data for the assessment of vehicle exhaust emissions: Application of a GPS-enhanced data collection tool. Transportation Research Part D-Transport and Environment 2010; 15: 117-122.

Beckx C, Panis LI, Uljee I, Arentze T, Janssens D, Wets G. Disaggregation of nation-wide dynamic population exposure estimates in The Netherlands: Applications of activity-based transport models. Atmospheric Environment 2009b; 43: 5454-5462.

Beckx C, Panis LI, Vankerkom J, Janssens D, Wets G, Arentze T. An integrated activity-based modelling framework to assess vehicle emissions: approach and application. Environment and Planning B-Planning & Design 2009c; 36: 1086-1102.

Beelen R, Hoek G, van den Brandt PA, Goldbohm RA, Fischer P, Schouten LJ, et al. Long-term effects of traffic-related air pollution on mortality in a Dutch cohort (NLCS-AIR study). Environmental Health Perspectives 2008; 116: 196-202.

Bjork J, Ardo J, Stroh E, Lovkvist H, Ostergren P-O, Albin M. Road traffic noise in southern Sweden and its relation to annoyance, disturbance of daily activities and health. Scandinavian Journal of Work Environment & Health 2006; 32: 392-401.

Boogaard H, Kos GPA, Weijers EP, Janssen NAH, Fischer PH, van der Zee SC, et al. Contrast in air pollution components between major streets and background locations: Particulate matter mass, black carbon, elemental composition, nitrogen oxide and ultrafine particle number. Atmospheric Environment 2011; 45: 650-658.

Bos I, De Boever P, Vanparijs J, Pattyn N, Panis LI, Meeusen R. Subclinical Effects of Aerobic Training in Urban Environment. Medicine and Science in Sports and Exercise 2013; 45: 439-447.

Bradshaw CJA, Giam X, Sodhi NS. Evaluating the Relative Environmental Impact of Countries. Plos One 2010; 5.

Brereton F, Bullock C, Clinch JP, Scott M. Rural change and individual well-being: the case of Ireland and rural quality of life. European Urban and Regional Studies 2011; 18: 203-227.

Brink M. Parameters of well-being and subjective health and their relationship with residential traffic noise exposure - A representative evaluation in Switzerland. Environment International 2011; 37: 723-733.

Buonanno G, Marks GB, Morawska L. Health effects of daily airborne particle dose in children: Direct association between personal dose and respiratory health effects. Environmental Pollution 2013; 180: 246-250.

Buonanno G, Stabile L, Morawska L. Personal exposure to ultrafine particles: The influence of time-activity patterns. Science of the Total Environment 2014; 468: 903-907.

Campen M, Robertson S, Lund A, Lucero J, McDonald J. Engine exhaust particulate and gas phase contributions to vascular toxicity. Inhalation Toxicology 2014; 26: 353-360.

Campen MJ, Lund A, Rosenfeld M. Mechanisms linking traffic-related air pollution and atherosclerosis. Current Opinion in Pulmonary Medicine 2012; 18: 155-160.

Cattani, Giorgio, Alessandro Di Menno di Bucchianico, and Marco Inglessis. "CAR COMMUTERS'PERSONAL EXPOSURE TO ULTRAFINE PARTICLES Extended abstract." Environmental Engineering and Management Journal 12.S11 (2013): 217-220.

Chuepeng S, Xu H, Tsolakis A, Wyszynski M, Price P. Particulate Matter size distribution in the exhaust gas of a modern diesel Engine fuelled with a biodiesel blend. Biomass & Bioenergy 2011; 35: 4280-4289.

Clark C, Crombie R, Head J, van Kamp I, van Kempen E, Stansfeld SA. Does Traffic-related Air Pollution Explain Associations of Aircraft and Road Traffic Noise Exposure on Childrens Health and Cognition? A Secondary Analysis of the United Kingdom Sample From the RANCH Project. American Journal of Epidemiology 2012; 176: 327-337.

Costello, Anthony, et al. "Managing the health effects of climate change: lancet and University College London Institute for Global Health Commission." The Lancet 373.9676 (2009): 1693-1733.

Creutzig F, Muehlhoff R, Roemer J. Decarbonizing urban transport in European cities: four cases show possibly high co-benefits. Environmental Research Letters 2012; 7.

Daniau C, Dor F, Eilstein D, Lefranc A, Empereur-Bissonnet P, Dab W. Study of self-reported health of people living near point sources of environmental pollution: A review. First part: Health indicators. Revue D Epidemiologie Et De Sante Publique 2013; 61: 375-387.

Dardiotis C, Fontaras G, Marotta A, Martini G, Manfredi U. Emissions of modern light duty ethanol flex-fuel vehicles over different operating and environmental conditions. Fuel 2015; 140: 531-540.

Davies H, Van Kamp I. Noise and cardiovascular disease: A review of the literature 2008-2011. Noise & Health 2012; 14: 287-291.

Davies HW, Vlaanderen JJ, Henderson SB, Brauer M. Correlation between co-exposures to noise and air pollution from traffic sources. Occupational and Environmental Medicine 2009; 66: 347-350.

de Hartog JJ, Ayres JG, Karakatsani A, Analitis A, ten Brink H, Hameri K, et al. Lung function and indicators of exposure to indoor and outdoor particulate matter among asthma and COPD patients. Occupational and Environmental Medicine 2010; 67.

de Kluizenaar Y, van Lenthe FJ, Visschedijk AJH, Zandveld PYJ, Miedema HME, Mackenbach JP. Road traffic noise, air pollution components and cardiovascular events. Noise & Health 2013; 15: 388-397.

de Kok TMCM, Driece HAL, Hogervorst JGF, Briede JJ. Toxicological assessment of ambient and traffic-related particulate matter: A review of recent studies. Mutation Research-Reviews in Mutation Research 2006; 613: 103-122.

de Nazelle A, Fruin S, Westerdahl D, Martinez D, Matamala J, Kubesch N, et al. Traffic Exposures and Inhalations of Barcelona Commuters. Epidemiology 2011; 22: S77-S78.

Dhondt S, Beckx C, Degraeuwe B, Lefebvre W, Kochan B, Bellemans T, et al. Health impact assessment of air pollution using a dynamic exposure profile: Implications for exposure and health impact estimates. Environmental Impact Assessment Review 2012; 36: 42-51.

Dills JE, Rutt CD, Mumford KG. Objectively Measuring Route-To-Park Walkability in Atlanta, Georgia. Environment and Behavior 2012; 44: 841-860.

Distaso A. Well-being and/or quality of life in EU countries through a multidimensional index of sustainability. Ecological Economics 2007; 64: 163-180.

Dons E, Panis LI, Van Poppel M, Theunis J, Wets G. Personal exposure to Black Carbon in transport microenvironments. Atmospheric Environment 2012; 55.

Dons E, Panis LI, Van Poppel M, Theunis J, Willems H, Torfs R, et al. Impact of time-activity patterns on personal exposure to black carbon. Atmospheric Environment 2011; 45: 3594-3602.

Dons E, Temmerman P, Van Poppel M, Bellemans T, Wets G, Panis LI. Street characteristics and traffic factors determining road users' exposure to black carbon. Science of the Total Environment 2013; 447: 72-79.

Dons, E., 2013. Air pollution exposure assessment through personal monitoring and activity-based modeling. PhD Thesis. Hasselt University, Diepenbeek, p. 302.

Dons E, Van Poppel M, Kochan B, Wets G, Panis LI. Implementation and validation of a modeling framework to assess personal exposure to black carbon. Environment International 2014; 62: 64-71.

Dratva J, Zemp E, Dietrich DF, Bridevaux PO, Rochat T, Schindler C, et al. Impact of road traffic noise annoyance on health-related quality of life: results from a population-based study. Quality of Life Research 2010; 19: 37-46.

Ducret-Stich R, Delfino RJ, Tjoa T, Gemperli A, Ineichen A, Wu J, et al. Home outdoor models for traffic-related air pollutants do not represent personal exposure measurements in Southern California. Inhaled Particles X 2009; 151.

EU commission, Directive 2002/49/EC of the European Parliament and of the Council of 25 June 2002 relating to the assessment and management of environmental noise - Declaration by the Commis-

sion in the Conciliation Committee on the Directive relating to the assessment and management of environmental noise, http://eur-lex.europa.eu/legal-content/EN/ALL/?uri=CELEX:32002L0049

EU commission, Directive 2015/996 of 16 May 2015. Estiablishing common noise assessment methods acoording to Directive 2002/49/EC of the European Parliament and the Council.

Feng, Yu, et al. "Ozone concentration forecast method based on genetic algorithm optimized back propagation neural networks and support vector machine data classification." Atmospheric Environment 45.11 (2011): 1979-1985.

Fontaras G, Franco V, Dilara P, Martini G, Manfredi U. Development and review of Euro 5 passenger car emission factors based on experimental results over various driving cycles. Science of the Total Environment 2014; 468: 1034-1042.

Foraster M. Is it traffic-related air pollution or road traffic noise, or both? Key questions not yet settled! International Journal of Public Health 2013; 58: 647-648.

Foraster M, Deltell A, Basagana X, Medina-Ramon M, Aguilera I, Bouso L, et al. Local determinants of road traffic noise levels versus determinants of air pollution levels in a Mediterranean city. Environmental Research 2011; 111: 177-183.

Fyhri A, Klaeboe R. Road traffic noise, sensitivity, annoyance and self-reported health-A structural equation model exercise. Environment International 2009; 35: 91-97.

Gallimore JM, Brown BB, Werner CM. Walking routes to school in new urban and suburban neighborhoods: An environmental walkability analysis of blocks and routes. Journal of Environmental Psychology 2011; 31: 184-191.

Gan WQ, Davies HW, Koehoorn M, Brauer M. Association of Long-term Exposure to Community Noise and Traffic-related Air Pollution With Coronary Heart Disease Mortality. American Journal of Epidemiology 2012; 175: 898-906.

Gan WQ, Koehoorn M, Davies HW, Demers PA, Tamburic L, Brauer M. Long-Term Exposure to Traffic-Related Air Pollution and the Risk of Coronary Heart Disease Hospitalization and Mortality. Environmental Health Perspectives 2011; 119: 501-507.

Gerlofs-Nijland, Miriam E., et al. "Toxicity of coarse and fine particulate matter from sites with contrasting traffic profiles." Inhalation toxicology 19.13 (2007): 1055-1069.

Guite HF, Clark C, Ackrill G. The impact of the physical and urban environment on mental well-being. Public Health 2006; 120: 1117-1126.

Haines, Andy, et al. "Climate change and human health: impacts, vulnerability and public health." Public health 120.7 (2006): 585-596.

Hankey S, Marshall J, Brauer M, Frank L. Within-city Variation in Exposures to Air Pollution and Physical Inactivity. Epidemiology 2011; 22: S77-S77.

Hankey S, Marshall JD, Brauer M. Health Impacts of the Built Environment: Within-Urban Variability in Physical Inactivity, Air Pollution, and Ischemic Heart Disease Mortality. Environmental Health Perspectives 2012; 120: 247-253.

Hannam K, McNamee R, De Vocht F, Baker P, Sibley C, Agius R. A comparison of population air pollution exposure estimation techniques with personal exposure estimates in a pregnant cohort. Environmental Science-Processes & Impacts 2013; 15: 1562-1572.

Hansson E, Mattisson K, Bjork J, Ostergren PO, Jakobsson K. Relationship between commuting and health outcomes in a crosssectional population survey in southern Sweden. Bmc Public Health 2011; 11.

Hao JY, Hatzopoulou M, Miller EJ. Integrating an Activity-Based Travel Demand Model with Dynamic Traffic Assignment and Emission Models Implementation in the Greater Toronto, Canada, Area. Transportation Research Record 2010: 1-13.

Hatzopoulou M, Miller EJ. Linking an activity-based travel demand model with traffic emission and dispersion models: Transport's contribution to air pollution in Toronto. Transportation Research Part D-Transport and Environment 2010; 15: 315-325.

Hausberger, Fuel consumption and emissions of modern passenger cars. University of Technology Graz, Institute for internal combustion engines and thermodynamics report Nr. I-25/10 Haus-Em 07/10/676 (2010)

Heimann D, Schafer K, Emeis S, Suppan P, Obleitner F, Uhrner U. Combined evaluations of meteorological parameters, traffic noise and air pollution in an Alpine valley. Meteorologische Zeitschrift 2010; 19: 47-61.

Hoek G, Beelen R, de Hoogh K, Vienneau D, Gulliver J, Fischer P, et al. A review of land-use regression models to assess spatial variation of outdoor air pollution. Atmospheric Environment 2008; 42: 7561-7578.

Hoek G, Kos G, Beelen R, Dijkema M, de Hartog J, Brunekreef B, et al. A Land Use Regression Model for Ultrafine Particles in Amsterdam. Epidemiology 2009; 20.

Holden, 2007, Achieving sustainable mobility: everyday and leisure-time travel in the EU. ISBN-13: 978-0-7546-4941-0.

Hu SS, Fruin S, Kozawa K, Mara S, Paulson SE, Winer AM. A wide area of air pollutant impact downwind of a freeway during pre-sunrise hours. Atmospheric Environment 2009; 43: 2541-2549.

ICRP, Human Respiratory Tract Model for Radiological Protection. International Commission on Radiological Protection (ICRP), Publication 66, Elsevier Science, Oxford, U.K, 1994.

Int Panis, L.; de Geus, B.; Vandenbulcke, G.; Willems, H.; Degraeuwe, B.; Bleux, N.; Mishra, V.; Thomas, I.; Meeusen, R., Exposure to particulate matter in traffic: A comparison of cyclists and car passengers. Atmospheric Environment 2010, 44, (19), 2263-2270.

Int Panis, Luc. "Cycling: health benefits and risks." Environmental health perspectives 119.3 (2011): A114.

Jacobs, Lotte, et al. "Subclinical responses in healthy cyclists briefly exposed to traffic-related air pollution: an intervention study." Environmental Health 9.1 (2010): 64.

Janssen NAH, Brunekreef B, van Vliet P, Aarts F, Meliefste K, Harssema H, et al. The relationship between air pollution from heavy traffic and allergic sensitization, bronchial hyperresponsiveness, and respiratory symptoms in Dutch schoolchildren. Environmental Health Perspectives 2003; 111: 1512-1518.

Janssen NAH, Hoek G, Simic-Lawson M, Fischer P, van Bree L, ten Brink H, et al. Black Carbon as an Additional Indicator of the Adverse Health Effects of Airborne Particles Compared with PM_{10} and $PM_{2.5}$. Environmental Health Perspectives 2011; 119: 1691-1699.

Janssen NAH, Lanki T, Hoek G, Vallius M, de Hartog JJ, Van Grieken R, et al. Associations between ambient, personal, and indoor exposure to fine particulate matter constituents in Dutch and Finnish panels of cardiovascular patients. Occupational and Environmental Medicine 2005; 62: 868-877.

Janssen, N. A., Gerlofs-Nijland, M. E., Lanki, T., Salonen, R. O., Cassee, F., Hoek, G., ... & Krzyzanowski, M. (2012). Health effects of black carbon (pp. 1-86). Copenhagen: WHO Regional Office for Europe.

Jensen SS, Berkowicz R, Hansen HS, Hertel O. A Danish decision-support GIS tool for management of urban air quality and human exposures. Transportation Research Part D-Transport and Environment 2001; 6: 229-241.

Jerrett M, Shankardas K, Berhane K, Gauderman WJ, Kunzli N, Avol E, et al. Traffic-related air pollution and asthma onset in children: A prospective cohort study with individual exposure measurement. Environmental Health Perspectives 2008; 116: 1433-1438.

Johns, Douglas O., et al. "Practical advancement of multipollutant scientific and risk assessment approaches for ambient air pollution." Environmental health perspectives 120.9 (2012): 1238.

Kaelsch H, Hennig F, Moebus S, Moehlenkamp S, Dragano N, Jakobs H, et al. Are air pollution and traffic noise independently associated with atherosclerosis: the Heinz Nixdorf Recall Study. European Heart Journal 2014; 35: 853-860.

Karner AA, Eisinger DS, Niemeier DA. Near-Roadway Air Quality: Synthesizing the Findings from Real-World Data. Environmental Science & Technology 2010; 44: 5334-5344.

Stylianos Kephalopoulos, Marco Paviotti, Fabienne Anfosso-Lédée (2012),Common Noise Assessment Methods in Europe (CNOSSOS-EU),EUR 25379 EN. Luxembourg, Publications Office of the European

Union, 2012, 180 pp.,European Commission Joint Research Centre, Institute for Health and Consumer Protection, TP 281, 21027 - Ispra (VA), Italy

Keuken M, Zandveld P, van den Elshout S, Janssen NAH, Hoek G. Air quality and health impact of PM(10) and EC in the city of Rotterdam, the Netherlands in 1985-2008. Atmospheric Environment 2011; 45: 5294-5301.

Kjellberg A, Landstrom U, Tesarz M, Soderberg L, Akerlund E. The effects of nonphysical noise characteristics, ongoing task and noise sensitivity on annoyance and distraction due to noise at work. Journal of Environmental Psychology 1996; 16: 123-136.

Klaeboe R, Kolbenstvedt M, Clench-Aas J, Bartonova A. Oslo traffic study - part 1: an integrated approach to assess the combined effects of noise and air pollution on annoyance. Atmospheric Environment 2000; 34: 4727-4736.

Knibbs LD, Cole-Hunter T, Morawska L. A review of commuter exposure to ultrafine particles and its health effects. Atmospheric Environment 2011; 45: 2611-2622.

Kornov L. Strategic Environmental Assessment as catalyst of healthier spatial planning: The Danish guidance and practice. Environmental Impact Assessment Review 2009; 29: 60-65.

Kovac D. Quality of life - a pressing challenge for science of the new millennium. Ceskoslovenska Psychologie 2001; 45: 34-44.

Kurra S, Morimoto M, Maekawa ZI. Transportation noise annoyance - A simulated-environment study for road, railway and aircraft noises, part 2: Activity disturbance and combined results. Journal of Sound and Vibration 1999; 220: 279-295.

Langrish, Jeremy P., et al. "Beneficial cardiovascular effects of reducing exposure to particulate air pollution with a simple facemask." Part Fibre Toxicol 6.8 (2009): 10-1186.

Langrish, Jeremy P., et al. "Reducing personal exposure to particulate air pollution improves cardiovascular health in patients with coronary heart disease." Environmental health perspectives 120.3 (2012): 367-372.

Laumbach RJ, Kipen HM. Respiratory health effects of air pollution: Update on biomass smoke and traffic pollution. Journal of Allergy and Clinical Immunology 2012; 129: 3-13.

Leslie E, Cerin E. Are perceptions of the local environment related to neighbourhood satisfaction and mental health in adults? Preventive Medicine 2008; 47: 273-278.

Leslie E, Saelens B, Frank L, Owen N, Bauman A, Coffee N, et al. Residents' perceptions of walkability attributes in objectively different neighbourhoods: a pilot study. Health & Place 2005; 11: 227-236.

Lee E.S. & Zhu Y. 2014. Application of a High-Efficiency Cabin Air Filter for Simultaneous Mitigation of Ultrafine Particle and Carbon Dioxide Exposures Inside Passenger Vehicles. Environmental Science & Technology, 48, 2328-2335.

Li LF, Wu J, Hudda N, Sioutas C, Fruin SA, Delfino RJ. Modeling the Concentrations of On-Road Air Pollutants in Southern California. Environmental Science & Technology 2013; 47: 9291-9299.

Lin HZ, Lo HP. ACTIVITY-TRAVEL-BASED LIFESTYLE CLASSIFICATION, 2007.

Lin HZ, Lo HP, Chen XJ. Lifestyle classifications with and without activity-travel patterns. Transportation Research Part a-Policy and Practice 2009; 43: 626-638.

Lioy PJ. Exposure Science: A View of the Past and Milestones for the Future. Environmental Health Perspectives 2010; 118: 1081-1090.

Lioy PJ, Smith KR. A Discussion of Exposure Science in the 21st Century: A Vision and a Strategy. Environmental Health Perspectives 2013; 121: 405-409.

Marshall JD, Brauer M, Frank LD. Healthy Neighborhoods: Walkability and Air Pollution. Environmental Health Perspectives 2009; 117: 1752-1759.

Marshall JD, Granvold PW, Hoats AS, McKone TE, Deakin E, Nazaroff WW. Inhalation intake of ambient air pollution in California's South Coast Air Basin. Atmospheric Environment 2006; 40: 4381-4392.

Marshall JD, Nethery E, Brauer M. Within-urban variability in ambient air pollution: Comparison of estimation methods. Atmospheric Environment 2008; 42: 1359-1369.

McCreanor J, Cullinan P, Nieuwenhuijsen MJ, Stewart-Evans J, Malliarou E, Jarup L, et al. Respiratory effects of exposure to diesel traffic in persons with asthma. New England Journal of Medicine 2007; 357: 2348-2358.

McMichael, Anthony J., Rosalie E. Woodruff, and Simon Hales. "Climate change and human health: present and future risks." The Lancet 367.9513 (2006): 859-869.

Michaud DS, Keith SE, McMurchy D. Annoyance and disturbance of daily activities from road traffic noise in Canada. Journal of the Acoustical Society of America 2008; 123: 784-792.

Miedema HME, Oudshoorn CGM. Annoyance from transportation noise: Relationships with exposure metrics DNL and DENL and their confidence intervals. Environmental Health Perspectives 2001; 109: 409-416.

Molitor J, Jerrett M, Chang C-C, Molitor N-T, Gauderman J, Berhane K, et al. Assessing uncertainty in spatial exposure models for air pollution health effects assessment. Environmental Health Perspectives 2007; 115: 1147-1153.

Morawska L, Ristovski Z, Jayaratne ER, Keogh DU, Ling X. Ambient nano and ultrafine particles from motor vehicle emissions: Characteristics, ambient processing and implications on human exposure. Atmospheric Environment 2008; 42: 8113-8138.

Mordukhovich, Irina, et al. "Black carbon exposure, oxidative stress genes, and blood pressure in a repeated-measures study." (2009).

Moro M, Brereton F, Ferreira S, Clinch JP. Ranking quality of life using subjective well-being data. Ecological Economics 2008; 65: 448-460.

Moser G, Robin M. Environmental annoyances: an urban-specific threat to quality of life? European Review of Applied Psychology-Revue Europeenne De Psychologie Appliquee 2006; 56: 35-41.

Moustris, Konstantinos P., Ioannis C. Ziomas, and Athanasios G. Paliatsos. "3-Day-ahead forecasting of regional pollution index for the pollutants NO2, CO, SO2, and O3 using artificial neural networks in Athens, Greece." Water, Air, & Soil Pollution 209.1-4 (2010): 29-43.

Nivison ME, Endresen IM. AN ANALYSIS OF RELATIONSHIPS AMONG ENVIRONMENTAL NOISE, ANNOYANCE AND SENSITIVITY TO NOISE, AND THE CONSEQUENCES FOR HEALTH AND SLEEP. Journal of Behavioral Medicine 1993; 16: 257-276.

Oberdörster, Günter. "Pulmonary effects of inhaled ultrafine particles." International archives of occupational and environmental health 74.1 (2000): 1-8.

OECD, 2004, “The OECD-JRC Handbook on Practices for Developing Composite Indicators”, paper presented at the OECD Committee on Statistics, 7-8 June 2004, OECD, Paris.

Oglesby L, Rotko T, Krutli P, Boudet C, Kruize H, Jantunen MJ, et al. Personal exposure assessment studies may suffer from exposure-relevant selection bias. Journal of Exposure Analysis and Environmental Epidemiology 2000; 10: 251-266.

Ohrstrom E. Longitudinal surveys on effects of changes in road traffic noise - annoyance, activity disturbances, and psycho-social well-being. Journal of the Acoustical Society of America 2004; 115: 719-729.

Padro-Martinez LT, Patton AP, Trull JB, Zamore W, Brugge D, Durant JL. Mobile monitoring of particle number concentration and other traffic-related air pollutants in a near-highway neighborhood over the course of a year. Atmospheric Environment 2012; 61: 253-264.

Panis LI, de Geus B, Vandenbulcke G, Willems H, Degraeuwe B, Bleux N, et al. Exposure to particulate matter in traffic: A comparison of cyclists and car passengers. Atmospheric Environment 2010; 44: 2263-2270.

Parks, A. Kearns, R. Atkinson, What makes people dissatisfied with their neighbourhoods?, in: Urban Studies, Vol. 39, No. 13, 2002, p. 2413-2438

Pattinson, Woodrow. "Cyclist exposure to traffic pollution: microscale variance, the impact of route choice and comparisons to other modal choices in two New Zealand cities." (2009).

Rojas-Rueda D, de Nazelle A, Tainio M, Nieuwenhuijsen MJ. The health risks and benefits of cycling in urban environments compared with car use: health impact assessment study. British Medical Journal 2011; 343.

Roswall, N., Høgh, V., Envold-Bidstrup, P., Raaschou-Nielsen, O., Ketzel, M., Overvad, K., ... & Sørensen, M. (2014). Residential Exposure to Traffic Noise and Health-Related Quality of Life—A Population-Based Study. PloS one, 10(3).

Rothen-Rutishauser, Barbara M., Stephen G. Kiama, and Peter Gehr. "A three-dimensional cellular model of the human respiratory tract to study the interaction with particles." American journal of respiratory cell and molecular biology 32.4 (2005): 281-289.

Rundle AG, Bader MDM, Richards CA, Neckerman KM, Teitler JO. Using Google Street View to Audit Neighborhood Environments. American Journal of Preventive Medicine 2011; 40: 94-100.

Sabaliauskas K, Jeong C-H, Yao X, Jun Y-S, Jadidian P, Evans GJ. Five-year roadside measurements of ultrafine particles in a major Canadian city. Atmospheric Environment 2012; 49: 245-256.

Schimmack U, Schupp J, Wagner GG. The influence of environment and personality on the affective and cognitive component of subjective well-being. Social Indicators Research 2008; 89: 41-60.

Schlesinger, Richard B., and Flemming Cassee. "Atmospheric secondary inorganic particulate matter: the toxicological perspective as a basis for health effects risk assessment." Inhalation toxicology 15.3 (2003): 197-235.

Schreckenberg D, Griefahn B, Meis M. The associations between noise sensitivity, reported physical and mental health, perceived environmental quality, and noise annoyance. Noise & Health 2010; 12: 7-16.

Setton E, Marshall JD, Brauer M, Lundquist KR, Hystad P, Keller P, et al. The impact of daily mobility on exposure to traffic-related air pollution and health effect estimates. Journal of Exposure Science and Environmental Epidemiology 2011; 21: 42-48.

Shen L, Kyllo JM, Guo XL. An Integrated Model Based on a Hierarchical Indices System for Monitoring and Evaluating Urban Sustainability. Sustainability 2013; 5: 524-559.

Shepherd D, Welch D, Dirks KN, Mathews R. Exploring the Relationship between Noise Sensitivity, Annoyance and Health-Related Quality of Life in a Sample of Adults Exposed to Environmental Noise. International Journal of Environmental Research and Public Health 2010; 7: 3579-3594.

Shepherd D, Welch D, Dirks KN, McBride D. Do Quiet Areas Afford Greater Health-Related Quality of Life than Noisy Areas? International Journal of Environmental Research and Public Health 2013; 10: 1284-1303.

Sirgy MJ, Widgery RN, Lee DJ, Yu GB. Developing a Measure of Community Well-Being Based on Perceptions of Impact in Various Life Domains. Social Indicators Research 2010; 96: 295-311.

Smyth R, Nielsen I, Zhai QG, Liu TM, Liu Y, Tang CY, et al. A study of the impact of environmental surroundings on personal well-being in urban China using a multi-item well-being indicator. Population and Environment 2011; 32: 353-375.

Staniswalis, Joan G., et al. "Temporal analysis of airborne particulate matter reveals a dose-rate effect on mortality in El Paso: indications of differential toxicity for different particle mixtures." Journal of the Air & Waste Management Association 55.7 (2005): 893-902.

Steerenberg PA, Withagen CET, van Dalen WJ, Dormans J, Heisterkamp SH, van Loveren H, et al. Dose dependency of adjuvant activity of particulate matter from five European sites in three seasons in an ovalbumin-mouse model. Inhalation Toxicology 2005; 17: 133-145.

Steinle S, Reis S, Sabel CE. Quantifying human exposure to air pollution-Moving from static monitoring to spatio-temporally resolved personal exposure assessment. Science of the Total Environment 2013; 443: 184-193.

Strak, M. M., et al. "Respiratory health effects of airborne particulate matter: the role of particle size, composition, and oxidative potential-the RAPTES project." Environmental health perspectives 120.8 (2012): 1183-1189.

Suh H, Zanobetti A. Impact of exposure error on the relationship between traffic-related air pollution and heart rate variability (HRV). Epidemiology 2006; 17: S213-S213.

Suh HH, Zanobetti A. Exposure Error Masks the Relationship Between Traffic-Related Air Pollution and Heart Rate Variability. Journal of Occupational and Environmental Medicine 2010; 52: 685-692.

Terzano C, Di Stefano F, Conti V, Graziani E, Petroianni A. Air pollution ultrafine particles: toxicity beyond the lung. European Review for Medical and Pharmacological Sciences 2010; 14: 809-821.

Tetreault LF, Perron S, Smargiassi A. Cardiovascular health, traffic-related air pollution and noise: are associations mutually confounded? A systematic review. International Journal of Public Health 2013; 58: 649-666.

Totlandsdal AI, Fudge N, Sanderson EG, van Bree L, Brunekreef B. Strengthening the science-policy interface: experiences from a European Thematic Network on Air Pollution and Health (AIRNET). Environmental Science & Policy 2007a; 10: 260-266.

Totlandsdal AI, Fudge N, Sanderson EG, van Bree L, Brunekreef B. Strengthening the science-policy interface: experiences from a European Thematic Network on Air Pollution and Health (AIRNET). Environmental Science & Policy 2007b; 10: 260-266.

United Nations, 2007, Glossary of Environment Statistics, Studies in Methods, Series F, No. 67, New York)

Van Poppel M, Panis LI, Govarts E, Van Houtte J, Maenhaut W. A comparative study of traffic related air pollution next to a motorway flyover. Atmospheric Environment 2012; 60: 132-141.

Warburton DER, Nicol CW, Bredin SSD. Health benefits of physical activity: the evidence. Canadian Medical Association Journal 2006; 174: 801-809.

Welch D, Shepherd D, Dirks KN, McBride D, Marsh S. Road traffic noise and health-related quality of life: A crosssectional study. Noise & Health 2013; 15: 224-230.

WHO, 2000, Carlos Corvalán, David Briggs, David John Briggs, Gerhard Zielhuis , Decision-making in Environmental Health: From Evidence to Action.

Wood, Simon N. "Stable and efficient multiple smoothing parameter estimation for generalized additive models." Journal of the American Statistical Association 99.467 (2004).

Wood, S. N., On confidence intervals for generalized additive models based on penalized regression splines. Australian & New Zealand Journal of Statistics 2006, 48, (4).

Xia, Tian, et al. "Quinones and aromatic chemical compounds in particulate matter induce mitochondrial dysfunction: implications for ultrafine particle toxicity." Environmental health perspectives (2004): 1347-1358.

Zhu, Yifang, et al. "In-cabin commuter exposure to ultrafine particles on Los Angeles freeways." *Environmental science & technology* 41.7 (2007): 2138-2145

Zuurbier M, Hoek G, Oldenwening M, Lenters V, Meliefste K, van den Haze P, et al. Commuters' Exposure to Particulate Matter Air Pollution Is Affected by Mode of Transport, Fuel Type, and Route. Environmental Health Perspectives 2010; 118: 783-789.

Zuurbier M, Hoek G, Oldenwening M, Meliefste K, Van den Hazel P, Brunekreef B. Acute Health Effects of Commuters' Exposure to Air Pollution. Epidemiology 2009; 20: S197-S197.

Zuurbier M, Hoek G, Oldenwening M, Meliefste K, van den Hazel P, Brunekreef B. Respiratory Effects of Commuters' Exposure to Air Pollution in Traffic. Epidemiology 2011; 22: 219-227.

Chapter 2 Person based evaluation of quality of life, exposure to noise and air pollution

2.1 Introduction

This chapter describes the analysis and development the person-based approach to investigate the quality of life and air pollution exposure. A unique model evaluates the traffic related component of the Quality of Life (QoL). In the transport research field, this is also referred to as 'Traffic Liveability'. Sixteen indicators are calculated for a virtual population including a simulated behavioural mobility pattern. The indicators are not only evaluated at the dwelling but when relevant also at the destinations and along the travelled routes. Aggregating the sixteen indicators to the top-level 'Traffic liveability index' (TLI) gets special attention and is an example of a composite indicator as introduced in 1.1.1.1. The methodology of the QoL model is summarized in 2.2; the results are presented in chapter 3.

The implementation is extended to process personal time activity patterns, on-person measurements and more complex indicators. In this generalized workflow, the indicators are not predefined but become a flexible component to resolve customized research questions. The extended functionality is mapped to the vison and strategy of Lioy and Smith (Lioy and Smith, 2013) and the 'eDPSEEA' model presented by Reis (Reis et al., 2013) as introduced in 1.1.2.

2.2 Traffic Liveability and Quality of Life model

This work was performed in collaboration of the IDM (Instituut voor Duurzame mobiliteit, institute for sustainable mobility, www.idm.ugent.be). This section is a compilation of different publications and reports available in the publication list (see 1.2.4). The relevant publications are authored or co-authored by Dominique Gillis.

2.2.1 Introduction

Quality of Life (QoL) is a research domain attempting to quantify the well-being of a population. QoL is typically investigated by using surveys on large samples of the population. A major component of the QoL relates to the impact of the environment on our well-being and health. When quality of life is narrowed down to traffic related burdens, it is typically referred to as 'Traffic Liveability'.

In the current standardized approaches, traffic liveability is evaluated on the traffic parameters near the dwelling or the living street of the subjects. In section 1.1.1.2, the state-of-the-art is already summarized. Within a project funded by the Flemish Government the traffic liveability is extended to including all aspects of traffic, not only the aspects near the dwelling but also along the travelled trajectories. Traffic Liveability (TL) also includes positive aspects since mobility is not only a burden but also fulfils needs like reachability of different functions in daily life (work, school, shops, family, etc…). This extension leads to the need to evaluate the full diurnal pattern. It has to include evaluation at home, along the travelled roads and at the destinations.

The well-being of a population is the sum of the well-being of its individuals each with their specific combination of dwelling location, travelled routes, modal choices (car, bike, public transport etc...) and the destinations (schools, workplaces, shops, recreational activities etc.). In an expert meeting, joining knowledge on mobility, traffic liveability and the different traffic related health effect paths, a layered set of indicators were defined (Figure 2.2.1) (Dekoninck et al., 2010).

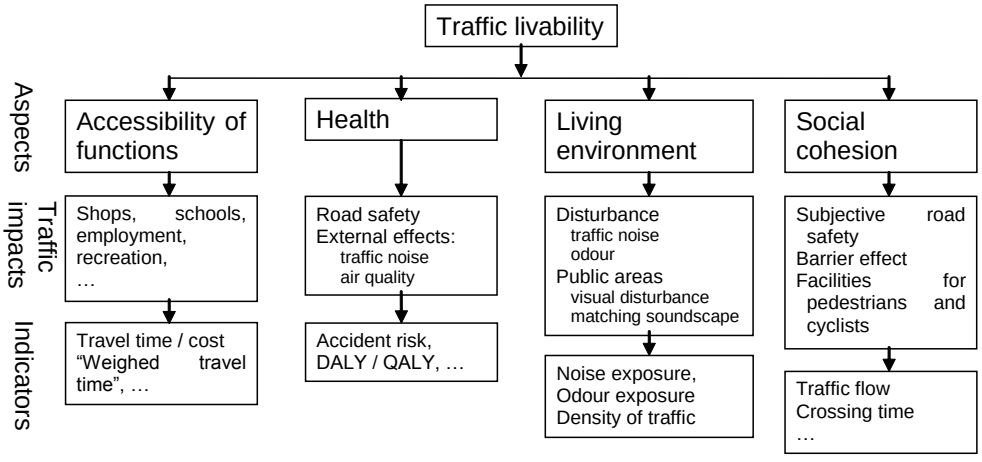

Figure 2.2.1: Definition of traffic liveability, containing several types of traffic impacts, each with their own indicators.

To be able to predict the quality of life for a full population and to be able to predict changes in the quality of life for different scenarios, a mathematical model mimics the responses of the public to their perception of the environment. In this specific application, the reference is a series of the Flemish quality of life surveys, repeated every five years (SLO-0, SLO-1 and SLO-2). The surveys contain questions related to different aspects of environmental quality (noise, odour, light pollution, traffic, etc…) and include some general questions about well-being and appreciation of the environment.

2.2.2 Extending the dwelling based traffic liveability

The environmental quality of the living environment is mainly linked to the direct and indirect impact of mobility in the neighbourhood of the dwellings. In the Flemish mobility and urban planning policy, the term 'liveability' is used focusing on the living conditions of people's home location (Asperges, 1998). In literature the term is normally used in a more general sense, taking into account the social, economic and environmental circumstances in a certain city or area. 'Traffic liveability' is used to describe the impact of all types of traffic on the liveability at a specific location. Some methodologies were developed to allow an objective measurement of the traffic impact on quality of life (references in section 1.1.1.2). Typically, these methods are based on very local road characteristics, such as the road width, traffic amounts and speeds, the presence of facilities for pedestrians and cyclists, etc. The liveability at a certain address is expressed as a function of the characteristics of the road section in front of the house.

This is a very narrow interpretation of traffic liveability. First of all, this presumes that quality of life is very locally determined by the location and situation of the house. This is contradictory to elementary planning theories, such as by Klaeboe (2007) or Appleyard (1981), both stating that quality of life is determined by the living neighbourhood, rather than only by the dwelling location. People judge their living quality during a vast set of activities, some taking place at home, some taking place at other locations (office, shop, sports centre …). We propose to extend 'liveability' over the locations of all the activities, including the trips to reach these places, taking the approach of Klaeboe and Appleyard one step further. A second limitation of the current methodologies is that they ignore the importance of networks in traffic planning (see 2.2.4).

An alternative methodology was developed for an objective measurement of the *impact of mobility on quality of the life* (Dekoninck et al., 2009, Dekoninck et al., 2011). Compared to the current practice, this new methodology aims at the following:

- The traffic liveability takes in account the pros and cons of traffic. We need the mobility to satisfy our needs, but traffic creates disturbance and pollution for all people in the larger area.

- The evaluation is not performed for the average person, but includes the individual needs and travel patterns, sampled from a household trip database with personal characteristics, representing the large diversity of the mobility needs. The methodology should reflect a daily activity pattern, including the travelled routes and destinations. The traffic liveability of a specific household in a specific area will reflect on the full extent of their needs at home, during the trips and at the destinations.
- Traffic liveability itself is measured by means of a broad set of indicators, representing different types of exposure and/or traffic impacts. Each individual indicator can express a non-linear effect. The separate indicators are combined into an aggregated traffic liveability.
- The application has to be able to calculate scenarios to evaluate changes in the population behaviour and changes in the driving forces. Changes in driving forces which affect multiple indicators will reflect the combined and secondary effects along the multi-level indicator aggregation steps.

2.2.3 Unravelling Quality of life

Based on a review of recent literature and with Maslow's pyramid in mind (Maslow, 1943), the 'traffic liveability' was unravelled into its separate components. In order to have enjoyable living conditions, people need access to some basic functions in the neighbourhood, need healthy living conditions, and an attractive environment (Lercher, 2003). The environment should stimulate the deployment of a social network. Noise and air pollution have effects both on the health conditions and on the attractiveness of the environment.

These aspects are focused towards 'traffic liveability' by restricting them into their purely traffic-related aspects. For example, from a traffic point of view, it is not sufficient to have the basic functions available, but it is necessary to have a fast, attractive and safe access to these basic functions. In this way, the above aspects of liveability are translated into six components of traffic liveability: accessibility of basic functions, traffic safety, external effects of traffic, disturbance of the surrounding functions, appreciation of public domain and social contact (Dekoninck et al., 2010, Dekoninck et al., 2011, Gillis et al., 2011).

For each of those aspects indicators can be designed that allow an objective measurement. Among the indicators are some commonly accepted evaluations like Number of Highly Annoyed Inhabitants (for noise). For some indicators, a modified or new dose-effect relation has to be formulated, awaiting more reviewed evaluations (e.g. availability of parking spaces, on road exposure to air pollution while cycling, etc.).

As a result, the term "traffic liveability" can be defined by means of a tree, representing the breakdown into its different aspects, the different traffic impacts, and the possible indi-

cators as show in Figure 2.2.3. The bottom arrows show which indicators are sensitive to on-road evaluation.

The weight of the different branches in the global traffic liveability is derived from the Liveability Survey (Schriftelijk Leefbaarheidsonderzoek – Flemish Government, LNE), which is executed by the Flemish Government every three years. The survey asks about the satisfaction of people about their living neighbourhood, and asks if people would recommend friends to live in this area, followed by an open question about reason why (not). The answers to this last open question were grouped according to the main aspects of traffic liveability, and were analysed to determine which aspects influence the appreciation in a positive or negative way.

Figure 2.2.2 shows the correlation between the (dis)satisfaction about the living environment and the appreciation of the several aspects of traffic liveability. The graph shows that noise disturbance and traffic bustle show the strongest correlation, both in a positive as in a negative direction. Both have a strong impact on the negative perception of a neighbourhood, while the absence of traffic noise and traffic bustle are strong assets for the neighbourhood. In addition, subjective safety has a strong impact, but mostly in the negative sense: a safe feeling is considered a normal characteristic for the living area.

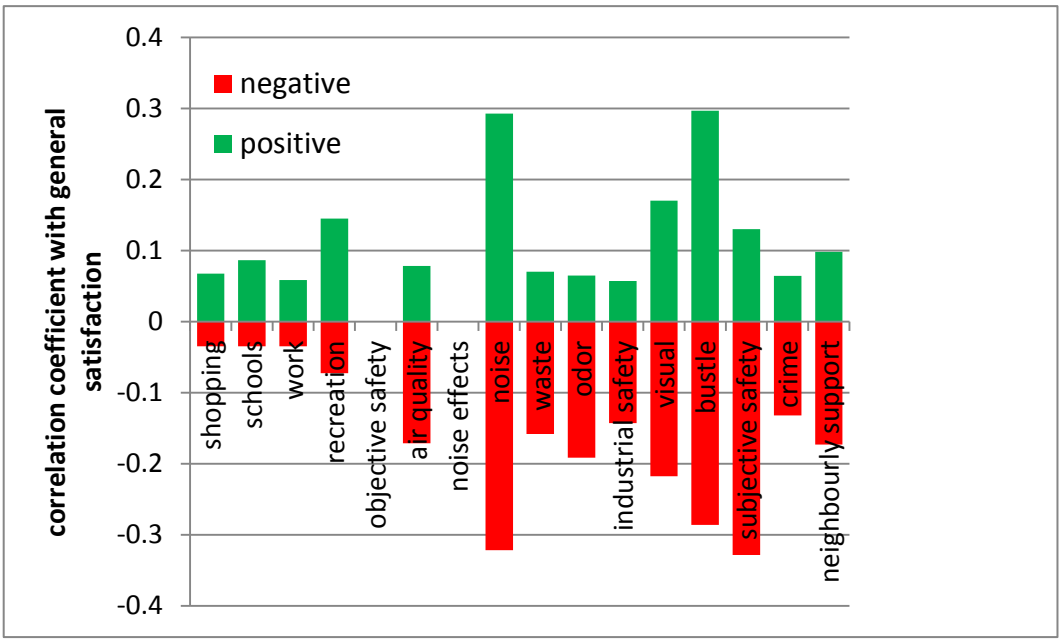

Figure 2.2.2: Correlation between the general satisfaction about the living neighbourhood and the aspects of traffic liveability.

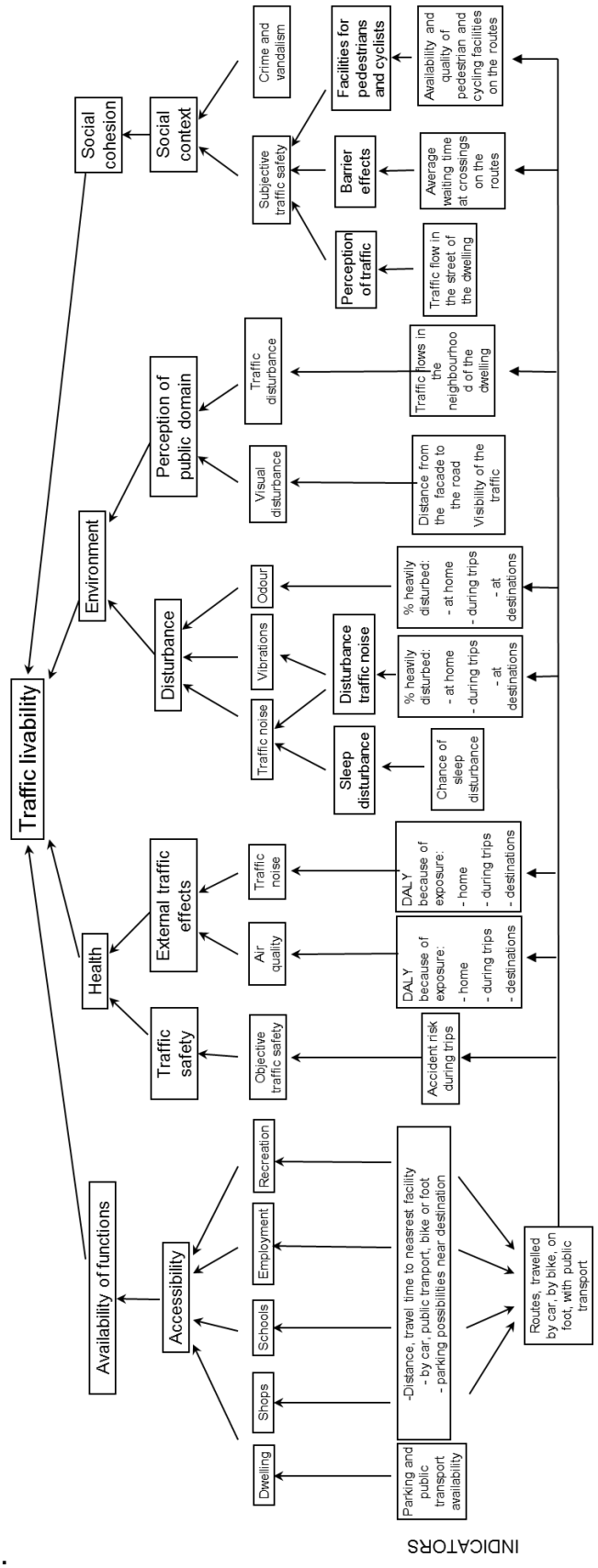

Figure 2.2.3: The term 'traffic liveability' unravelled into its aspects and matching indicators. The bottom arrows show which indicators are sensitive to on-road evaluation.

2.2.4 Innovating the exposure simulation

Looking at the collected indicators of traffic liveability, the conclusion is that a lot of them are network characteristics, rather than local point or road characteristics. Traffic noise and traffic emissions are spatially distributed impacts, affecting also houses in nearby streets. Traffic congestion or road unsafety affect not only people living at this location, but also harms all people using this road for their transportation needs. For this reason, these aspects should be measured as a spatial attribute for the larger neighbourhood, instead of restricting the evaluation to the road section near to the home address, as is the current practice in existing methodologies.

Therefore, a new evaluation methodology was developed, aiming at a more realistic representation of the individual living pattern, of which only a part takes place at home. By incorporating also the activities at other locations, and even the trips to these locations, a better estimation of the living quality is obtained.

This is achieved by simulating the individual trip behaviour, based on the regional trip diary survey (Onderzoek Verplaatsingsgedrag), a large-scale trip survey covering over 5.000 households in the whole of Flanders. This survey collected a large database of individual trip patterns per person during two days. In order to evaluate the quality of the living environment on a certain home address, a random household is chosen from the database (taking into account some of the location characteristics, such as the distance to the nearest bus stop or train station), with the unique travel pattern of all its members.

For each single trip, a logical trip destination is chosen from a database of available destinations (e.g. the nearest school for school trips, the shopping centre for shopping trips …). Using a traffic model, the best transport mode and route from the home address to this destination is calculated (Dekoninck et al., 2009). This results in a set of routes that is representative for the daily trips to and from the house for all the members of the household, for all purposes and all transportation modes (Figure 2.2.4).

With this set of routes, the quality of the living environment for this address is evaluated. The indicators are evaluated not only at the home address, but also on the different routes to and from home, and on the destination locations. This means that the traffic liveability will get a negative impact if for example; traffic safety is bad on the surrounding roads, if bicycle or walking trips leave the home via noisy routes, or if activities take place in bad conditions, (e.g. schools or sports facilities with high noise levels or air pollution levels).

By sampling a sufficient number of households within a certain street or neighbourhood, and aggregating the results, the global quality of the living environment in this area becomes available.

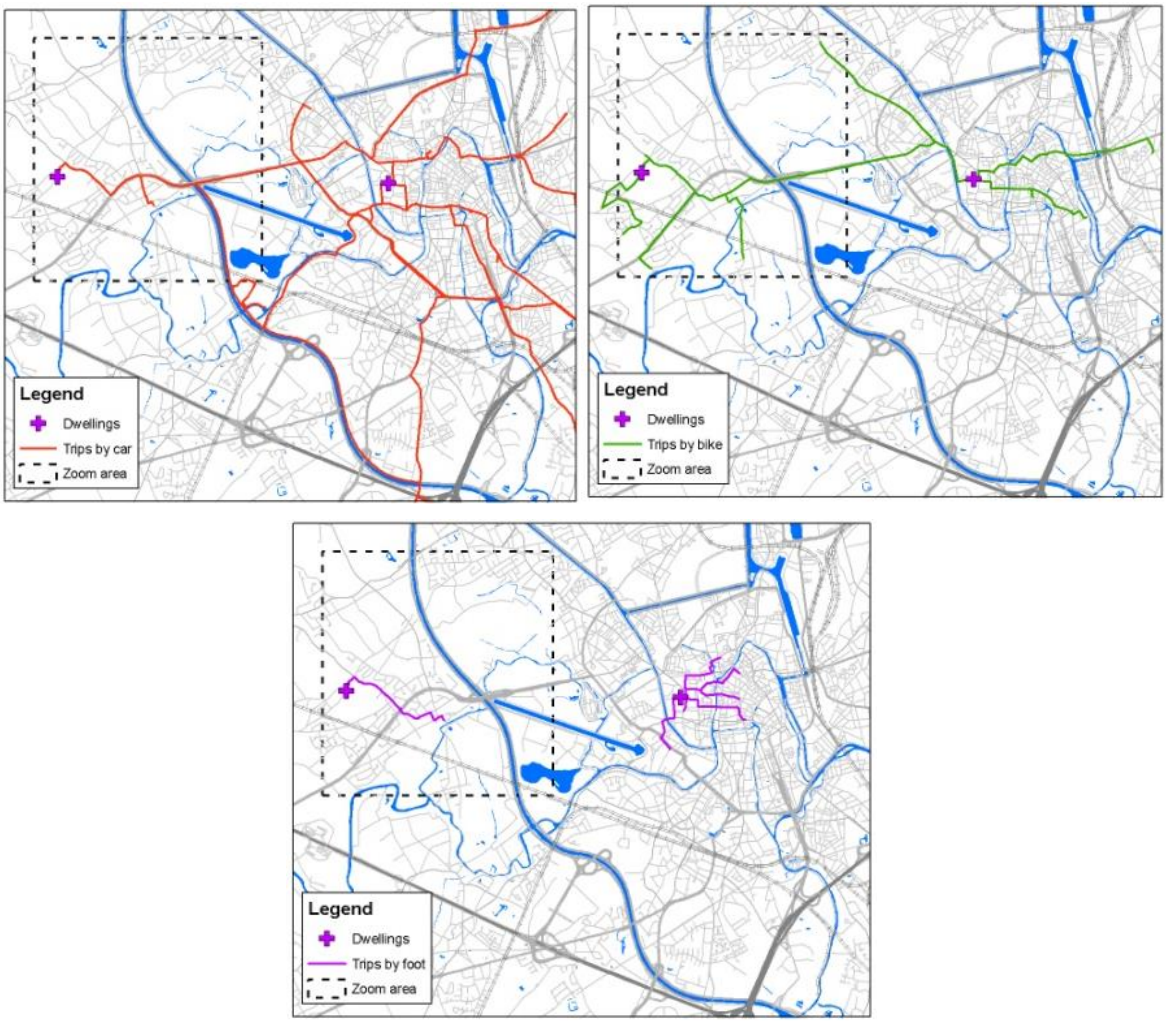

Figure 2.2.4: The calculated routes by the sampled households in two dwellings, including the trips by car (top left), by bike (top right) and on foot (bottom).

2.2.5 Technical model structure

The implementation of the exposure model relies on four major components: the GIS layers and input databases, the traffic model, the exposure simulation, and the indicator aggregation (Figure 2.2.5). The input components are the GIS layers containing attributes about the infrastructure, traffic, dwellings, points of interest, population density and databases containing demographic statistics (trip and time usage) (Dekoninck et al, 2009).

Based on the available trip statistics, the locations of dwellings and the distance to different commodities, a local origin-destination traffic demand matrix is compiled. A traffic model is used to calculate the transportation mode and the route for these trips. This model is also used to generate the overall traffic flows and traffic characteristics such as traffic speed and congestion, which are used to derive traffic noise levels and air pollution maps, evaluate safety risks, etc. The core of the method is the exposure evaluation. For each household included in the simulation, a trip pattern is sampled from the trip database and linked to suit-

able routes obtained from the traffic model. The resulting diurnal patterns are used to sample exposure to noise, air pollution, and safety risks from calculated maps. These maps mainly rely on traffic data generated by the local traffic behaviour. Trips also give information about the destination and thus exposure at the destination can be included if the destination falls within the scope of the study area.

The final component is the indicator aggregation. Two alternatives can be considered: Firstly, the different components of quality of the living environment (and quality of life by extension) can first be aggregated for every person in the sample individually. This approach has the huge advantage over existing techniques that it allows to accurately account for combined exposures. Secondly, aggregation can be performed at a population level for every component of the quality of the living environment to obtain a population averaged effect. With this order of aggregating, the model keeps its explanatory value: when certain measures or scenarios result in an improvement or reduction of the liveability, this change can be re-traced, in order to detect which aspects of liveability or which indicators cause these changes.

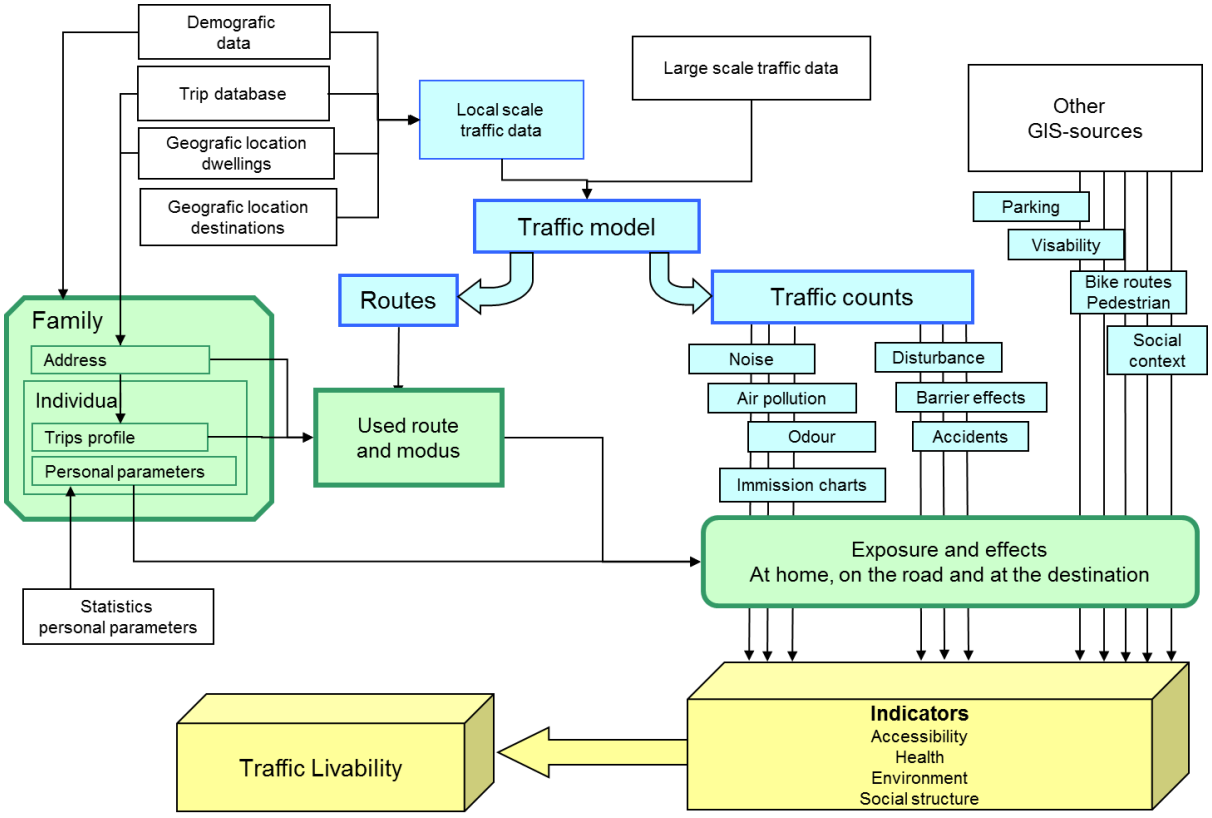

Figure 2.2.5: Building blocks of the implementation of the proposed model for traffic related aspects of the quality of the living environment. (White = input data, blue = traffic and GIS data, green = personal data, routes and evaluation, yellow = indicator evaluation and aggregation.

2.2.6 Aggregation scheme of the indicators

To be able to sum the different indicators, the indicator values are mapped to a standardize scale, arbitrarily chosen as a continuous variable between -2 and +2. For each of the indicators a reference framework is defined to decide how the physical value of the underlying indicator is mapped to the standardized continuous variable. The full set of indicators including the calculation method and the indicator conversion are available in Dutch in a detailed report for the Flemish Government (Dekoninck et al., 2011). Two branches of the aggregation scheme (Figure 2.2.3) are presented as examples of the technique: 'external traffic related health effects' and 'disturbance'.

The external traffic related health effects are evaluated through the concept of Disability Adjusted Life Years (DALYs) (Table 2.2-1). The environmental disturbance path is evaluated through a set of weighted noise annoyance and sleep disturbance functions and also includes an odor exposure pathway. The values in the tables map a specific result of the indicator to the standardized continuous variable. The chosen mapping is expert based but uses as much external global or local references as possible (WHO, Flemish environmental thresholds, etc.). Each individual pathway gets a relative weight within the evaluation branch. These weights are a combination of expert choices and weights derived from the appreciation of the aspects by the subjects in the questionnaire (see Figure 2.2.2).

	2	1	0	-1	-2
Effects of air pollution	**Thresholds**				
Health					
DALY	3‰	6‰	10‰	15‰	>10‰
Effects of noise	**Thresholds**				
Health					
DALY	1‰	2.5‰	5‰	10‰	>10‰

Table 2.2-1: Conversion and thresholds of the external traffic health effects for noise and air pollution.

	2	1	0	-1	-2	Weight
Disturbance by noise						
Noise annoyance by road traffic, % moderately of highly anno	10	20	30	50	>50	1
Noise annoyance by railway traffic, % moderately of highly an	5	7.5	10	15	>15	0.25
Sleep disturbance, LAmax, indoor	40	45	50	55	>55	1
Quiet Façade (deltaMaxMinFacade, Lday>55)	-10	-5	0	0	0	1
Disturbance by odour						
Exposure too odour by road traffic (ou/m3)	0.05	0.1	0.2	0.3	>0.3	1

Table 2.2-2: Conversion and thresholds of the disturbance indicator for traffic related exposure.

For the aggregation from the separate indicators to an appreciation of each aspect, and from the aspects to a global traffic liveability evaluation, a Choquet integration is applied (Botteldooren et al., 2006, Verkeyn et al., 2011, Dekoninck et al, 2011). This method makes a weighted sum, giving most weight to the strongest components. This simulates human evaluation, as one extreme (positive or negative) aspect will dominate the perception and will

rarely be compensated by one or more moderately good or bad aspects. This way, the model combines advantages from a weighted sum and a strongest component aggregation.

2.2.7 Population simulation

The quality of life model is assessed in case study for the city of Ghent, simulating 10,000 households in and around the city of Ghent (Dekoninck et al., 2011, Gillis et al., 2010, Gillis et al., 2011, Dekoninck et al, 2012)). The results of the traffic liveability model are summarized in Chapter 3.

2.3 Personal activity indicator framework

2.3.1 Introduction to 'exposome'

In recent literature, the investigation of the health effects due to multiple simultaneous exposures to environmental stressors is referred to as the 'eco-exposome': the sum of all environmental burdens where a person is exposed to and how to address, interpret and disentangle the health effects of the different stressors. This introduction extends on the information given in 1.1.2. Two recent publications originating from the NRC committee for exposure compile two sets of recommendations regarding the vision and strategy on the exposome (Lioy and Smith, 2013). The first set addresses the more general concerns on the highly multidisciplinary nature of the exposure field and expresses the need to align research from many different fields. It also reaches out to the policy domain. The research should result in better support of regulatory and societal challenges. The scientific efforts have to result in better human and ecosystem protection. The document emphasizes strongly the grey area and need for interaction between personal exposure, external dose, internal dose and toxicology pathways of the pollutants. The gathering of data in this field through participatory sensing campaigns and mobile measurements is expensive and requires a lot of technical support. However, even with larger population samples it will be difficult to achieve representative population samples. The difficulty to extrapolate the exposure measurements to representative populations for epidemiological research and governmental policy is recognized as the most important issue to be solved in the exposome research (Lioy and Smith, 2013).

The second set of recommendations the NRC committee sums up some more detailed concerns on the interactions between several components in the exposure data flow and it acknowledges the importance of personal time-activity patterns, activity related dose corrections, the potential effects of behavioural changes and several feedback mechanisms. The explicit inclusion of the upstream forcers is on the wish list as well.

In another recent review "Integrating health and environmental impact", a modified ecosystem enriched Drivers, Pressures, State, Exposure, Effects and Actions or 'eDPSEEA' model is proposed, addressing similar concerns due to the "continuing failure to truly integrate human health and environmental impact analysis..." (Reis et al., 2013). Many of the data flow properties of the eDPSEEA approach match the recommendations of the NRC committee documents, and it explicitly expresses the need to extend the conceptual models to include "an effective and robust science-policy interface". In a sense, the approach of the eDPSEEA model is a larger scale and economic indicators driven vision for environmental

evaluations and enhanced policy support, while the eco-exposome builds on the biomedical indicators, biomarkers and toxicological parameters, both are expressing the same concern.
Other reviews focus on the good practice for the actual personal exposure measurement campaigns that will feed the eco-exposome research. The personal exposure research field is performing mobile and/or participatory sensing measurement campaigns and several authors have discussed more specific requirements. A state of the art overview of current practice in participatory sensing measurements is presented by Steinle, evaluating numerous 'must-have' properties of the research setups (Steinle et al., 2013). One of the basic concepts is monitoring of specific microenvironments enabling detailed modelling of the microenvironment specific spatial and temporal variability. Other investigations rely on diaries and questionnaires. Recently some equipment became available to measure the actual exposure of the individuals and due to the availability of GPS and other location-aware technology; individuals can now be tracked to complement the diary registrations. The most cumbersome part of the personal monitoring is the cost of the equipment and high support cost for those personal exposure measurement campaigns. As mentioned before, due to the high costs it is very difficult to reach a representative sample of the population by actually measuring the personal exposure. In this section, the conceptual model for the quality of life dataflow framework will be extended for processing and analysing participatory sensing campaigns. The extended data flow framework will also attempt to include many of the general requirements listed by Lioy. A special effort will be made on extrapolating exposure measurement campaigns to representative populations. The eDPSEEA approach will be partially achieved since results will be driven by the population distribution of individual time-activity pattern as the driving force of the exposure of a population. The actions in the eDPSEEA scheme result in expected changes in the population behaviour. The indicators are evaluated for the new population and the results support the policy decisions. This functionality was already available in the QoL model.

The following functionalities should be available:

- Activity based evaluation with customizable activity parameters.
- Person data from any source: simulations, tracking data, mobile experiments and participatory sensing data.
- Extend the external data to any temporal or spatiotemporal data.
- Indicators can be calculated for different population data sources.
- Indicators can be reported at any level (model resolution, activity, day, person, population).
- A project specific report phase enables evaluation in any available dimension.
- Composite indicators are aggregated in the reporting phase.

The next section will present this person centred activity based data workflow. It starts with the requirements and challenges expressed by different authors for environmental aspects of health and policy support as introduced in general in 1.1.2.

2.3.2 Framework components

2.3.2.1 Spatiotemporal objects and the exposome

In the introduction (1.1.2 and 1.1.5), it is shown that many solutions focus on the activity as the key object in a personal time-activity pattern. The basic reporting level of a methodology to calculate personal exposure is the person object. A person's time activity pattern is a sequence of activities. The person's whereabouts can be described as a so-called "spatiotemporal object", a changing location in time with a set of activity specific features. The instantaneous position of the subject is a coordinate and a time (position, time). The daily personal time-activity can be visualized as a line in a three dimensional space with coordinates (x,y,t).

The temporal resolution used to evaluate the activity can change according to the needs and requirements of the research question at hand. Within this PhD, activities at fixed location are evaluated at a temporal resolution of 5 minutes. The in-traffic activities are evaluated at a temporal resolution of 10 seconds. The environmental burdens themselves also change in space and time and are spatiotemporal objects as well. They can be visualized as two-dimensional surfaces changing in time. Those surfaces do not have to exist as such. The only requirement is that they can be calculated for each relevant time and position when required in the personal spatiotemporal object.

The indicator is the evaluation of the environmental burdens for a specific time activity pattern. The indicator calculation is based on the intersection of the two spatiotemporal objects for person and burden. The eco-exposome for a personal activity pattern is in essence the evaluation of the person's activity pattern for all environmental burdens (see Figure 2.3.1).

Figure 2.3.1: Exposure, dose and indicators are a combination of two spatiotemporal object, the first describing the behaviour of the person, the second the behaviour of the environmental burdens. The result is the personal exposure, in general terms referred to as the 'exposome'.

In an object oriented development, all components will become objects, attributes or methods. An object represents a specific entity of information and has attributes and methods. Attributes organize the relevant information about the object. Methods are actions that can be performed on the objects and alter objects and their attributes. In the next sections, the objects for the exposome compatible indicator model are presented. The dataflow framework will be referred to as MEX, modelling the exposure/exposome.

2.3.2.2 Person object structure

A person is a multi-layered object. The top-level person object includes all personal attributes and contains one or more activity patterns objects. An activity pattern includes matching attributes and a set of activity objects. The activity is the central object, includes matching attributes but has four standard attributes: the time/episode, the purpose, the micro-environment and the location or route. The standard attributes contain the basic information to evaluate the activity for the environmental burdens. The combination of the purpose and micro-environment is referred to as the *'activity typology'* and will act as the link between the activity object and the indicator object (see 2.3.2.4). For all person related objects, project specific attributes can be defined, including any relevant information from the personal input data useful for future indicator calculations. At the level of the activity, attributes can be single values or time series objects. When an activity object is created, the location attribute is by default a time series containing a sequence of (x,y,t), defining the position of the person in time. Other attributes with time series include any relevant ubiquitous information. This will be explained in detail in 2.3.3.2.

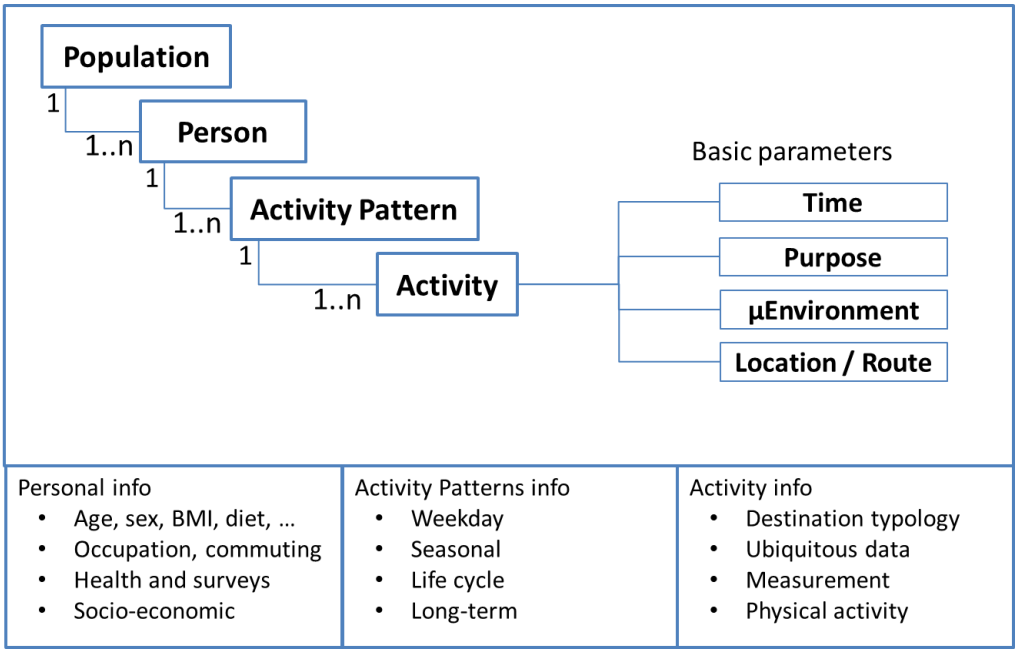

Figure 2.3.2: Persona objects structure and examples of the objects attribution.

When an activity object is created and evaluated for a specific indicator (see 2.3.2.6), it results in a temporary spatiotemporal activity object (STA) which contains all information gathered on the person, activity pattern and activity with a temporal resolution matching the type of the activity and the project specifications.

2.3.2.3 The activity purpose and micro-environment

The activity typology organizes the indicator calculations and is a crucial concept. The purpose of the activity is a basic attribute of an activity in mobility research and activity

modelling. It defines why the activity takes place. The set of values can be defined project specific, but it is good practice to use a generalized set of purposes. The typical set is: “work”, “school”, “shop”, “recreation”, “social”, “service”, “bring and get” (Beckx et al., 2009, Beckx et al., 2013).

The micro-environment of the activity is a basic attribute in exposure modelling. The exposure dynamics depend strongly on the micro-environment (1.1.5.2). The set of values can be defined by project. An attribute of the micro-environment object groups the micro-environments into indoor and outdoor microenvironment. Similar to the purpose, a generalized but customizable set is defined: “Home-indoor”, “Home-outdoor“, “Office”, “School”, “Work” (non-office work locations), “Walk”, “Bike”, “Car”, “Rail”, “Light Rail”, “Bus”, “Metro”, “In-transit” (in between modal choices), etc.

2.3.2.4 Indicator object structure

The indicator object contains all relevant definitions to calculate the indicator and is referred to as the *“Indicator definition”*. The evaluation of an indicator is by design sensitive to the properties of the activity. The indicator definition contains a set of objects each defining the behaviour of the indicator for a specific type of activity, referred to as an ‘Activity Specific Model’ (ASM). The activity is not only the central object in the description of the person, but it defines the behaviour of the *indicator definition*. The first action when evaluating an activity is dispatching the STA to the matching ASM (Figure 2.3.3). For example, if the indicator is the exposure to BC, the ASMs will describe the specific exposure dynamics for the different micro-environments. The activity will in this case, be dispatched to the ASM matching its micro-environment attribute. Dispatching can be organized by any *‘activity typology’*. More sensitive subdivisions can be organized within the ASMs.

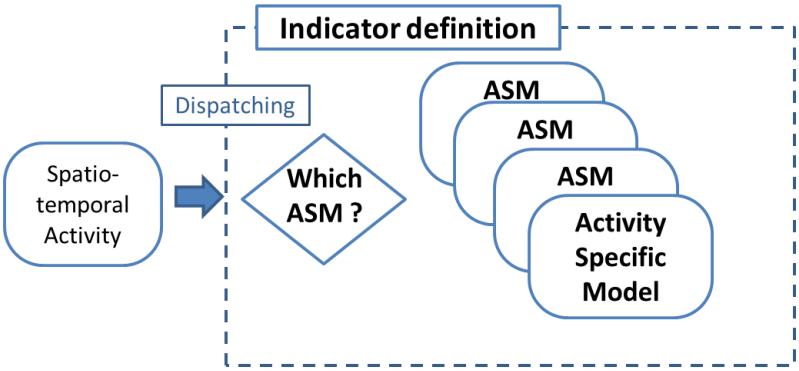

Figure 2.3.3: Step 1 in the indicator definition is dispatching the spatiotemporal activity to the matching activity specific model.

The ASM object organizes all information necessary to actually calculate the indicator. Gathering the information is a stepwise process, matching the logical flow of the information. It defines the necessary external data sources where information has to be retrieved from and defines the type of data retrieval. It also defines any function necessary to calculate any feature of the activity necessary to perform the next step in the stepwise process.

Each step is referred to as an *'Activity Calculation'* (AC). An AC can use any piece of information available in the STA at that moment. This includes all personal parameters, time-activity pattern parameters, all activity parameters and all new attributes gathered in the stepwise process so far, at the predefined activity specific temporal resolution. The AC returns an extended STA for the following step. An important reason why the attribution of the activity is organized stepwise is the speed of the calculations. Getting a thousand points from a specific data source is much faster than triggering a thousand times the retrieval of a single point, which would be the case if the calculations are organized by the time step matching the temporal resolution. The stepwise process is illustrated in Figure 2.3.4.

The core of the ASM is the *'activity specific function'* (ASF), the function that actually calculates the indicator. The ASF is triggered at the moment when all necessary attributes are available. The ASF is technically also an activity calculation but is added as a specific component for different reasons. First of all, it does not have to be a 'classical' analytical function. It can be any external function or procedure. The only technical limitation is the possibility to execute the function from within Python, the chosen implementation technology. In the ASMs for BC exposure presented in this PhD, the ASF is the prediction function of a "*Generalized Additive Model*" (GAM), triggered externally in the statistical open source R environment. The ASF can also be a validated function from a scientific publication or external report. In that case, the scientific reference supports the ASM at full and the ACs are only gathering the input data. The outcome of the ASF is an exposure, a dose or an indicator. The three outcomes are available in parallel if relevant. More details will be given in 2.3.2.7. Additional ACs can organize the conversion from exposure to dose and/or indicator, again capable of using any available data of the STA (not show in figure). These ACs can have scientific references as well and can bring additional parameters into the STA in the process.

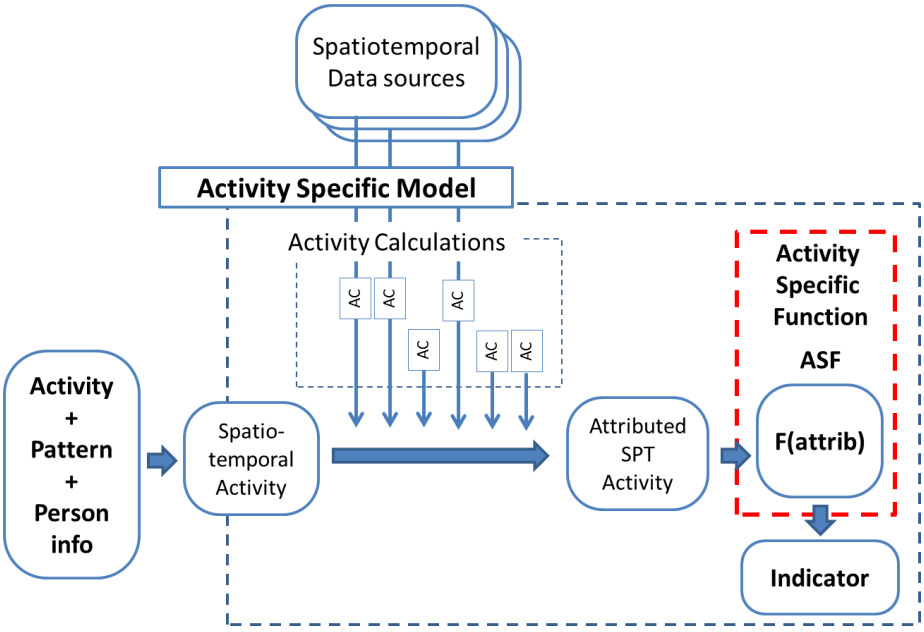

Figure 2.3.4: Data workflow in activity specific model (ASM) and the Activity Specific Function (ASF).

2.3.2.5 Activity calculation types

The activity calculations gather the relevant external data. Within the spatiotemporal modelling, a large variety of data sources are available. A short list of the functionalities is summarized. The STA has the position and time as basic features. The position is used to retrieve data from spatial grids, search for closest points or polylines, retrieve attributes, calculate distances and bearings and several other geographic operations. Keys and attributes can be retrieved from GIS layers. The time stamp of the STA can retrieve information from external time series. More complex spatiotemporal operations are available to retrieve data by combining time and position information: multiple GIS layers with time annotations, time series with position annotations. The implementation is extendible to include new data types if necessary.

2.3.2.6 MEX processing and low level reporting

The processing is visualized for a single indicator with only one activity specific model in Figure 2.3.5. The *'person factory'* builds the personal objects (2.3.2.2) from external population data. The different options for the population data will be presented in 2.3.2.8.

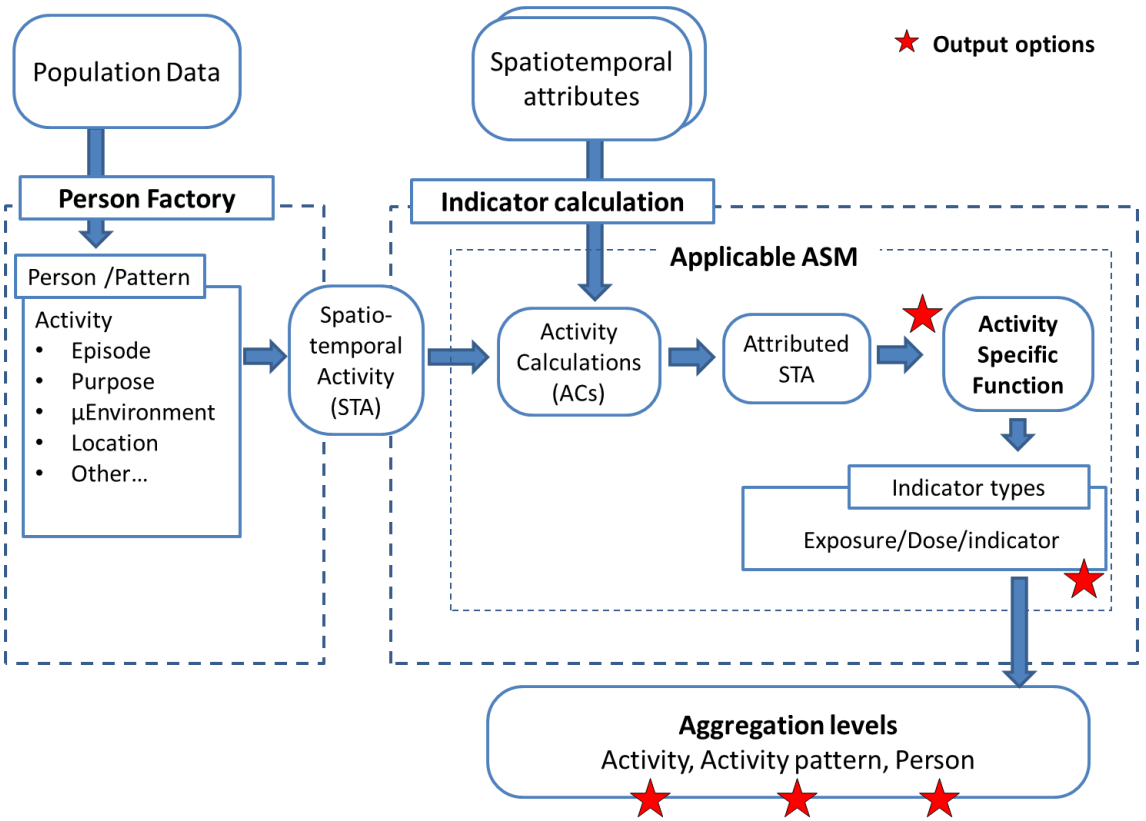

Figure 2.3.5: The person factory creates the person, time-activity pattern and activity objects from the external population data. The Spatiotemporal Activity (STA) assembles all personal data and triggers the indicator calculation. The applicable ASM contains a sequence of Activity Calculation retrieving the external data and performs other relevant actions on the data. This results in an attributed STA. The Activity Specific Function (ASF) is applied and results in an indicator. The red stars identify the stages in the process where data can be retrieved and reporting is initiated.

The calculation of the indicator is triggered at the level of the activity object since the indicator evaluation is activity based. The STA is created and the sequence of activity calculations is applied to the STA. The outcome values (exposure, dose, and indicator) are calculated in the ASF. The results exist at this stage with the same temporal resolution as the definition in the applied ASM. The data is available for detailed analysis and contains all temporary results of all activity calculations (the full STA, including the outcomes of the ASF).

2.3.2.7 Personal indicator reporting

The indicator calculation is available at the temporal resolution of the ASM. At this stage the detailed results are aggregated to the different relevant levels of the personal objects. By default, the indicator is aggregated by activity, diurnal pattern and person. By default, the flagged outcomes (exposure, dose, and indicator) will be aggregated. The aggregation function can be a customized function matching the properties of the calculated indicator. Every other customized reporting level can be applied in a post-processing and reporting phase on the resulting data for the full population.

2.3.2.8 MEX projects and scenarios

A scenario is the combination of a person factory and a set of indicator definitions. Different scenarios can be compared and evaluate the effect of the changes in the person factory and/or the indicator definitions. A project is a set of scenarios built to answer a specific research question.

Feedback loops between changing population behaviour and the external data sources for the indicator calculations are not explicitly covered but can be achieved by implemented sequences of scenarios, combined with customized reporting. The population simulation results in a set of individuals travelling the network. Aggregating the data by network segment results in an estimate of traffic on all segments. This is an example of a reporting action orthogonal to the person data for that specific scenario. This technique is used to improve the local traffic estimates in the Traffic Liveability model (see 3.2.3 and 3.2.4). Customized reporting or expert decisions can be used to adjust or recalculate the external data sources and enable the implementation of feedbacks.

2.3.2.9 Applying indicator definition on other populations

The processing of the person data and the calculation of the indicator are at this point only connected by the temporary SPA object. The only restriction to apply an indicator definition on another population is the availability of the relevant input data:

- Can the person factory deliver the SPA and the relevant personal attributes to match the indicator definition to be applied?
- Is the external data to calculate the indicator available in the project area?

- Is the available Activity Specific Function valid for the investigated episode, region or subpopulation?

If all answers are positive, the indicator can be calculated at once. If one of the answers is negative, additional expert decisions can result in an adjusted indicator definition or person factory to calculate a result with a reasonable error and/or acceptable reduced sensitivity.

2.3.3 The person factory types

2.3.3.1 Simulated populations

The first type of person factory is the simulated population. Simulated populations are the basic input in the QoL indicator described in 2.2. The external population data is a set of people attributed with enough information to estimate the time-activity pattern of the individual. The trip information will include an origin, destination and a modal choice. A route planner provides the simulated trip (Figure 2.3.6).

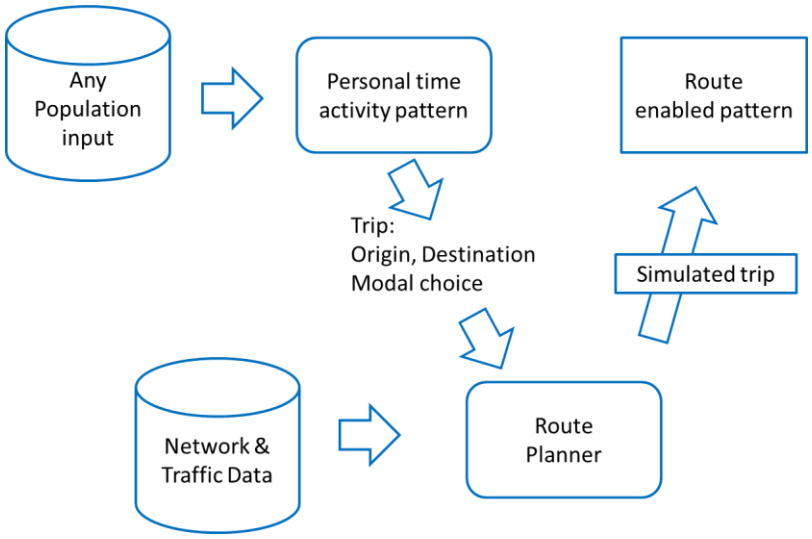

Figure 2.3.6: Simulating a personal time- activity pattern through a route planner.

Two options are available. The person factory can include an internal routing solution, providing data similar to the QoL model (see 2.2.4). The second option is to rely on external data. Building simulated populations based on traffic scenarios is a highly specialised technique in the traffic and mobility research field. An example of a potential external application to build virtual populations is the Feathers model (Bellemans et al., 2010). The person factory then only maps the external dataset to the dataflow framework input objects. The internal routing option is however very useful for other specific research questions. The exposure of bicyclists is sensitive to the travelled route. A potential bicyclist related policy application builds person factories with different variants of the routing network with in-

creased alternative biking facilities. The network routing parameters can evaluate the shortest path and the low exposure paths and will provide information for local government on effectivity of biking facilities. Different indicator definitions can be calculated (exposure to air pollution, bicycle accident risk, etc.), each sensitive to the specific traffic network. The results can be used to create awareness to the reduction potential of bicycle facility and will support the modal transition towards biking.

2.3.3.2 Participatory sensing

Performing in-traffic exposure research requires mobile measurements. Scientists perform controlled experiments or select a group of volunteers to carry equipment to measure their personal exposure. Each specific action of the subjects becomes an activity. Note that the person factory does not need to result in a full diurnal activity pattern. A person factory processing only in-traffic activities is valid as well.

The data includes personal features, trip registrations, exposure measurements, personal activity diaries, GPS-tracks, vehicle choice and characteristics, activity specific attributes etc. The person factory will map this variety of data to the three objects: Person, Activity Pattern and Activity. The diaries build the matching activity pattern. All activity specific information is mapped to the activity. The activity attributes can be simple parameters or more complex spatiotemporal data series. The physical location of the dwelling or the destination and their properties are simple parameters of the stationary activities. The modal choice (bike, car, rail...) for a specific in-traffic activity is a standardized parameter. The registered GPS track and the simultaneous exposure measurements are two examples of spatiotemporal information linked to the activity. The GPS and the measurement equipment will typically not result in time series with matching time stamps. It is one of the explicit functionalities of the person factory to align the time series to a standardized and activity specific temporal resolution. If necessary, the data is interpolated to match the required temporal resolution. Any indicator can be calculated using the full detail of the behavioural pattern of the subjects.

2.3.3.3 Measurement based Activity Specific Function

The core of the MEX data workflow is the Activity Specific Function. The real challenge in the exposome research is establishing these functions. This is one of the most important functionalities of the MEX model. In a typical setup, the exposure/indicator is the unknown in the data workflow. Participatory sensing campaigns not only capture the personal information but also personal exposure measurements. The personal exposure is known within the participatory sensing campaign and can be entered into the data workflow as an activity attribute. The only unknown object in the scenario is the *"Activity Specific Function"*. The data output option before the ASF delivers the attributed dataset necessary to test, build and

evaluate a function to predict the measurement performed in the participatory sensing campaign. That is exactly the use of the MEX model in 0: building the ASF.

The MEX functionality provides also the possibility to perform the external validation. An independent dataset is used to supply similar activities including the indicator measurements as an attribute of the activity. Applying the acquired ASF results in a measurement and a prediction and enables the external validation.

2.3.3.4 Epidemiological databases

Cohorts and other epidemiological datasets are an obvious target of the MEX model. The person factory will add health parameters to the dataset. For the subjects in the health study, the time activity pattern has to be simulated. This requires a set of personal attributes to simulate the behavioural pattern, similar to 2.3.3.1. Any available indicator definition can be calculated. Including effects of changing behaviour over time is organized by calculating the indicator of different time-activity patterns. Multiple time-activity patterns can be attributed to a single person, each describing the typical time-activity pattern for that specific episode in the life of the subject. If the subjects moved or changed occupation or modal choice, the indicator can be made sensitive to those changes.

The potential in the epidemiological studies is only limited by the available personal information and the availability of valid external data and activity specific models for the investigated episode. Expert decisions can adjust for the missing data. Relative indicators within a certain time window might be an option to tackle this issue. A person could get an evaluation like 'in the top 10 percentile of personal exposure in decade X'.

2.3.4 Implementation

The indicator framework is developed with available open source technology in an object oriented open source programming language: Python. Python is a multiplatform programming language with as most import feature, the huge community using Python in almost all software and science fields. The second main open source package used is R, a state of the art statistical project embodying the newest techniques in statistics. All work in this PhD is highly depending on the solid work performed by these open source communities. The most important external libraries used in this work will be simply listed here.

Python libraries:
Pandas, shapelib, shapely, numpy, matplotlib, networkx, gdal, rpy, rpy2 and other
R libraries: mgcv, spatial and many others
Postgresql, PostGis, QGis
Open Street Map: spatial data and network enabled road datasets

2.3.5 Conclusions

A multi-purpose indicator dataflow frame is presented. The list of functionalities mentioned in 2.3.1 is achieved. A large variety of external data can be processed. Activity specific functions can be retrieved from the measurement campaigns. Every indicator definition becomes an independent result, enabling the extrapolation of the indicator to custom populations. The Activity Specific Function can be any type of evaluation, including complex statistical prediction models.

The evaluation path can be affected by different research fields. Multidisciplinary cooperation is necessary to match the available data to the specific features of the investigated indicator. The data workflow is open to multiple types of research initiatives. Extrapolation to representative populations combined with scenario building enables advanced health research and policy support.

2.4 References

Appleyard, D. Livable Streets. Berkeley: University of California Press,1981

Asperges, Impact van verkeersonveiligheid en –onleefbaarheid – objective en subjectieve factoren: methodiek objectieve verkeersleefbaarheid, oktober 1998

Beckx C, Lefebvre W, Degraeuwe B, Vanhulsel M, Kochan B, Bellemans T, et al. Assessing the environmental impact associated with different trip purposes. Transportation Research Part D-Transport and Environment 2013; 18: 110-116.

Beckx C, Panis LI, Arentze T, Janssens D, Torfs R, Broekx S, et al. A dynamic activity-based population modelling approach to evaluate exposure to air pollution: Methods and application to a Dutch urban area. Environmental Impact Assessment Review 2009; 29: 179-185.

Beckx, W. Lefebvre, B. Degraeuwe, M. Vanhulsel, B. Kochan, T. Bellemans, S. Dhondt, L. Int Panis, Assessing the environmental impact associated with different trip purposes, Transportation Research Part D: Transport and Environment, Volume 18, January 2013, Pages 110-116, ISSN 1361-9209, http://dx.doi.org/10.1016/j.trd.2012.10.002.

Bellemans, T., Kochan, B., Janssens, D., Wets, G., Arentze, T., & Timmermans, H. (2010). Implementation framework and development trajectory of FEATHERS activity-based simulation platform. Transportation Research Record: Journal of the Transportation Research Board, 2175(1), 111-119.

Botteldooren D, Verkeyn A, De Baets B, Lercher P, Ieee. Fuzzy integrals as a tool for obtaining an indicator for quality of life. IEEE International Conference on Fuzzy Systems, Vancouver, CANADA, 2006, pp. 1065-1071.

Botteldooren D., Dekoninck L., Gillis D. The Influence of Traffic Noise on Appreciation of the Living Quality of a Neighborhood. International Journal of Environmental Research and Public Health. 2011; 8(3):777-798.

Dekoninck, L., Gillis, D., Botteldooren, D., & Lauwers, D. (2010). Methodologie voor het objectief meten van het effect van verkeer op de leefbaarheid : een aggregatietechniek om de lokale effecten van verkeer (veiligheid, gezondheid en kwaliteit van de omgeving) , thuis, onderweg en op de bestemming te evalueren op basis van het individueel tijdsgebruik en verplaatsingsgedrag : theoretisch kader. Steunpunt Mobiliteit & Openbare Werken.

Dekoninck, L., Gillis, D., Botteldooren, D., & Lauwers, D. (2011). Indicatoren voor verkeersleefbaarheid: uitwerking en toepassing van een model voor het meten van verkeersleefbaarheid. Steunpunt Mobiliteit & Openbare Werken.

Dekoninck, L., Gillis, D., Botteldooren, D., & Lauwers, D. (2012). Ruimtelijke ontwikkeling, verkeer, geluidshinder en impact op leefbaarheid. Steunpunt Mobiliteit & Openbare Werken.

Klaeboe R. 2007. Are adverse impacts of neighbourhood noisy areas the flip side of quiet area benefits? Applied Acoustics, 68, 557-575.

Klaeboe R. Are adverse impacts of neighbourhood noisy areas the flip side of quiet area benefits? Applied Acoustics 2007; 68: 557-575.

Lercher P. Which health outcomes should be measured in health related environmental quality of life studies? Landscape and Urban Planning 2003; 65: 65-74.

Lioy P.J. & Smith K.R. 2013. A Discussion of Exposure Science in the 21st Century: A Vision and a Strategy. Environmental Health Perspectives, 121, 405-409.

Maslow, A.H. (1943). "A Theory of Human Motivation," Psychological Review 50(4): 370-96.

Ministerie van de Vlaamse Gemeenschap, Departement Leefmilieu en Infrastructuur, Onderzoek Verplaatsingsgedrag – Analyse opdracht – Eindverslag, 1996

Ministerie van de Vlaamse Gemeenschap, Departement Leefmilieu en Infrastructuur - Mobiliteitscel, Onderzoek Verplaatsingsgedrag Vlaanderen 2, 2004

Ministerie van de Vlaamse Gemeenschap, Departement Mobiliteit en Openbare Werken, Onderzoek Verplaatsingsgedrag Vlaanderen 3 – Verkeerskundige interpretatie van de belangrijkste tabellen, 2009

Parks, A. Kearns, R. Atkinson, What makes people dissatisfied with their neighborhoods?, in: Urban Studies, Vol. 39, No. 13, 2002, p. 2413-2438

Python Software Foundation. Python Language Reference, version 2.7. Available at http://www.python.org

R Core Team (2013). R: A language and environment for statistical computing. R Foundation for Statistical Computing, Vienna, Austria. URL http://www.R-project.org/.

Reis et al., 2013, “Integrating health and environmental impact analysis”, Public Health, 2013, doi:10.1016/j.puhe.2013.07.006

Steinle S, Reis S, Sabel CE. Quantifying human exposure to air pollution-Moving from static monitoring to spatio-temporally resolved personal exposure assessment. Science of the Total Environment 2013; 443: 184-193.

Tetreault L.F., Perron S. & Smargiassi A. 2013. Cardiovascular health, traffic-related air pollution and noise: are associations mutually confounded? A systematic review. International Journal of Public Health, 58, 649-666.

Verkeyn A, Botteldooren D, De Baets B. Genetic learning of fuzzy integrals accumulating human-reported environmental stress. Applied Soft Computing 2011; 11: 305-314.

Chapter 3 Noise and Quality of Life

3.1 Introduction

This chapter presents a strongly restricted selection of the results generated with the TL model within a Flemish Government funded project on Traffic liveability and is focussing on the relevance of using detailed noise assessments along the road network. More details can be found in the co-authored publications with Dominique Gillis (1.2.4). In the first section, the full QoL indicator model is applied on the city of Ghent and vicinity. The second part summarizes a publication (available in the appendix C), which focusses on the perception of the surroundings of the dwelling in relation to the exposure to noise at the facade and the noise levels along the routes near the dwelling. The third section identifies the potential use of in-traffic noise assessments as a proxy for air pollution exposure.

3.2 QoL Case study: City of Ghent and vicinity

This section is partially based on the conference paper:

Dekoninck, L., Gillis, D., & Botteldooren, D. (2011). Perceived quality of the living environment and noise. In 10th International Congress on Noise as a Public Health Problem (ICBEN-2011) (Vol. 33, pp. 921-928). Institute of Acoustics.

3.2.1 Input data

The traffic related quality of life methodology was applied in a case-study for the city of Ghent. The intermediate results will be used in order to illustrate the different steps in the calculation, and to clarify the improvements brought by the developed methodology.

The study area includes the city centre of Ghent, and some of the south-western suburbs (Figure 3.2.1). The map compiles of a number of GIS-layers with the road infrastructure, rail-roads and waterways. For the model calculation each road segment is represents one model

zone, containing data about the traffic origins (number of households) and traffic destinations (e.g. schools, shops, sport and recreation facilities, large companies, etc.), representing the traffic generation and traffic attraction for each road segment. The traffic attraction strength of a zone distinguishes for the different purposes: commuting traffic, shopping traffic, recreational traffic, etc.

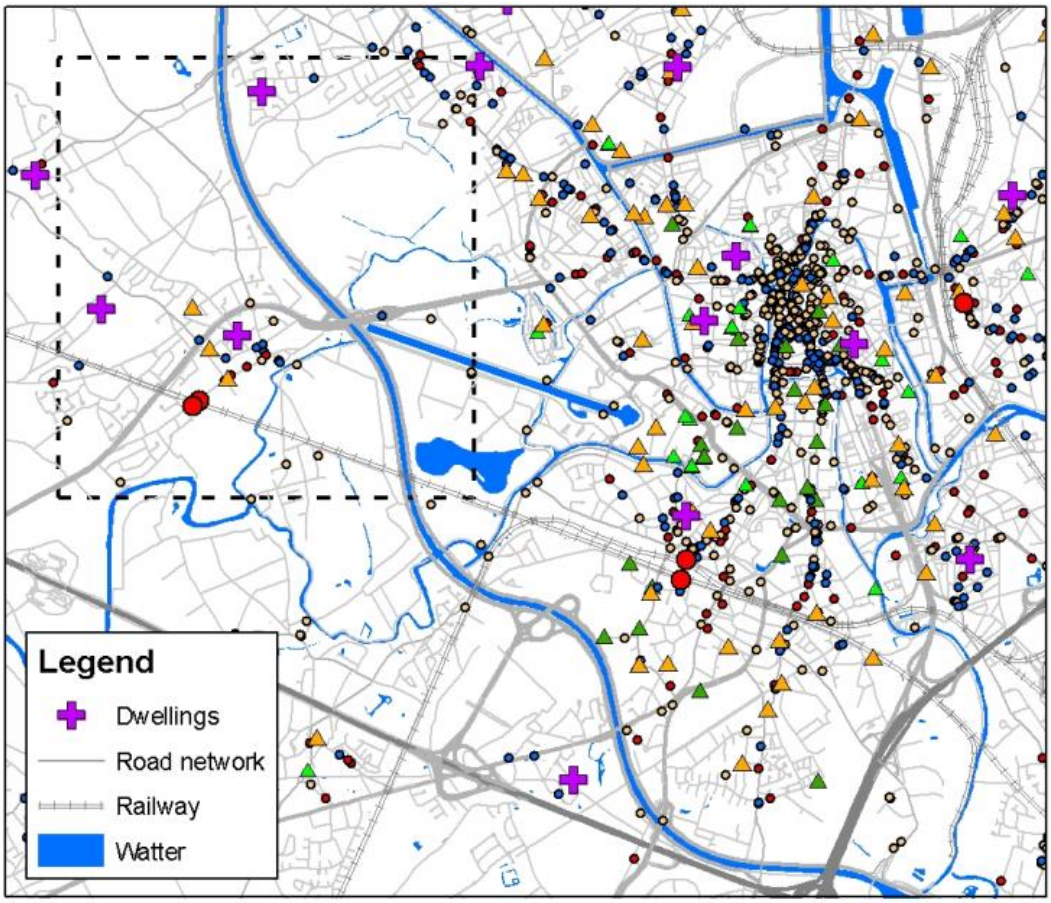

Figure 3.2.1: A sample of the study area with 11 randomly selected dwellings and a complete set of frequented destinations of the simulated households in the selected dwellings. The triangles and dots in different colours present selection of different types of destinations (shops, schools, work places,etc…).

3.2.2 Sampling of a household

The first phase in the calculation is the sampling of individual travel patterns. For each dwelling in the study area, a family is sampled from the Flemish trip diary survey, with its own household characteristics (e.g. number of persons, age of the persons, employment …) and daily trips (amount of trips, trip purpose, transportation mode …). By sampling a realistic destination address for each of these trips, it is possible to define the optimal transport mode and route for each trip.

For each dwelling, this results in an overview of all the trips to and from this address during one day. Graphically this can be represented as a map showing all the routes travelled by all household members, distinguishing between the transport modes. An example is shown

in Figure 3.2.2, which displays the travel patterns for two households, one living in the centre of Ghent, and the other one living in one of its suburbs. Both are households with three teenage children, resulting in a rather high daily amount of trips. It is obvious that in the city centre, the share of short distance trips is larger, which increases the potential for active mobility (trips by foot or by bike).

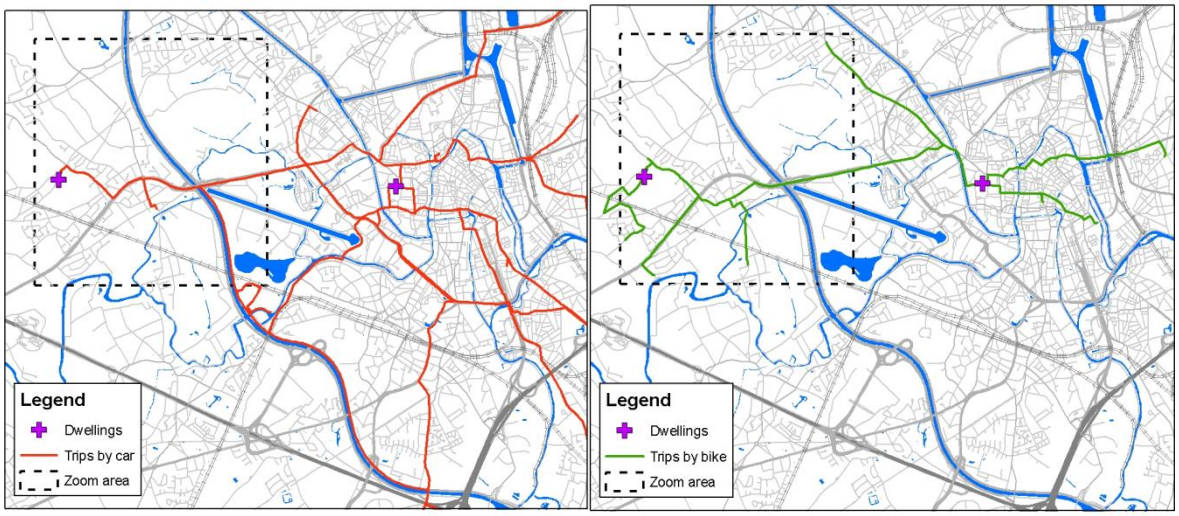

Figure 3.2.2: Trip patterns per mode for a household living in the city centre and a household living in the suburbs (Left panel: car trips; Right panel: active trips (bike, walk omitted).

From this figure, it is clear that the house location can have an important impact on the travel behaviour according to the proposed model, both in terms of traffic mode used and direction taken to leave the house.

In addition, the household characteristics are of big importance: the household size, age of the members, employment … will all influence the number and type of trips (trip purpose, transportation mode, etc.). In case of a less active household, the trip patterns equivalent to Figure 3.2.3 would count fewer trips, mainly of a shorter distance. As a consequence, for these people the quality of the living environment would be determined strongly by the more local conditions, closer to the dwelling, as opposed to a household with teenagers which has a potential larger radius of action.

When developing the methodology for the measurement of quality of the living environment or traffic liveability, this means that it is important to repeat the simulation for a sufficient number of house addresses, and for a sufficient variety of household types. The first issue will be countered by making an evaluation for every existing address location. The second issue is solved by using the trip diary survey, which contains a large selection of households, which has been stratified according to the age of the house owner.

3.2.3 Adding local traffic to the evaluation

The same simulation of the trip patterns is performed for all households within the complete model area. Aggregating the sampled car or public traffic trips at local street segment level will result in a map of traffic generated by the local inhabitants. By merging this information to the macroscopic traffic flows, a more refined input dataset for the noise immission and air pollution calculation is obtained. All other indicators in the model depending on the traffic in the road at the dwelling can be calculated at this moment. When overlaying the car flows with the other modes, the conflicts between both become visible. Figure 3.2.3 shows the aggregation of all trips by car for just a small selection of dwellings. At each dwelling location – that is assumed representative for a street segment as far as local traffic intensity is concerned – different households are simulated. The intensities of local traffic already give a very good picture of the impact of local traffic on the overall traffic intensities.

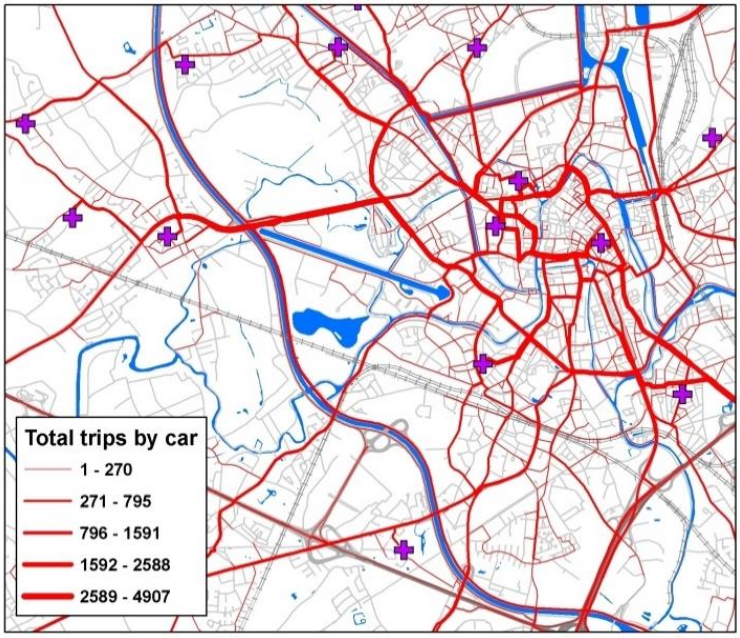

Figure 3.2.3: Aggregation of all trips by car for a selection of dwellings (crosses) populated by several sampled households.

3.2.4 Improve the noise map

The aggregated trajectories for each road segment are used to recalculating the noise maps, now including the estimate of the local traffic. This resolves the missing traffic data and improves the spatial resolution of the QoL model. Improving the spatial variability of the external data sources, in this specific case the local traffic count, based on the results of the population simulation is an important asset in the modelling approach. Building virtual populations with different activity patterns and different mobility patterns resulted in the potential

to feedback the differences in the mobility scenarios. It enables the evaluation of local changes including the cumulative effect of secondary changes in multiple indicators into the combined QoL indicator.

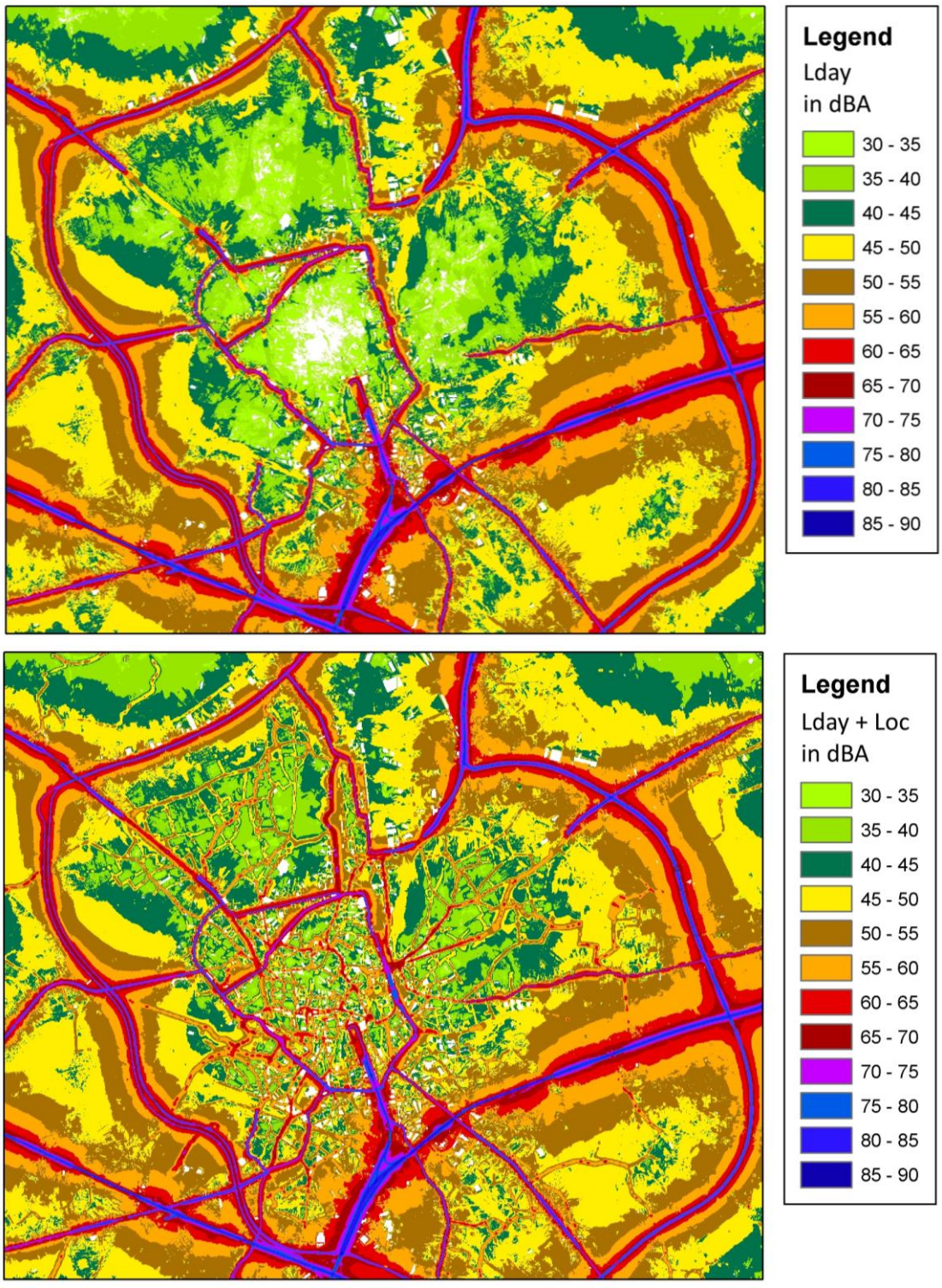

Figure 3.2.4: Improvement of the noise maps by including the aggregated simulated trips for roads not included in the large scale traffic data sources. Top panel: traffic data, 2008, bottom panel: traffic data 2008 + weighted simulation of local traffic.

3.2.5 Indicator evaluation

This way, the full set of indicators is evaluated, covering all aspects of traffic liveability according to the indicator scheme presented in Figure 2.2.3. Each indicator is evaluated for each sampled person in the model area. In the following aggregation step, the separate indicators are aggregated both geographically (from individual perceptions to segment or street level) and thematically. Indicators are grouped in four separate aspects of traffic liveability: accessibility, health, living environment and social cohesion.

For the aggregation from the separate indicators to an appreciation of each aspect, and from the aspects to a global traffic liveability evaluation, the method of Choquet integration is applied (Botteldooren et al., 2006). This method makes a weighted sum, giving most weight to the strongest components. This simulates human perception, as one extreme (positive or negative) aspect will dominate the perception and will rarely be compensated by one or more moderately good or bad criteria. The model combines advantages from a weighted sum and a strongest component aggregation.

Traffic noise is incorporated in the model in two ways: it has an impact on the "Health" aspect (for the health effects by traffic noise) and on the "Living environment" aspect (for the perceived annoyance by traffic noise). As an illustration, the model result for the impact of traffic noise through the health path is shown in Figure 3.2.5, combining traffic and railway noise. Figure 3.2.6 shows the noise annoyance evaluation in the environment path.

The histograms show the distribution of the evaluations for the sampled persons. The majority of the sampled population have a rather bad score for the health effects because of traffic noise. This is partially an overestimation of the health effects, as the underlying noise map does not take into account the shielding effect of buildings. The map shows that the health impact of traffic noise is mainly concentrated in the south of the city, because of the concentration of two highways with the main entrance road to the city centre, two railroads and the ring road.

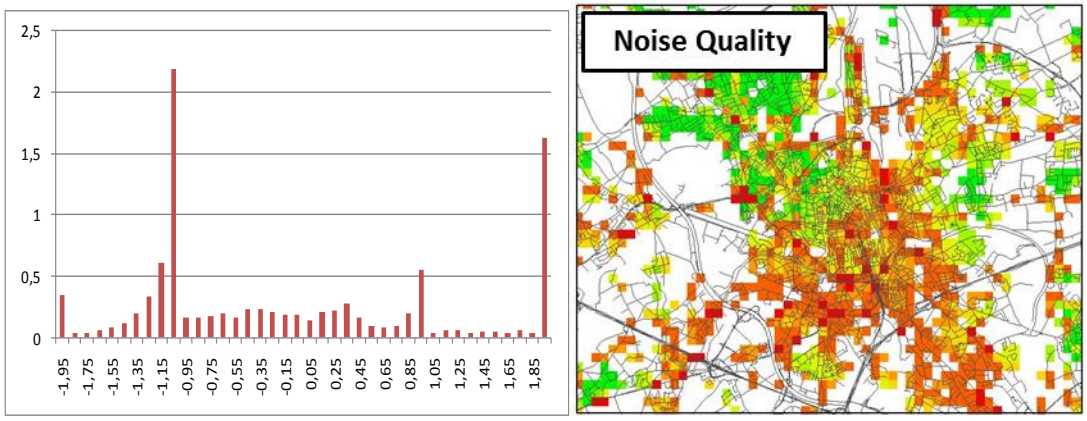

Figure 3.2.5: Illustrations of the 'Health' effects of traffic noise: the frequency graph of the individual evaluations (left) and a model plot showing good (green) to bad (red) evaluation of the health impact by traffic noise

Concerning traffic noise annoyance the distribution shows a generally much more positive evaluation, mainly because this annoyance is only evaluated at home. This means that only people living on the major traffic roads experience annoyance and people living more quiet streets do not experience annoyance by traffic noise. Figure 3.2.6 also confirms this where we recognise the Ghent ring road and the main entrances to the city centre.

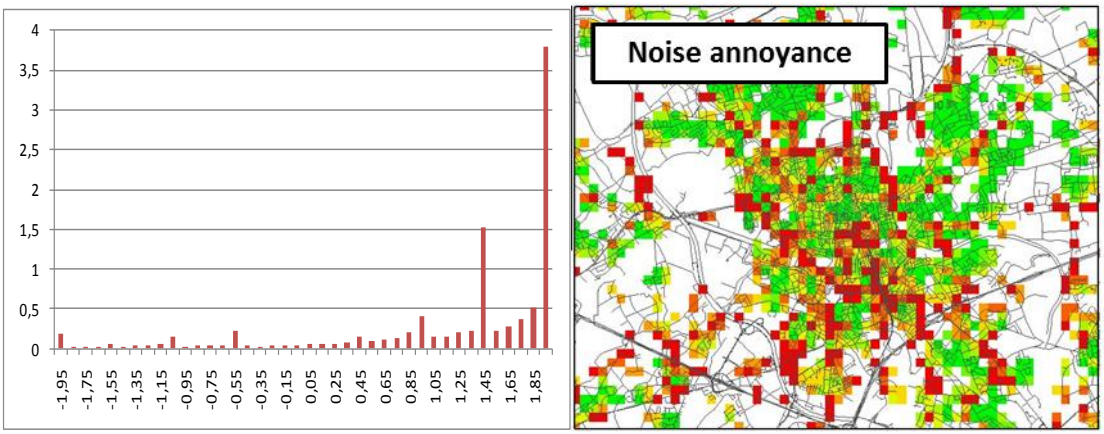

Figure 3.2.6: Illustrations of some model results annoyance by traffic noise: the frequency graph of the individual evaluations (left) and a model plot showing good (green) to bad (red) evaluation of the annoyance by traffic noise

The other evaluation paths are calculated in a similar way and aggregated in the indicator at the top (Figure 2.2.3). The resulting total appreciation of traffic liveability index (TLI) is presented in Figure 3.2.7. Again, some well-known black spot areas appear from this plot, such as the Ghent ring road, some radial arteries and the highways and railroads passing near the city.

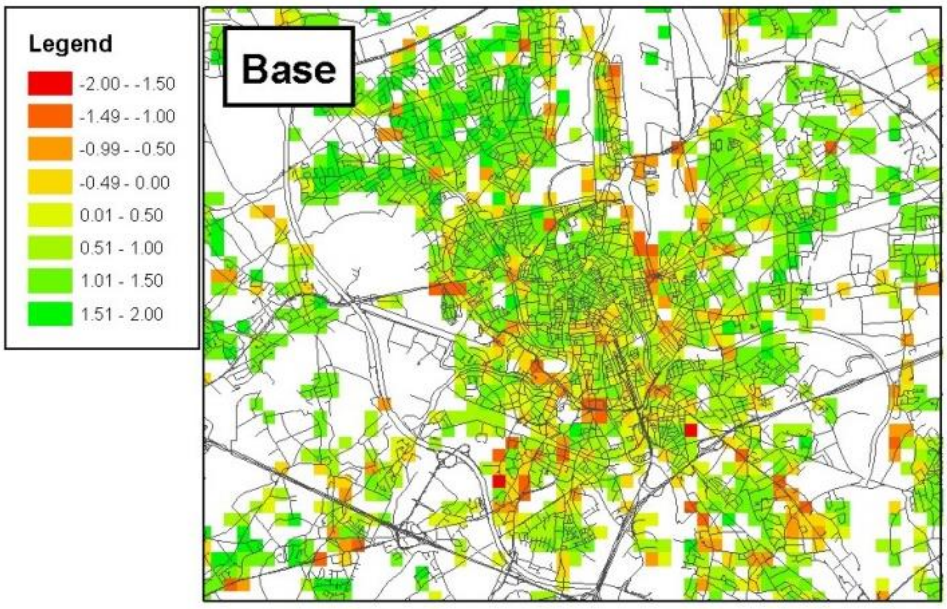

Figure 3.2.7: Model plot showing the average traffic liveability index (TLI) using a 200 m raster aggregation of the current situation (Base), other scenarios are reported in detail in specific reports.

3.2.6 Relation to the reported satisfaction

In order to assess the quality of the proposed model, the model results are compared to the data from the Written Liveability Survey (SLO, "Schriftelijk Leefbaarheids-Onderzoek"). This large scale survey asks people from all over Flanders about their appreciation of their living environment. For the further analysis, only the survey data from the Ghent area are used. Since no detailed information is available about the individual families of the subjects in the survey and due to the sensitivity of the evaluation to the selected diurnal pattern of the subject, multiple families are simulated in the dwellings of the survey subjects. The resulting traffic liveability at a certain dwelling is the average of the traffic liveability of 20 families evaluated for the full indicator scheme at each dwelling of the survey.

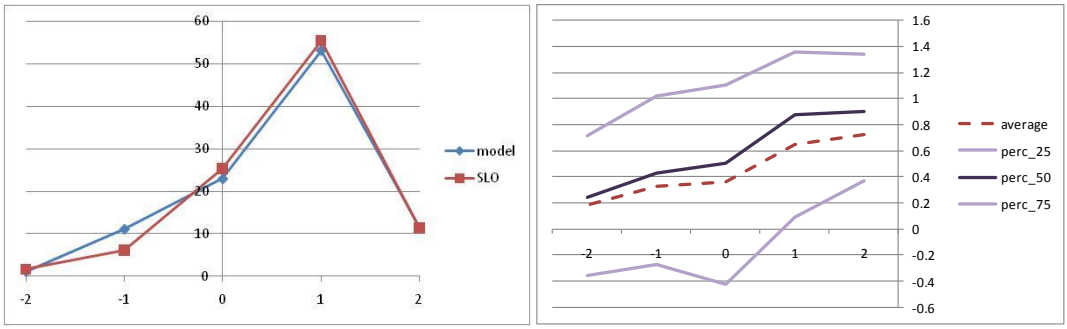

Figure 3.2.8: Frequency plot of the traffic liveability evaluation according to the traffic liveability model and the reported satisfaction in the SLO-survey (Panel A; Left). The relation between the reported satisfaction from the SLO-survey (x-axis) and the calculated evaluation (y-axis), according to the traffic liveability model, showing the average and median value in each class and the 25- and 75-percentile values (Panel B; Right).

In Figure 3.2.8A the resulting traffic liveability appreciation from the survey and the model are grouped into five satisfaction classes. The graph shows that the traffic liveability model gives a very good reproduction of the reported satisfaction from the SLO-survey: the majority of the people (about 65%) are satisfied to very satisfied (classes 1 and 2) while only 10% state to be dissatisfied or (very) dissatisfied (classes -1 and -2).

For a more detailed comparison of the results, the model results are reduced in order to make both sets geographically comparable. The dwellings that were included in the SLO-surveys are drawn on the model map, and from the model only the simulated persons that are in the immediate vicinity of the SLO-surveys are retained. This guarantees that both datasets represent the same geographical dwelling locations. Finally, the model results are split into five classes, according to the reported satisfaction in the corresponding SLO-survey dwelling. This allows comparing the calculated traffic liveability to the reported satisfaction. The results are visualized in Figure 3.2.8B, where the horizontal axis contains the reported satisfaction (SLO-survey) and the vertical axis shows the calculated appreciation according the model. The model results are clearly related to the reported satisfaction. Although the results show a large deviation, the over-all behaviour reproduces the survey results well.

3.2.7 Conclusions

An innovative model is presented for objectively measuring the traffic liveability. Whereas classical methods focus on the traffic impacts at the dwelling location, the proposed method incorporates the whole activity pattern and trip behaviour in the evaluation. This is achieved by a simulation of households, including their reported trip behaviour, matching the Flemish Trip Behaviour Survey. The application of the traffic liveability model in the city of Ghent indicates that the model offers a realistic reproduction of the reported satisfaction of the living environment.

3.2.8 References

T. Asperges, "Impact van verkeersonveiligheid en –onleefbaarheid – objectieve en subjectieve factoren: methodiek objectieve verkeersleefbaarheid", oktober 1998

Studiegroep Omgeving, "Onderzoek naar de draagkracht"

Klaeboe, R. and Engelien, E. and Steinnes, M., Mapping neighbourhood soundscape quality, Proceedings of the 33th International Congress and exposition on Noise Control Engineering Internoise 2004

D. Appleyard, Livable streets, 1981

Ministerie van de Vlaamse Gemeenschap, Afdeling AMINABEL, "Uitvoeren van een schriftelijke enquête ter bepaling van het percentage gehinderden door geur, geluid en licht in Vlaanderen, SLO1-meting: eindverslag, dossiernummer: 03/1361", 2004

Botteldooren, D., Verkeyn, A., De Baets, B., Lercher, P., Fuzzy Integrals as a Tool for Obtaining an Indicator for Quality of Life, IEEE International Conference on Fuzzy Systems, 2006

Botteldooren D., Dekoninck L., Gillis D. The Influence of Traffic Noise on Appreciation of the Living Quality of a Neighborhood. International Journal of Environmental Research and Public Health. 2011; 8(3):777-798.

Dekoninck L., Gillis D., Botteldooren D. and Lauwers D., Methodologie voor het objectief meten van het effect van verkeer op de leefbaarheid, september 2010

Ministerie van de Vlaamse Gemeenschap, Departement Leefmilieu en Infrastructuur, Onderzoek Verplaatsingsgedrag – Analyse opdracht – Eindverslag, 1996

Ministerie van de Vlaamse Gemeenschap, Departement Leefmilieu en Infrastructuur - Mobiliteitscel, Onderzoek Verplaatsingsgedrag Vlaanderen 2, 2004

Ministerie van de Vlaamse Gemeenschap, Departement Mobiliteit en Openbare Werken, Onderzoek Verplaatsingsgedrag Vlaanderen 3 – Verkeerskundige interpretatie van de belangrijkste tabellen, 2009

3.3 The influence of traffic noise on appreciation of the living quality of a neighbourhood

This section starts with a summary of full article "The influence of traffic noise on appreciation of the living quality of a neighbourhood", available in Appendix C. This analysis is based on 800 locations with survey results for the QoL survey and the evaluation of an extended set of noise parameters along the trajectories of the subjects (an extension on the Traffic Liveability model presented in 2.2 and 3.2). The noise parameters along the trips are calculated with different aggregation options. These parameters are compared with different questions in the QoL survey.

In a second step, the resulting strongest parameter, the equivalent noise level along the roads within 300 m from the dwelling ($L_{T,300,eq}^{eq}$), is evaluated towards the calculated traffic liveability index (TLI) for the entire simulated population presented in the previous section (3.2).

3.3.1 Summary of the publication

Short abstract

The perception of the surroundings of the dwelling is evaluated in relation to the exposure to noise at the facade and the noise levels along the routes near the dwelling. Noise levels along the routes near the dwelling prove to be an important modifier on top of the facade noise levels to predict the response of the inhabitants on the traffic related quality of life question. If the aggregated noise level along roads within 300 m of the dwelling is low, the appreciation of the environment improves and vice versa. Living is a locally shielded area near a major road is evaluated as a lower quality compared to a similar exposure at the facade with lower amounts of traffic in the vicinity.

Full conclusion of the paper

The relationship between traffic noise and perceived quality of life in the neighbourhood was investigated by comparing the results of a survey with new types of exposure indicators focusing on noise exposure during trips from the house. The latter are calculated in an innovative way by sampling origins, destinations (shops, schools, etc.) and typical travel behaviour from several databases and reconstructing all possible trips leaving the dwelling.

The importance of traffic and traffic noise in reported quality of life in a neighbourhood is observed by analysing open questions on positive and negative aspects of coming to live in

this neighbourhood; by analysing the relationship between the quality of life question and a standard noise annoyance question; and most importantly by obtaining multiple logistics models relating quality of life in the neighbourhood to noise exposure. The relationship between reported noise annoyance and quality of the living environment suggest that the pathway is a direct one, not relying on underlying hidden variables. Combining this analysis with a question on traffic intensity in the neighbourhood further suggests that the pathway from traffic through noise to quality of life in the neighbourhood accounts for the strongest relationship between traffic and quality of life. Other paths may contribute, but most probably to a much lesser extent.

Traffic noise exposure in the neighbourhood is assessed by estimating where people would drive their car and where they would walk close to their house while leaving for work, school, shopping or whatever other reason. In that way, the exposure indicators for noise exposure during trips account for the access routes and the location of the most important attraction poles close to the house, rather than merely considering a circular area around the house as the neighbourhood. Several ways of aggregating noise over the length of the trip and between trips are compared. Statistical analysis showed that calculating an equivalent level over the first 300m of each trip and aggregating over all trips using an equivalent level as well, $L_{T,300,eq}^{eq}$, results in the most significant improvement of models for noise annoyance at home and quality of the living environment. In addition, a restriction to trips made on foot or by bike improves the predictability of satisfaction with the quality of the living environment, but not of dissatisfaction with it. For noise annoyance at home, the level at the most exposed facade is still a dominant indicator. Adding the above mentioned indicator for noise exposure during trips improves the model for moderate to extreme annoyance and also the model for no annoyance at all. The positive effect of access to a quiet side on noise annoyance at home is not recovered probably because quiet side levels were not calculated accurately enough.

Most surprisingly at first sight, the indicator for noise exposure during trips is the most significant contributor to a model for quality of life in the neighbourhood. Adding facade exposure to the model gives no improvement, which is a rather surprising result that is however understandable since the neighbourhood has a wider spatial meaning than just one's own dwelling. Similarly surprising is the observation that the same exposure indicator performs best in a model for perceived traffic intensity in the neighbourhood, more so than a traffic count on the street of the dwelling itself. At this point, it is only possible to propose a few hypotheses to explain this observation: traffic intensity might be judges via noise or the traffic aggregation embedded in the noise exposure indicator might be just the way to aggregate traffic intensities over an area that corresponds best to perceptive evaluation.

The logistic models obtained in this work provide an interesting step forward for building a general model for evaluating the overall impact of land use planning and mobility planning on the quality of life of a neighbourhood.

3.3.2 Noise in and around the dwellings and Traffic Liveability Index

In the paper "The influence of traffic noise on appreciation of the living quality of a neighbourhood" (Botteldooren et al., 2011), the equivalent noise level along the roads within 300 m from the dwelling ($L^{eq}_{T,300,eq}$) was a strong indicator. Since the strength of this indicator towards the Quality of Life questions is strong, it's relation towards the calculated Traffic Liveability Index (TLI) can be evaluated as well. This is a valid approach since the $L^{eq}_{T,300,eq}$ indicator is not an explicitly included in the set of sixteen indicators of the TLI model (2.2).

In Figure 3.3.1 the relation between the two noise exposure parameters ($L_{DEN,facade}$ and $L^{eq}_{T,300,eq}$) and TLI is presented. In the population simulation of the TLI (10% of the population in the city of Ghent and its vicinity) the TLI is be visualized as a function $L_{DEN,facade}$ and $L^{eq}_{T,300,eq}$. The TLI is presented in a continuous scale from -2 to +2. The two noise exposure parameters are used on the X and Y axes, the QoL-indicator is presented in a gradual colour scheme with green and orange the positive QoL evaluations and the red to bleu scheme for the negative QoL outcomes.

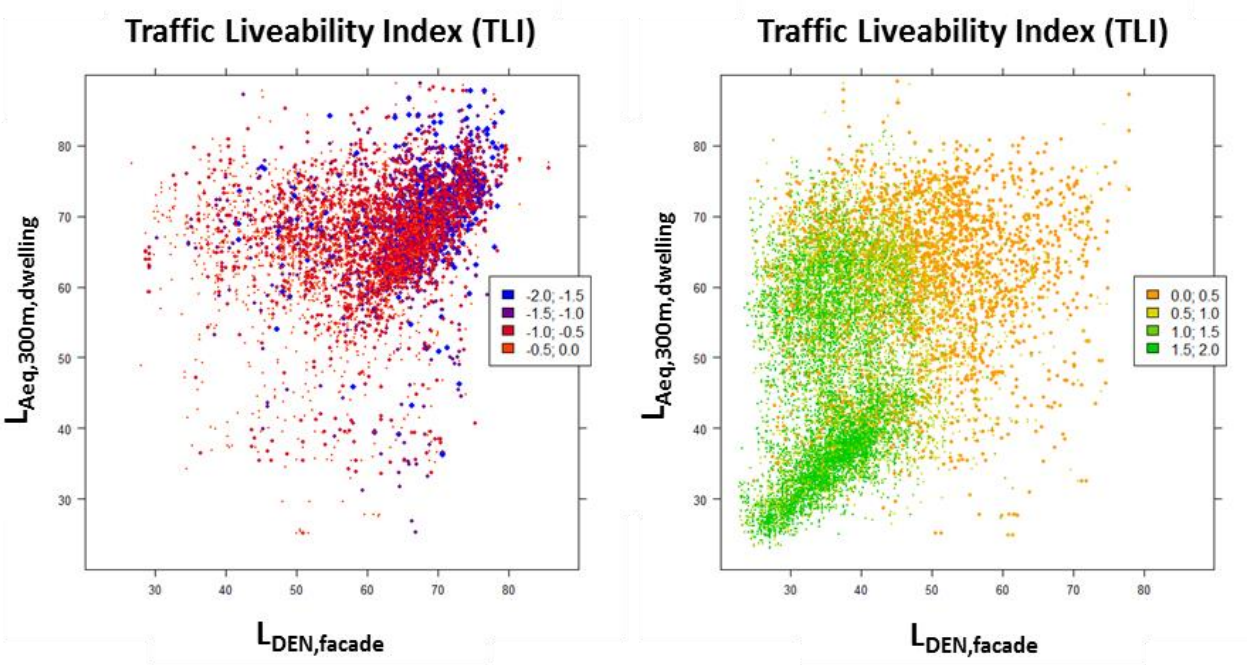

Figure 3.3.1: Calculated Traffic Liveability Index (TLI) presented by exposure at the dwelling facade and the noise exposure along the first 300 m near the dwelling: unsatisfied individuals (left) and satisfied individuals (right). The TLI is expressed in a continuous scale between -2 and + 2.

The negative TLI is mainly related to the high noise levels at the facade, but people are also dissatisfied at lower noise levels at the facade when high noise evaluations along the roads near the dwelling occur. The positive TLI are mainly located at low exposure for both parameters, but the less satisfied people (orange) experience low noise levels at the facade and high noise levels along the roads near the dwelling. The variation indicates the influence

of the other indicators in the TLI aggregation. This illustrates the relevance of noise assessments as a proxy for the subjective perception of the traffic related component in the quality of the environment.

3.4 Conclusions

3.4.1 The importance of noise in QoL

Predicting the personal perception of the quality of life is successful mainly due the noise related indicators. Noise exposure is the strongest component is the overall satisfaction about the dwelling and the neighbourhood in the vicinity of the dwelling in the SLO surveys and consequently also in the QoL indicator aggregation scheme. The noise evaluations captured both the positive and negative aspects of the personal evaluation. The second and third strongest components are traffic count related and are therefore directly related to the noise evaluation. The aggregation model was based on a strongest component technique that favours the noise indicator paths, matching the human perception scheme. The on-road evaluation of the noise exposure is a valid method to include the exposure characteristics near the dwelling and add additional power to the prediction of the personal perception. The overall conclusion is that noise exposure at the dwelling, combined with the on-road evaluation near the dwelling is a very good indicator of the perceived Quality of Life.

3.4.2 Lack of data or spatial resolution in the driving forces

For most of other indicators, an external dataset can be found to perform a qualitative evaluation of the indicator. In some cases the external data source is not available for the whole region of Flanders which inhibits extrapolation to a regional scale. Some of the indicators not be quantified in a dynamical way due to lack of external functions or geographic attributes. In the direct path to health, through traffic accidents, no dynamic traffic accident risk prediction function was available. A traffic accidents function should be based on type of roads, traffic density, type of crossing and availability and quality of bicycle infrastructure.

For air pollution exposure the available maps (yearly averaged PM_{10}) did not express a spatial resolution matching the capabilities of the in-traffic evaluation model. Especially for the in-traffic exposure, not a lot of data was available. Since the presented techniques could evaluate noise exposure along the travelled routes, the basic concept of the PhD emerged. Traffic emits simultaneous noise and air pollution. Can we use the spatial detail for the noise evaluations in the QoL model to improve the resolution for the air pollution exposure?

Chapter 4 Noise based micro-environment specific BC exposure models

4.1 Introduction

A correlation can be expected between the exposure to noise and the exposure to air pollution while being in traffic. The basic research question 'can noise exposure be used as a proxy for in-traffic air pollution exposure' was tested first on the micro-environment with the most direct exposure to noise and air pollution: the bicycle. Both strong spatial effect and strong meteorological effects were to be expected. The combined measurements were performed while commuting by bicycle from home to the office over a one year period. Many different alternative routes were selected in an attempt to cover as much spatial variability during the rush hour.

After communication on this result at the ISEE 2013 conference at Basel, Julian Marshall and Steve Hankey of the University of Minneapolis showed high interest in this approach. A cheap and automated mobile noise measurement implementation, a result from the IWT funded IDEA project, was shipped to Bangalore, India. A pilot study was started to validate the instantaneous exposure model in completely different conditions. In parallel the model was expanded to convert a mobile noise biked map into a yearly average BC exposure along the selected trajectory, introducing a fast and cheap way to map the spatial variability of the noise and air pollution exposure for bicyclists.

A similar measurement campaign was performed for in-vehicle exposure to Black Carbon. Since in-vehicle noise is not useful for modelling, an available noise map is used to evaluate the 'virtual' exposure of the passengers. The next challenge is an indoor BC exposure model. The bicycle measurements are used to recalibrate the noise map and used to predict the indoor BC exposure.

At the end of this chapter, a pilot study with simultaneous monitoring of BC and noise at a high exposed dwelling facade the diurnal pattern of the noise exposure is used to model the local traffic component of the BC exposure at the dwelling.

4.2 An instantaneous spatiotemporal model to predict a bicyclist's Black Carbon exposure based on mobile noise measurements.

Published: Dekoninck L., Botteldooren D. & Int Panis L. 2013. An instantaneous spatiotemporal model to predict a bicyclist's Black Carbon exposure based on mobile noise measurements. Atmospheric Environment, 79, 623-631.

4.2.1 Introduction

Exposure to particulate matter is currently regulated in PM standards, that only distinguish between the size of the particles (PM_{10}, $PM_{2.5}$…). The soot fraction, Black Carbon (BC) is the part of the PM directly related to combustion processes. Recent evidence, summarized by the world health organization, documents the relevance of BC for evaluating traffic related health effects (WHO Europe, 2012). Recent epidemiological results for BC suggest health effects per mass may be up to 10 times higher than PM_{10} (Janssen et al., 2011). Further research into health effects is hampered by the difficulty to measure or model BC concentrations. An important reason for this is the strong spatial variability of BC compared to PM_{10} (Karner et al., 2010). Building a monitoring network for BC would be a daunting task because of the large spatio-temporal gradients. In addition, efforts are now made to standardize BC measurements as a first step to including BC in the set of official air pollution standards. For these reasons, this paper takes a closer look at an innovative way to predict a bicyclist's Black Carbon exposure.

Large personal exposure measurement campaigns prove the relevance of the in-traffic exposure contribution (Dons et al., 2011, 2012). Technology for mobile air pollution measurements is however scarce and expensive. On the one hand, cheap implementations do not meet quality requirements, on the other hand high quality equipment is often highly demanding on the operator (e.g. changing filters or liquids, limited portability). In contrast, mobile noise measurements can be done with low intrusive measurement equipment like dosimeters and new mobile technologies. Mobile noise measurements are a popular theme in noise exposure modelling (Eisenman et al., 2009; Kanjo et al., 2010, Maissonneuve et al., 2009). Noise levels are strongly correlated with traffic related air pollution levels and might be a good proxy to model personal air pollution exposure (Dekoninck et al., 2012; Can et al., 2011; Eisenman et al. 2009). Since in-traffic personal air pollution exposure is a major component of the total personal diurnal exposure and diurnal activity patterns are very diverse within the population, epidemiology would benefit from including exposure differences due

to different activity patterns when investigating the health effects of air pollution (von Klot et al., 2011; Dons et al., 2012). The use of a proxy which is easy to monitor could result in improved personal exposure estimates on larger population samples at a reasonable cost.

Numerous efforts have been made to quantify the exposure and health effects of cycling in dense traffic since the current trends in sustainable mobility focus on establishing modal shifts towards biking and walking (de Nazelle et al., 2011; Int Panis et al., 2010; Berghmans et al., 2009; de Hartog et al., 2010). Exposure of cyclists is directly influenced by the distance to the local traffic, strongly related to local traffic conditions (congestion, traffic lights etc.) and highly influenced by meteorological conditions. Since cyclists often travel along low-traffic-density roads however, there is in general no traffic data available from either counting loops or traffic models. The most important exposure parameter is therefore unknown in most studies. Local traffic on low density roads is also highly variable in both space and time. A suitable traffic description should reflect these short-term effects with an adequate spatial and temporal resolution. Mobile noise exposure therefore has the potential to become this key indicator to predict the local component of traffic related air pollution exposure.

Based on theoretical aspects of traffic dynamics, the relationship between noise and particulate matter emission and the potential to extract one from the other have been discussed earlier (Dekoninck et al. 2012). The focus there was on the selection of noise descriptors correlating best with vehicular particulate matter emissions for typical traffic dynamics. However, noise exposure close to the source is not strongly influenced by the meteorological conditions while air pollution is strongly affected by the meteorological conditions. This is one of the reasons why the average of repeated noise exposure measurements will converge faster compared to repeated air pollution exposure measurements. So, if mobile noise measurements are proven to be a valid proxy for air pollution exposure, fewer measurements will be needed to predict the personal exposure at a higher spatial and temporal resolution.

To establish an instantaneous relationship between noise exposure and air pollution exposure meteorological conditions have to be taken into account. A major concern is the influence of long term meteorology and long distance air pollution transport on the background concentrations influencing the actual personal exposure. In this paper two major research questions are addressed: (1) is a prediction model for BC exposure improved by separating out long term variations in the background concentration; (2) can the instantaneous local Black Carbon exposure be predicted based on instantaneous local noise exposure and meteorological conditions. For the latter, the question how to derive the local traffic dynamics that influence the instantaneous Black Carbon exposure from noise measurements is addressed. Section 4.2.2 will address the methodology including the definition of the models and the noise exposure parameters. Section 4.2.3 gives the results of the models and the model validations. Results are discussed in Section 4.2.4.

4.2.2 Methodology

4.2.2.1 Measurement equipment and setup

The experimental setup contains a basic GPS (in a HTC Desire smart phone), a Type 1 Noise Level Meter (Svantek 959) and a micro-aethalometer (Model AE51 MageeScientific, 2009) to measure Black Carbon. The measurements were performed while commuting by bicycle from the villages to the west of Ghent (Belgium) into the city centre, thus covering the sparsely build areas in the villages, the city centre, open recreational areas and natural reserves in between. A total of 209 biking trips were performed, covering a distance of 2300 kilometre, a total measurement time of 128 hours at an average speed of 18 km per hour. More than 75 km of distinct roads were sampled at least 3 times. Almost all measurements were made between 7:30h-9:30h and 16:30h-18:30h. Some of the longer trips, for example when sampling in the vicinity of the highway, were partially made outside these time windows.

The details of the measurement setup, temporal resolution, pre-processing, meteorological data and the spatial mapping on aggregation points p_x along the network with a spatial resolution of 50 m are available in the supplementary data. In the instantaneous model only one spatial attribute, the street canyon index $StCan_{p_x}$ at aggregation point p_x is included, identifying 'street canyon likeliness' of the built-up area along the trip trajectories. More detail on the calculation of $StCan_{p_x}$ is available in the supplementary data.

4.2.2.2 Black carbon, background and local contribution

The BC exposure during a cycling trip consists of a contribution of local sources and a background contribution. The latter varies only little over a large area and can thus easily be obtained from a well-located fixed measurement station. The background contribution strongly depends on long-term meteorological conditions. The proposed model assumes that the dominant source of BC in the vicinity of the cyclist is the local traffic on the travelled road. An additive approach is used; the BC exposure is viewed as the sum of the background level $BC_{j,bg}$ during trip j and the "local" contribution BC_{loc}. Similar procedures are used in exposure estimations where regional and local scale models are added to estimate personal exposure (Isakov et al., 2009). The available background measurements are averaged concentrations over half an hour (see supplementary data). Subtracting a fixed measurement with a temporal resolution of a half hour from mobile BC measurements sampled at 1 second time interval is not trivial. When sampling air pollution at a shorter time interval, concentrations below the "background" concentrations can be measured at some of the low traffic locations. Adjusting for the background concentration could then result in negative local concentrations. The proposed models will use a logarithm of BC as an outcome variable because noise is also measured on a logarithmic scale and hence negative values cannot be allowed.

For this reason the background concentration is not removed completely but replaced by a typical but constant low background concentration. The choice of this constant is not very critical since it will be added again to the model outcome and constants do not affect the model. This approach enables the dataset to retain spatial variation also for low density roads. Nevertheless a physical reference to the ambient concentration is useful, therefore the long term first quartile concentration over the whole measurement period, $Q1(BC_{bkg,lt})$, equal to 775 ng/m^3, is used. This value does not depend on the route choice of the sampled trip which is an additional benefit. The relation between the measured BC_{raw} and the local contribution BC_{loc} for a location *i* and during a trip *j*, can be written as:

$$BC_{raw,i,j} = BC_{loc,i,j} + (BC_{bkg,j} - Q1(BC_{bkg,lt})) \quad (1)$$

Where $BC_{bkg,j}$ is the background concentration obtained from the continuous measuring station averaged over the whole duration of the trip j. At each aggregation points p_x on the network, the arithmetic average of all *n* measurements of trip j in this collection is calculated as:

$$BC_{loc,p_x,j} = \frac{1}{n}\sum_{\in P_{px,j}} BC_{loc,i,j} \quad (2)$$

4.2.2.3 Noise parameters and physical interpretation

Details of noise parameter calculations are available in the supplementary data. For an even more detailed description of the theoretical and empirical relations of the noise parameters with the BC exposure the reader is referred to Dekoninck et al, 2012. The main arguments for selecting particular noise indicators to be included in the model, based on their physical and technical interpretations, are briefly reminded to the reader. Three noise parameters were included in the instantaneous modelling. The harmonized calculation method used for noise map calculations for the European Union (END Directive) separates the noise emission into an engine contribution and a rolling noise contribution. Engine noise is dominant in the low frequencies; rolling noise is dominant in the high frequencies at higher speeds. The two first parameters are directly related to these emission features. The first parameter $L_{OLF,p_x,j}$ (100 – 200 Hz) describes the engine noise of the nearby traffic at point p_x for trip j. High throttle increases the engine noise. $L_{HLF,p_x,j}$ (1000 – 2000 Hz) is related to the rolling noise. The second parameter $L_{HFmLF,p_x,j}$ is the difference between high and low frequencies in the noise spectrum at point p_x for trip j. High levels of $L_{HFmLF,p_x,j}$ indicate a relatively stronger contribution of high frequencies, compared to low frequencies, indicating more rolling noise than engine noise due to the nearby traffic, hence traffic at higher speed. The third parameter $(L_{Aeq} - L_{Amin})_{p_x,j}$ referred to as the short term dynamics of the noise at point p_x for trip j, indicates the presence of noise events. If noise levels $L_{Aeq,100\ ms}$ within a single second change rapidly, the passing vehicles can individually be detected in the noise

measurements. If $(L_{Aeq} - L_{Amin})_{p_x,j}$ is low, noise levels are constant, indicating constant flow traffic with many sources in the vicinity.

4.2.2.4 GAM modelling

Generalized additive models (GAMs) are regression models where smoothing splines are used instead of linear coefficients for the covariates. This approach has been found to be particularly effective for handling the complex non-linearity associated with air pollution research (Dominici et al., 2002, Pearce et al., 2011). The additive model in the context of spatial exposure modelling can be written in the form:

$$log(BC_{px,j}) = \sum_{z=1}^{n} s_z\,(v_{z,px,j}) + \varepsilon_{x,j} \qquad (3)$$

Where v_z is the z^{th} covariate evaluated for trip j at location p_x; $s_z(v_{z,px,j})$ is the smooth function of z^{th} covariate, n is the total number of covariates, and $\varepsilon_{x,j}$ is the corresponding residual with $var(\varepsilon_{x,j}) = \sigma^2$, which is assumed normally distributed. Smooth functions are developed through a combination of model selection and automatic smoothing parameter selection using penalized regression splines, which optimize the fit and try to minimize the number of dimensions in the model. The main advantage of GAM modelling is the possibility to adjust for non-linear relationships between the covariate and the outcome. The analysis was constructed using the GAM modelling function in the R environment for statistical computing (R development Core Team, 2009) with the package 'mgcv' (Wood, 2006).

Two modelling approaches will be discussed. The first option is to model the measurements on the basic aggregation level: one value for each parameter for each trip at each aggregation point p_x. This dataset contains about 37.700 records and will be referred to as the basic dataset (BDS). The second approach starts the modelling after aggregating the BDS to a dataset averaging the BC exposure for the classified parameters included in the aggregation models. Each of the retained parameters is classified according to a set of predefined percentile classes (see supplementary data). For each of these two approaches the models will be evaluated for both the raw BC result (BC_{raw}) as for the local contribution BC_{loc} to assess the relevance of handling background concentrations separately.

4.2.3 Results

In this section, the following terminology will be used to refer to the different models that will be compared:

- BC_{bkg} model: this model simply assumes that exposure during cycling trips equals concentrations measured at a regional background measurement station.
- BC_{raw} model: uses GAM to obtain BC directly from noise, weather, and geometrical data.

- BC_{loc} model: uses GAM to obtain BC_{loc} and adds measured BC_{bkg} to obtain the overall concentration as shown in Eqs. (1).
- Aggregated BC_{raw} and BC_{loc} models: same as above but with predictive variables categorized in percentile classes.

4.2.3.1 BC_{loc} and BC_{raw} model

The BC_{loc} model is based on the BDS dataset and includes the three noise parameters, wind speed WS_{trip}, temperature $Temp_{trip}$ and street canyon index $StCan_{p_x}$. The parameters of the GAM models are shown in Table 4.2-1. The quality of a GAM model and the relative strength of its parameters are described by the deviance explained, the intercept, the F and p-value for each of its covariates. Since the number of data points in the models is large compared to the number of covariates, the degrees of freedom is large and the p-values are in general too small to be used to compare the covariates. The F-parameters present the relative strength of the covariates instead. In the BC_{loc} model the intercept and the $L_{OLF,p_x,j}$ have a similar strength; the wind speed is about half the strength of $L_{OLF,p_x,j}$.

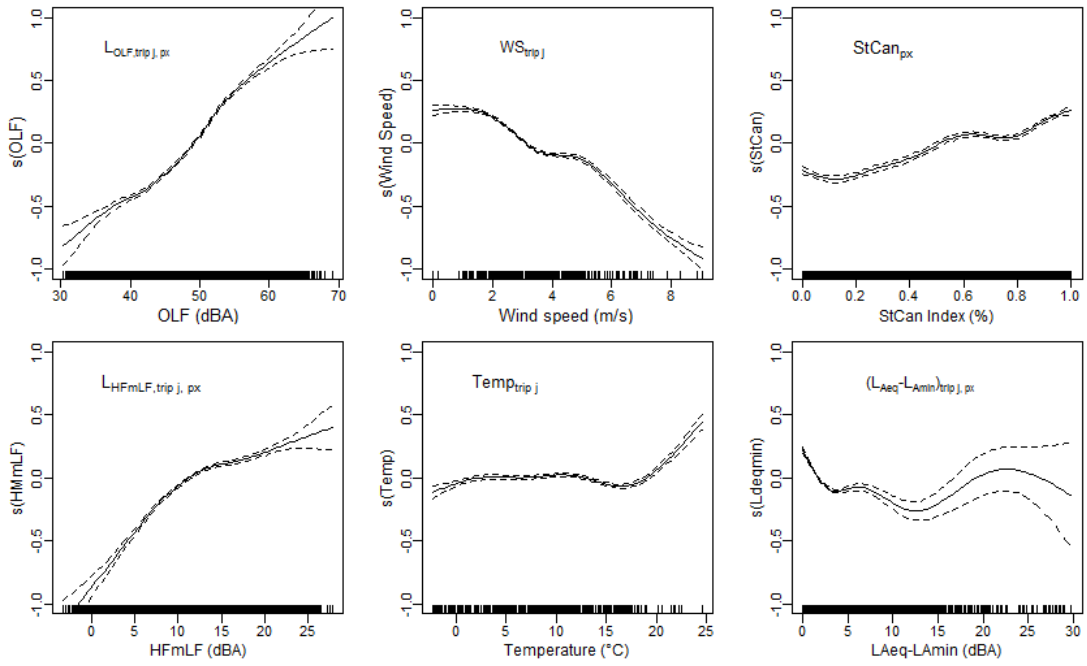

Figure 4.2.1: Splines of the six covariates of the BC_{loc} GAM model, ordered by strength within the model (top-left to bottom-right).

The plots of the splines created by the GAM modeling show the relation of the parameter to the outcome log(BC_{loc}) (Figure 4.2.1). In the BC_{loc} model the $L_{OLF,p_x,j}$ is the strongest component and has a linear relation with log(BC_{loc}). $L_{HFmLF,p_x,j}$ saturates for higher levels. Log(BC_{loc}) decreases for high wind speeds. The street canyon effect is visible as a steady increase of the exposure with a higher street canyon index $StCan_{p_x}$. The temperature is not very important; the steep upward trend is based on only a few trips performed at tempera-

tures above 20 °C. Log(BC_{loc}) increases strongly for very small values of $(L_{Aeq} - L_{Amin})_{p_x,j}$ indicating episodes with almost constant noise levels result in higher BC concentrations.

The BC_{raw} model shows a slightly higher deviance explained than the BC_{loc} model (Table 4.2-1). The BC_{raw} model also has a higher intercept. Wind speed is the strongest component. The low frequency noise level L_{OLF} and temperature have a similar strength.

	BC_{loc}		**BC_{raw}**	
	F	p-value	F	p-value
Intercept	7.82 (2600 ng/m3)		8.14 (3400 ng/m3)	
Intercept (t value)	1961		1755	
$StCan_{p_x}$	165	<2e-16	102	<2e-16
$L_{OLF,p_x,j}$	704	<2e-16	441	<2e-16
WS_{trip}	505	<2e-16	805	<2e-16
$Temp_{trip}$	46	<2e-16	434	<2e-16
$L_{HFmLF,p_x,j}$	245	<2e-16	168	<2e-16
$(L_{Aeq} - L_{Amin})_{p_x,j}$	77	<2e-16	62	<2e-16
Deviance explained	25.9%		26.3%	
Number of datapoints	37722		37722	
Total estimated degrees of freedom	34.47		34.08	

Table 4.2-1: Comparing the results of the BC_{loc} and BC_{raw} models, F-value and p-value.

4.2.3.2 Aggregated BC_{loc} and BC_{raw} models

The aggregated models are built including respectively 3, 4 and 5 parameters. The temperature is not included since it proved to be of little relevance in the BC_{loc} model. In Table 4.2-2 the results of the aggregated models are assembled, including the number of unique combinations of the classified parameters. Again similar changes between the $BC_{raw,Xp}$ and $BC_{loc,Xp}$ models can be detected (where X is the number of aggregation parameters). In Figure 4.2.2 the splines of the five parameter model $BC_{loc,5p}$ are shown. The deviance explained is higher and the splines are smoother compared to the BC_{loc} model due to the aggregation process. In the 3 parameter model L_{OLF} the only acoustic parameter describing the source has the strongest importance in the model, but as other traffic descriptors, L_{HFmLF} and (L_{Aeq}-L_{Amin}) are added, wind speed becomes the most important covariate.

	$BC_{loc,3p}$	$BC_{raw,3p}$	$BC_{loc,4p}$	$BC_{raw,4p}$	$BC_{loc,5p}$	$BC_{raw,5p}$
Intercept	8.1 3300 ng/m3	8.4 4447 ng/m3	8.0 2980 ng/m3	8.3 4020 ng/m3	7.9 2700 ng/m3	8.2 3640 ng/m3
T-value	805	891	908	883	1274	1197
F-statistics						
$StCan_{p_x}$	60	40	134	85	232	148
$L_{OLF,p_x,j}$	271	203	363	605	441	228
WS_{trip}	237	364	301	378	520	744
$Temp_{trip}$						
$L_{HFmLF,p_x,j}$			150	92	224	144
$(L_{Aeq} - L_{Amin})_{p_x,j}$					59	36
Deviance explained	87.0%	86.1%	63.8%	56.1%	41.6%%	35.0%%
Number of data points	360	360	2020	2020	8990	8832
Total estimated degrees of freedom	11.07	10.55	14.27	11.94	18.54	17.59

Table 4.2-2: Comparing the results of the aggregated models.

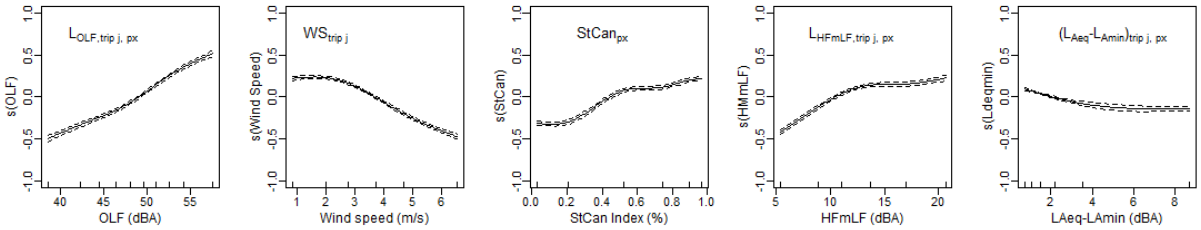

Figure 4.2.2: Splines of the five covariates of the GAM $BC_{loc,5p}$ model.

4.2.3.3 Comparing the fit of the models

The BC exposure during individual trips is reconstructed based on the models presented above. The results for the BC_{bkg}, BC_{loc} and BC_{raw} models are shown in Figure 4.2.3. The second row shows the results of the BC_{loc} model, and the third row the results of the BC_{raw} model. Each point in the charts represents a single trip. The x-axis shows the measured BC exposure, the y-axis the model outcome.

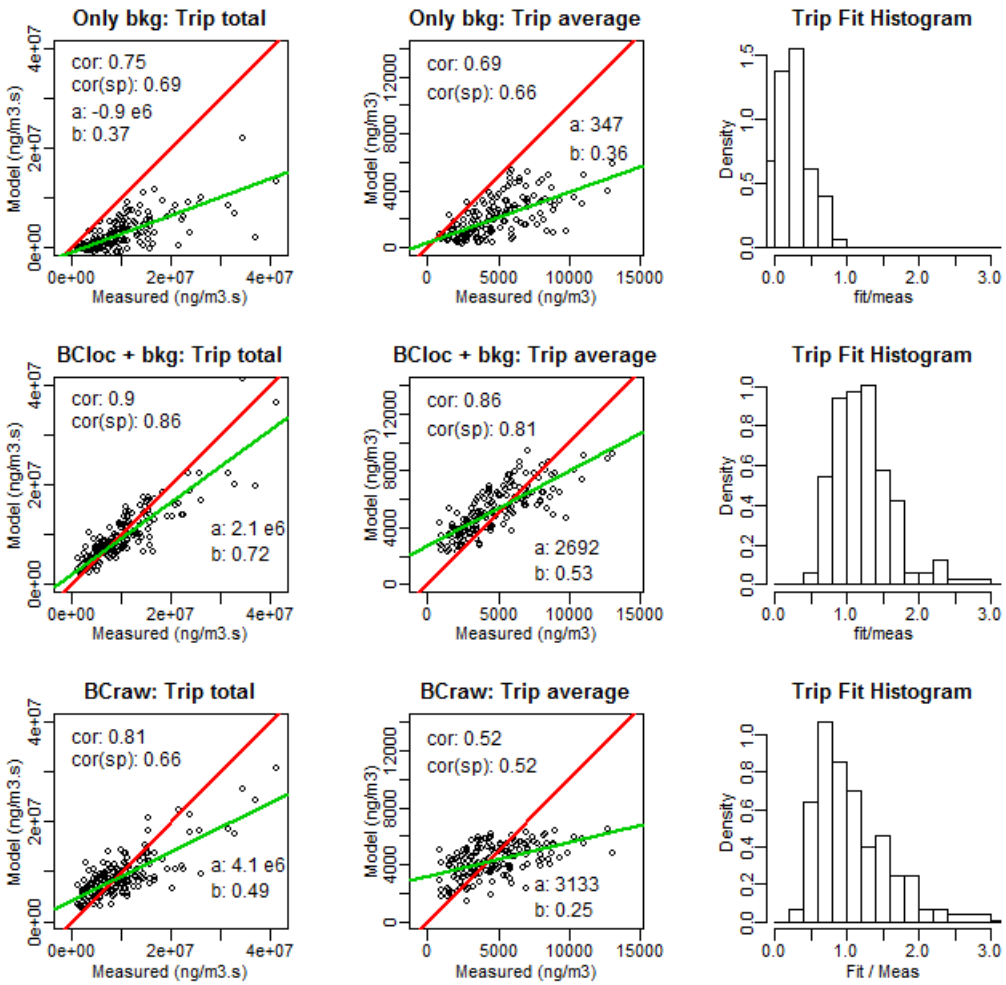

Figure 4.2.3: Evaluation of the model fit of the BC_{bkg}, BC_{loc} and BC_{raw} models. Each point in the charts represents a single trip. The first row shows the results of the BC_{bkg} model, the second row the results of the BC_{loc} model, the third row the results of the BC_{raw} model.

The first column shows the total trip exposure (as ng/m^3 * seconds), the second column the average exposure over the trip. Both are relevant, but the correlation in the first column is strongly influenced by the duration of the trip. The predictive quality of the models is best determined by the ability to predict the trip averaged exposure. In each of these charts, the diagonal (red) and the linear fit (green) on the results are shown and the correlation and the spearman's correlation between model and measurement are given. The properties (intercept and slope) of the linear fit are shown to evaluate the model fits. The third column shows the distribution of the relative prediction: total model BC divided by total measured BC, presenting the under- and overshoots of the trip total exposure prediction, which is identical for the total and averaged evaluation.

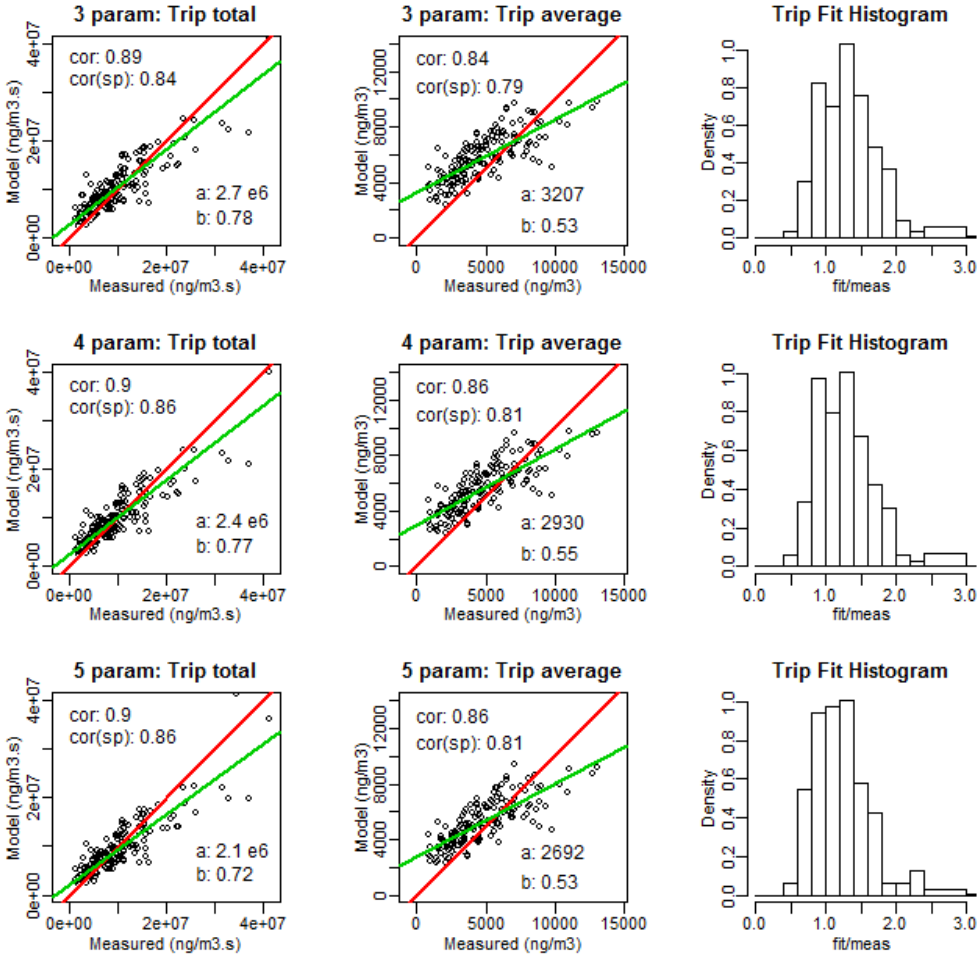

Figure 4.2.4: Evaluation of the model fit of the aggregated BC_{loc} models for 3, 4 and 5 parameters.

A similar procedure is performed for the aggregated models. For each passage at an aggregation point the corresponding classification is used to estimate BC exposure. Summing all results over the full trajectory reconstructs the total trip exposure. In Figure 4.2.4 the fitting properties of the reconstructed trips of the $BC_{loc,Xp}$ models are shown for the three aggregated models on BC_{loc}. The aggregated BC_{raw} model evaluations are not shown.

4.2.3.4 Comparing the predictive strength of the models

The predictive strength of the models is checked by building variants of the models based on a random subset of 75% of the available trips and then predicting the remaining trips. This procedure is repeated 50 times. For each trip, a set of approximately 13 predictions for different model variants are thus available. The average BC trip exposure is calculated for the trips used to build the model (referred to as 'fitted trips') and predicted for the trips left out of the model (referred to as 'predicted trips'). The Pearson correlation of the fitted trips versus the measurements and the predicted tips versus the measurements are calculated for each model variant. The distributions of the correlations of the fitted trips of the model variants and the distributions of correlations of predicted trips out of the model variants are shown by model type in Figure 4.2.5. The mean correlations of the total exposure of the fitted trips for the models (as ordered in Figure 4.2.5) are 0.90, 0.86, 0.88, 0.89 and 0.89, the mean correlations of the total exposure of the predicted trips are 0.88, 0.84, 0.89, 0.90 and 0.90. The mean correlations of the averaged exposure of the fitted trips for the models are 0.78, 0.71, 0.75, 0.77 and 0.77; the mean correlations of the averaged exposure of the predicted trips are 0.75, 0.67, 0.75, 0.78 and 0.74. Models BC_{loc}, $BC_{loc,4p}$ and $BC_{loc,5p}$ have similar distributions for both the fitted trips and the predicted trips. The predicted trips show wider distributions compared to the fitted trips. BC_{raw} and $BC_{loc,3p}$ perform significantly worse than BC_{loc}, $BC_{loc,4p}$ and $BC_{loc,5p}$. The correlation of the predicted trips of BC_{raw} model is extremely sensitive to the trip selection. Figure 4.2.5C shows the relation between the correlations of the fitted and predicted trips for the individual model variants. Correlations of the predicted trips are not necessarily lower than the fitted trips. The correlation of the predictions can be higher than the correlation of the fitted trips, especially for the BC_{loc} and $BC_{loc,xp}$ models (Figure 4.2.5C).

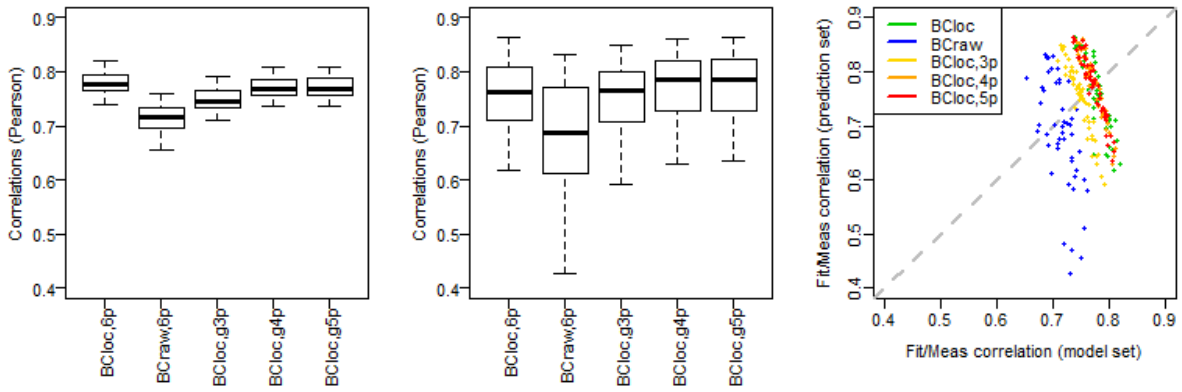

Figure 4.2.5: Distributions of the model variants correlation of the fitted trips (A), distributions of the model variants correlation of the predicted trips (B) and the relations between the correlation of the fitted trips and the correlation of the predicted trips for the individual model variants (C).

For each set of predictions of a single trip obtained from a model variant, the average prediction and the standard deviation of the trip predictions is calculated. The relative prediction (average of the total trip predictions divided by the total measured for trip j) and the

standard deviation of the trip j predictions divided by the trip j total exposure are used to compare the predictive strength and sensitivity of the model variants to the random sampling strategy. The results are shown in two charts in Figure 4.2.6. The BC_{loc} model is slightly underestimating the exposure, BC_{raw} and $BC_{loc,3p}$ are overestimating, the $BC_{loc,4p}$ and $BC_{loc,5p}$ models are centred around 1.0. The interquartile range of the distribution of the relative trip predictions for the BC_{loc} model is 0.38, the ranges are slightly larger for the $BC_{loc,4p}$ and $BC_{loc,5p}$ models, respectively 0.47 and 0.43. The interquartile range of the BC_{loc} model is 3.1, the BC_{raw} model performs much worse (IQR 5.8). The best IQR is found for the $BC_{loc,5p}$ model with 1.8. All aggregated models perform better than the BC_{loc} model for the distribution of the standard deviation of the trip predictions.

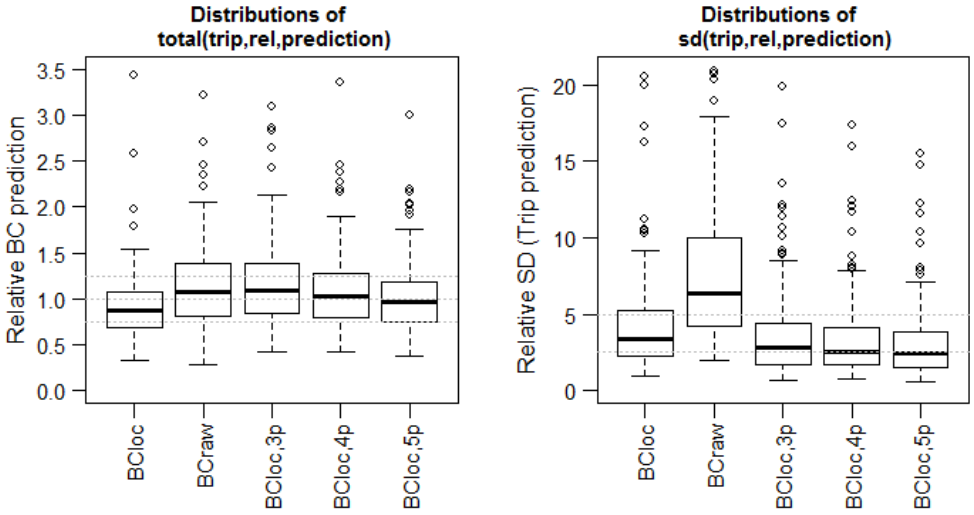

Figure 4.2.6: Distribution of the average of the relative trip predictions (A) and the distribution of the standard deviations of the trip prediction relative to the trip total measured BC (B), presented by model.

4.2.4 Discussion

The first research question investigates whether a prediction model for BC exposure could be improved by separating out long term variations in the background concentration; the second research question whether the instantaneous local Black Carbon exposure could be predicted on the basis of local noise exposure and meteorological conditions. The first research question is addressed by comparing BC_{bkg}, BC_{loc} and BC_{raw} models. The second research question is addressed by evaluating the features of BC_{loc}, $BC_{loc,3p}$, $BC_{loc,4p}$, $BC_{loc,5p}$ models.

The BC_{bkg} model accounts on average for 30-40% of the total trip exposure only, but the slope in the relation between modelled and measured exposure is as large as 0.36 (Figure 4.2.3). High average trip exposure is partially related to higher background concentrations. Although the BC_{raw} model on average results in a good estimate of the average exposure during cycling trips, the trend line connecting prediction to measurement (Figure 4.2.3)

slopes at 0.25. The strong influence of wind speed and temperature indicates that this model mainly tries to resolve the temporal variations in the background contributions and fails to include indicators for local exposure. Integrating the GAM model for BC_{loc} with measured BC_{bkg} combines best of both worlds: temporal variability of the BC_{bkg} with spatial variability of the BC_{loc} model and results in a slope between modelled and measured average trip exposure of 0.53.

A similar conclusion can be drawn when evaluating the predictive power of the models in Section 3.4. The wide distribution of the correlations of the predicted trips in the model variants of the BC_{raw} model (Figure 4.2.5B) and the high relative standard deviation of the individual trip prediction (Figure 4.2.6B) illustrate the sensitivity of the BC_{raw} model to the trip selection. All variants of the BC_{loc} model perform significantly better. The BC_{loc} model is slightly sensitive to over fitting for the low exposure values, which is reflected in the underestimation of the relative trip prediction (Figure 4.2.6A).

As it is now established that the BC_{loc} models outperform models that aim at predicting the whole exposure at once, let us now look in detail at the choice of predictive variables for these models. In the BC_{loc} model $L_{OLF,p_x,j}$ is the strongest component and wind speed the second strongest. The negligible importance of temperature in the model can be explained as follows. Temperature is expected to affect emission and is an indicator for meteorological conditions that influence dispersion. The background concentration indeed shows a distinctive seasonal pattern and temperature is related to season (see supplementary data 1.9 figure S3). BC_{bkg} seems to include the temperature dependence sufficiently thereby reducing the relevance of temperature in the BC_{loc} model. Wind speed has a similar relationship with background concentration as temperature (supplementary data 1.9 figure S4). The strength of the wind speed covariate is therefore also reduced in the BC_{loc} compared to its strength in the BC_{raw} model but in contrast to the temperature, it is still highly relevant. This is explained by the observation that wind speed not only influences background concentrations but also instantaneous dispersion of the local emissions. Higher wind speeds reduce the local exposure of cyclists. StCAN and L_{HFmLF} are also stronger in the BC_{loc} model compared to the BC_{raw} model probably because major confounders are eliminated by treating BC_{bkg} separately. The BC_{loc} model becomes more sensitive to spatially varying variables such as vehicle speed and local air pollution accumulation. The latter effect and its dependence on street canyon geometry (measured here as StCAN) is confirmed by physical calculations of street canyon accumulation, validated with measurements, such as the one presented by Berkowicz et al (2008).

High-degree-of-freedom models such as the GAM model risk to over fit the data that they are based on while losing the ability to generalize to other situations. This can be prevented by reducing the number of input variables (covariates) and –in the particular case of GAM models – also by reducing the number of values that the variable can take. Classification of the covariates indeed reduces the degrees of freedom (Table 4.2-2) in the model. Because of

the change in number of data points, the goodness-of-fit parameters and the strength of the covariates in the models cannot be compared directly, the quality of the models is determined by evaluating the properties of the predictions. In addition, a lower number of variables reduces the complexity of the model and simplifies implementation.

Turning to the model prediction evaluation shown in Figure 4.2.5 and Figure 4.2.6, it is clear that the $BC_{loc,g3p}$ model performs worse than the BC_{loc} model in predicting the average exposure. This is not unexpected as the information used in the prediction is significantly reduced. The reduction in number of covariates and the clustering of values is expected to make the model less sensitive to trip sampling. For $BC_{loc,g3p}$ the aggregation is too strong to observe this positive effect. The $BC_{loc,g4p}$ and $BC_{loc,g5p}$ models slightly outperform the BC_{loc} model when evaluated for correlation between model and the measurement data not used for fitting (Figure 4.2.5B). The distribution of relative trip predictions (Figure 4.2.6A) is wider for the $BC_{loc,g4p}$ and $BC_{loc,g5p}$ models compared to the BC_{loc} model, but the distributions are centred around 1. The relative standard deviation of the individual trip prediction (Figure 4.2.6B) is slightly better. The $BC_{loc,g5p}$ outperforms the BC_{loc} model despite the fact that it only reduces the number of data points from 37722 to 8832. The aggregation process removes the lowest values in the basic dataset, resulting in a better prediction of the total trip BC exposure.

It is more difficult to distinguish between the $BC_{loc,g4p}$ and $BC_{loc,g5p}$ models. The only relevant difference is the reduction of the intercept in the $BC_{loc,g5p}$ model. The short term dynamics (L_{Aeq}-L_{Amin}) covariate – the variable differentiating $BC_{loc,g5p}$ from $BC_{loc,g4p}$ – distinguishes between two different traffic conditions: low values can be linked to situations of congested traffic, many cars with constant noise emission (idling) result in constant noise levels; high values indicate short distinct events, typically a single car passing by at a relatively high speed. This last traffic situation is however rare during the rush hour and is under represented in our (rush hour only) database. When similar measurements would be performed outside the rush hour, this covariate might prove more relevant. With the available measurements it cannot be concluded that the $BC_{loc,5p}$ model is better than $BC_{loc,4p}$ model.

In general, the simplification of the model improves its quality as long as the 4 or 5 most significant parameters are kept. The models suggested in this paper perform well mainly due to the unique choice of noise indicators that are directly related to relevant traffic dynamics. The L_{OLF} covariate detects traffic volume including acceleration both linked to higher particulate emissions. L_{HFmLF} indicates the traffic speed; emissions increase with speed at low speeds, but saturate at higher speeds because constant high speeds result in more efficient combustion processes and lower particulate emissions. Similar relationships were reported for nanoparticles in Uhrner et al., 2011 and for gaseous emissions in De Vlieger et al., 2000. This also explains why models based on L_{Aeq} are less successful: L_{Aeq} is related to human loudness perception and does allow distinguishing situations with different traffic dynamics (Boogaard et al., 2008). Ross et al., 2011 relates a spectral noise evaluation to air pollution

on a fixed monitoring station. Although these measurements are not directly comparable with the measurements in this paper, the same frequency bands are found to be relevant.

4.2.5 Conclusions

This paper proves that it *is* possible to predict instantaneous BC exposure based on mobile noise measurements. The in-traffic exposure to Black Carbon of bicyclists is determined by background concentration, distance to source, local traffic density and speed, local traffic dynamics, local street geometry, and meteorological conditions. Spectral evaluation of (mobile) noise measurements can be used to implicitly detect local traffic conditions directly related to the local BC emission. Predicting personal BC exposure of cyclists proved only successful after splitting the model into a background contribution and a local component. In particular, it was shown that the spatial variability due to the local traffic contribution can be modelled using four parameters: the low frequency noise L_{OLF} related to the traffic volume and engine throttle, the difference between high and low frequencies L_{HFmLF} related to the traffic speed, the instantaneous wind speed and the street canyon index both related to the local accumulation of BC. The overall trip exposure is predicted by the four categorized parameters GAM model, $BC_{loc,g4p}$, with a correlation of 0.90. The average trip exposure is predicted with a correlation of 0.78.

The structure of the model presented in this paper can be expected to be valid for different areas in the world since parameters are chosen with a physical background in mind and because the model has been well validated. Since fleet composition and driving behaviour might differ between different parts of the world, it is suggested that each mobile noise measurement campaign is accompanied with a partial BC sampling to re-establish the model coefficients. The measurement underlying the specific model presented here, are performed in a typical (European) environment, a medium size city including suburbs and green areas, representative for the living environment of the majority of the population in Europe. The exact same model including model coefficients is expected to be applicable in any city sufficiently similar to this situation.

Mobile noise measurements on bicycles have the potential to provide the spatial detail and high temporal resolution that is necessary to predict the urban exposure to black carbon, including the local effects of route choice. Mobile noise measurements therefore have the power to replace large scale in-traffic personal air pollution exposure measurements and can be performed on larger populations at a significantly lower cost than traditional participatory sampling techniques. In this way the results obtained in this study could be useful for raising public awareness, changing personal behaviour by selecting low exposure routes and to perform large scale epidemiological research on the impact of personal BC exposure on health.

4.2.6 References

Berghmans, P.; Bleux, N.; Int Panis, L.; Mishra, V. K.; Torfs, R.; Van Poppel, M., Exposure assessment of a cyclist to PM(10) and ultrafine particles. Science of the Total Environment 2009, 407, (4), 1286-1298.

Boogaard, H.;Borgman F.;Kamminga J.; Hoek G.; Exposure to ultrafine and fine particles and noise during cycling and driving in 11 Dutch cities. Atmosferic environment 43 (2009) 4234-4242.

Berkowicz R., Ketzel M., Jensena S.S, Hvidberg M., Raaschou-Nielsen http://www.sciencedirect.com/science/article/pii/S1364815207000783 - aff2 O., Evaluation and application of OSPM for traffic pollution assessment for a large number of street locations, Environmental Modelling & Software 2008, 296-303.

Can, A.; Botteldooren, D., Towards Traffic Situation Noise Emission Models. Acta Acustica United with Acustica 2011, 97, (5), 900-903.

Can, A.; Leclercq, L.; Lelong, J.; Botteldooren, D., Traffic noise spectrum analysis: Dynamic modeling vs. experimental observations. Applied Acoustics 2010, 71, (8), 764-770.

de Hartog, J. J.; Boogaard, H.; Nijland, H.; Hoek, G., Do the health benefits of cycling outweigh the risks? Environ Health Perspect. 2010 August; 118(8): 1109–1116.

de Nazelle, A.; Fruin, S.; Westerdahl, D.; Martinez, D.; Matamala, J.; Kubesch, N.; Nieuwenhuijsen, M., Traffic Exposures and Inhalations of Barcelona Commuters. Epidemiology 2011, 22, (1), S77-S78.

Dekoninck, L.; Botteldooren, D.; Int Panis, L., Guidelines for participatory noise sensing based on analysis of high quality mobile noise measurements. Internoise 2012 (conference), 394-402

De Vlieger I., D De Keukeleere D., Kretzschmar J.G., Environmental effects of driving behaviour and congestion related to passenger cars, Atmospheric Environment, Volume 34, Issue 27, 2000, Pages 4649-4655

Dominici, F.; McDermott, A.; Zeger, S. L.; Samet, J. M., On the use of generalized additive models in time-series studies of air pollution and health. American Journal of Epidemiology 2002, 156, (3), 193-203.

Dons, E.; Int Panis, L.; Van Poppel, M.; Theunis, J.; Willems, H.; Torfs, R.; Wets, G., Impact of time-activity patterns on personal exposure to black carbon. Atmospheric Environment 2011, 45, (21), 3594-3602.

Dons, E.; Int Panis, L.; Van Poppel, M.; Theunis, J.; Wets, G., Personal exposure to Black Carbon in transport microenvironments. Atmospheric Environment 2012, 55.

Eisenman, S. B.; Miluzzo, E.; Lane, N. D.; Peterson, R. A.; Ahn, G.-S.; Campbell, A. T., BikeNet: A Mobile Sensing System for Cyclist Experience Mapping. Acm Transactions on Sensor Networks 2009, 6, (1).

Foraster, M.; Deltell, A.; Basagana, X.; Medina-Ramon, M.; Aguilera, I.; Bouso, L.; Grau, M.; Phuleria, H. C.; Rivera, M.; Slama, R.; Sunyer, J.; Targa, J.; Kunzli, N., Local determinants of road traffic noise levels versus determinants of air pollution levels in a Mediterranean city. Environmental Research 2011, 111, (1), 177-183.

Int Panis, L.; de Geus, B.; Vandenbulcke, G.; Willems, H.; Degraeuwe, B.; Bleux, N.; Mishra, V.; Thomas, I.; Meeusen, R., Exposure to particulate matter in traffic: A comparison of cyclists and car passengers. Atmospheric Environment 2010, 44, (19), 2263-2270.

Isakov, V., J. S. Touma, et al. (2009). "Combining Regional- and Local-Scale Air Quality Models with Exposure Models for Use in Environmental Health Studies." Journal of the Air & Waste Management Association 59(4): 461-472.

Kanjo, E., NoiseSPY: A Real-Time Mobile Phone Platform for Urban Noise Monitoring and Mapping. Mobile Networks & Applications 2010, 15, (4), 562-574.

Maisonneuve, N.; Stevens, M.; Niessen, M. E.; Steels, L., NoiseTube: Measuring and mapping noise pollution with mobile phones. Information Technologies in Environmental Engineering 2009, 215-228.

Pearce, J. L.; Beringer, J.; Nicholls, N.; Hyndman, R. J.; Tapper, N. J., Quantifying the influence of local meteorology on air quality using generalized additive models. Atmospheric Environment 2011, 45, (6), 1328-1336.

Ross Z., Kheirbek I., Clougherty J., Ito K., Matte T., Markowitz S., Eisl H., Noise, air pollutants and traffic: Continuous measurement and correlation at a high-traffic location in New York City. Environmental Research, 2011, 1054-1063.

Uhrner, U., M. Zallinger, et al. (2011). "Volatile Nanoparticle Formation and Growth within a Diluting Diesel Car Exhaust." Journal of the Air & Waste Management Association 61(4): 399-408

von Klot, S.; Cyrys, J.; Hoek, G.; Kuhnel, B.; Pitz, M.; Kuhn, U.; Kuch, B.; Meisinger, C.; Hormann, A.; Wichmann, H. E.; Peters, A., Estimated Personal Soot Exposure Is Associated With Acute Myocardial Infarction Onset in a Case-Crossover Study. Progress in Cardiovascular Diseases 2011, 53, (5), 361-368.

WHO Europe, 2012: Health effects of black carbon, ISBN: 978 92 890 0265 3.

Wood, S. N., On confidence intervals for generalized additive models based on penalized regression splines. Australian & New Zealand Journal of Statistics 2006, 48, (4).

4.3 Using city-wide mobile noise assessments to estimate bi-cyclists annual exposure to Black Carbon

Published: Dekoninck, Luc, Dick Botteldooren, and Luc Int Panis. "Using city-wide mobile noise assessments to estimate annual exposure to Black Carbon.", *Environment international* 83 (2015): 192-201

ABSTRACT

Several studies have shown that a significant amount of daily air pollution exposure, in particular Black Carbon (BC), is inhaled during bicycle trips. Previously, the instantaneous BC exposure of cyclists was modelled as the sum of a background concentration and a local traffic related component based on a local assessment of traffic noise. We present a fast and low cost methodology to achieve a city-wide assessment of yearly average BC exposure of cyclists along their trips, based on a city-wide mobile noise sensing campaign.

The methodology requires participatory sensing measurements of noise, partially combined with BC and/or other air pollutants sensitive to local traffic variations. The combined measurements cover the spatial and meteorological variability and provide the data for an instantaneous exposure model. The mobile noise-only measurements map the full city; and yearly meteorology statistics are used to extrapolate the instantaneous exposure model to a yearly average map of in-traffic air pollution exposure. Less than four passages at each segment along the network with mobile noise equipment are necessary to reach a standard error of 500 ng/m^3 for the yearly average BC exposure.

A strong seasonal effect due to the BC background concentration is detected. The background contributes only 25% to the total trip exposure during spring and summer. During winter the background component increases to 50-60%. Engine related traffic noise along the bicyclist's route is a valid indicator of the BC exposure along the route, independent of the seasonal background. Low exposure route selection results in an exposure reduction of 35% in winter and 60 % in summer, sensitive to the weather conditions, specific trip attributes and the available alternatives.

The methodology is relevant for further research into the local effects of air pollution on health. Mobile noise mapping adds local traffic data including traffic dynamics into the air pollution exposure assessments. Local policy makers and urban planners can use the results to support the implementation of low exposure infrastructure, create awareness through route planners and achieve behavioural changes toward active travel modes.

4.3.1 Introduction

Exposure to particulate matter is currently regulated in PM standards that only distinguish between the size of the particles but not between the composition and thus origin of the particulate matter. The soot fraction or Black Carbon (BC) is a fraction of the PM directly related to combustion processes. Recent evidence, summarized by the World Health Organization (WHO), documents the relevance of BC for evaluating traffic related health effects (WHO Europe, 2012). BC is more sensitive to traffic emissions and is able to detect local exposure differences not available in the PM_{10} evaluations. The first epidemiological results based on BC exposure detect health effects up to ten times stronger compared to the similar evaluations based on PM_{10} (Janssen et al. 2011).

Large personal exposure measurement campaigns prove the relevance of the in-traffic exposure contribution to daily personal exposure (Dons et al., 2011, 2012). Technology for mobile air pollution measurements is however scarce and expensive. The high variability of the in-traffic exposure is partially due to the strong influence of meteorology on the exposure, swamping the variability due to the local traffic densities and dynamics (Dons et al., 2013). In previous work of the authors, an instantaneous spatiotemporal model based on mobile noise measurements for cyclists was proposed (Dekoninck et al., 2013). It was shown that noise measurements are a good proxy for local traffic intensity and local traffic dynamics. The instantaneous spatiotemporal model splits the BC exposure of a cyclist into a background component and a component of local origin. In the Flemish region, only one continuous monitoring station was available at the time of the measurement campaign that can act as a background concentration (Antwerpen-Linkeroever – 40AL01). After adjusting for the background contribution the local variation in the traffic density and traffic dynamics successfully predicts the BC exposure of the cyclists using four parameters: the low frequency noise (L_{OLF}) related to the traffic volume and engine throttle, the difference between high and low frequencies (L_{HFmLF}) relating to the traffic speed, the instantaneous wind speed and the street canyon index (StCan). Wind speed and street canyon features affect the dispersion of BC. The background adjusted model significantly reduced the temperature dependency of the bicyclist exposure. All temperature dependency, regardless of the origin (other BC sources, meteorology or vehicle fleet related aspects) is resolved in the background contribution. In other work, the instantaneous model approach was validated in completely different traffic conditions (Bangalore, India). The quality of the background adjustment was related to the properties of the background measurement location (Dekoninck et al, 2015). Meteorological conditions thus enter this model directly through the wind speed and indirectly via temperature and wind speed in the background BC concentration. Wind direction was not included in the model. The strongest component in the local traffic related exposure is the traffic within meters from the cyclists, resulting in correlation of 0.86 with only four parameters. Wind direction is not relevant at such small distances to the source. The noise

measurements quantify the local traffic and traffic dynamics. The strengths of the method are based on the possibility to quantify the local traffic properties and by adding missing traffic data at low density traffic roads.

For many applications however, there is a strong interest in annual average rather than instantaneous levels of exposure. The internal validation of the instantaneous model - predicting 25% of the trips using models fit on the other 75% of the trips- resulted on average in a correlation of the trip averaged BC exposure of 0.77 (Dekoninck et al., 2013). The intrinsic quality of the instantaneous model to predict a single trip under any meteorological conditions or trajectory is strong and enables the simulation of yearly average exposure during bicycle trips without further validation. One of the remaining questions is whether subtracting a measured background concentration results in a valid local contribution that can actually be interpreted as the contribution of the local traffic (BC_{loc}). If this is the case, the model should result in BC_{loc} approaching zero with low traffic intensity. As an alternative, the behavior of the strongest component in the spatiotemporal model, L_{OLF} is proposed as a good indicator of the background adjustment since this component is directly related to the presence of traffic. When the spatiotemporal model reveals a linear relationship between L_{OLF} and $\log(BC_{loc})$, the background adjusted exposure will by consequence only include local traffic related exposure. For low L_{OLF}, the local contribution in the instantaneous model dwindles to values close to the detection limit of the BC measurement equipment. Therefore the background location and the applied background correction are valid.

In each mobile measurement campaign only a limited number of potentially occurring situations is sampled. Bias is introduced into the measurements due to the combination of route choice, instantaneous meteorological conditions and instantaneous background exposure, each of them subject to unintended selection bias. It is therefore impossible to perform a measurement campaign covering all combinations of the exposure variables with unbiased exposure as the result. This paper will therefore introduce a methodology to convert a map of biased mobile measurements into a yearly average unbiased BC exposure map building upon the available instantaneous model (Dekoninck et al., 2013). This will be achieved in two phases. First the instantaneous exposure will be extrapolated to a yearly average by applying the spatiotemporal model for all meteorological situations to all available mobile noise measurements. In the second phase the instantaneous noise exposure is replaced by the average noise exposure at that location. In this way all dependence on meteorology can be removed, and the typical traffic situation at each location along the network is characterized using mobile noise measurements from a small but sufficient number of passages. This results in a spatial model, only based on local traffic related features (derived from noise) and a street canyon index (a parameter describing the accumulation of BC in narrow streets).

Several research questions will be addressed: how can a mobile noise measurement campaign be used to predict the annual average BC exposure for cyclists and how many noise measurement trips are necessary to reliably estimate the local traffic contribution. In addi-

tion, the effect of seasonal meteorological changes on the local traffic related BC exposure and on the total exposure will be illustrated. The potential exposure reduction by choosing low exposure routes is quantified.

4.3.2 Methodology and data processing

4.3.2.1 Methodology

The instantaneous model is based on 209 rush hour commuting trips by bicycle from the villages to the west of Ghent (Belgium) into the city centre. More than 75 km of distinct roads were sampled at least 3 times. The BC measurements are performed with the micro-aethalometer AE51 (Aethlabs.com, San Francisco). The details are available in Dekoninck et al., 2013 and the supplementary data. The instantaneous log-transformed model will be referred to as $BC_{loc,temporal}$ in this paper. The subscript 'temporal' is added to avoid confusion with the spatial yearly average models that will be developed in this work. Thus, to obtain a meteorology averaged BC exposure of cyclists, only wind speed and background concentration have to be accounted for. To implement a correction towards yearly representative meteorological conditions, the meteorological conditions are categorized according to the meteorological dependencies in $BC_{loc,temporal}$: wind speed and background concentration. A joint distribution over these two variables should be used because background BC concentration itself strongly depends on wind speed. The meteorological classes are presented in Section 4.3.2.2.

To obtain a yearly averaged value, the $BC_{loc,temporal}$ model is applied for a sufficiently large number of bicycle commuting trips passing through each evaluation point along the road network for each combined meteorological - background concentration class observed during a year. This means that the instantaneous wind speed and background concentration of that specific trip are replaced in the model by the wind speed and background concentration of the evaluated meteorological class. For each spatial evaluation point, the resulting dataset contains a BC estimate for each noise-measuring trip and each meteo/background class, Met_{cl}. A weighted average is applied according to the frequency of occurrence during a year of Met_{cl}, merging the results spatially for all trips passing by at a specific location.

In mathematical form, the procedure is summarized as follows. The local contribution to the measured BC concentration $BC_{loc,meas,i,j}$ for a location *i* and during a trip *j*, is written as:

$$\mathrm{BC}_{\mathrm{loc,meas,i,j}} = \mathrm{BC}_{\mathrm{tot,meas,i,j}} - \mathrm{BC}_{\mathrm{bg,j}} \quad (1)$$

Using the previously derived model, this contribution is approximated using Generalized Additive Models (GAM) (Wood, 2006). Several authors in air pollution research have applied this technique successfully (Dominici et al., 2002, Pearce et al., 2011, Li et al., 2013). The modeled BC concentration is obtained for each location i during trip j as:

$$\mathrm{BC_{loc,temporal,i,j}} = \exp(\mathrm{gamBC_{loc,temporal}}(\mathrm{L_{OLF,i,j}}, \mathrm{L_{HFmLF,i,j}}, \mathrm{StCan_i}, \mathrm{WS_j})) \quad (2a)$$

$$\mathrm{BC_{tot,temporal,i,j}} = \exp(\mathrm{gamBC_{loc,temporal}}(\mathrm{L_{OLF,i,j}}, \mathrm{L_{HFmLF,i,j}}, \mathrm{StCan_i}, \mathrm{WS_j})) + \mathrm{BC_{bg,j}} \quad (2b)$$

Note that all spatiotemporal dependence of the GAM model is implicitly included via the model covariates and that the background contribution is assumed location independent. Applying the wind speed and BC background concentration for all meteorological conditions $\mathrm{Met_{cl}}$ on each trip j:

$$\mathrm{BC_{loc,year,i,j}} = \frac{1}{\sum_{\mathrm{Metcl}} \mathrm{w_{Metcl}}} \sum_{\mathrm{Metcl}} \mathrm{w_{Metcl}} \left(\mathrm{gamBC_{loc,temporal,i,j}}\right) \quad (3)$$

$$\mathrm{BC_{tot,year,i,j}} = \frac{1}{\sum_{\mathrm{Metcl}} \mathrm{w_{Metcl}}} \sum_{\mathrm{Metcl}} \mathrm{w_{Metcl}} \left(\mathrm{gamBC_{tot,temporal,i,j}}\right) \quad (4)$$

Note that this result still has a weak dependence on trip number, and thus time, via the measured sound parameters and via the chosen route at that specific time. By aggregating all measurement trips to a spatial point p_i along the network, the spatial distribution is obtained:

$$\mathrm{BC_{loc,year,i}} = \frac{1}{\mathrm{n}} \sum_{\mathrm{j}} \mathrm{BC_{loc,year,i,j}} \quad (5)$$

$$\mathrm{BC_{tot,year,i}} = \frac{1}{\mathrm{n}} \sum_{\mathrm{j}} \mathrm{BC_{tot,year,i,j}} \quad (6)$$

Where for each spatial point p_i the collection of trips j passing point p_i contribute to the yearly average. In the last phase, the instantaneous noise levels are replaced by the average noise levels at each location p_i. (eq. 7 and 8). All meteorological variability is included in the input data (eq. 5 and 6) and no instantaneous meteorological covariates are necessary in the yearly meteorology based GAM models (eq. 9 and 10):

$$\mathrm{L_{OLF,i,map}} = \frac{1}{\mathrm{n}} \sum_{\mathrm{j}} \mathrm{L_{OLF,i,j}} \quad (7)$$

$$\mathrm{L_{HFmLF,i,map}} = \frac{1}{\mathrm{n}} \sum_{\mathrm{j}} \mathrm{L_{HFmLF,i,j}} \quad (8)$$

$$gamBC_{loc,year} \equiv \log(\mathrm{BC_{loc,year,i}}) = gam \quad (L_{OLF,i,map}, L_{HFmLF,i,map}, StCan_i) \quad (9)$$

$$gamBC_{tot,year} \equiv \log(\mathrm{BC_{tot,year,i}}) = gam \quad (L_{OLF,i,map}, L_{HFmLF,i,map}, StCan_i) \quad (10)$$

This results in a function that converts the average mobile noise measurement map to an average BC map, independently of the trip sampling paths. In Figure 4.3.1, the spatial variability of the two noise covariates ($L_{OLF,i,map}$ and $L_{HFmLF,i,map}$) and the street canyon index $StCan_i$ are illustrated, as well as the background adjusted local component of the BC measurements ($BC_{loc,meas,i,map}$) spatially averaged in a similar way as the noise covariates (eq. 7 and 8). Local BC contributions are highly variable and are affected by local traffic variability.

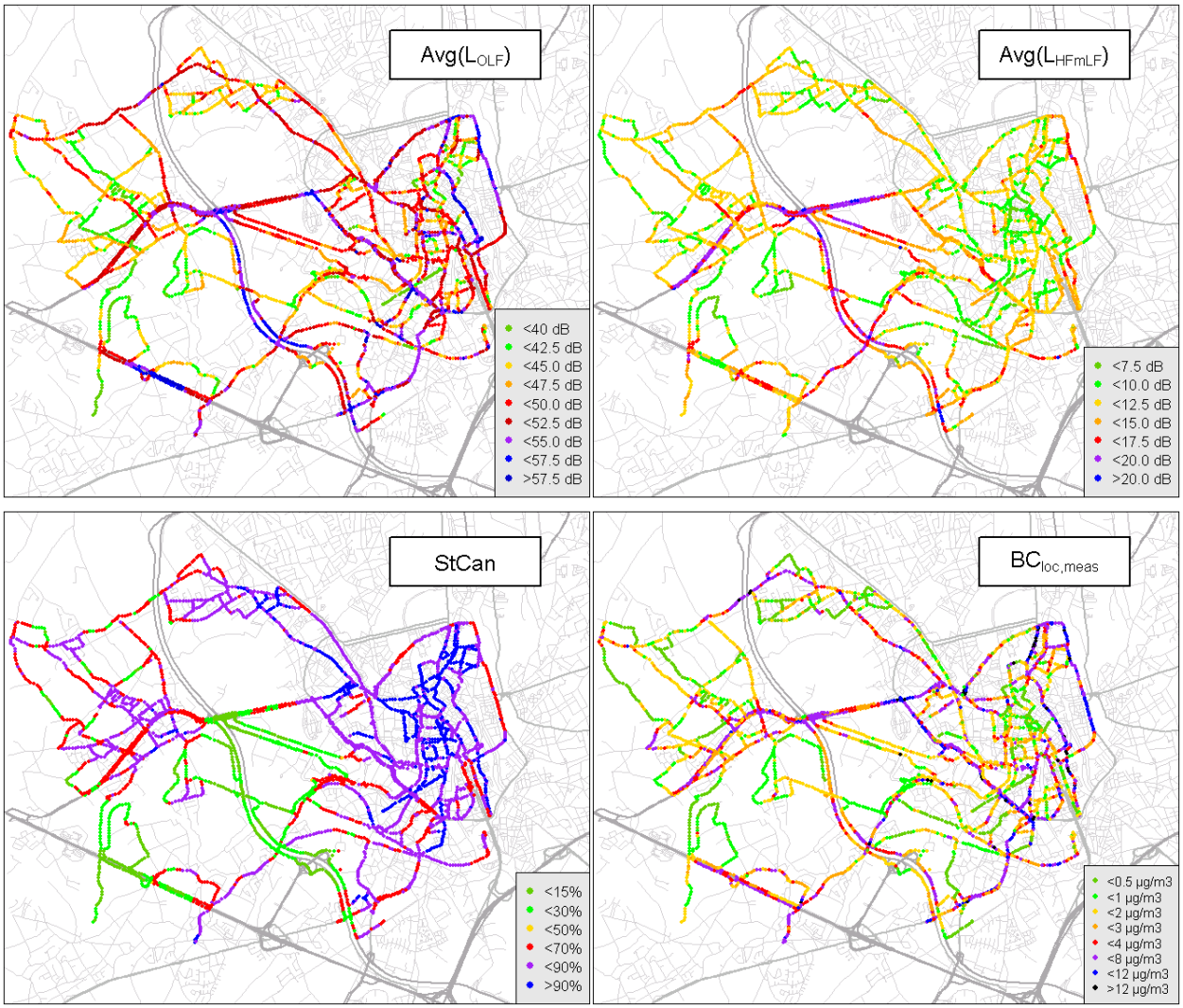

Figure 4.3.1: Three maps showing the spatial covariates ($L_{OLF,i,map}$, $L_{HFmLF,i,map}$ and $StCan_i$). The fourth map shows the average local contribution to the BC exposure measurements: $BC_{loc,meas,i,map}$.

4.3.2.2 Meteorology classes

The combined mobile noise and BC measurement campaign stretched from November 2010 till November 2011. The yearly averaged exposure was calculated for the calendar year 2011. A full year of hourly meteorological data for 2011 was retrieved from the national meteorological institute of Belgium (KMI). The measuring site is located in Melle, less than 10 km south of the city centre of Ghent. BC background data covering the full year 2011 was made available by the environmental institute of Flanders (VMM) for the nearest station at

Antwerpen-Linkeroever (40AL01). The same data were used for the background adjustment in the spatiotemporal model. Further information is available at http://www.irceline.be.

Only the meteorological conditions during the rush hour (7:00-10:00h and 16:00-19:00h) were included in the statistics, since the model is only based on rush hour measurements. For the year 2011 this resulted in 160 distinct meteorological / background concentration classes (referred to as Met_{cl}), each class occurring in the year 2011 with a weight $wMet_{cl,2011}$. The wind speed classes ranged from 0 to 11 m/s and the BC background concentrations from 0 to 16 µg/m^3. The distribution of the wind speed classes, BC background classes and the combined occurrences are presented in Figure 4.3.2. The size of the circles is proportional to the occurrence $wMet_{cl,2011}$ of the meteorological situations. The sparse BC background values above 7 µg/m^3 were added to the 7 µg/m^3 class for easy presentation in the plot only.

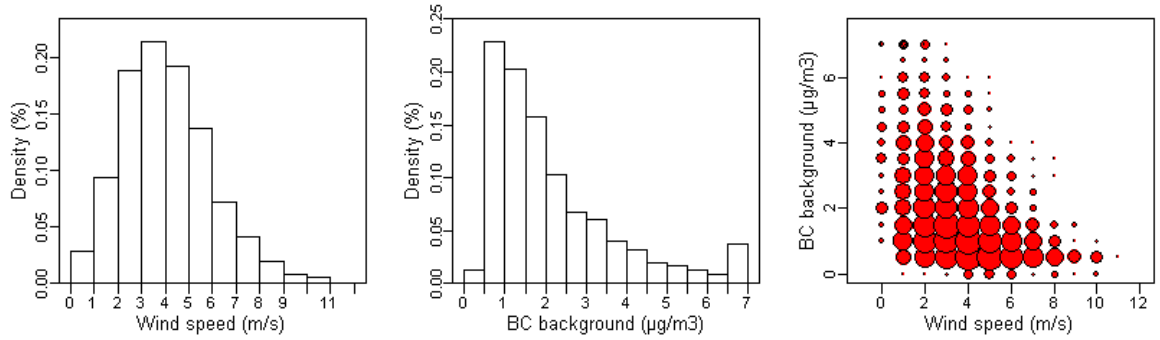

Figure 4.3.2: Histograms of the wind speed (A), BC background exposure (B) and the combined occurrence of wind speed and background exposure (based on hourly wind speed data in Melle and 30 minute BC data for station 40AL01 obtained respectively from VMM and KMI).

4.3.3 Results

4.3.3.1 A model for yearly averaged BC concentration

The data processing is based on data from Dekoninck et al, 2013, referred to as BDS. After applying Eq.(3) and (4) on BDS the yearly meteorology adjusted BC exposure is available as $BC_{year,loc,i,j}$ and $BC_{year,tot,i,j}$ for each location i and each trip j. The new datasets are representative for the yearly averaged meteorological condition, removing the bias due to the not representative sample of meteorology of the trips that passed at location i. A new GAM model containing only three parameters, L_{OLF}, StCan and L_{LFmHF}, can be extracted from the new dataset, since the variability due to the wind speed is removed. The resulting models, gam-$BC_{loc,year}$ and the gam$BC_{tot,year}$ are presented in Table 4.3-1. The GAM models are almost trivial and virtually perfect, since they are based on the output of the $BC_{loc,temporal}$ GAM model. The only variability left in these GAM models is the difference in the instantaneous noise evaluation covariates L_{OLF} and L_{HFmLF} for the trips contributing to the location i.

Model	Intercept	$L_{OLF,i,map}$	$L_{HFmLF,i,map}$	StCan	Deviance explained	Number of points	AIC
		F-value			%	N	
$gamBC_{loc,year}$	8.11 (3.3 µg/m³)	37427	10272	18874	99.5	3827	-17064
$gamBC_{tot,year}$	8.60 (5.4 µg/m³)	17766	4395	8046	98.9	3827	-17980

Table 4.3-1: Model results comparison, showing intercept, F-values, deviance explained and AIC.

The $gamBC_{loc,year}$ model is the strongest model. The engine related noise covariate L_{OLF} is the strongest component in both models. In Figure 4.3.3, the three spline plots including the residuals for L_{OLF}, L_{HFmLF} and StCan are shown for $gamBC_{loc,year}$ and $gamBC_{tot,year}$. In $gamBC_{tot,year}$ the low traffic condition (small L_{OLF}) converges to an lower limit, related to the yearly average BC background concentration. In the L_{OLF} covariate of $gamBC_{loc,year}$ a very linear relation is found, even for low values. Traffic evaluation through noise assessment has a perfect linear log-log relationship with the engine related noise after adjusting for the yearly meteorology distribution. The speed related covariate L_{HFmLF} converges to a maximum. In situations with high traffic speed the BC exposure does not increase any further for equal L_{OLF}. In the street canyon index a step-like solution is visible. Below 0.5 the location is in rather open area, above 0.5, dispersion is significantly reduced.

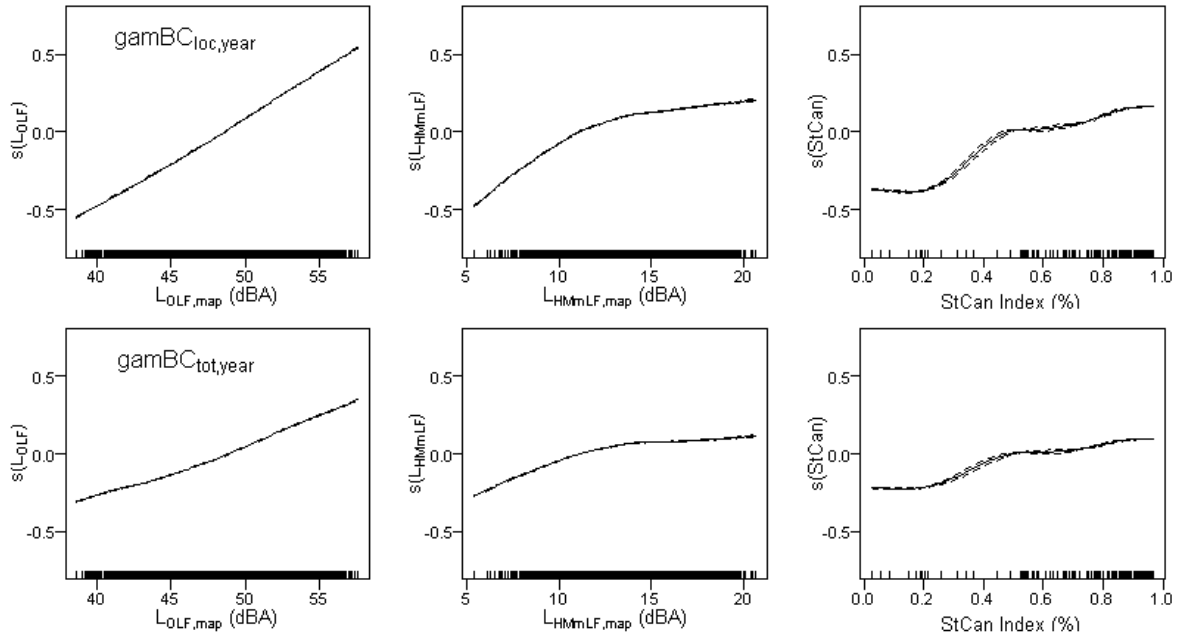

Figure 4.3.3: Splines of three covariates of the $gamBC_{loc,year}$ (top) and $gamBC_{tot,year}$ (bottom) models show strong linear behavior between the L_{OLF} and log(BC). In the total exposure the effect of the background exposure emerges, limiting the decrease of the exposure for low L_{OLF}..

Now we illustrate the effect of the different steps in modelling the yearly meteorology adjusted BC exposure using mobile noise data. A sequence of evaluations in Figure 4.3.4 illustrates the consecutive adjustments of the meteorology related effects on the bicyclist's exposure. The first evaluation (plot A) shows $BC_{tot,meas,j}$, the averaged measured BC exposure by

trip (each dot is one trip) as a function of the strongest covariate $L_{OLF,meas,j}$, the averaged measured noise level L_{OLF} along trip j. The correlation is low. After adjusting the exposure for the background contribution ($BC_{loc,meas,j}$) in plot B the correlation increases, but the wind speed is still an important variable in the personal exposure (see Dekoninck et al, 2013). The linear fit of the previous plot is repeated in the dashed line as a reference for each of the consecutive steps. In plot C the exposure is extrapolated to the yearly average meteorological conditions $BC_{loc,year,j}$ for each trip j. The correlation is enhanced up to 0.88 expressing the removal of the meteorology induced bias in the mobile measurement campaign. Several of the extremely high exposure trips are drastically reduced by applying the yearly average meteorology. The y-axis is adjusted to the new range. Plot D investigates the effect of replacing the actual noise measured along the trip by the average noise level for all passages at each location i passed by trip j, thus evaluating the trips according to the average mobile noise map for both noise covariates $L_{OLF,i,map}$ and $L_{HFmLF,i,map}$. Only a small change is detected for shifting from instantaneous noise level to the average over multiple passages, supporting the validity of replacing the instantaneous noise levels by the average noise levels. The correlation increases due to the removal of differences in the noise evaluation for trips passing at the same location i. Plot E replaces $BC_{loc,year,j}$ by $BC_{tot,year,j}$. The correlation is not affected since the difference is only related to the change in background exposure. The yearly average background adjustment is added.

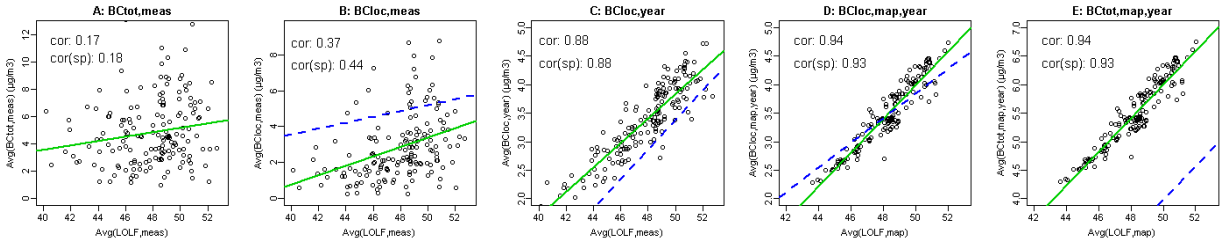

Figure 4.3.4: Visual representation of the sequential improvements of mobile measurements as a function of the trip average engine noise L_{OLF}: average measured $BC_{tot,meas,j}$ (A) along the trip and different exposure modeling steps: $BC_{loc,meas,j}$, $BC_{loc,year,j}$ $BC_{loc,year,map,j}$ and $BC_{tot,year,map,j}$.(B, C, D, E). Each plot includes a linear fit on the trip evaluation (green). The linear fit of the previous plot is repeated in dashed blue on the next plot. Note the changes in the x and y-axis in the different steps.

The spatial result of the $gamBC_{loc,year}$ and $gamBC_{tot,year}$ is presented in Figure 4.3.5. These maps are the yearly meteorological adjusted version of $BC_{loc,meas,i}$ as presented in Figure 4.3.1. The maps are much smoother due to the removal of meteo-related variability. They illustrate the sensitivity of the exposure to the local amount of traffic, traffic dynamics and the distance of the bicyclist to the local traffic. The difference between $BC_{loc,year}$ and $BC_{tot,year}$ is a constant, the yearly averaged background adjustment.

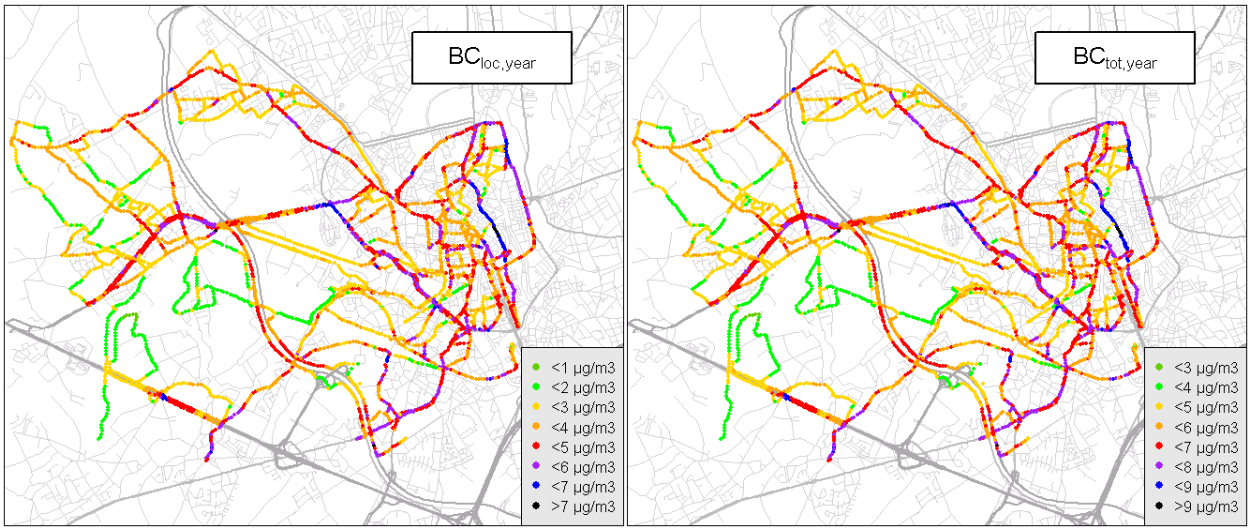

Figure 4.3.5: Visual representation of the yearly meteorology adjusted and noise mapped exposure based BC exposure for cyclists: local component $BC_{loc,year}$ (left) and total exposure $BC_{tot,year}$ (right).

4.3.3.2 Number of noise measurements necessary for yearly averaged BC prediction

Since bicyclist's BC exposure is highly sensitive to the meteorology, it is virtually impossible to achieve a representative sample of measurements for all possible combinations of local traffic and meteorological situations at a given location. Since the noise exposure at location i is not sensitive to the BC background concentrations and much less sensitive to wind speed and wind direction compared to BC exposure, it is expected that much less measurement repetition will be needed to quantify the local noise exposure at location i compared to BC exposure. Hence, the measurement error on the yearly averaged BC exposure is also expected to drop considerably with increasing number of trips. To confirm this expectation, the measurement error (standard deviation over all trips divided by the square root of the number of trips that contribute to the average) is calculated for each location *i* with two or more passages. Figure 6 shows box plot statistics over all locations of this standard error for six parameters: $L_{OLF,i}$, $L_{HFmLF,i}$, $BC_{tot,meas,i}$, $BC_{loc,meas,i}$, $BC_{tot,year,i}$ and $BC_{loc,year,i}$ as a function of the number of passages *n*. For $BC_{tot,meas,i}$ the standard error is not significantly improving with increasing number of passages if the number of passages is below 10, illustrating the high meteorology induced variability. That conclusion is also valid for $BC_{loc,meas,i}$, which is surprising since a large portion of the meteorological effects is already removed from the dataset by adjusting for instantaneous background exposure. For the yearly meteorology adjusted $BC_{tot,year,i}$ the standard error is reduced dramatically. With as little as four passages, the Q3 of the standard error of $BC_{loc,,year,i}$ is smaller than 0.5. µg/m^3. In this dataset 95% of all locations have a standard error for L_{OLF} below 2.0 dB and result in a standard error below 0.5 µg/m^3 for $BC_{loc,,year,i}$. For $BC_{tot,,year,i}$ four passages result in a Q3 smaller than 0.7. µg/m^3 and 90% of all locations in this dataset have a standard error for L_{OLF} below 2.0 dB and result in a

standard error below 0.75 µg/m^3. Evaluating L_{OLF} within 2 dB accuracy is more than sufficient to characterize the yearly averaged traffic related BC exposure.

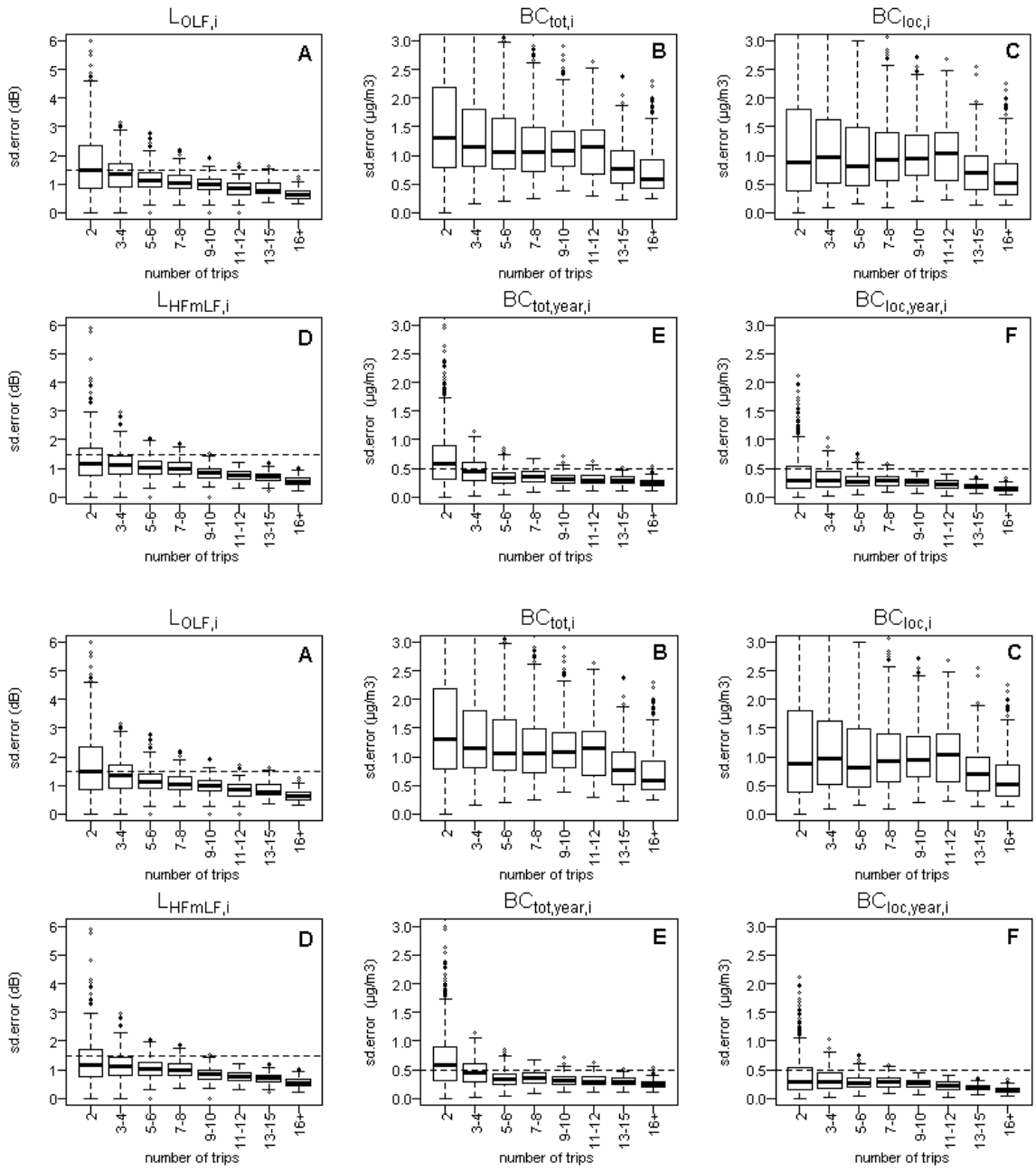

Figure 4.3.6: Distributions of the standard error by number of passages at location i for $L_{OLF,i}$, $BC_{tot,meas,i}$, $BC_{loc,meas,i}$, $L_{HFmLF,i}$, $BC_{tot,year,i}$ and $BC_{loc,year,i}$. Drop lines at 1.5 dB and 0.5 µg/m^3 are added for comparison.

4.3.3.3 Monthly variation in BC exposure

In many countries the actual use of bicycles and the time spent outdoors depends on weather conditions and season. Hence, to correctly assess the yearly averaged exposure as well as to give advice to reduce personal exposure, one may need to account for the annual variation in meteorological conditions. In Figure 4.3.7A the evaluation over all trips is presented,

while restricting the meteorological weighting to the occurrence of the meteorological conditions for that specific month: $BC_{loc,month,j}$ and $BC_{tot,month,j}$. The distributions indicate the range of the high to low exposure trips. The corresponding monthly meteorological statistics for the wind speed and background concentrations are shown in Figure 4.3.7B. Note the atypical conditions in December 2011 with high wind speeds and low background exposure. The variability of the wind speed by month does not show a strong seasonal pattern, and since this is the only meteorological covariate in the GAM model for $BC_{loc,month,j}$, $BC_{loc,month,j,}$ does not show a seasonal pattern either. In this local situation, a yearly representative sample of wind speeds occurs each month. A strong seasonal effect on the $BC_{tot,year,j}$ is visible, expressing the strong seasonal effect of the background exposure. In Figure 4.3.7C the relative contribution of the background exposure to the local traffic component is shown. In summer, the local contribution is almost 75% of the total contribution, in winter it drops to 50%. For the larger part of the year, the local contribution is more than 60% of the total exposure.

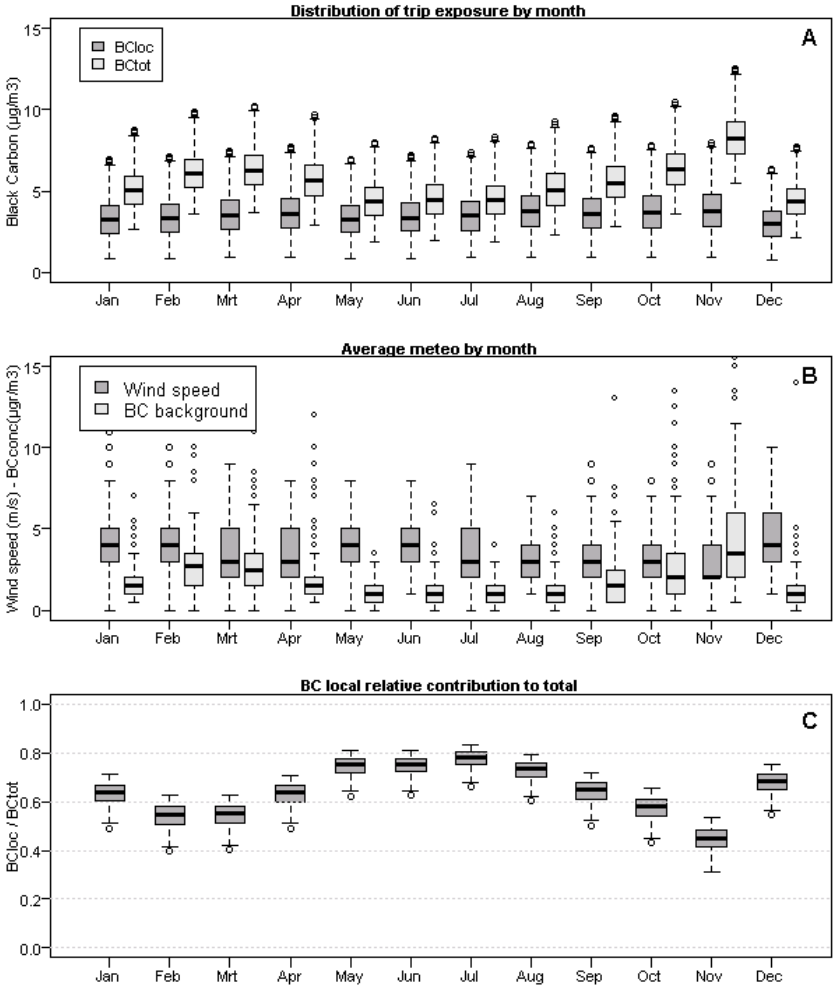

Figure 4.3.7: Monthly variation of the distribution of the local and total BC exposure by trip (A). Background BC and Wind speed show the effect of changing meteorological conditions over the year (B). Relative contribution of the local contribution to the total exposure (C).

4.3.3.4 City-wide mapping and low exposure routes

The proposed methodology for data collection uses mobile measurements on bicycle and consists of two simultaneous actions: during a limited set of trips BC and noise are measured jointly, preferably covering the full range of meteorological conditions and traffic conditions. These data are used to tune the coefficients in a local version of the $BC_{loc,temporal}$ model to the specific emission of the local vehicle fleet, meteorological conditions and background concentrations. The $BC_{loc,temporal}$ model is converted to the yearly meteorology adjusted GAM models as described in 4.3.2.1. An extensive mobile noise only measurement campaign can be performed to obtain spatial detail for a more extended area. In a numerical example: a city-wide participatory campaign with ten cheap noise measurement units, used by one-hundred participants for two weeks each can be completed in half a year. With a typical bicycle route of 10 km, each measuring their standard route and a set of alternatives will result in approximately 100 persons x 20 trips x 10 km or 20,000 km of mobile noise data. If the participants' origins and destinations are well distributed over the investigated city and suburbs, the majority of roads will be sampled adequately. The mobile noise measurements result in city-wide noise maps $L_{OLF,i,map}$ and $L_{HFmLF,i,map}$. Mapping any bicycle trajectory to the mobile noise maps (within the extent of the map) and applying the $BC_{loc,temporal}$ results in an instantaneous meteorological sensitive estimate of the BC trip exposure. Applying the yearly or monthly meteorology adjusted models results in yearly or monthly averaged BC exposure, according to the requirements of the application.

To estimate the potential exposure improvement of alternative route choice, we take a closer look at the trips used for deriving the models presented in this article (Figure 4.3.4). Figure 4.3.4D and Figure 4.3.4E show that trips performed during rush hour result in differences in L_{OLF} of up to 10 dB with a matching reduction of over 50% in $BC_{loc,year}$ and 35% in $BC_{tot,year}$. A reference trip with an average $L_{OLF,map,trip}$ of 50 dB and an alternative trip of 46 dB will result in a decrease of 1.3 µg/m3, a reduction of 33% for the local traffic component and 22% on the total exposure in a far from extreme trip change scenario. In interpreting the results one should take into account that the travelled routes in this dataset were not optimized to detect the low exposure routes. The travelled routes were by design always switching from high to low exposure road segments to capture as much variability in traffic for similar meteorological conditions within a single trip. A systematic choice for a low exposure route for commuting could easily result in a 35 to 60% reduction in personal exposure depending on the season, but this also depends on the specific commute and the available alternatives for that trip.

4.3.4 Discussion

4.3.4.1 Predictive quality of the methodology

At first sight the GAM models deviance explained is extremely high. When considering the procedure and the importance of the wind speed covariate in the spatiotemporal model, this is not surprising. All remaining variability that is not explained by the spatiotemporal model is -by design- not available in the yearly extrapolation. More important than the fact that the $gamBC_{loc,year}$ and $gamBC_{tot,year}$ models are virtually perfect, is that all locations are included, even those that were sampled only once or twice, without affecting the quality of the GAM model. It was expected that the dataset should be restricted to a minimum number of passages to build a valid GAM model, but this was clearly not necessary. The quality of the model in the locations with low sampling is also visible in Figure 4.3.6E and Figure 4.3.6F. 75% of the points with only two passages reach a yearly standard error below 500 ngr/m^3 for the $gamBC_{loc,year}$ and almost 50% reach this value for the $gamBC_{tot,year}$ model. The procedure to adjust each individual trip to the yearly averaged meteorological situation is effective. Dekoninck et al. (2012) concluded that an estimate of L_{OLF} resulted in a standard error of approximately 1.5 dB after ten samples at a specific location in similar traffic conditions. The results in this paper show that a standard error of 1.5 dB does not have to be achieved to successfully apply this methodology. A standard error of 2.0 dB is more than sufficient to result in a valid prediction of the yearly BC exposure, which is achieved with four passages for a specific traffic condition. The data showed that it is extremely difficult to achieve a valid averaged BC exposure by increasing the number of passages without using the proposed modeling approach, as illustrated by the low reduction by number of trips in Figure 4.3.6B and Figure 4.3.6C. Noise measurements adequately quantify the local traffic situation and enable the disaggregation of the variability in the BC measurements into local traffic related and meteorology related contributions. This is valid for the instantaneous model and the yearly meteorology extrapolated model.

4.3.4.2 Comparison with other mobile measurements

A general review by Bigazzi and Figliozzi (2014) summarized 42 studies on the exposure of bicyclists. Fourteen studies addressed BC or EC. The studies are combined and evaluated according to the reported differences between high and low exposure road segments. The exposure on high exposure segments is 8 times higher than low exposure segments across the studies when excluding rural assessments. In the measurements for the instantaneous model (reported in $BC_{loc,i,meas}$) the high exposure locations reach levels up to 25 times the low exposure locations when including rural data and up to 10 times when excluding rural data (see Figure 4.3.5). The evaluations in the instantaneous model are aggregated by 50 m segments. In the review the data is aggregated by physical street segments. The measure-

ments in the instantaneous model also include high wind speed conditions and extreme background conditions, typically not sampled in bicycle campaigns. These differences in the measurement setup (spatial detail and sampled meteorological conditions) explain the larger detected ranges. Despite the differences in the measurement setup, the measurement ranges are comparable with the results in the review.

4.3.4.3 Potential of background adjusted models

The additive modelling approach has the potential to be more than a mathematical method to disentangle the meteorological and background exposure effects from the local traffic contribution. Several authors investigated the particle size distribution in relation to the distance to the source (Karner et al., 2010, Boogaard et al., 2011, Strak et al., 2011, Kingham et al., 2013, Holder et al., 2014). All results show similar trends; closer to the source the size distributions show higher numbers of small particles. In health effects of air pollution exposure research, the importance of the particle size and particle count has been investigated by different authors (Strak et al., 2010, Seaton et al., 1995). Although the smallest particles may enter the body in different ways (e.g. through the olfactory nerve (Oberdorster, 2004)), specific health effects or different toxicity estimates (based on particle mass or on particle number and size distributions) have proven hard to detect (Osunsanya et al., 2001). The additive approach -splitting exposure in background particles (aged and larger) and local contribution (fresh and small)- can be a base for adjusting the exposure to particle size corrected exposures and to verify if high local contributions result in adverse health effects. Quantifying the particle size distribution adjustments for the local and background contribution is subject to further research. Similar measurement campaigns measuring UFP particle counts or particle size distributions can add significant value in this respect. A smaller measurement campaign has already shown that this technique is also valid for UFP (Dekoninck et al., 2015). UFP shows a steeper relation to L_{OLF} compared to BC and the additive approach is less sensitive to the background concentrations compared to BC.

4.3.4.4 Diurnal variability, vehicle fleet composition and policy support

The main limitation in the presented results is the restriction to rush hour exposure and traffic, the data limitation of the underlying instantaneous model. Since most policy measures are mainly focusing on commuting, the presented results are applicable in that context. The proven effectiveness of the noise sampling implies that mapping the traffic related exposure has the potential to be extended to capture the diurnal variability with only a small extension of the sampling strategy to include trips outside the rush hour and adding the hour of the day as a new dimension in the models. Only few passages on different types of routes for different times of the day could reveal the diurnal patterns of the BC exposure. Implementing this technique in other countries and/or continents requires recalibration of the

instantaneous model. Vehicle fleet, vehicle fleet evolution, driver behaviour, biking facilities, city characteristics, meteorological conditions and air pollution background concentration all have their specific influence on the relationship between noise and local traffic related air pollution. The sensitivity of the spatiotemporal model at different locations should be evaluated for other dependencies (temperature, humidity etc.). Validating new implementations is crucial and will not only illustrate the proposed methodology but will also detect effects of different vehicle fleets. This must be seen as one of the most important applications of the combined methods (instantaneous modeling and yearly meteorology adjusted maps). The instantaneous models will adjust and resolve the bias between the different mobile measurement campaigns for meteorology, background concentrations, route choice and traffic dynamics. The remaining difference can be attributed to the different fleet composition. In Belgium more than 60% of the vehicles use diesel, a well-known source of BC. Large changes in the relationship between noise and BC in other countries are probable and will be relevant for policy decisions in Belgium. Consecutive calibration measurement campaigns are relevant to quantify the changes in the vehicle fleet emission over time and require similar control over the sampling biases to reveal the vehicle fleet related component in the evolution of the BC exposure. The effects of changes in the local and the background exposure due to changes in the vehicle fleet emission or other BC sources are automatically included through the background adjusted approach of the instantaneous model. This leads us to an important feature of the mobile noise based traffic assessments. Noise emission of the vehicle fleet is much less sensitive to change over time due to much less restrictive and less effective legislation for the noise emission of the vehicle fleet. The traffic quantification is therefore valid for longer periods of time. Only reduced combined noise-BC measurement campaigns are required to reassess the noise-BC relation. In response to local policy based traffic changes, small dedicated 'noise-only' measurements can reassess the traffic densities and traffic dynamics. The burden and costs of performing large air pollution measurement campaigns can be reduced significantly while the results cover much larger areas.

From a scientific point of view, the improvement of personal exposure assessment for bicyclists to traffic related air pollution is the most important goal of this methodological exercise. From the cyclist's point of view, the awareness of their route choice on the related exposure is the most important aspect. Only if people are aware of an issue, they can react and change their behavior accordingly. The main traffic related challenge of the local governments is reducing car use within cities and promoting a shift to other modes of transportation. A campaign similar to the proposed setup can inform the public on low exposure routes for cyclists and the local government can use this information to improve the quality, availability and dissemination of the alternative routes. Missing links in the biking network can be detected and benefits of investing in these trajectories can be quantified and used in the dissemination process. Alternative routes and improved bicycle infrastructure will also re-

duce the number of bicycle accidents (Reynolds et al., 2009, Vandenbulcke et al., 2014, Molino et al., 2009).

4.3.4.5 Multidisciplinary aspects and LURs

The mobile noise mapping should not be only performed for air pollution assessments but can also be a part of extended multidisciplinary evaluations of in-city traffic related liveability. Strong synergies exist between local air pollution exposure assessments and traffic noise related burdens. Local traffic assessment along the roads near the dwellings improves noise annoyance and wellbeing evaluations of the inhabitants (Botteldooren et al., 2010). Mobile noise measurements include more detail than calculated noise maps and have the potential to add value to all environmental noise related evaluations. They also provide a proxy for traffic on low-density roads where no external traffic data is available. An important application is the improvement of the traffic related air pollution land-use regression models. The mobile noise map provides traffic data for the LUR models on low density roads including local traffic dynamics. In the acoustic field, the combination of mobile and fixed noise monitoring stations will enable dynamic noise maps (Can et al., 2011, Can et al., 2014). City-wide mobile noise evaluation is therefore a strong tool to improve in-city liveability in a multidisciplinary approach.

4.3.5 Conclusions

We have successfully extended an instantaneous exposure model for bicyclists to a yearly meteorology averaged exposure model. Strong seasonal effects were detected. Mapping the local variability of in-traffic exposure to BC for cyclists based on mobile noise measurements can be achieved with a small number of passages, since the noise exposure assessments are much less influenced by meteorological conditions and are therefore more efficient compared to in-traffic air pollution assessments. Extending the presented models to diurnal exposure models becomes feasible.

In low background conditions the background BC exposure accounts for less than 25% of the bicyclist's exposure, whereas in high background exposure conditions the contribution is 40 to 60%. Low exposure route choice can reduce the local traffic exposure with at least 35-60% depending on the available alternative trajectories and the season. Local governments can use mobile noise mapping to support investments in alternative networks for cyclists.

The results support the potential of the additive approach defining personal exposure as the sum of a background contribution and a local traffic contribution. Applying this technique enables international comparison of both the local traffic related particulate matter exposure and the background exposure levels. Applying the methodology on a city-wide scale will result in a detailed spatial and accurate yearly averaged exposure map. The influ-

ence of instantaneous meteorology on air pollution exposure can be quantified through a partial participatory sensing campaign measuring one or more traffic related air pollutants for the full range of meteorological conditions in parallel to the mobile noise measurement campaign mapping the full city. Extrapolation to yearly local and total exposure with or without seasonal adjustments is inherently available in the methodology. This low cost methodology quantifies the local traffic in an unprecedented spatial resolution and fits in a multidisciplinary approach of evaluating and improving personal exposure, liveability, well-being and health in large urban and suburban context.

4.3.6 References

Bigazzi, A. Y., & Figliozzi, M. A. (2014). Review of Urban Bicyclists' Intake and Uptake of Traffic-Related Air Pollution. Transport Reviews, 34(2), 221-245.

Bigazzi, A. Y., & Figliozzi, M. A. (2014). Review of Urban Bicyclists' Intake and Uptake of Traffic-Related Air Pollution. Transport Reviews, 34(2), 221-245.

Boogaard H., Kos G.P.A., Weijers E.P., Janssen N.A.H., Fischer P.H., et al. 2011. Contrast in air pollution components between major streets and background locations: Particulate matter mass, black carbon, elemental composition, nitrogen oxide and ultrafine particle number. Atmospheric Environment, 45, 650-658.

Botteldooren D., Dekoninck L. & Gillis D. 2011. The Influence of Traffic Noise on Appreciation of the Living Quality of a Neighborhood. International Journal of Environmental Research and Public Health, 8, 777-798.

Can A., Dekoninck L. & Botteldooren D. 2014. Measurement network for urban noise assessment: Comparison of mobile measurements and spatial interpolation approaches. Applied Acoustics, 83, 32-39.

Can A., Van Renterghem T., Rademaker M., Dauwe S., Thomas P., et al. 2011. Sampling approaches to predict urban street noise levels using fixed and temporary microphones. Journal of Environmental Monitoring, 13, 2710-2719.

Dekoninck, L.; Botteldooren, D.; Int Panis, L., Guidelines for participatory noise sensing based on analysis of high quality mobile noise measurements. Internoise 2012 (conference), 394-402

Dekoninck L., Botteldooren D. & Int Panis L. 2013. An instantaneous spatiotemporal model to predict a bicyclist's Black Carbon exposure based on mobile noise measurements. Atmospheric Environment, 79, 623-631.

Dekoninck L., Botteldooren D., Panis L.I., Hankey S., Jain G., et al. 2015. Applicability of a noise-based model to estimate in-traffic exposure to black carbon and particle number concentrations in different cultures. Environment International, 74, 89-98.

Dominici F., McDermott A., Zeger S.L. & Samet J.M. 2002. On the use of generalized additive models in time-series studies of air pollution and health. American Journal of Epidemiology, 156, 193-203.

Dons E., Panis L.I., Van Poppel M., Theunis J. & Wets G. 2012. Personal exposure to Black Carbon in transport microenvironments. Atmospheric Environment, 55.

Holder A.L., Hagler G.S.W., Yelverton T.L.B. & Hays M.D. 2014. On-road black carbon instrument intercomparison and aerosol characteristics by driving environment. Atmospheric Environment, 88, 183-191.

Janssen N.A.H., Hoek G., Simic-Lawson M., Fischer P., van Bree L., et al. 2011. Black Carbon as an Additional Indicator of the Adverse Health Effects of Airborne Particles Compared with PM10 and PM2.5. Environmental Health Perspectives, 119, 1691-1699.

Karner A.A., Eisinger D.S. & Niemeier D.A. 2010. Near-Roadway Air Quality: Synthesizing the Findings from Real-World Data. Environmental Science & Technology, 44, 5334-5344.

Li L.F., Wu J., Hudda N., Sioutas C., Fruin S.A., et al. 2013. Modeling the Concentrations of On-Road Air Pollutants in Southern California. Environmental Science & Technology, 47, 9291-9299.

Molino J.A., Kennedy J.F., Johnson P.L., Beuse P.A., Emo A.K., et al. 2009. Pedestrian and Bicyclist Exposure to Risk Methodology for Estimation in an Urban Environment. Transportation Research Record, 145-153.

Oberdorster G., Sharp Z., Atudorei V., Elder A., Gelein R., et al. 2004. Translocation of inhaled ultrafine particles to the brain. Inhalation Toxicology, 16, 437-445.

Osunsanya T., Prescott G. & Seaton A. 2001. Acute respiratory effects of particles: mass or number? Occupational and Environmental Medicine, 58, 154-159.

Pearce J.L., Beringer J., Nicholls N., Hyndman R.J. & Tapper N.J. 2011. Quantifying the influence of local meteorology on air quality using generalized additive models. Atmospheric Environment, 45, 1328-1336.

Reynolds C.C.O., Harris M.A., Teschke K., Cripton P.A. & Winters M. 2009. The impact of transportation infrastructure on bicycling injuries and crashes: a review of the literature. Environmental Health, 8.

Seaton A., Macnee W., Donaldson K. & Godden D. 1995. PARTICULATE AIR-POLLUTION AND ACUTE HEALTH-EFFECTS. Lancet, 345, 176-178.

Strak M., Boogaard H., Meliefste K., Oldenwening M., Zuurbier M., et al. 2010. Respiratory health effects of ultrafine and fine particle exposure in cyclists. Occupational and Environmental Medicine, 67, 118-124.

Strak M., Steenhof M., Godri K.J., Gosens I., Mudway I.S., et al. 2011. Variation in characteristics of ambient particulate matter at eight locations in the Netherlands - The RAPTES project. Atmospheric Environment, 45, 4442-4453.

Vandenbulcke G., Thomas I. & Panis L.I. 2014. Predicting cycling accident risk in Brussels: A spatial case-control approach. Accident Analysis and Prevention, 62, 341-357.

WHO Europe, 2012: Health effects of black carbon, ISBN: 978 92 890 0265 3.

Wood S.N. 2006. On confidence intervals for generalized additive models based on penalized regression splines. Australian & New Zealand Journal of Statistics, 48.

4.4 Applicability of a noise-based model to estimate in-traffic exposure to black carbon and particle number concentrations in different cultures

Published: Dekoninck, Luc, Dick Botteldooren, Luc Int Panis, Steve Hankey, Grishma Jain, Karthik S, Julian Marshall. "Applicability of a noise-based model to estimate in-traffic exposure to black carbon and particle number concentrations in different cultures" Environment International, Volume 74, January 2015, Pages 89–98.

ABSTRACT

Several studies show that a significant portion of daily air pollution exposure, in particular Black Carbon (BC), occurs during transport. In previous work, a model for the in-traffic exposure of bicyclists to BC was proposed based on spectral evaluation of mobile noise measurements and validated with BC measurements in Ghent, Belgium. In this paper, applicability of this model in a different cultural context with a totally different traffic and mobility situation is presented. In addition, a similar modelling approach is tested for Particle Number (PN) concentration.

Indirectly assessing BC and PN exposure through a model based on noise measurements is advantageous because of the availability of very affordable noise monitoring devices. Our previous work showed that a model including specific spectral components of the noise that relate to engine and rolling emission and basic meteorological data, could be quite accurate. Moreover, including a background concentration adjustment improved the model considerably. To explore whether this model could also be used in a different context, with or without tuning of the model parameters, a study was conducted in Bangalore, India. Noise measurement equipment, data storage, data processing, continent, country, measurement operators, vehicle fleet, driving behaviour, biking facilities, background concentration, and meteorology are all very different from the first measurement campaign in Belgium. More than 24 hours of combined in-traffic noise, BC, and PN measurements were collected. It was shown that the noise-based BC exposure model gives good predictions in Bangalore and that the same approach is also successful for PN. Cross validation of the model parameters was used to compare factors that impact exposure across study sites. A pooled model (combining the measurements of the two locations) results in a correlation of $r = 0.84$ when fitting the total trip exposure in Bangalore. Estimating particulate matter exposure with traffic noise measurements was thus shown to be a valid approach across countries and cultures.

4.4.1 Introduction

Particulate matter (PM) is currently regulated in Europe, the US, India and other countries based on specific particle size fractions (e.g., PM_{10}, $PM_{2.5}$). Black Carbon (BC) and Particle Number (PN) concentrations are associated with transportation emissions but are typically unregulated. The World Health Organization suggests including BC when evaluating traffic-related health effects (WHO Europe, 2012). Recent epidemiological results for BC suggest health effects per mass may be up to 10 times higher than PM_{10} (Janssen et al., 2011). Research into the health effects of traffic-related particulates is constrained by the stronger spatial variability for BC and PN concentrations relative to PM_{10} and $PM_{2.5}$. Detailed measurements for near-road settings have shown large spatial gradients for certain aspects of particulate air pollution. For example, ultrafine particles and BC show decreases of over 50% within the first 150 m from the edge of the road (Karner et al., 2010) and significant street-to-street differences in PN and BC have been reported by several authors (Boogaard et al., 2011, Dons et al., 2012-2013). Building a fixed-site monitoring network for PN and BC to provide robust estimates of exposure patterns, would therefore be a daunting task.

In previous work a novel way to predict a bicyclist's in-traffic BC exposure was presented based on mobile measurements of traffic-related noise and BC in Ghent (Belgium) (Dekoninck et al., 2013). The noise-based model yields spatially and temporally precise estimates of BC based on traffic noise measurements. The additive model successfully split the BC exposure of a bicyclist into a background component and a local, traffic-related component. The local component included the wind speed, a street canyon index and a noise-based characterization of instantaneous traffic volume and dynamics; specifically, an engine throttle noise component and a rolling noise component.

Here we extend our prior work by exploring the same category of modelling (correlating real-time measurement of noise with real-time pollution measurements) in Bangalore, India. Relevant environmental differences between Bangalore and Ghent include vehicle fleet and fuel use, driving patterns, speeds, densities, and behaviour; levels of ambient and traffic-related noise and pollution, meteorological conditions, and limited biking facilities. Three important differences between the current investigation (Bangalore) and the prior investigation (Ghent) are: (1) a different location, with very different traffic conditions relative to the prior study, (2) measurement procedures were automated to allow use by bicyclists unfamiliar with the equipment, and (3) we study two pollutants (PN and BC) rather than only BC.

4.4.2 Methodology

4.4.2.1 Measurement equipment and setup

The original experimental setup for the measurement campaign in Ghent (Dekoninck et al., 2013) was based on a manually operated smartphone GPS, a Type 1 Noise Level Meter (Svantek 959) and a micro-aethalometer. The data was processed and merged manually. These labour intensive procedures needed to be automated to enable large scale, low support measurement campaigns. A low-cost noise measurement setup designed by the acoustics group at the Ghent University was modified to enable automated mobile measurements at a much lower hardware cost (Can et al., 2011a, Can et al., 2011b, Van Renterghem et al., 2011, Dauwe et al., 2012). The noise measurement module is extended with a GPS (Haicom HI-204 III USB), a micro-aethalometer (AE51, Aethlabs, San Francisco, CA) and a battery for off-grid operation (Figure 4.4.1). Software was developed to automatically capture the 1-second data stream from the micro-aethalometer. The mobile node is designed to be mounted on the handlebar of a bicycle. In addition, a condensation particle counter (CPC 3007, TSI Inc., Shoreview, MN) was carried in a backpack by the bicyclist to measure PN. After each sampling run the mobile node was connected to the internet and the data was uploaded to a database on the server at the University of Ghent. An automated process synchronizes and merges the noise, GPS and BC data based on the timestamp of the mobile node. The CPC data was joined with the other data in a separate post-processing sequence.

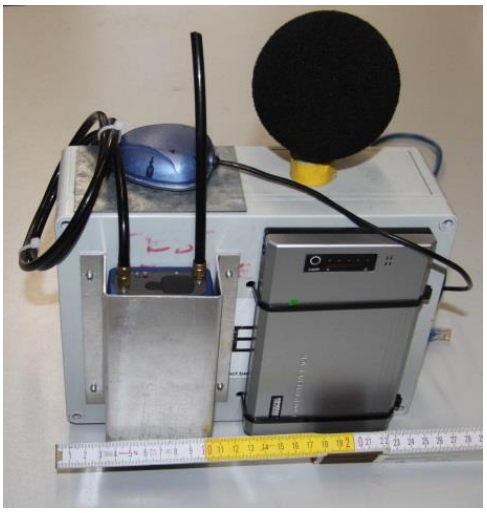

Figure 4.4.1: Inexpensive mobile noise measurement equipment including the micro-aethalometer and GPS. The box containing all instruments is 23cm by 9 cm wide and 17 cm high.

4.4.2.2 Measurement location, strategy and processing

Measurements were carried out north of the city center of Bangalore, India, (elevation: 920m; metropolitan population: ~10 million; land area: 1,276 km^2). The mobile measurements were performed while cycling a predefined route around the Armana Nagar neigh-

bourhood including roads with different traffic conditions instead of the random sampling used by Dekoninck et al. (2013). The route was selected to alternate on a regular basis between high and low traffic roads to assess small scale spatial and temporal differences in exposure. The sampling route was completed 15 times during the morning rush-hour and 5 times in the evening rush-hour during the sampling period (11 November 2013-15 January 2014; total duration: 24.5 hours). The sampling route is shown in Figure 4.4.2. The sampling runs also included stationary roadside measurement to explore the possibility of using stationary noise measurements. The results of the stationary measurements are not reported in this article. Some additional 'random' runs (not on the sampling route) were included to increase the coverage of small roads in several neighbourhoods.

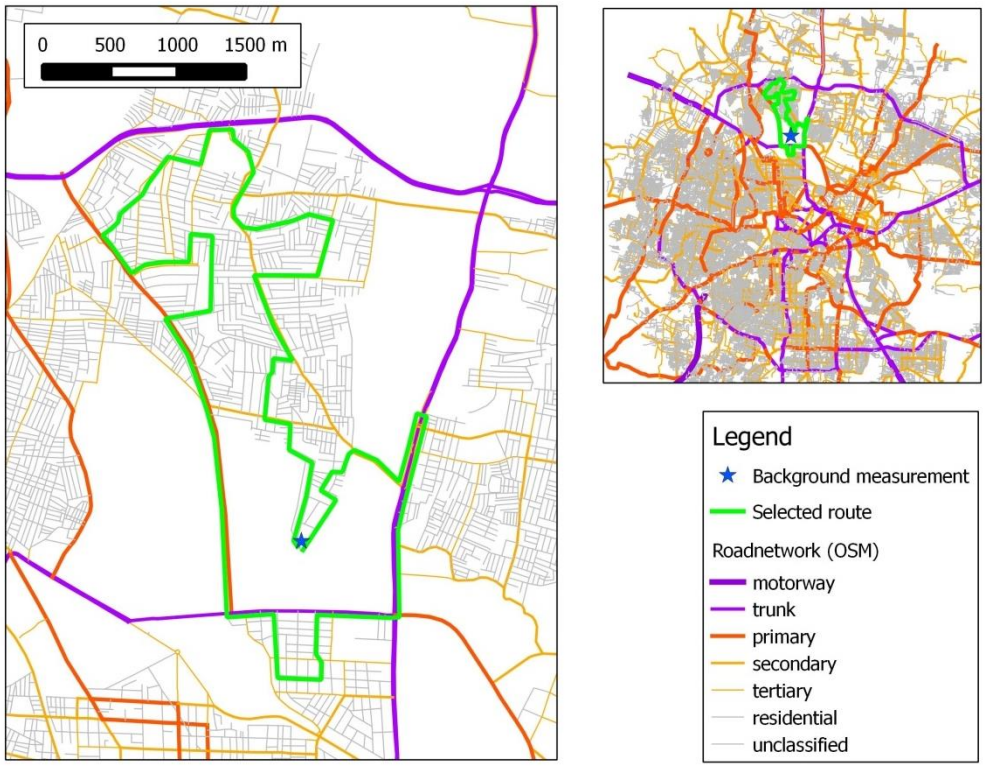

Figure 4.4.2: Map of the sampling route in Bangalore. The blue star shows the location of the background measurement location (BG).

The noise measurements are performed in one-third octave band spectra, at a sampling rate of 8 measurements per second; these sound measurements are later aggregated to 1-second averages, to match the temporal resolution of the GPS, BC and PN measurements. The basic traffic-related noise parameters $L_{OLF}(t)$ and $L_{HFmLF}(t)$ as defined in Dekoninck et al. (2013) are then calculated. The parameter $L_{OLF}(t)$ is the sum of the (A-weighted) 100 to 200 Hz one-third octave bands and describes the engine noise of the nearby traffic at timestamp t. It increases with increasing engine throttle, increasing traffic volume, and increasing fraction of heavy vehicles. The second parameter $L_{HFmLF}(t)$ is related to the ratio of rolling noise and engine noise. The high frequencies in rolling noise are caused by tire-road interaction and are related to the size and pattern of the tire profile and the road surface grain size (see

for example Sandberg and Ejsmont, 2002). $L_{HFmLF}(t)$ is defined as the difference between the high (1000 to 2000 Hz) and the low frequencies (100 to 200 Hz) in the noise spectrum at timestamp t. High levels of $L_{HFmLF}(t)$ indicate that rolling noise dominates over engine noise, which indicates higher driving speed.

The noise, BC and PN measurements are smoothed by applying a running average of 20 seconds on the 1-second time series. The smoothed 1-second time series are then aggregated to the mean of each 10-second interval. The data set with 10 second temporal resolution is used as input for the exposure models.

The noise-BC relation is evaluated on the uncorrected standard output of the aethalometer or CPC and reported on this basis in the detailed results, but several BC and PN correction functions to improve the quality of the data processing are available in the literature. Some measurement quality issues were related to bumps along the bicycle route as reported in the past by other authors (Apte et al., 2011, Cai et al., 2013). We checked the validity of the noise-BC relation for a selection of commonly used correction functions to test the sensitivity of our results. Two correction functions aim at cleaning the short-term time series of BC by removing spikes and potentially erroneous aethalometer readings due to vibration errors (Apte et al., 2011, Hagler et al., 2011). Two particle loading correction functions for BC and one correction function for PN are applied as well (Virkkula et al., 2007, Kirchstetter et al., 2007 and Westerdahl et al., 2007). Each of the correction functions are applied to the raw output of the aethalometer or CPC. Where the correction function requires the use of the ATN value of the BC measurements it is applied as documented in the references.

4.4.2.3 Black Carbon: background and local contribution

The approach used to model the local BC exposure in Dekoninck et al. (2013) was based on an adjustment for the background concentration at a fixed measurement site in the official air pollution network. Since no fixed BC background measurement stations were available at the time of the measurements in Bangalore, an alternative procedure was designed for the background adjustment. A second micro-aethalometer was set up in Bangalore near a dwelling in a low exposure area next to a park (background measurement location [BG] shown in Figure 4.4.2). The BC concentration at the background location was measured simultaneously with the mobile concentrations at a one second temporal resolution. At the same site a semi-professional meteorological station was set up to acquire wind speed and temperature conditions. To mimic the resolution of the background concentrations available in the original (Belgium-based) model, the basic statistics of the BC at the background location BG are evaluated at a temporal resolution of 15 minutes. Instantaneous values of the in-traffic measurements can be lower than the 15 minute background evaluations. Due to the frequent occurrence of episodes with high background exposure concentrations in the Bangalore experiment, the background adjustment had to be restricted. A maximum adjustment is introduced in the procedure. The background adjustment for Bangalore is thus defined as:

$$BC_{loc,j}(t) = \max(BC_{raw,j}(t) - \min(BC_{bc,limit}, BC_{bkg,15min,Q1,j}), 500) \quad (1)$$

Where $BC_{bkg,15min,Q1,j}$ is the first quartile of background concentration of the 15 minute interval at the start of the bicycle trip j. The minimum level for the $BC_{loc}(t)$ component was set to 500 ng/m^3, a slightly higher value than in Belgium. Setting a minimum value is necessary to reduce the range of $\log(BC_{loc}(t))$ for episodes with very low exposure. The value $BC_{bkg,limit}$ is chosen while evaluating the GAM model on $\log(BC_{loc}(t))$, ensuring a maximum positive effect on the prediction of the trip segments with low amounts of local traffic.

A similar approach was developed for PN. No simultaneous measurements at the background location were performed since only one CPC 3007 was available. Instead, to adjust for day-to-day variability in background concentrations, all instruments were co-located at the reference site for 30 minutes before and 30 minutes after each sampling run. This data was used to assess the background concentration of PN during the bicycle trip. To be consistent with the background adjustment for BC the average of the first quartile of the 15 minute periods before and after the measurement period are used to estimate the background concentration of PN. The PN_{loc} adjustment is defined as:

$$PN_{loc,j}(t) = \max(PN_{raw,j}(t) - \min(PN_{bc,limit}, mean_j(PN_{bkg,15min,Q1}), 500) \quad (2)$$

Where $mean_j(PN_{bkg,15min,Q1})$ is the mean of the first quartile of the 15 minute intervals at the background location before and after the trip j. Variants of the local components are calculated for the different correction functions listed in the previous section.

4.4.2.4 GAM modelling

Generalized additive models (GAMs) are regression models where smoothing splines are used instead of linear coefficients for the covariates. This approach has been found to be particularly effective for handling the complex non-linearity associated with air pollution research (Dominici et al., 2002, Pearce et al., 2011, Dekoninck et al. 2013). The mathematical form of GAM models is reduced to a time stamp of the measurement and a reference to the measurement node j and can be written in the form:

$$\log(BC(t)) = \sum_{z=1}^{n} s_z(v_z(t)) + \varepsilon(t) \quad (3)$$

Where $v_z(t)$ is the z^{th} covariate evaluated at timestamp t; $s_z(v_z(t))$ is the smooth function of z^{th} covariate, n is the total number of covariates, and $\varepsilon(t)$ is the corresponding residual with $var(\varepsilon) = \sigma^2$, which is assumed to be normally distributed. Smooth functions are developed through a combination of model selection and automatic smoothing parameter selection using penalized regression splines, which optimize the fit and try to minimize the number of dimensions in the model. The main advantage of GAM modelling is the possibility to adjust for non-linear relationships between the covariate and the outcome. The analysis was constructed using the GAM modelling function in the R environment for statistical computing (R

development Core Team, 2009) with the package 'mgcv' (Wood, 2006). The covariates are restricted to L_{OLF}, L_{HFmLF}, wind speed and BC background.

4.4.3 Results

4.4.3.1 General statistics and background correction

Basic statistics of the BC and PN measurements are assembled in Table 1. The distributions are presented in Figure 4.4.3A. The background correction limit $BC_{bkg,limit}$ is set to 6,000 ng/m^3 in this measurement campaign, close to the average background. Higher correction limits did not improve the BC_{loc} models. In contrast to BC, the PN concentrations at the background locations are small compared to the in-traffic PN concentration. The $PN_{bkg,limit}$ could be set to 16000 pt/cc, close to the maximum of the PN background concentration without disturbing the PN_{loc} model. This could express a physical difference between the PN and BC particle behaviour at the background location, but also a difference in the measurement technique. Particles coagulate while the distance to the source increases. This strongly influences the particle count, but has less influence on mass related measurements.

	P10	P25	Median	Mean	P75	P90
$BC_{bkg,15min,Q1}$	2,993	3,567	4,966	6,687	6,457	10,983
$BC_{raw}(t)$	3,347	6,096	12,890	26,240	28,470	59,412
$BC_{loc}(t)$	500	2,597	9,284	22,840	25,260	54,956
$PN_{bkg,15min,Q1}$	5,070	5,765	8,842	8,854	10,710	13,302
$PN_{raw}(t)$	3,786	5,946	12,940	23,210	32,190	59,210
$PN_{loc}(t)$	500	500	4,259	15,980	23,570	50,075

Table 4.4-1: Descriptive statistics of the BC and PN (background, raw and local) datasets in ng/m^3 for BC, pt/cc for PN.

Box plots of air pollution measurements and the model covariates are shown in Figure 4.4.3A and Figure 4.4.3B. The wind speed in Bangalore is very low and never exceeded 2 m/s (wind speeds during the sampling in Belgium averaged 3 m/s). The noise measurements in Bangalore are high with L_{Aeq} reaching values over 100 dBA and L_{OLF} reaching 90 dB compared to Ghent where these levels were 70 dBA and 65 dB respectively. The difference between L_{Aeq} and L_{OLF} is shown in Figure 4.4.3C. Differences larger than 25 dB are not unusual in Bangalore and are related to the regular use of (high frequency) vehicle horns. Several reports are available on the frequent honking while driving in India (Banerjee et al., 2009, Sen et al., 2010). No data was removed to accommodate the potential disturbances of the models due to the honking. In Figure 4.4.3D the $BC_{10sec}(t)$ concentration is shown as a function of

$L_{OLF,10sec}(t)$ as an illustration of the physical relation between noise and particulate matter exposure.

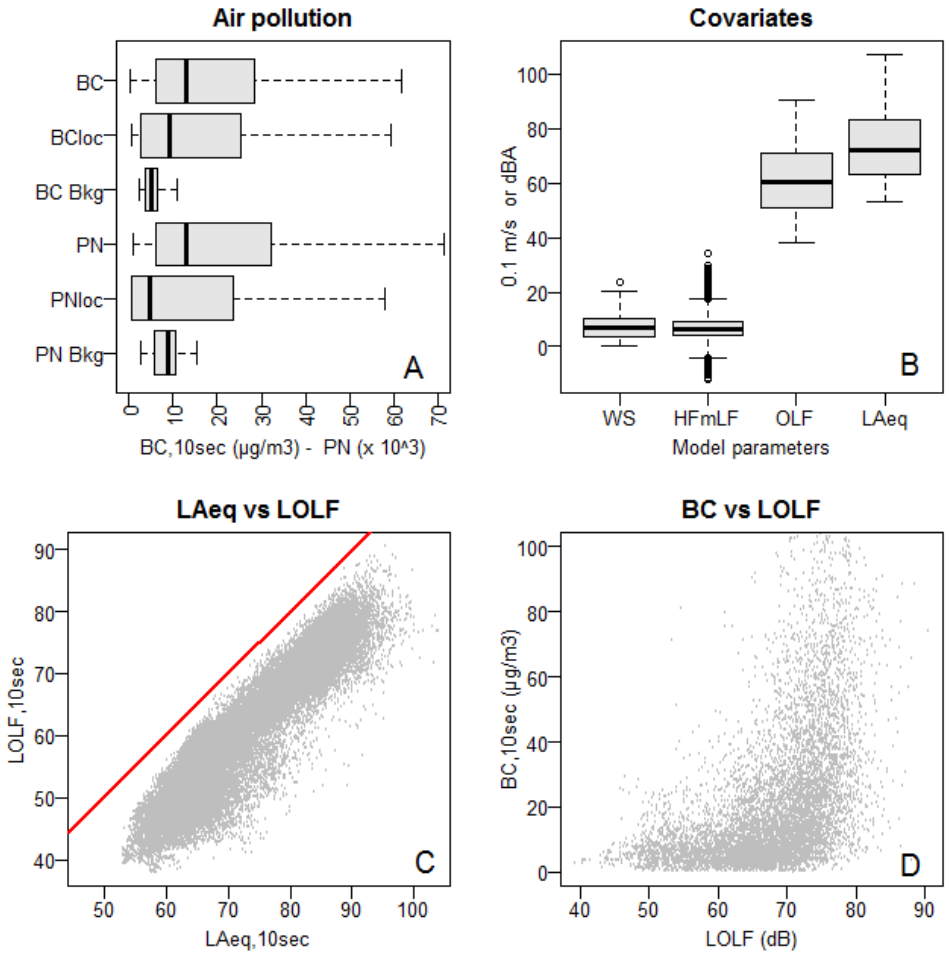

Figure 4.4.3: Distributions of the air pollution measurements: BC and BC_{loc} while biking, BC at the background location, PN and PN_{loc} while biking and PN at the background (A), distributions of the model covariates, wind speed, L_{HFmLF}, L_{OLF} and L_{Aeq} (B), relation between $L_{Aeq,10sec}$ and $L_{OLF,10sec}$ (C), relation between BC_{10sec} while biking and $L_{OLF,10sec}$ (D). Boxes represent interquartile range; whiskers represent 5th and 95th percentile. Plot B shows outliers as dots.

4.4.3.2 Black Carbon and Particle Number models

Models of BC and PN were developed using two types of dependent variables: measurements (1) unadjusted and (2) adjusted for background concentrations. The BC_{raw} model is based on measured BC concentrations $BC_{raw}(t)$ and investigates the relationship between $BC_{raw}(t)$ and the covariates L_{OLF}, L_{HFmLF}, wind speed and the logarithm of the background concentration $\log(BC_{bkg}(t))$. The BC_{loc} model is based on background adjusted BC exposure $BC_{loc}(t)$ as described in equation (1) and the same set of covariates. The BC_{loc} model investigates the potential to describe the actual BC exposure in an additive model similar to the approach in Dekoninck et al., 2013. The parameters of the GAM models are shown in Table 4.4-2. The quality of a GAM model and the relative strength of its parameters are described

by the deviance explained, the intercept, as well as the F-parameter and p-value for each of its covariates. Since the number of data points in the models is large compared to the number of covariates, the degrees of freedom is large and the p-values are in general too small to be used to compare the covariates. The F-parameters present the relative strength of the covariates instead. In the BC_{raw} model the intercept and the L_{OLF} have similar strength; the other covariates are almost ten times less important compared to L_{OLF}. The plots of the splines for both models show the relation of the parameter to the outcome $\log(BC_{loc})$ (Figure 4.4.4, top and second row). In the BC_{loc} model, L_{OLF} is even stronger compared to the BC_{raw} model. The influence of the background adjustment is visible in the stronger linearity of the spline of the L_{OLF} covariate for smaller L_{OLF}. The relative strength of the wind speed and L_{HFmLF} covariate compared to $\log(BC_{bkg})$ in the BC_{loc} model is higher than in the BC_{raw} model illustrating the effect of the background adjustment. Compared to Dekoninck et al. (2013), the strength of the wind speed covariate is low and this is likely due to the low variability of the wind speed in Bangalore during the measurement campaign. Note that the intercept of the BC_{raw} model in Bangalore is more than three times the value observed in Ghent and twice the value of the BC_{loc} model. The splines in the Bangalore model are similar to the model for Ghent.

	BC_{raw}		BC_{loc}		PN_{raw}		PN_{loc}	
	F	p-value	F	p-value	F	p-value	F	p-value
Intercept	9.50 (13,359 ng/m^3)		8.96 (8,103 ng/m^3)		9.54 (13,800cm^{-3})		8.29 (3,984 cm^{-3})	
Intercept (t value)	1,050		706		1,079		516	
L_{OLF}	1,692	<2e-16	1,792	<2e-16	1,421	<2e-16	1,376	<2e-16
WS	160	<2e-16	121	<2e-16	176	<2e-16	100	<2e-16
L_{HFmLF}	116	<2e-16	118	<2e-16	187	<2e-16	165	<2e-16
$\log(BC_{bkg})$	136	<2e-16	51	<2e-16				
$\log(PN_{bkg})$					133	<2e-16	11	6.0e-7
Deviance explained	45.7%		43.6%		35.8%		33.6%	
Number of datapoints	8,819		8, 819		8, 819		8, 819	

Table 4.4-2: Results of the BCraw, BCloc, PNraw and PNloc exposure models

We also developed a model for particle number concentrations to explore if PN behaves similarly to BC. The results are available in Table 4.4-2 and the splines are shown in the two bottom rows of Figure 4.4.4. The PN_{raw} and PN_{loc} models behave similarly to the BC_{raw} and BC_{loc} models for all covariates. The intercept of the PN_{raw} model is 13.8 x10^3 cm^{-3} and is reduced to 3,900 for the PN_{loc} model due to the background adjustment. L_{OLF} is the strongest component in both models; L_{HFmLF} is the second strongest component. The importance of the background PN concentration and the wind speed is relatively low in both models and

drops in importance in the PN_{loc} model compared to the PN_{raw} model and is more effective compared to the BC models. The wind speed covariate is weaker in the PN models than the BC models. The strength of the L_{OLF} covariate increases in most of the local models, expressing an improved noise-BC/PN relation after background adjustment.

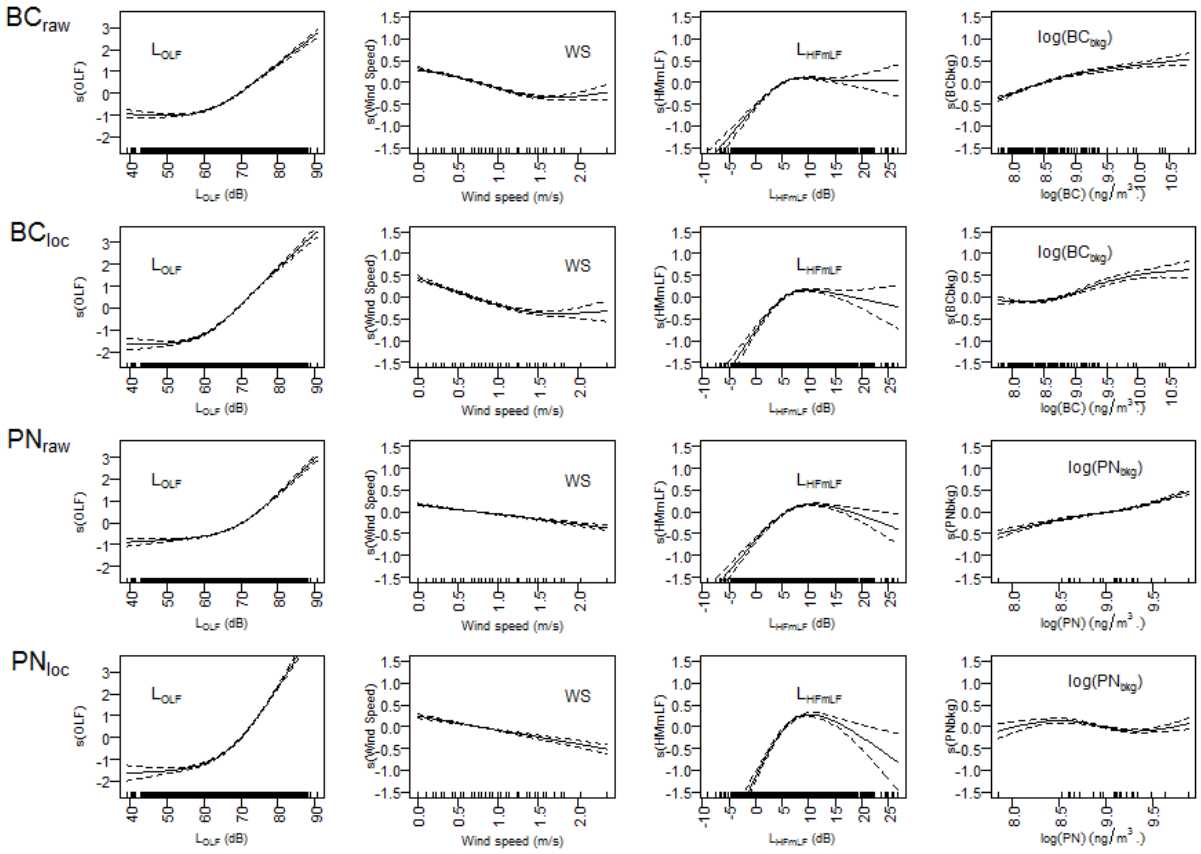

Figure 4.4.4: Splines of the four covariates for the BC_{raw}, BC_{loc}, PN_{raw} and PN_{loc} GAM models. Note the different scale used for L_{OLF} as compared to the other covariates since this covariate strength is an order of magnitude larger compared to the other covariates.

In Table 4.4-3 the results of the variants of the GAM models for the different correction functions are presented. The basic model using unadjusted BC measurements shows the highest F-value for the L_{OLF} covariate and the highest deviance explained. The noise-BC relation is consistent in all other models. In the background adjusted models the strength of L_{OLF} increases and the strength of $log(BC_{bkg})$ decreases; the deviance explained does not increase in these models due to loss of resolution in the dataset for low BC exposure. The alternative approach, removing the measurements below the instantaneous background does not improve the local models.

BC raw models								
Model	Intercept	F(L_{OLF})	F(WS)	F(L_{HFmLF})	F(log(BC_{bkg}))	deviance explained	count	AIC
BC (base)	13,324	1,692	159	115	135	45.7%	8,819	22,204
BC (Virk)	19,456	1,652	140	119	136	44.9%	8,819	21,772
BC (Kirch)	20,936	1,595	131	117	126	43.9%	8,819	21,840
BC (Hagler)	13,039	1,482	126	115	137	43.0%	8,819	23,587
BC (Apte)	13,165	1,456	150	78	143	46.0%	7,834	19,499
BC (Hagler+Virk)	18,962	1,385	105	114	133	41.1%	8,819	23,615
BC (Apte+Kirch)	20,267	1,371	129	79	145	44.3%	7,834	19,269
BC (Hagler +Kirch)	20,388	1,331	98	112	125	40.1%	8,819	23,741
BC local models (background adjusted)								
Model	Intercept	F(L_{OLF})	F(WS)	F(L_{HFmLF})	F(log(BC_{bkg}))	deviance explained	Count	AIC
BC_{loc} (base)	7,862	1,792	121	118	50	43.6%	8,819	28,109
BC_{loc} (Hagler)	7,907	1,750	118	128	57	43.3%	8,819	28,171
BC_{loc}_(Virk)	13,684	1,673	106	120	77	43.0%	8,819	26,506
BC_{loc} (Kirch)	15,079	1,605	102	119	75	42.0%	8,819	26,417
BC_{loc}_(Hagler+Virk)	13,655	1,599	100	130	81	42.2%	8,819	26,810
BC_{loc} (Apte)	7,646	1,589	137	81	53	44.5%	7,834	24,624
BC_{loc} (Hagler +Kirch)	15,023	1,529	95	128	78	41.2%	8,819	26,773
BC_{loc} (Apte+Kirch)	14,459	1,416	113	87	86	42.9%	7,834	23,149
PN models (raw + background adjusted)								
Model	Intercept	F(L_{OLF})	F(WS)	F(L_{HFmLF})	F(log(PN_{bkg}))	deviance explained	count	AIC
PN (base)	13,800	1,421	176	187	133	35.8%	8,819	21,724
PNloc (base)	3,984	1,376	100	165	11	33.6%	8,819	32,600
PN (Westerdahl)	14,045	1,422	175	185	132	35.8%	8,819	21,828
PNloc (Westerdahl)	4,004	1,401	100	164	11	33.6%	8,819	32,714

Table 4.4-3: GAM model evaluation for the BCraw and BCloc models for different correction and loading functions, sorting based on F(LOLF). The models based on the unadjusted data from Table 2 are added as a "base" case to allow for comparison. The abbreviated names relate to the first authors of the applied correction functions as listed in paragraph 2.2.

4.4.3.3 International comparison of the noise-based models

Upon completion of data collection in Bangalore it was possible to compare model results from Belgium and India. To make this comparison the total BC exposure is reconstructed by applying the prediction function of the GAM local models on an identical sequence of L_{OLF} while keeping other covariates constant and adding a background adjustment for the matching location. Wind speed was set to 1 m/s, L_{HFmLF} to 5 dB (relatively low traffic speed) and the street canyon index (Belgium-based model only) is set to a value that represents an urban environment (0.7). As background exposure the median of the difference between BC_{raw} and

BC_{loc} is used for each location. The results are plotted in Figure 4.4.5A for Ghent and Bangalore; predictions outside the range of measured values are shown as dashed lines. The model in Bangalore lacks resolution for the small L_{OLF} values, resulting in an almost constant exposure below 65 dB. The BC concentrations in Bangalore are almost exponential for the higher values of L_{OLF}. A second observation is that for the range of 50 to 70 dB, BC concentrations in Ghent are higher compared to Bangalore. In addition, a third model was developed for pooled data from the two sampling campaigns (giving each dataset equal weight in the GAM model). The pooled data model could only include covariates that were available in both cities and is therefore restricted to L_{OLF}, wind speed and L_{HFmLF}. The authors are aware that the pooled data model implies similar noise-BC emission relations for both locations, despite the extremely different fleet composition. Higher air pollution emission could relate to the noise emission of the vehicles and is assumed valid within the scope of this comparison. In Figure 4.4.5B; the resulting simulations are presented for the pooled model with the local matching BC background (3,600 ng/m^3 for Bangalore and 1,600 ng/m^3 for Ghent). The simulation is evidently higher for Bangalore compared to Ghent over the full range.

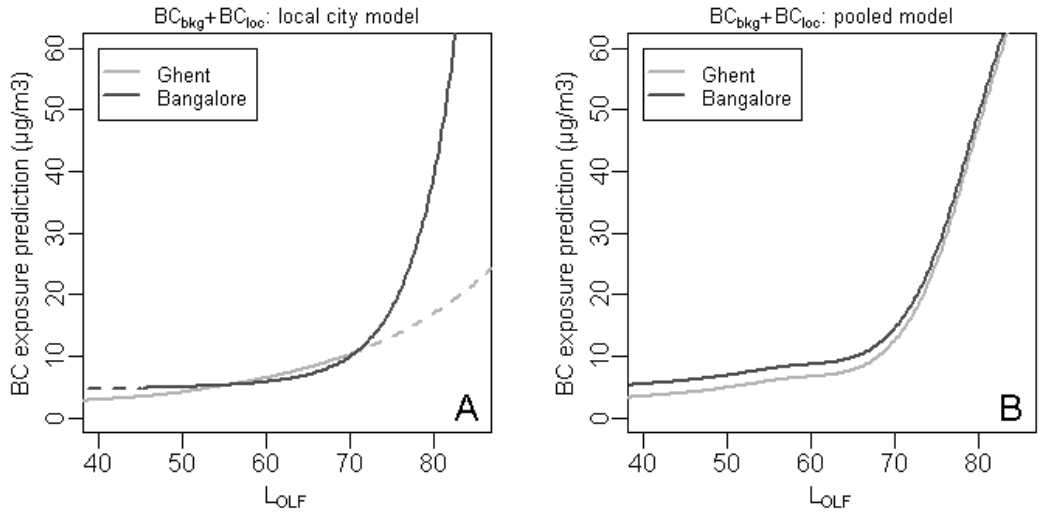

Figure 4.4.5: Comparison of Ghent and Bangalore BC prediction for fixed wind speed and L_{HFmLF} values, dashed lines present extrapolated results outside the measured range of L_{OLF} (A) and the BC prediction by location based on the pooled data model with matching background adjustment by location (B).

The second step to compare the Ghent and Bangalore models is to perform a cross validation by predicting the measurements in Ghent with the model based on the measurements in Bangalore and vice versa and predicting both measurement campaigns with the pooled data model. The predicted exposure is aggregated for each sampling trip and compared to the actual measurements for that trip (see Figure 4.4.6). The measured vs. modelled prediction correlations are weaker when transferring models between cities; this result parallels the L_{OLF}-BC relationship for the two models shown in Figure 4.4.5A. The slope and absolute prediction of the Ghent trips is lower due to the underestimates of the Bangalore model for L_{OLF} of 50 to 70 dB; the opposite effect is visible for the trips in Bangalore predicted with the

Ghent model for L_{OLF} larger than 70 dB. The pooled data model is almost identical to the Ghent model for L_{OLF} below 70 and performs well on the Ghent trips. The combined model improves the prediction of the Bangalore trips compared to the Bangalore model significantly due to the improvement of resolution in the combined model for L_{OLF} below 70 dB. The pooled data better specifies the L_{OLF} parameter and improves the prediction for the Bangalore data despite the fact little data was collected in Bangalore below 70 dB. This results in correlation of 0.84 for the total trip exposure fit with the pooled model.

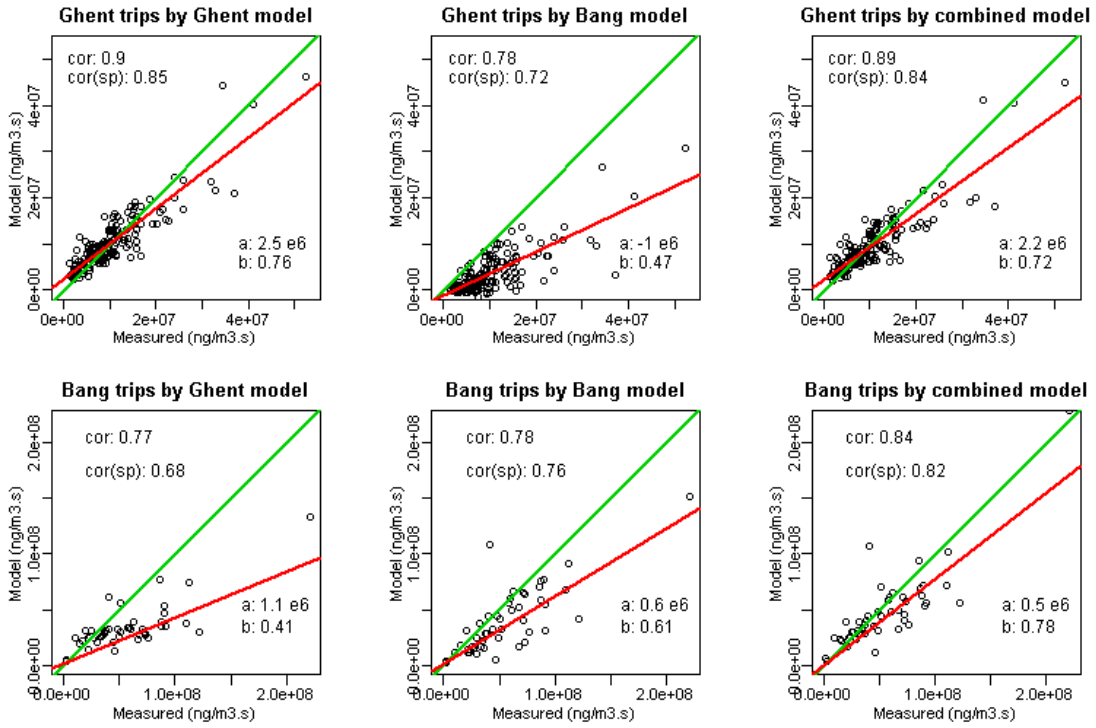

Figure 4.4.6: Trip-based comparison and cross validation of the Ghent and Bangalore models. Each dot represents the total predicted exposure by trip compared to the measurement. The green line indicates the perfect fit; the red line presents the linear fit on the total trip exposure predictions. Correlations (Pearson and Spearman) and linear fit parameters of the trip prediction are shown for each plot.

4.4.4 Discussion

A monitoring campaign was conducted for independently cross validating a previously designed model for predicting cyclist exposure to black carbon on the basis of noise measurements (Dekoninck et al., 2013) in a completely different socio-economic context. The results show that indeed the exposure to noise and black carbon are significantly higher in Bangalore, India, than in Ghent, Belgium. The bicyclist's exposure to BC in Bangalore exceeds the exposure in Belgium by a factor of four. The range of noise levels observed is at least 10 dBA higher. The observed between-city difference in the range of measured L_{OLF} could be due to a variety of factors. The first candidate is the fleet composition; the number of motorcycles and motorcycle-like vehicles is large compared to Belgium and the individual vehicle noise is

high. There are few noise regulations and reducing the individual-vehicle noise is not considered a priority in India. The second candidate is the lack of bicycle facilities. During sampling the cyclists travelled among other vehicles (especially close to motorcycles). Since the concentrations of BC increase exponentially with smaller distance to the tail-pipe, cyclists in India are exposed to less-diluted exhaust emissions and comparatively high noise levels.

In addition to the context, the monitoring campaign conducted in Bangalore also differed slightly in design from previous measurements. An important technical difference is the use of consumer grade microphones and data acquisition rather than high-quality IEC class 1 graded measurement equipment. As we stated before, using noise as a proxy for particulate air pollution is beneficial because noise measuring equipment is significantly cheaper. However this difference in cost is not high unless noise measurements can be done with consumer grade equipment. It has been shown previously that consumer electrets can be used for traffic noise monitoring over long time intervals (Van Renterghem et al., 2011) but it is also known that these devices may exhibit noise floors of 35 to 40 dBA. Comparing these values to the range of observations in Figure 4.4.3 it becomes clear that they will cause no deviations in measurements of noise in streets. The new back-end database and internet based communication with the mobile measurement equipment showed that it is possible to seamlessly collect, manage and process measurements of noise and particulate matter simultaneously. The automated post-processing of the measurements resulted in quick reporting allowing evaluation of the progress of the measurement campaign on a daily basis. The monitoring campaign in Bangalore has shown the feasibility of internet-based measurement campaigns for noise and air pollution with low latency data storage and processing distributed across the globe (India, Belgium, USA).

Based on a one-year dataset of commuting noise and black carbon measurements, two parameters derived from the noise spectrum were found to be most suitable for explaining 10 second aggregated BC exposure of cyclists: L_{OLF} and L_{HFmLF}. In addition, it was found that including wind speed measured at a nearby weather station and an indicator for the street geometry – expressing how strong it resembles a canyon – improved the performance of the proposed GAM model. In the current study, street geometry could not be included. Nevertheless, the goodness of fit of the GAM model extracted in this study confirms that the choice of (noise) parameters is valid also in a completely different socio-cultural context. With this fixed choice of noise parameters, the proposed prediction of in-traffic exposure to black carbon can thus be used in a variety of international settings using a small dataset of combined noise and BC measurements to validate the model coefficients. Aethalometer-based black carbon measurements are sensitive to measurement error and therefore several corrections and loading functions have been proposed in literature (Apte et al., 2011, Hagler et al., 2011, Virkkula et al., 2007, Kirchstetter et al., 2007 and Westerdahl et al., 2007). It was found (Table 3) that the choice of correction and loading function has a limited influence on the model coefficients and hardly affects model performance (deviance explained and AIC).

The model is robust against these corrections. A possible explanation for this is that the model already smooth out most of the measurement errors that are also eliminated by the aforementioned corrections.

Based on the theoretical consideration that measured levels of BC have both a local origin, mainly caused by traffic, and a more regional origin including industrial, heating, and distant traffic, the measured BC concentration is split in a local and a background concentration. The rationale for treating a background contribution separately in the proposed models is that noise levels could be an indicator for the local traffic contribution to the overall level but are not expected to be indicative for the origin of background contributions. However, it has also been pointed out that a measured background concentration could also be a good indicator for dispersion of air pollutants in general since it strongly depends on weather conditions (Dominici et al, 2002). In the proposed models the former is included by subtracting the background from the raw measurement data, the latter is partially captured by a multiplicative factor included as a $\log(BC_{bkg})$ factor in the GAM model for $\log(BC_{loc})$. The factor $\log(BC_{bkg})$ in the GAM model for $\log(BC_{raw})$ is added to illustrate the effect of the additive approach in the models. Because of the strong non-linearity of the GAM, there is no strict separation between additive and multiplicative. Yet, the fact that the strength of the $\log(BC_{bkg})$ factor decreases once an additive correction for background has been applied indicates that the additive approach is valid. It results in a model explaining 45.6% of variance and could therefore be a valid alternative for the explicit background correction introduced in Section 2.3. An important issue however is how well the background measurements capture the background exposure variation due to long term meteorological conditions. Here, the background measurement location is inside the city of Bangalore and might be influenced by the diurnal pattern of in city traffic related air pollution exposure partially masking the long term background conditions. The quality and the properties of the BC background measurement location are important when employing an additive modelling approach. Still, this method for taking into account background concentrations could serve as a source of inspiration for mobile air pollution measurement processing in general.

A model using the same noise parameters was also established for particle number. The variance explained by this model is somewhat lower than for the BC model. PN concentration is also mainly related to traffic exhaust, but even more variable than BC, the lower variance explained is therefore expected. The background adjustment did not require strong restrictions through $PN_{bkg,limit}$ to achieve a performant BC_{loc} model. This suggests a different spatial behaviour of the relation between local and background exposures for PN compared to BC. BC background is probably more sensitive to local non-traffic related exposure compared to PN. Also physical differences between the two quantities could explain this difference. BC is mass based and does not distinguish between the sizes of the particles. PN is known to increase near tail-pipes and decreases strongly due to the coagulation processes at larger distances from the source, reducing the number of particles faster with distance

from the source compared to mass based quantities. The meteorological situation is therefore likely to have less influence on the background PN compared to background BC. The noise-PN relationship can be stronger compared to noise-BC relationship.

When comparing the models for Ghent and Bangalore, it is clear that the Bangalore model lacks observations for L_{OLF} below 65 dB and overestimates BC below that level as compared to the model for Ghent (Figure 4.4.5). Similarly, the dataset collected in Ghent lacks observations with L_{OLF} above 70 dB which results in underestimation of BC concentration at high noise levels in an extrapolated model. Extracting model parameters from the pooled data (Figure 4.4.5B) results in a single smooth relationship which is indicative for a common ground truth in the relationship between L_{OLF} and log(BC). When cross-validating the average exposure to BC during bicycle trips by comparing model predictions to measurements some interesting conclusions can be drawn. As expected, the correlation between model and measurement decreases when model coefficients from the other area are used. However, using the model based on pooled data, the correlation improves for the Bangalore trips (Figure 4.4.6 bottom right) while it does not deteriorate for the Ghent data (Figure 4.4.6 top right) both compared to the correlation with the model based on local data. This suggests a strong underlying relationship between noise and BC concentrations capable of distinguishing spatial variability beyond the disturbance of background and meteorological effects on the air pollution exposure measurements.

The authors suggest extending these measurement campaigns and using similar approaches for other traffic-related air pollutants in different countries. The quality of the background measurement site is an issue worth further investigation for future international deployment of this approach. Detecting and quantifying the contribution of the local traffic to the instantaneous exposure in environments where emissions from local traffic are low as compared to the ambient concentrations is crucial to improve the models. This can and should be achieved by several adjustments in the measurement setup. Extending the measurements to more variable meteorological conditions and extending the scope of the measurements to cover more spatial variability are two potential improvements. This technique attributes mobile measurements based on physical parameters, adding value to the current practice of manual qualification of traffic based on video footage. The simultaneous noise measurements add knowledge to the exposure measurements in an unprecedented temporal resolution enabling the disentanglement of the variation of the in-traffic exposure into a local traffic related component, the meteorological influences and background exposure. It also enables the use of random sampling in participatory measurement campaigns since the traffic is instantaneously documented in space and time. As illustrated in the Table 4.4-3, the technique can be used in the future to compare the BC correction functions, potentially distinguishing between short term variation related to actual physical changes in the instantaneous exposure and variation related to instrumentation errors.

4.4.5 Conclusions

Exposure to traffic-related air pollution is strongly related to local traffic dynamics which can be characterized by spectral noise measurements. The physical relationship between noise and particulate air pollution was confirmed using an inexpensive noise measurement node in an entirely different socio-cultural setting (Bangalore, India) than previous work in Belgium with high-quality noise measurement equipment. The consumer grade noise measurement setup results in mobile noise measurements that are accurate enough to predict air pollution exposure. The full technical setup consisting of inexpensive measurement nodes combined with a back-end database and data post-processer enabled fast and accurate in-traffic sampling and reporting. Despite the significant differences between the local traffic conditions in Ghent, Belgium and Bangalore, India the mobile BC models behave similar. Moreover, trip exposure estimates based on a model fitted on pooled data from both monitoring campaigns correlates better with measurements. Sampling strategy has a strong impact on the properties of the models, low exposure route sampling is as important in the measurement campaigns as achieving proper quantification along the high exposure roads. Splitting the measurements in an instantaneous background concentration and a local contribution gave similar results as in previous work; however, high background concentrations can reduce the spatial resolution of the method in low exposure streets. The characteristics of the background measurement location have a strong impact on the additive modelling approach and should be carefully considered in future projects. As an alternative, introducing background concentration as a log-additive term in the GAM model also increased the explained variance in a way that is partly complementary to separating background concentrations in an additive way.

Implementing this technique in places where only a few parameters change has the potential to disaggregate the effects of factors influencing in-traffic exposure (e.g., vehicle fleet, biking facilities, driving behaviour and meteorology). For example, in the case of Belgium with its high number of diesel vehicles, a comparison with a similar European city but with a different fleet mix could allow for the quantification of the impact of diesel fuel related policy.

An identical model with the same noise covariates is valid as well for the mobile PN measurements, extending the potential of the methodology. The first results on PN for the additive modelling approach suggest that PN is less sensitive to properties of the background measurement location compared to BC. The international validation of this method for two important traffic-related pollutants (BC and PN) demonstrates the potential to evaluate within-city spatial patterns of particulate air pollution based on noise measurements in a variety of urban settings.

4.4.6 References

Apte J.S., Kirchstetter T.W., Reich A.H., Deshpande S.J., Kaushik G., et al. 2011. Concentrations of fine, ultrafine, and black carbon particles in auto-rickshaws in New Delhi, India. Atmospheric Environment, 45, 4470-4480.

Boogaard H., Kos G.P.A., Weijers E.P., Janssen N.A.H., Fischer P.H., et al. 2011. Contrast in air pollution components between major streets and background locations: Particulate matter mass, black carbon, elemental composition, nitrogen oxide and ultrafine particle number. Atmospheric Environment, 45, 650-658.

Banerjee et al., Appraisal and mapping the spatial-temporal distribution of urban road traffic noise, Int. J. Environ. Sci. Tech, 6, (2), 325-335, 2009.

Cai J., Yan B.Z., Kinney P.L., Perzanowski M.S., Jung K.H., et al. 2013. Optimization Approaches to Ameliorate Humidity and Vibration Related Issues Using the MicroAeth Black Carbon Monitor for Personal Exposure Measurement. Aerosol Science and Technology, 47, 1196-1204.

Can A., Dekoninck L., Rademaker M., Van Renterghem T., De Baets B., et al. 2011. Noise measurements as proxies for traffic parameters in monitoring networks. Science of the Total Environment, 410, 198-204.

Can A., Van Renterghem T., Rademaker M., Dauwe S., Thomas P., et al. 2011. Sampling approaches to predict urban street noise levels using fixed and temporary microphones. Journal of Environmental Monitoring, 13, 2710-2719.

Dauwe S., Van Renterghem T., Botteldooren D. & Dhoedt B. 2012. Multiagent-Based Data Fusion in Environmental Monitoring Networks. International Journal of Distributed Sensor Networks. International Journal of Distributed Sensor Networks, Volume 2012 (2012), http://dx.doi.org/10.1155/2012/324935

Dekoninck L., Botteldooren D. & Int Panis L. 2013. An instantaneous spatiotemporal model to predict a bicyclist's Black Carbon exposure based on mobile noise measurements. Atmospheric Environment, 79, 623-631.

Dominici F., McDermott A., Zeger S.L. & Samet J.M. 2002. On the use of generalized additive models in time-series studies of air pollution and health. American Journal of Epidemiology, 156, 193-203.

Dons E., Int Panis L., Van Poppel M., Theunis J. & Wets G. 2012. Personal exposure to Black Carbon in transport microenvironments. Atmospheric Environment, 55, 392-398.

Dons E., Temmerman P., Van Poppel M., Bellemans T., Wets G., Int Panis L. 2013. Street characteristics and traffic factors determining road users' exposure to black carbon. Science of The Total Environment, 447C:72-79. DOI:10.1016/j.scitotenv.2012.12.076

Hagler G.S.W., Yelverton T.L.B., Vedantham R., Hansen A.D.A. & Turner J.R. 2011. Post-processing Method to Reduce Noise while Preserving High Time Resolution in Aethalometer Real-time Black Carbon Data. Aerosol and Air Quality Research, 11, 539-546.

Janssen N.A.H., Hoek G., Simic-Lawson M., Fischer P., van Bree L., et al. 2011. Black Carbon as an Additional Indicator of the Adverse Health Effects of Airborne Particles Compared with PM_{10} and $PM_{2.5}$. Environmental Health Perspectives, 119, 1691-1699.

Karner A.A., Eisinger D.S. & Niemeier D.A. 2010. Near-Roadway Air Quality: Synthesizing the Findings from Real-World Data. Environmental Science & Technology, 44, 5334-5344.

Kirchstetter T.W. & Novakov T. 2007. Controlled generation of black carbon particles from a diffusion flame and applications in evaluating black carbon measurement methods. Atmospheric Environment, 41, 1874-1888.

Pearce J.L., Beringer J., Nicholls N., Hyndman R.J. & Tapper N.J. 2011. Quantifying the influence of local meteorology on air quality using generalized additive models. Atmospheric Environment, 45, 1328-1336.

Sandberg and Ejsmont, 2002. Tyre/road noise reference book, published by INFORMEX.

Sen R. et al., Horn-ok-please, MobiSys '10 Proceedings of the 8th international conference on Mobile systems, applications, and services. ACM New York, NY, USA 2010, ISBN: 978-1-60558-985-5, 137-150,

Van Renterghem T., Thomas P., Dominguez F., Dauwe S., Touhafi A., et al. 2011. On the ability of consumer electronics microphones for environmental noise monitoring. Journal of Environmental Monitoring, 13, 544-552.

Virkkula A., Makela T., Hillamo R., Yli-Tuomi T., Hirsikko A., et al. 2007. A simple procedure for correcting loading effects of aethalometer data. Journal of the Air & Waste Management Association, 57, 1214-1222.

Westerdahl D., Fruin S., Sax T., Fine P.M. & Sioutas C. 2005. Mobile platform measurements of ultrafine particles and associated pollutant concentrations on freeways and residential streets in Los Angeles. Atmospheric Environment, 39, 3597-3610.

WHO Europe, 2012: Health effects of black carbon, ISBN: 978 92 890 0265 3.

Wood S.N. 2006. On confidence intervals for generalized additive models based on penalized regression splines. Australian & New Zealand Journal of Statistics, 48.

4.5 Instantaneous in-vehicle BC exposure.

This section will be submitted in an adjusted form as a full research paper.

ABSTRACT

Several studies have shown that a significant amount of daily air pollution exposure is inhaled during trips. We set-up a campaign during which car drivers assessed their own exposure under real conditions. 223 hours of data was collected. In-vehicle exposure is highly dynamical and is strongly related to the local traffic dynamics. An extensive set of potential covariates including wind speed, temperature, background concentrations, vehicle speed, acceleration, relative speed to the local speed limit, traffic counts are investigated in a temporal resolution of 10 seconds. Traffic data is retrieved directly from traffic databases and indirectly by attributing the trips to L_{DEN} noise maps as an alternative proxy.

Modelling by generalized additive models (gam) shows strong non-linear effects for meteorology, traffic dynamics and traffic count attribution. A diurnal traffic count attribution fails to predict the diurnal patterns of the in-vehicle exposure. Comparing the strength of traffic and noise map based traffic attribution reveals significant potential for noise attribution. External validation showed strong discrepancies. Only half of the absolute level of the exposure in a four year old validation set could be explained with the model despite high correlation (0.8). Several potential biases were identified. The recent implementation of the EU PM Euro 5 emission standard can explain between 30% and 40% of the discrepancy between the two participatory campaigns. This change matches the evolution of the passenger car fleet in Belgium (80% of the vehicle-km are driven with diesel).

Instantaneous modelling at high temporal resolution can provide successful prediction models without the need of disentangling the underlying complex interaction of the relevant covariates. Noise maps are a valid proxy for in-vehicle exposure mapping.

4.5.1 Introduction

Exposure to particulate matter is currently regulated in PM standards that only distinguish between the size of the particles (PM_{10}, $PM_{2.5}$…). The soot fraction, Black Carbon (BC) is the part of the PM directly related to combustion processes and is not yet regulated. Recent evidence, summarized by the world health organization, documents the relevance of BC for evaluating traffic related health effects (WHO Europe, 2012). Recent epidemiological results for BC suggest health effects per mass may be up to 10 times higher than PM_{10} (Janssen et al., 2011). Large personal exposure measurement campaigns prove the relevance of the in-traffic exposure contribution (Dons et al., 2011, 2012). Further research into health effects is hampered by the difficulty to measure or model the actual personal exposure to BC. An im-

portant reason for this is the strong spatial variability of BC compared to PM_{10} (Karner et al., 2010).. Assessing exposure in vehicles is a complex issue, reported extensively by several authors, each investigating a subset of relevant parameters. Outdoor concentrations are reported to be very dynamic along trajectories. An extensive study on bicyclists Black Carbon exposure detect local changes of a factor 15 to 20 only due to changing local traffic dynamics and instantaneous meteorology (Dekoninck et al., 2013). Especially in the immediate vicinity of traffic lights and complex traffic situations high exposure levels were found. Other authors reported similar effects based on road classification for different air pollutants (Dons et al. 2013, Hudda et al, 2012).

Ventilation settings and influence of vehicle speed on the ventilation is addressed by several authors (Hudda et al., 2011, Knibbs et al., 2010, Fruin et al., 2011). When investigating the effect of ventilation settings the lag between outdoor and indoor concentrations changes. An extensive literature study on the ventilation settings and effects of in-vehicle exposure result in an important conclusions. With 'outdoor air ventilation' settings, outdoor exposure changes are registered very fast inside the vehicle. Lags between 30 and 60 seconds are detected. The driving force of the personal exposure inside the vehicle will be the outside concentration.

The first instantaneous in-vehicle personal exposure models are based on traffic counts, road types, the number of lanes, speed of the traffic and a set of meteorological parameters (Carslaw, 2007). The largest study is based on about 300 kilometres of data on a predefined route covering a period of six weeks (Li et al, 2013). The authors focus on the comparison of linear models and gam models in their attempts to model the in-vehicle exposure. They conclude that the gam models capture more of the non-linear features in the highly diverse set of exposure descriptors. The model is adjusted by road classification and does not attempt to describe the local traffic dynamics. The authors also mention lack of instantaneous traffic data and tested the use of more general traffic parameters such as the annual average daily traffic (AAWT, only weekdays). Effort to predict instantaneous particulate matter exposure in-vehicle have not been very successful at this point due to the interactions between meteorological conditions, local traffic dynamics, ventilation settings, vehicle properties, etc..

In this work, we attempt to build a LUR model with high spatial and temporal resolution. Spatiotemporal modelling of bicyclist's black carbon exposure based on simultaneous noise measurements proved to be successful (Dekoninck et al., 2013). A similar approach will now be tested for the in-car micro-environment. An important feature of noise maps is the high spatial resolution of the calculations,. The sources and receivers are positioned with a spatial detail of meters, a spatial detail that is rarely available in air pollution maps. These types of noise maps are available for all major cities and all major roads in Europe through the environmental noise directive of the European Committee (END; (European Commission 2002/49/EC)). A strong synergy is possible if the noise maps can also be used for personal air pollution assessments. A few research questions will be addressed in this paper: How does

the in-vehicle exposure relate to the different spatial and temporal covariates? Can a noise map be a proxy for the traffic attribution? Can a reduced model be built without including local traffic dynamics derived from the GPS tracking? Section 4.5.2 addresses the measurement campaign, the methodology and the definition of the covariates. Section 4.5.3 will present the data exploration and the models. In section 4.5.4 an external validation is performed and the discrepancies are investigated in detail. Results are discussed in section 4.5.5.

4.5.2 Methodology

4.5.2.1 Measurement equipment and setup

A low-cost noise measurement setup enables automated mobile measurements at a much lower hardware cost (Can et al., 2011a, Can et al., 2011b, Van Renterghem et al., 2011, Dauwe et al., 2012). The noise measurement module is extended with a GPS (Haicom HI-204 III USB), a micro-aethalometer (AE51, Aethlabs, San Francisco, CA) and a battery. Software was developed to automatically capture the 1-second data stream from the micro-aethalometer. After a set of measurements, the mobile node was connected to the internet and the data uploaded to a database. An automated process synchronizes and merges the noise, GPS and BC data based on the timestamp of the mobile node. Within this evaluation only the BC and the GPS data are used. The equipment was used in an exposure experiment in Bangalore, India. More details on the equipment can be found in Dekoninck et al, 2015 (see also 0).

To model real life exposure conditions, a 'un-controlled' participatory campaign is performed with little knowledge on the vehicle types and personal preferences of the drivers towards the ventilation settings. Nine volunteers carried the equipment on the passenger seat while travelling their typical trajectories. Two of the people are sales representatives, travelling long distances. The participants perform their commutes within their daily behaviour. The measurements cover a full year and the whole region of Flanders. Rush hour and off-peak traffic situation are sampled. The in-vehicle measured exposure is evaluated every 10 seconds. 340 individual car trips were performed during weekdays with a total measurement time of 223 hours between December 2012 and November 2013. The random trips result in an uncontrolled combination of multiple variables: meteorological conditions, background concentration, number of measurements during the different episodes during the day, route choice, actual ventilation settings, participants vehicle fleet and so on. The dataset is assumed to express real-life use and traffic conditions. The measurements are attributed with meteorology and background concentrations; local traffic dynamics are added through the GPS tracking. Traffic is attributed from various spatial and spatiotemporal data

sources. An L_{DEN} noise map will be used as a proxy for the local traffic attribution and is compared with the traffic count on the road segments.

4.5.2.2 Model covariates

The BC measurements are attributed with a set of potential relevant attributes for detailed analysis. In this section we provide a short summary of the covariates, more information on the basic data sources is available in Appendix B; detailed information on the pre-processing of the in-vehicle data is available Appendix E. Traffic dynamics related parameters, speed and acceleration, are deduced from the GPS positions. The wind speed and temperature are retrieved from the closest of five meteorological stations. The meteorological data was made available by the royal meteorological institute of Belgium. The BC background concentrations are retrieved from a background measurement location (Linkeroever-Antwerpen, ref 40AL01). Traffic is available as an hourly average by day of the week and includes the diurnal pattern. Traffic is available on 80,000 links in the Flemish area with a resolution of roads connecting the smallest villages. The traffic is linked to the segments to match the closest road. The speed limit of the road is retrieved from the same dataset. The alternative traffic attribution is based on a regional noise map (MIRA 2013), based on the same traffic data (data for the year 2012). The yearly changes in traffic are typically below 1 percent per year and 2012 data are therefore representative for the measurement period. The noise map is the L_{DEN} with correction for the day, evening and night exposure as requested by END noise directive. This is a single value for each point in space, not including diurnal details. This type of noise map is chosen because it is available for all major agglomerations of the European community and available for each road with more than 60,000 vehicles per year and for all cities with more than 50.000 inhabitants since the end of 2014. An example of the spatial detail of the noise map is available in Appendix B.

Next to the strong potential local contribution of the traffic on the in-vehicle exposure, more macroscopic dynamics can be expected. Large cities with many roads and higher traffic densities also coincide with increased activities with mid-range impacts on the background levels. To accommodate this mid-range spatial variability, a PM_{10} air pollution map with a resolution of five kilometres is used for the Flemish region (see Appendix B). Also the street canyon effect is included in the models based on a custom build street canyon index as was defined in previous work (supplementary data of Dekoninck et al., 2013 and Appendix B).

4.5.2.3 GAM modelling

Generalized additive models (GAMs) are regression models where smoothing splines are used instead of linear coefficients for the covariates. This approach has been found to be particularly effective for handling the complex non-linearity associated with air pollution

research (Li et al., 2013, Carslaw, 2007). The additive model in the context of spatial exposure modelling can be written in the form:

$$\log\big(BC_j(t)\big) = \sum_{z=1}^{n} s_z\,(v_{z,j}(t)) + \varepsilon_{x,j}(t) \qquad (3)$$

Where v_z is the z^{th} covariate evaluated for trip j at time stamp t; $s_z(v_{z,j}(t))$ is the smooth function of z^{th} covariate, n is the total number of covariates, and $\varepsilon_{x,j}(t)$ is the corresponding residual with $var(\varepsilon_{x,j}(t)) = \sigma^2$, which is assumed normally distributed. Smooth functions are developed through a combination of model selection and automatic smoothing parameter selection using penalized regression splines, which optimize the fit and try to minimize the number of dimensions in the model. The main advantage of GAM modelling is the possibility to adjust for non-linear relationships between the covariate and the outcome. The analysis was constructed using the GAM modelling function in the R environment for statistical computing (R development Core Team, 2009) with the package 'mgcv' (Wood, 2006).

4.5.3 Data exploration and models

In appendix E.2.1, the lag between the instantaneous traffic conditions and the in-vehicle exposure is investigated. The model using an accumulated lag of 60 seconds shows the highest deviance explained. The accumulated lag is the average of six 10 second values at and after the evaluated timestamp, referred to as LAG60. Also a weighting function based on the exposure levels is applied to increase the predictive strength on trip total exposure. The dataset contains few extreme exposure values and this weighting is chosen to achieve a high trip fit predictions (see Figure 4.5.2, details in the next paragraph). All results are based on the LAG60 exposure dataset, this model is referred to as BC_LAG60_WBC, the model with all covariates, an implemented lag of 60 seconds and weighting applied to the BC to reach proper trip fits. First the non-linear exposure in-vehicle characteristics are presented and commented. In the second section the different traffic attributes are compared.

4.5.3.1 Non-linear in-vehicle exposure characteristics

In this section the model BC_LAG60_WBC is presented including all covariates. The strength of the different covariates is available in appendix E, Table 1. The aim is to illustrate the variability in the measurements and map the specific non-linear characteristics of all the covariates to the potential origins of the in-vehicle exposure variation. The hourly traffic counts and noise attribution are presented within a single model to illustrate the relative behaviour and strength (Figure 4.5.2).

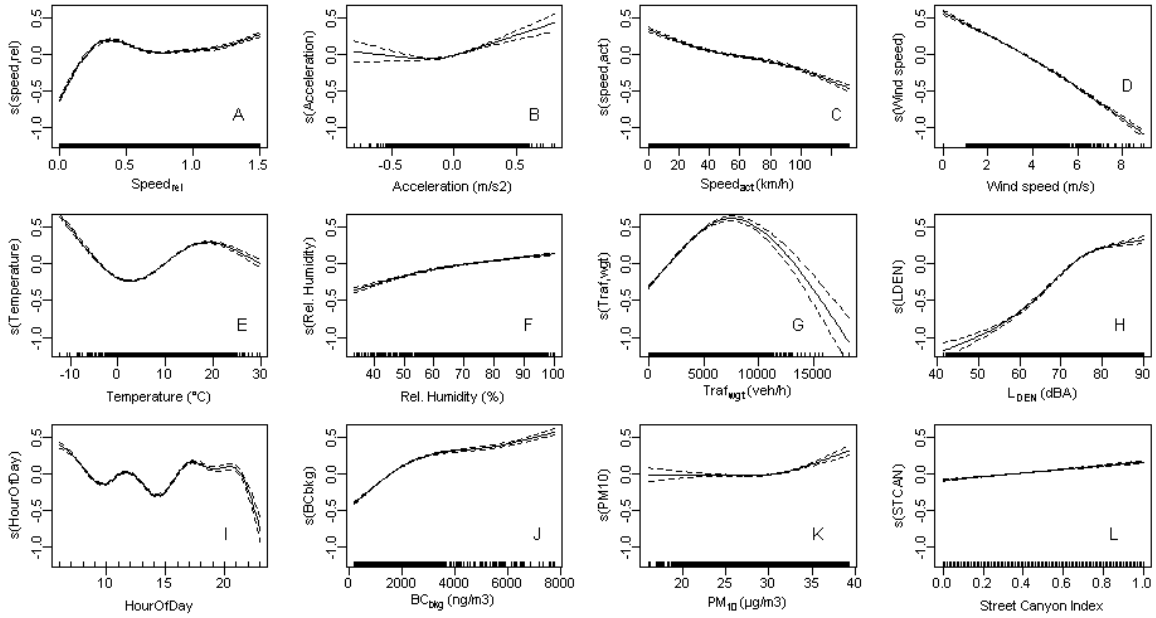

Figure 4.5.1: Splines of the BC_LAG60_WBC gam model, expressing the non-linear properties of the covariates. The local traffic dynamics are shown in A, B and C, the meteorological covariates in D, E and F, the traffic related covariates in G, H and I. The temporal background exposure level in J, the general spatial related attributes in K and L.

The speed relative to the speed limit ($speed_{rel}$) shows a maximum when $speed_{rel}$ is below 0.5. The peak can relate to dynamic traffic with start- and stops and/or congested traffic. Short distances between vehicles in these traffic conditions and changes PM emission dynamics result in higher in-vehicle concentrations. The acceleration is the weakest covariate and highly sensitive to the quality of the GPS readings but behaves as expected; increased levels when accelerating and decreased levels with moderated deceleration. Strong deceleration, related to actual stops in traffic, shows high variability that can relate to the short distance to source when waiting and idling in a queue at a traffic light. The bulk of the data shows little or no acceleration and this is reflected in the very low strength of the covariate. The actual speed ($speed_{act}$) shows higher values at low speeds and higher values at high speed. The increased levels at low speed can find their origin in congested traffic as well. The reduction of in-vehicle exposure at high speeds could be linked to the higher efficiency of the ventilation systems at higher speed as mentioned by Xu (Knibbs, 2010, Xu et al., 2011). Higher speeds also relate to free flow traffic with higher distances between the vehicles. Other interactions with other covariates are also possible, the actual speed does for example also relate to the type of road travelled. $Speed_{act}$ is lower in strength compared to $speed_{rel}$, expressing the different and often contradicting driving forces for this covariate.

The in-vehicle exposure decreases with high wind speeds as expected (Li et al., 2013, Carslaw et al., Xu et al, 2011). Wind speed is by far the strongest covariate. The temperature shows a distinctive and complex pattern. Very low temperatures and moderate temperatures result in high exposure, low and very high temperatures result in lower exposure. The high exposure at very low temperatures can relate to the cold periods with high background

levels, stable atmosphere and/or due to cold start increased vehicle emission. The high exposure for moderate temperatures and the lower exposure for the highest temperatures can be linked to the changing ventilation settings. At moderate temperatures fresh outdoor air is enough for cooling and refreshing the vehicle interior, at higher temperatures air condition is turned on and changes the air flow to recirculation with strong effects on the in-vehicle concentration (Xu and Bin, 2014, Lee et al., 2014). Relative humidity shows increased levels at high values. This potentially links to the light scattering properties of water saturated BC particles which can trigger an increased response in the µ-aethalometer (Cai et al., 2013). Xu and Bin reported a reduced efficiency of vehicle cabin air filter in humid conditions (Xu et al., 2014).

The large scale spatial covariate (K) introduced in the model through the PM_{10} map has an interesting feature. For low values, the covariate is not significant but at high levels -typically near the major cities- adds value to the model, expressing augmented in-vehicle concentrations in larger cities. This links to the higher density of roads and traffic in and around the cities through several mechanisms (higher urban background, increased traffic congestion, etc.). The street canyon index correlates with the PM_{10} map but adds spatial detail compared to PM_{10}.

The two traffic related data sources, L_{DEN} and weighted traffic $Traf_{wgt}$, are similar in strength despite the fact that L_{DEN} is only a spatial covariate and $Traf_{wgt}$ is a spatiotemporal covariate. The hourOfDay covariate expresses the expected pattern, including the higher concentrations in the morning rush hour, compared to the evening rush hour, matching the well-known diurnal pattern of PM. It is also possible that this pattern is a result of increased emission related to stronger traffic dynamics in the morning rush hour. The traffic related covariates will be investigated in detail in section 4.5.3.2.

To evaluate the models a standardized graphical report is designed, including four charts: an evaluation of the total trip exposure estimate and the average trip exposure estimate as a function of the measurements, the relative trip fit results for the all trips in the dataset and a similar evaluation by participant. Models should result in good correlations between measurement and simulation and show a narrow distribution of the relative fit prediction and be independent of the participant.

The model fitting strength is tested by evaluating the total and average trip prediction versus the measured BC trip exposure. The results are presented in Figure 4.5.2. The total trip prediction is strong, but the slope of the linear fit on the average trip exposure prediction is somewhat lower (0.63).

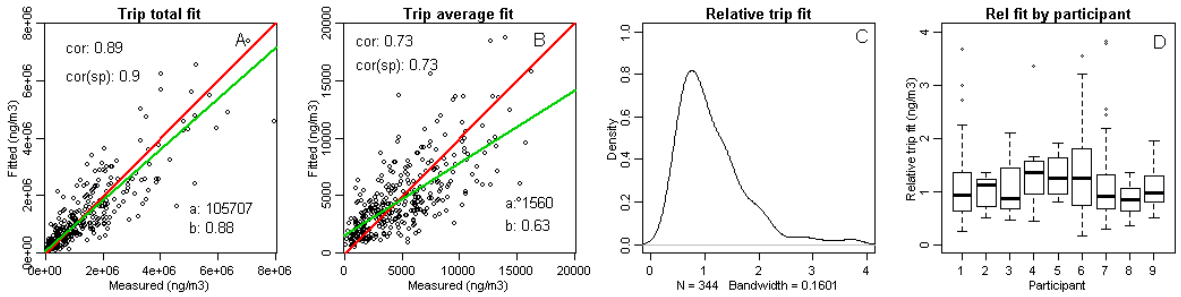

Figure 4.5.2: Trip fitting evaluation of the model BC_LAG60_WBC: Total trip fit versus measurement (A), average trip fit versus measurement (B), relative trip fit distribution (C) and relative trip fit distribution by person.

4.5.3.2 Comparing traffic related data sources

The next focus is on the comparison of the strength of the traffic related data sources and how they correlate with the diurnal pattern of the BC exposure. The spatial covariates with a direct relation to road categorization are not included because we want to investigate only the effect of the traffic covariates. The traffic data is available in two variants: the hourly traffic attribution $Traf_{wgt}$ and a daily average for weekdays ($TAAWT_{wgt}$). The first one includes a diurnal pattern; the $TAAWT_{wgt}$ is a single value valid for a weekday at a certain road segment. The alternative traffic data are the noise covariates L_{DEN} and L_{DAY}. The L_{DAY} covariate is L_{DEN} including a diurnal correction based on an average diurnal traffic pattern expressed in dBA (see Appendix E1.1.4). The correction from L_{DEN} to $L_{Aeq,hour}$ is equal for the whole study area and is not locally specified to the local diurnal pattern of the local road. The covariates to compared are $Traf_{wgt}$, $TAAWT_{wgt}$, L_{DEN} and $L_{Aeq,hour}$ with and without the influence of the diurnal pattern covariate HourOfDay. This way the relative strengths of the traffic data sources can be evaluated. The relative changes in the models with or without the HourOfDay covariate will reveal the interaction between the diurnal patterns of traffic data, hour of the day and the in-vehicle BC exposure. A similar set of models is built with exclusion of the GPS derived covariates ($Speed_{rel}$ and Acceleration). This set can determine how important the traffic dynamics are in the evaluation in relation to the diurnal pattern adjustment through HourOfDay. In Table 4.5-1 the gam models parameters are summarized. The models are sorted by deviance explained.

The models that include traffic dynamics are the strongest, and within those models, the noise based models are the strongest. The same observation is valid for the models excluding traffic dynamics. The BC_LDAYWH model has a similar evaluation as BC_LDENWH, but the relative importance of the HourOfDay covariate does not behave as expected. Since L_{DAY} includes a diurnal pattern, less influence of the covariate is expected. The F-values of the BC_LDAYWH is higher compared to BC_LDENWH. This indicates a higher adjustment for the covariate spline. This phenomenon is visualized in the splines of the different models in Appendix E2.2).

		F-values of covariates												
	Intercept (ng/m3)	Wind speed	Tempe-rature	BCbkg	StCan	Speed relatve	Accel	Hour Of Day	Traffic (hourly)	Traffic (AAWT)	LDEN	Lday	Deviance explaine d	AIC
Investigating traffic covariates (including traffic dynamics)														
BC_LDAYWH	4056	2869	843	879	318	497	28	587				3429	44.0%	256387
BC_LDENWH	4058	2666	862	882	117	475	27	314			3364		44.0%	256393
BC_TRAFWAADTH	4061	2145	833	971	81	567	67	284		3241			43.7%	256759
BC_TRAFWH	4056	2151	825	950	71	571	65	282	3037				43.3%	257301
BC_LDENW	4076	2616	764	1250	151	521	24				3382		42.2%	258859
BC_TRAFWAADT	4077	2496	735	1311	73	637	66			3305			42.1%	258994
BC_TRAFW	4072	2649	677	1274	62	654	65		3108				41.7%	259521
BC_LDAYW	4091	2654	672	1323	21*	564	25					2611	40.7%	260928
Investigating traffic covariates (without traffic dynamics)														
BCR_LDENWH	4081	2627	852	769	151			346			3858		42.2%	258916
BCR_LDAYWH	4081	2636	830	762	152			634				3806	42.1%	259031
BCR_TRAFWAADTH	4092	2322	769	839	116			336		3408			41.3%	260132
BCR_TRAFWH	4087	2338	754	819	114			342	3200				40.9%	260686
BCR_LDENW	4103	2794	749	1144	148						3852		40.1%	261631
BCR_TRAFWAADT	4114	2721	662	1191	123					3435			39.3%	262765
BCR_TRAFW	4109	2867	601	1156	114				3207				38.8%	263370
BCR_LDAYW	4122	2876	651	1218	50							3000	38.4%	263932

Table 4.5-1: Results of the gam models to investigate the strength of the traffic related data sources of the in-vehicle exposure for different traffic sources, the influence of the HourOfDay and the traffic dynamics. The F-values of the acceleration marked with * express a p-value higher than 2.0 e^{-16} but are still significant.

The diurnal pattern of the exposure is easier explained when not including a diurnal pattern in the traffic covariate. This phenomenon in visible is many other features in the model comparison. The hourly traffic covariates typically score less than the daily traffic covariates, even when the HourOfDay covariate is not included. When the traffic dynamics are removed, a completely similar evaluation can be performed (BCR models are the BC models in a reduced form excluding speed and acceleration). The models including hourly traffic covariates without HourOfDay have reduced deviance explained compared to the models with daily traffic covariates, confirming the mismatch between the traffic diurnal pattern and the BC exposure diurnal pattern. The diurnal pattern of the traffic related covariates is clearly too strong or too different from the BC in-vehicle exposure to be a good and useful covariate.

The BCR_LDENWH model has similar strength as BC_LDENW. The hourOfDay covariate in the reduced model can compensate for the variability explained in the BC exposure by the traffic dynamics in the BC_LDENW model. Variation in the traffic dynamics is typically induced near complex traffic interaction (traffic lights and crossings). In the noise maps these areas have increased noise exposure since the noise emissions of all roads in the vicinity are added. In the traffic based models this interaction near crossings is not available. The combined noise exposure in the noise maps is partially mimicking the local effects off the traffic dynamics in the models. The noise map evaluation is also much smoother when roads with high and low density connect, smoothing out the traffic covariate on the low density roads in the vicinity of the roads with higher density. The L_{DEN} based models are the strongest models. In the remainder of the paper the BCR_LDENWH is used as the reference model. The applicability of the model is broader since the actual traffic dynamics are not necessary to

estimate the BC exposure. The trip fit evaluation is available in Figure 4.5.3. The correlations and slopes are slightly reduced compared to BC_LAG60_WBC. The distribution width is reduced in the BCR_LDENWH compared to BC_LAG60_WBC. The six covariates in BCR_LDENWH predict the trip exposure properly. The Pearson and Spearman correlations for the trip total fit are 0.89 and 0.89 and 0.7 and 0.69 for the trip average, removing the effect of the duration of the trip.

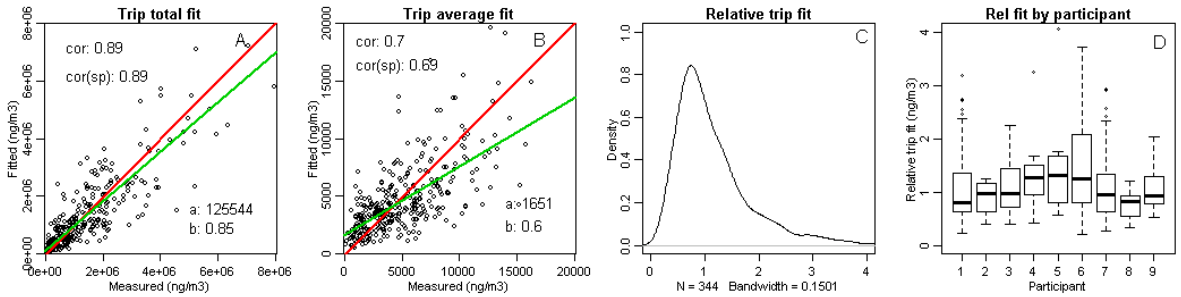

Figure 4.5.3: Trip fitting evaluation of the model BCR_LDENH : Total trip fit versus measurement (A), average trip fit versus measurement (B), relative trip fit distribution (C) and relative trip fit distribution by person.

4.5.4 External validation

A large participatory campaign for BC exposure was performed in the region of Flanders (Dons et al. 2011, Dons et al. 2012, Dons et al. 2013). The in-vehicle data of this participatory campaign used here as an external validation dataset (see Appendix A). In the following section this dataset is referred to as EX_PSC, the external participatory campaign. The independent participatory campaign presented in this Section is referred to as PSC.

4.5.4.1 Comparison of the participatory campaigns

First the potential biases in the two measurement campaigns for the most important covariates are investigated and evaluated towards potential biases in the measurements. The distributions of the BC measurements and the covariates are presented in Figure 4.5.4. The summary statistics of the two BC participatory campaigns differ significantly ($p < 2.2e-16$ for F test and t-test). The Q1, median, mean and Q3 of the validation data (EX_PSC) are 3805, 6147, 7187 and 9508 ng/m^3, and 2040, 4146, 5644 and 7637 ng/m^3 for the PSC. The difference in low values is expected due to the different measurement resolution. The EX_PSC is measured in a resolution of five minutes, the PSC in one second and evaluated by ten seconds. Note that the reported values of EX_PSC in the dataset differ from the reported data by Dons since trips or trip segments are included only if the BC measurement, GPS data and diary entries are available. Some data points were discarded when external data sources were not available.

For several of the covariates the distributions are equal in the two campaigns (wind, temperature, diurnal pattern). For BC_background, traffic, L_{DEN}, PM_{10} the PSC campaign shows

distribution to higher values of the covariates, suggesting larger exposure in PSC while the actual BC exposure in the PSC is much lower compared to the EX_PSC. Only for the Street Canyon Index and the relative humidity the EX_PSC results in distributions that suggest higher exposure for EX_PSC.

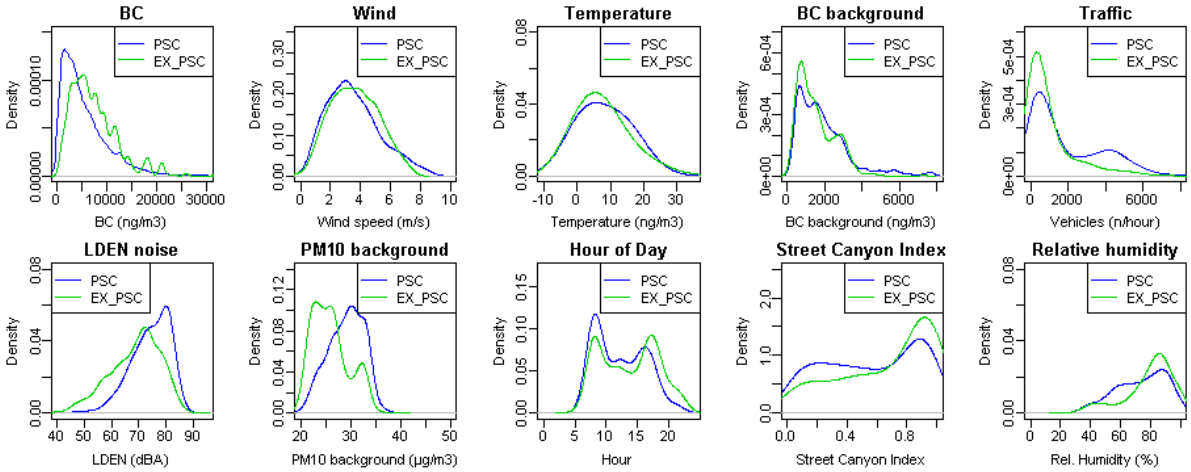

Figure 4.5.4: Comparison of the distributions of the investigated covariates for both measurement campaign (green= validation set EX_PSC, blue = instantaneous model PSC).

4.5.4.2 External validation

The prediction function of the gam implementation in R is used to estimate the in-vehicle exposure in the external participatory sensing campaign. The trips with valid GPS recordings of the external dataset are attributed with the same data sources described in section 4.5.2.2. The evaluation of these trips is performed at a temporal resolution of 10 seconds to match the resolution of the models presented in this section. For the BC values only the average value of the five minute result is available in the EX_PSC but a validation is possible when the instantaneous predictions in a 10 second resolution are aggregated to the full trip. The results are aggregated to individual trips, for each trip the evaluation is restricted to the number of valid 10 second samples for the trip. The missing data within the first and last five minute interval of the evaluated trip will introduce an error in the exposure evaluation of the EX_PSC. In Figure 4.5.5 the external validation is illustrated. The correlations are strong for the total trip prediction (Pearson 0.82 and Spearman .78) but strongly reduced for the average trip prediction (Pearson 0.47 and Spearman .48). The Q1, median, mean and Q3 of the relative trip fit are 32%, 49%, 67% and 74%, expressing a strong underestimation of the exposure measured in the EX_PSC.

When evaluating the behaviour of the trip fit quality for each the strongest covariates, a strong underestimation is detected on the wind speed covariate (Figure 4.5.6). The measurements in EX_PSC are less sensitive to the wind speed, compared to PSC measurements. Especially for high wind speeds large discrepancies emerge. Short trips (less than 10 minutes) are in the EX_PSC only characterized by two partial 5 minute exposure evaluations

and are removed from the data. Also high wind speeds (> 7 m/s) are removed since the models fail for such high wind speed conditions. The Q1, median, mean and Q3 of the relative trip fit are only moderately modified by these restrictions to 34%, 50%, 68% and 75%. The IQR is 34%.

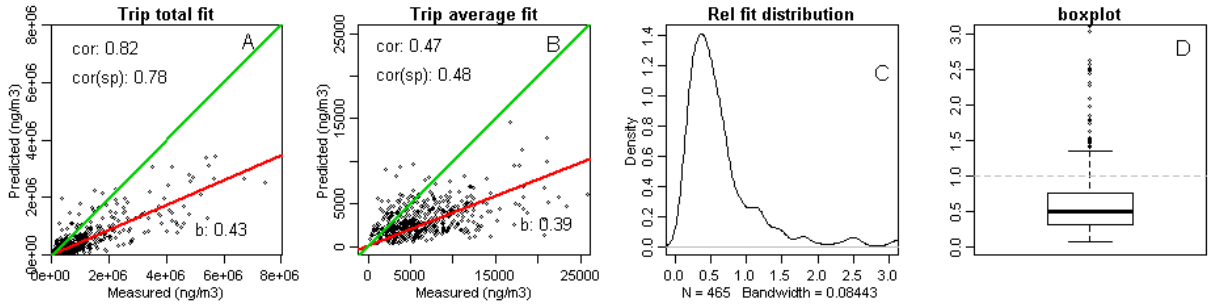

Figure 4.5.5: External validation based on BCR_LDENWH: Total trip fit versus measurement (A), average trip fit versus measurement (B), relative trip fit distribution (C) and relative trip fit box plot (D).

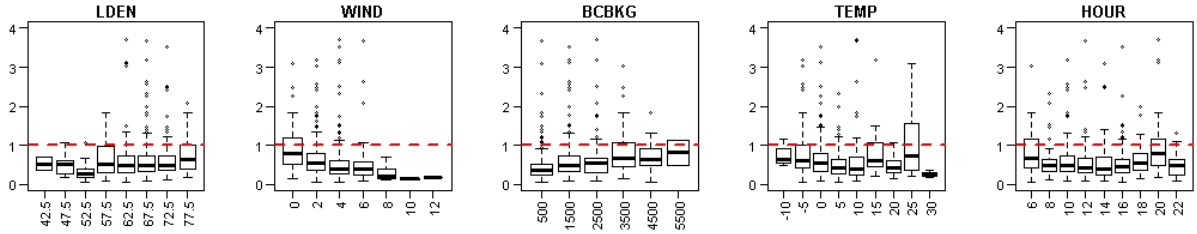

Figure 4.5.6: Trip fit behaviour for the five strongest covariates for prediction with BCR_LDENWH. Strong underestimates occur for higher wind speeds.

4.5.4.3 Investigating the discrepancy

The discrepancy is mainly expressed in the absolute predicted exposure value, not in the correlation in the total trip fit evaluations. In this section the potential origins of the discrepancy are evaluated. As mentioned before no control was available on the actual use and settings of the ventilation system. The people in PSC were however asked to avoid the in-vehicle circulation and set the ventilation to their normal operation. This unknown factor can influence the in-vehicle exposure strongly for individual trips but it is not expected to affect the measurements to the determined magnitude. Two new cars, driven by sales representatives, collected a large portion of the dataset. The bulk of their contribution was collected off-peak and large parts were collected on highways and major roads. Their measurements were collected in spring of 2013. This was a much colder and windy period compared to other years. The potential influence of these atypical weather conditions were tested by building the gam model without the two sales persons (persons 6 and 7), but the validation did not improve when removing these two persons (Appendix E2.3).

An extensive study by Fruin builds a model to predict the air flow rate based on age, mileage, speed of the car and a manufacture specific adjustment (Fruin et al., 2011). The discrepancy between the participants in this participatory campaign can partially be related to the age and the vehicle of the participants. In the Appendix E2.4, a variant of the

BCR_LDENWH model is presented including the year of build of the vehicle of the participant. This approach fits the individual differences between the participants with the age of the vehicle, attempting to isolate the influence of the vehicle from the participant specific trip behaviour. The model shows strong improvement of the deviance explained and trip fit quality. A vehicle age attribution is tested on the external participatory campaign. Vehicle age is in the EX_PSC only available in an indirect manner. For each household, the number of vehicles is known, fuel type and an annotation referring to the age of the car 'before 2009' is available. It is unknown which person drives which vehicle at any time in the campaign. Yet this data was attributed to the trips based on gender. The newest car is attributed to the man if two vehicles are available to the household. The adjusted model validation results in an increase for Q1, median, mean and Q3 of 32% to 38%, 49% to 50%, 68% to 74% and 75% to 81% compared to the BCR_LDENWH validation. The correlation of the trip average exposure fit increased from 0.47 to 0.5 (Spearman) and is equal for Pearson's correlation. Despite the poor quality of the vehicle information in the EX_PSC, the validation improves slightly. This is an indication that age and/or quality of the ventilation system of the vehicle is part of the discrepancy in the validation. It does not explain the large discrepancy in the validation, only closes the gap with about 6%.

The two participatory campaigns were performed with three years difference in time. In 2009 more stringent EU-legislation (Euro 5) reduced particulate matter emission limits for diesel vehicles. The EU limits for PM exhaust is reduced from 0.025 g/km to 0.005 g/km between Euro 4 and Euro 5. The new legislation was hardly influencing the fleet composition at the time of the external participatory campaign (2010-2011). In 2013 strong changes in the vehicle fleet emission can be expected due to the Euro5 legislation. In Appendix E3.1, a detailed estimate of the modified fleet is documented. Data on the fleet composition by environmental class is only available since 2011. An estimate of the evolution from 2010 to 2013 sets the minimum reduction of the vehicle fleet emission to 33%, not accounting the effect of more mileage performed by newer vehicles. A reduction of at least 40% of the PM emission due to the Euro5 legislation can be expected over this short span of time. External evidence of the effectiveness of the Euro5 legislation was found in the BC concentration in the measurements performed by the Flemish Government. The results are shown in Appendix 3.2. A reduction of 30 to 40% is found for BC during rush hour and 20 to 30 % in the off-peak periods. The strongest decreases are found at sites with high traffic exposure.

A third potential relevant discrepancy is found in the differences in the distribution of the street canyon index. In the PSC campaign relatively few measurements were performed in build-up area. The main part of the PSC campaign is performed outside the cities. The effect of this potential effect cannot be quantified.

In an adjusted model BCR_LDENWH_VH_AGE_EU5 the two quantified discrepancies are added to the BCR_LDENWH model. It combines the adjustment for the vehicle age and quality and an emission reduction at the source is presented. The external validation is visible in

Figure 4.5.7. The details of the implementation of the age of the vehicle and the changes in the vehicle PM emission are available in Appendix 3.2).

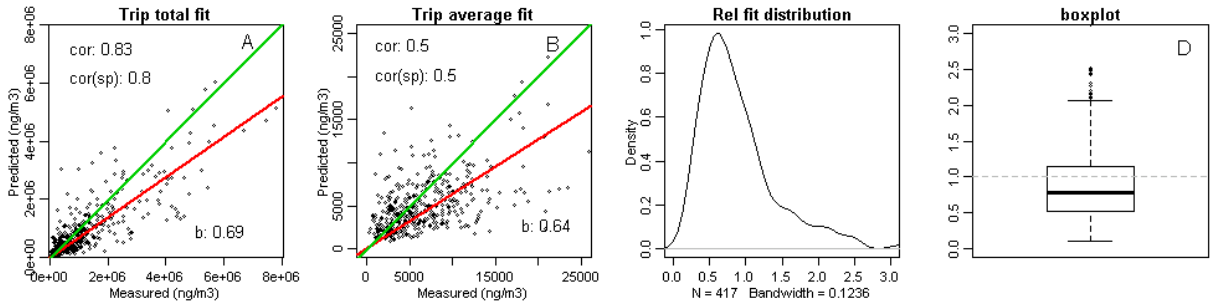

Figure 4.5.7: External validation based on BCR_LDENWH_VH_AGE_EU5: Total trip fit versus measurement (A), average trip fit versus measurement (B), relative trip fit distribution (C) and relative trip fit distribution (D).

The Q1, median, mean and Q3 of the relative trip fit are increasing from 38% to 53%, 50% to 79%, 74% to 104% and 81% to 114% compared to the BCR_LDENWH_AGE validation. The correlation of the trip average exposure remains the same, the total trip correlations increase slightly. The average is increased with 36%, from 68% to 104% similar to the increase at the near roadside long-term measurement location. The IQR is 51%.

4.5.5 Discussion

In-vehicle exposure dynamics: In section 4.5.3.1 the complexity of the in-vehicle exposure is illustrated. The technique to evaluate the in-vehicle exposure in an extreme detailed temporal resolution, combined with equally detailed traffic attribution, results in important information. The approach chosen in this article, modelling real-life in-vehicle personal exposure, contrasts with other approaches to evaluate predesigned in-vehicle exposure experiments. Most focus on a single aspect of the complex in-vehicle exposure dynamics. From a scientific point of view, the chosen approach will fail in quantifying the individual relations between the different relevant parameters influencing in-vehicle exposure. For epidemiological extrapolation however, the total combined effects of all potential influences will determine the actual personal exposure. This approach fits in the so-called ‘data science’ field, an emerging scientific field with a focus on data exploration to extract relevant relationships from the gathered data without the need for an analytical or a physical solution for the resulting relations. The high temporal resolution of the measurements and model covariates can disentangle the biases in the participatory sensing data and direct new measurements campaigns towards improved attribution and sampling.

Noise maps as ubiquitous traffic data source: The evaluation in section 4.5.3.2 has shown the potential of noise maps as a proxy for the local traffic data. The differences between the traffic based models and the noise map based models is not statistically significant. This is not surprizing since the noise maps is based on the identical set of traffic data. The quality of

the spatial attribution of both the noise and traffic is identical due to the 'map matching' data cleaning procedure, linking the traffic to the actual physical road. This is important to produce valid noise maps. An important advantage of the noise mapping approach is the availability of such spatially detailed noise maps. All EU cities larger than 50,000 inhabitants are required these maps to be compliant with the END noise directive. An import synergy is possible.

Noise maps accumulate the noise exposure from different roads when they are in each other's vicinity. This results in higher values at crossings and complex traffic situations, matching the areas with high traffic dynamics. In this way the additive nature of the noise maps seems to mimic the traffic emission behaviour. It was not possible to fully quantify the benefits of this built-in property.

External validation: The external validation underestimates the exposure by almost 50 %. The correlations are however very good. Three discrepancies with significant potential are identified:

- vehicle age and quality influencing the indoor PM levels due to changes of the vehicle intake filters and ventilation
- a potential bias in the sampling (more in-city measurements in the external data)
- the reduced emission of the vehicle fleet

The potential biases could only be investigated due to the detailed spatiotemporal attribution of the measurements. The origin of the discrepancies requires further research. The vehicle age and air intake filter quality will complicate exposure estimates even more in the future. Recent publications mention the improved quality and active development of UFP filters for vehicle ventilation systems. A reduction of 80 to 90% is achieved with certain specific filters (Lee, 2014). It is unknown to what extent these types of filters or less performant filter are available in the operational vehicle fleets at this moment. The change in the PM emission standard for diesel vehicles (Euro5) is the most plausible argument for the discrepancy in the external validation. Background measurements at remote and kerbside locations detect a decrease in the BC concentrations similar to the estimate based on the evolution of the vehicle fleet. Adjusting for the changed emission of the vehicle fleet is valid approach. The actual underlying spatial and temporal changes of the emission due to the Euro5 legislation is unknown but the chosen correction curve, adjusted stronger for high exposure episodes in the instantaneous model seems to explain the discrepancy between the two measurement campaigns. Further investigation of the changing emission dynamics of the vehicle fleet over time is crucial.

Participatory sensing: It is clear that the vehicle is a complex micro-environment with strong interactions with outside and driving conditions and strongly influenced by vehicle and driver specific parameters. As a result, this large set of influences can include unexpected biases in the sampling, including route choice, time of day, meteorology and age and

quality of the vehicles. The fast changing environment due to effective legislation adds more complexity. The strongest limitation in the measurement campaign is the small sample of vehicles. The high complexity of the in-vehicle exposure, combined with fast changing fleet emission and individual vehicle air intake quality hampers the quantification of each individual covariate. Large participatory campaigns are necessary to quantify the trend of personal exposure in the vehicles. The approach taken in this PhD, to sample and predict real-life conditions, will be important to be able to quantify the combined effects of the fast changing external influences and the high traffic dynamics and route sensitive in-vehicle exposure.

4.5.6 Conclusions

A large participatory sensing campaign of in-vehicle BC exposure is conducted and a high resolution spatiotemporal model is build. Several relations influencing the internal dynamics of the in-vehicle exposure can be detected (effects of speed, acceleration, wind speed, temperature, traffic density, diurnal pattern of PM dynamics…). The traffic dynamics and diurnal traffic patterns do not resolve the diurnal patterns of the in-vehicle exposure at full. Traffic attribution is achieved through traffic counts and through noise mapping. An in-vehicle exposure model based on six parameters with L_{DEN} in combination with a fitted diurnal pattern, resolves spatiotemporal variability. Noise maps are a valid proxy for air pollution without actual knowledge of the local traffic dynamics. The noise maps are widely available due to the EU END directive and enable a strong synergy in local policy making for cities and agglomerations with available noise maps.

The external validation with a four year old participatory campaign showed strong underestimations but the data analysis revealed two main components explaining the discrepancies: vehicle age and quality and PM emission changes due to the recent EU euro5 legislation. Adjusting for changes in vehicle quality and changed emission due to the effective legislation is possible. The chosen approach to sample real life exposure, combined with high resolution spatiotemporal modelling can provide good prediction models without the need of disentangling the underlying complex interaction of the underlying parameters.

4.5.7 References

Can A., Dekoninck L., Rademaker M., Van Renterghem T., De Baets B., et al. 2011. Noise measurements as proxies for traffic parameters in monitoring networks. Science of the Total Environment, 410, 198-204.

Can A., Van Renterghem T., Rademaker M., Dauwe S., Thomas P., et al. 2011. Sampling approaches to predict urban street noise levels using fixed and temporary microphones. Journal of Environmental Monitoring, 13, 2710-2719.

Carslaw D.C., Beevers S.D. & Tate J.E. 2007. Modelling and assessing trends in traffic-related emissions using a generalised additive modelling approach. Atmospheric Environment, 41, 5289-5299.

Dauwe S., Van Renterghem T., Botteldooren D. & Dhoedt B. 2012. Multiagent-Based Data Fusion in Environmental Monitoring Networks. International Journal of Distributed Sensor Networks. International Journal of Distributed Sensor Networks, Volume 2012 (2012), http://dx.doi.org/10.1155/2012/324935

de Nazelle A., Seto E., Donaire-Gonzalez D., Mendez M., Matamala J., et al. 2013. Improving estimates of air pollution exposure through ubiquitous sensing technologies. Environmental Pollution, 176, 92-99.

Dekoninck L., Botteldooren D. & Int Panis L. 2013. An instantaneous spatiotemporal model to predict a bicyclist's Black Carbon exposure based on mobile noise measurements. Atmospheric Environment, 79, 623-631.

Dekoninck L., Botteldooren D. & Int Panis L. 2015. Applicability of a noise-based model to estimate in-traffic exposure to black carbon and particle number concentrations in different cultures. Environment International, 74, 89-98.

Dons E., Int Panis L., Van Poppel M., Theunis J. & Wets G. 2012. Personal exposure to Black Carbon in transport microenvironments. Atmospheric Environment, 55, 392-398

Dons E., Panis L.I., Van Poppel M., Theunis J., Willems H., et al. 2011. Impact of time-activity patterns on personal exposure to black carbon. Atmospheric Environment, 45, 3594-3602.

Dons E., Temmerman P., Van Poppel M., Bellemans T., Wets G., et al. 2013. Street characteristics and traffic factors determining road users' exposure to black carbon. Science of the Total Environment, 447, 72-79.

EU Commission, The Environmental Noise Directive (2002/49/EC), http://ec.europa.eu/environment/noise/directive.htm.

Fruin S.A., Hudda N., Sioutas C. & Defino R.J. 2011. Predictive Model for Vehicle Air Exchange Rates Based on a Large, Representative Sample. Environmental Science & Technology, 45, 3569-3575.

Hudda N., Eckel S.R., Knibbs L.D., Sioutas C., Delfino R.J., et al. 2012. Linking in-vehicle ultrafine particle exposures to on-road concentrations. Atmospheric Environment, 59, 578-586.

Janssen N.A.H., Hoek G., Simic-Lawson M., Fischer P., van Bree L., et al. 2011. Black Carbon as an Additional Indicator of the Adverse Health Effects of Airborne Particles Compared with PM_{10} and $PM_{2.5}$. Environmental Health Perspectives, 119, 1691-1699.

Karner A.A., Eisinger D.S. & Niemeier D.A. 2010. Near-Roadway Air Quality: Synthesizing the Findings from Real-World Data. Environmental Science & Technology, 44, 5334-5344.

Knibbs L.D., de Dear R.J. & Morawska L. 2010. Effect of Cabin Ventilation Rate on Ultrafine Particle Exposure Inside Automobiles. Environmental Science & Technology, 44, 3546-3551.

Lee E.S. & Zhu Y. 2014. Application of a High-Efficiency Cabin Air Filter for Simultaneous Mitigation of Ultrafine Particle and Carbon Dioxide Exposures Inside Passenger Vehicles. Environmental Science & Technology, 48, 2328-2335.

Li L.F., Wu J., Hudda N., Sioutas C., Fruin S.A., et al. 2013. Modeling the Concentrations of On-Road Air Pollutants in Southern California. Environmental Science & Technology, 47, 9291-9299.

WHO Europe, 2012: Health effects of black carbon, ISBN: 978 92 890 0265 3.

Wood S.N. 2006. On confidence intervals for generalized additive models based on penalized regression splines. Australian & New Zealand Journal of Statistics, 48.

Xu B., Wu Y., Lin Z. & Chen Z. 2014. Investigation of Air Humidity Affecting Filtration Efficiency and Pressure Drop of Vehicle Cabin Air Filters. Aerosol and Air Quality Research, 14, 1066-1073.

4.6 Instantaneous indoor BC model

4.6.1 Introduction

In current epidemiological practice, exposure to air pollution at the dwelling is often modeled and estimated with land-use regression models (LURs). The typical spatial resolution of the parameters in LUR models is about 100 m to 1 km in most solutions (Hoek et al., 2008, Beelen et al., 2013, Dons, 2013). Recently it became clear that the spatial variability of the Black Carbon and UFP exposure is much larger compared to PM_{10} and $PM_{2.5}$ (see 1.1.4). The variability in the exposure is related to the local traffic variability, the distance to local roads or highways and strong meteorological influences. A higher spatial variability implies the need for spatially more detailed land-use regression models. In Section 4.2 and 4.4 it was shown that noise measurements act as traffic attribution for particulate matter measurements. It is possible to disentangle the variability in the BC/UFP measurements into a local and a background component. Noise maps are valid as an alternative traffic attribution for in-vehicle exposure (4.5). In this perspective, it is interesting to investigate the potential of noise maps to act as a proxy for the traffic related indoor BC exposure as well. The participatory sensing campaign of VITO (see Appendix A) will be used as an independent external validation in a similar fashion as for the in-vehicle model. The basic concept is visualized in Figure 4.6.1.

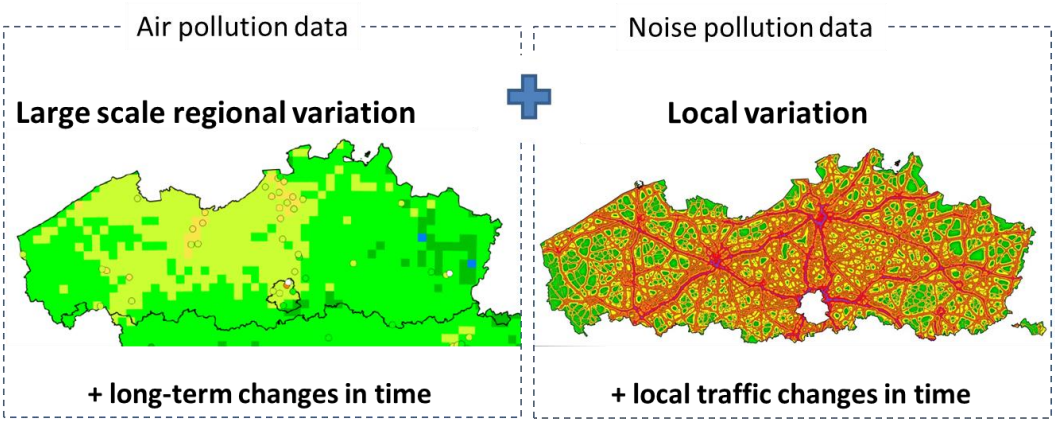

Figure 4.6.1: Basic concept of the noise based indoor BC exposure model: the large scale variation is described by air pollution data sources, the local variation by noise map data. Temporal changes with different resolution are added independently for the two contributions.

The large scale variability and long term variation of the BC concentrations is available in the air pollution discipline. Noise maps provide exposure to traffic in a spatial resolution of meters. Each discipline covers a matching temporal variation. The BC concentration at a dwelling will be described as the sum of a large-scale background contribution and a local traffic contribution:

$$BC_{dwel} = BC_{bkg}(p,t) + BC_{local\ traffic}(p,t) \qquad (1)$$

To result in a valid additive model, the two components should become as independent as possible. The background component should not be influenced by local traffic and vice versa.

This approach will require a function to convert the noise exposure at the dwelling into a BC exposure in a similar fashion as the noise measurements were converted in BC exposure for the bicyclists (4.2 and 0). The first question is which independent dataset of BC measurements can be used as a primary source to build an indoor model. For evident reasons, the external validation BC data measured at the dwellings cannot be used. No other independent third party measurement dataset at the dwellings is available to establish a noise-BC conversion for indoor exposure, so an alternative approach is tested. The BC exposure for bicyclists will be mapped on a noise map and will be used as a spatial assessment of the indoor BC exposure for the dwellings. In other words, the instantaneous bicyclist exposure model is now assessed with the underlying noise map instead of the instantaneous noise measurements and by doing so; provide a link between the noise map and BC exposure. The model will lose its capability to account for the traffic dynamics through the engine related L_{OLF} and rolling noise related L_{HFmLF} (see 4.2) since this is not available in the noise map.

4.6.2 Model hypothesis in detail

The instantaneous BC concentration in the dwellings is approximated as the sum of a large scale background variation and a local traffic variation. The large scale variation is captured by the available air pollution data, mainly driven by the changing meteorological conditions and wide range properties of the BC sources. The local noise immission is expected to capture the local traffic variation and consequently also the local contribution of the traffic related air pollution.

First we address the noise map based local variation. The noise map is presumed to match the spatial variability of the traffic related BC exposure of the dwellings. In other words, the decay of the sound energy is assumed to be similar to the decay of the BC concentration with the distance to the road. In first order, noise decays as $1/r^2$ neglecting reflections and other effects. In first order, particulate matter decays by expanding a sphere in a similar rate of $1/r^2$, neglecting meteorological, coagulation and other effects. The exact difference in the distance to source behavior is though not critical since the non-linear splines of the gam models intrinsically include this conversion factor. The fact that there is a match in first order, only simplifies the splines of the dominant covariates in the gam model.

Sampling the exposure by bicycle is by design limited to the road network and by consequence, not at the position of the buildings. The potential error due to this sparse spatial sampling is neglected and presumed to not affect the results. New variants of instantaneous gam models will be built to fit the BC exposure of the bicyclists using the noise map, while still including the meteorological attributes and the street canyon index (Dekoninck et al.,

2013, section 4.2). The BC exposure is assessed in and around the city of Ghent in a variety of buildup areas (in-city, suburb and open field). It is assumed that the local traffic related component of BC assessed in this variety of environments is valid for the whole Flemish region. The bicycle dataset was however only collected during morning and evening rush hours. The input data for the gam model will therefore not include information on the diurnal pattern of the exposure. A diurnal traffic pattern will be added to adjust to daily exposure. The details of the L_{DEN} noise map, the other data sources and the model variants will be presented in 4.6.3 and4.6.4. More details on the external data sources are available in Appendix B.

Next we address the large scale variation. The temporal variation of the BC concentration over the region is a combination of temporal changes with different frequency (day, week, weather patterns and season). The daily pattern is potentially available in both the local and the large scale variation and will a major topic in the discussion. It is also investigated in section 5.2 and in the general discussion (5.3) since this issue affects all micro-environments. For the evaluation period (2009-2010) only one background measurement station is available, an important restriction in the available data. The temporal variation enters the model through the time series of the BC concentration in the background measurement station.

The estimation of the exposure at the dwellings has to be performed region-wide (Flanders, Belgium) to match the extent of an external exposure validation dataset. The temporal pattern of the BC concentration at the background measurement location is expected to valid for the Flemish region, but the absolute value itself is not expected to be valid for the entire region. A spatial correction is necessary but no large-scale spatial data source for the background data source BC is available for the evaluation period. A large scale spatial data source is available for PM_{10}, the large fraction (< 10µm) of the particulate matter. BC is the soot fraction within the PM_{10} and the long-term relative contribution of Black Carbon in the PM_{10} concentration is constant for measurement location with a reasonable distance from major roads (about 6 to 7% of the PM_{10} value). The annual average concentration map of PM_{10} can be used as the spatial distribution of the average background concentration of BC over the Flemish area. The use of a regional wide map with no local variability related to local major traffic sources (e.g. highways) is part of the requirements to disentangle the background and local contribution.

The spatial and temporal prediction of BC results in outdoor exposure levels and requires a correction from the outdoor to the indoor micro-environment. A fixed outdoor-indoor ratio (I/O ratio) from literature will be used (see details in 4.6.4.4). The conversion factor is sensitive to the season since natural ventilation of the dwellings can vary strongly by the season. This feature will be an important part of the model.

4.6.3 Model description

4.6.3.1 Noise map based GAM models

The instantaneous bicycle model was built in two variants, once based on the raw measurement data (BC_{raw}) and on the background adjusted measurements (BC_{loc}), see 4.2.3.1. Each point p_x in the bicycle dataset is mapped to the L_{DEN} noise map to replace the noise measurements. The model properties are available in Table 4.6-1. The splines of the $BC_{raw,noisemap}$ gam model are presented in Figure 4.6.2.

		F-values of covariates						
	Intercept (ng/m3)	Wind speed	BC_{bkg}	L_{DEN}	StCan	# samples	Deviance explained	AIC
Investigating LAG and weight								
$BC_{raw,noisemap}$	3228	902	2777	2193	380	34914	40.8%	78788
$BC_{loc,noisemap}$	1781	890		2019	253	35048	19.9%	109853

Table 4.6-1: The $BC_{raw,bike,noisemap}$ and the $BC_{loc,bike,noisemap}$ gam models with respectively 4 and 3 parameters.

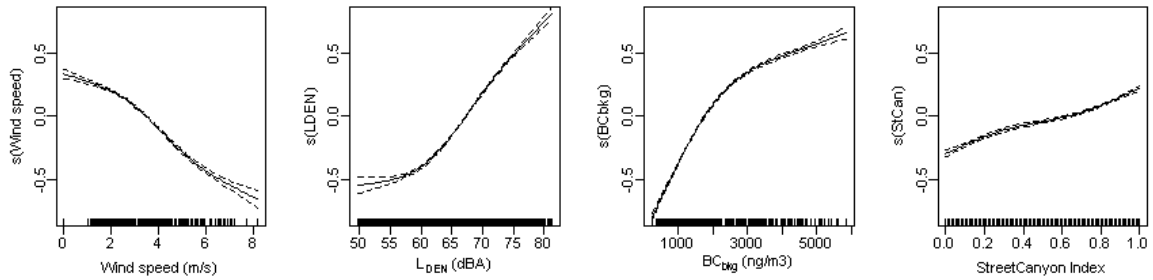

Figure 4.6.2: Splines of the four covariates of the $BC_{raw,bike,noisemap}$ GAM model.

Wind speed and background concentration are included in the $BC_{raw,noisemap}$ gam model as meteorological parameters. The covariates cover the following physical parameters: the traffic estimate through the L_{DEN} noise map, instantaneous dispersion of the pollution through wind speed, the influence of the background concentration and an adjustment of the dispersion based on the street canyon features of the location. This gam model is only valid for the rush hour since only rush hour measurements are included. Most splines are almost linear except for the BC_{bkg}. It is clear that above 3000 ng/m^3, the background concentration at the measurement location is not expressed in the bicycle measurements. This traffic based model is not useful for the additive approach since it includes the BC_{bkg} covariate and is by design not independent from the background contribution.

The $BC_{loc,noisemap}$ gam model is based on the background adjusted measurements of the biking dataset. The splines of the $BC_{loc,noisemap}$ gam model are presented in Figure 4.6.3. In this model, the influence of the background is not included. The background adjusted $BC_{loc,noisemap}$ gam model shows stronger and more linear slopes compared to the $BC_{raw,noisemap}$ gam model.

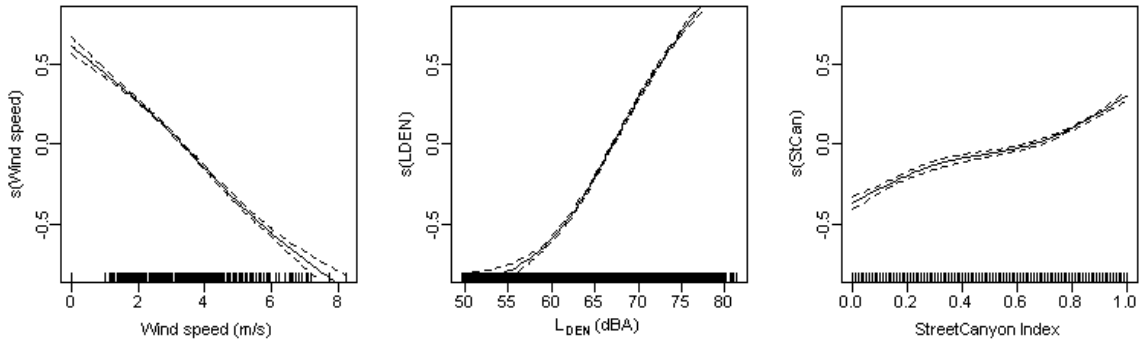

Figure 4.6.3: Splines of the three covariates of the $BC_{loc,bike,noisemap}$ GAM model.

The instantaneous wind is still relevant, in a similar fashion as in 4.2. In this model, the temperature covariate cannot be added since this would introduce a seasonal component into the model. This model has the potential to act as the conversion between the L_{DEN} noise map and an instantaneous BC concentration across the noise map.

4.6.3.2 The background adjusted BC model (BCBA)

The indoor exposure is defined by two components. The background component is an instantaneous function of location and time; the local component is an instantaneous function of the noise level at the dwelling which acts as a proxy for the traffic, the time of day and a set of other exposure modifiers. An outdoor-indoor correction has to be applied. The basic mathematical form is:

$$BCBA_{indoor} = (BCBA_{bkg,outd}(p,t) + BCBA_{loc,outd}(p,t,\dots)).OutIn_{cor}$$

The $BC_{loc,noisemap}$ gam model is used as the local traffic component $BCBA_{loc,outd}$. An adjustment has to be applied to extrapolate the model to the full diurnal pattern. In this approach, the local traffic related component should only include traffic information; the diurnal traffic correction has to be solely based on traffic information. No traffic data is available at the dwellings in the external validation data. A standard diurnal profile will be used for all dwellings (definition in 4.6.4.3). To implement this diurnal pattern, the noise level supplied to the gam model is adjusted for the hour of the day using the diurnal pattern. This assumes that the changes in BC concentration due to diurnal changes in the noise levels are similar as the changes of the BC concentration spatial changes of the noise levels during the rush hour. Since a noise levels expresses a certain amount of traffic, this assumption is correct in first order but neglects the effects of changing traffic dynamics throughout the day. The $BC_{loc,noisemap}$ gam model is by design not sensitive to the traffic dynamics. No large effects on the model are expected. The local component is expressed as follows:

$$L_{DEN,T}(p,t) = L_{DEN}(p) + Traf_{diurn,cor,dB}(\text{hour\_of\_day}(t))$$

$$\mathrm{BCBA_{loc,outd}(p,t)} = \mathrm{gam_{loc,noisemap}}\left(\mathrm{L_{DEN,T}}(p,t), \mathrm{WS(t)}, \mathrm{StCan(p)}\right)$$

Now we address the $BCBA_{bkg,outd}$. In the $BC_{raw,noisemap}$ model, the non-linear behavior of the background covariate is visible in the saturation the spline for high levels (see Figure 4.6.2). When the total background is used, large overestimations in the indoor model are detected for high background levels (not reported in the results). This relates to the local features of the background measurement station. It is very close to the largest city in Flanders, in between the harbor and the city. At high background episodes -typically meteorological situations with low dispersion- the background measurement station seems to be encapsulated in the expanding area of influence of the city, disturbing its representativity as a background for the rest of Flanders in these extreme conditions. Since no alternative background measurement location for the period of 2010-2011 is available, the background concentration will be adjusted for the high background episodes. The observed variation in the background concentration will be applied till 3000 ng/m^3 and only half of the excess concentration above 3000 ng/m^3 is added. This mimics the behavior of the BC background covariate in the $BC_{raw,bike,noisemap}$ GAM model. This results in:

$$BC^*_{bkg} = min(3000, BC_{bkg}\ (t)) + \frac{1}{2}\max(0.0, (BC_{bkg}\ (t) - 3000))$$

The large scale spatial adjustment over the full region is based on the ratio of the annual PM_{10} concentration at the dwelling and the annual PM_{10} concentration at the BC background measurement location:

$$PM10_{spat,cor} = \frac{PM10(dwel_{XY})}{PM10(BC_{bkg,XY})}$$

The background component has to be compatible with the background adjustment performed on the biking dataset (based on Q1 of the background concentration during rush hour, for details see Dekoninck et al., 2013, see also section 4.2). The resulting mathematical form of the models is shown below.

$$BCBA_{bkg,outd} = PM10_{spat,cor} \,.\max(0, BC^*_{bkg}(t) - BC_{bkg,Q1}\ ))$$

The sum of the two components is presumed to be an estimate of the outdoor concentration at the dwelling facade. The last step is adding the outdoor to indoor correction and is applied in two variants. The basic implementation is based on fixed correction for the full year available from literature (see 4.6.4.4). A seasonal influence on the I/O ratio is reported frequently. The seasonal effect of the I/O ratio will be evaluated based on the fixed correction and the resulting linear regression will be applied to the model as the expected I/O ratio. The two variants will be referred to as $BCBA_{const}$ and $BCBA_{season}$. The validity of this approach will be evaluated in the discussion.

4.6.4 Data sources and external parameters

4.6.4.1 External data sources

In Table 4.6-2 an overview of the external data is available, including references to the first use of the data in this work.

L_{DEN} noise map	Spatial layer (Identical map as used in CAR model, see section 4.5 and Appendix C). The noise map does not include screening by buildings.
Bicyclist BC exposure	Bicyclist BC exposure datasets (see section 4.2).
Meteorological data in gam models	Meteorological variability in the bicyclist data (wind speed, temperature, humidity), identical to data in section 4.2) Meteo data from Melle, measurement location closest to Ghent (KMI.be).
Meteorological data in for validation set	Wind speed, temperature, humidity from identical data source (KMI.be) for 5 different points distributed over the Flanders region. The closest meteorological station is used in the prediction.
BC background	BC measurements at background monitoring station AL01 Antwerpen-Linkeroever as used in section 4.2, 4.3 and 4.5). Temporal resolution of 30 minutes (3 hour minimum running smooth is applied on the time series)
PM_{10} map	Yearly PM_{10} map for Flanders (2010, source www.irceline.be). Identical to data in section 4.5 To link the PM_{10} map to the temporal variability of the background, the level of PM_{10} at the BC background monitoring station (AL01-Antwerpen Linkeroever) is retrieved. The level of PM_{10} at the background monitoring station is 35 $\mu g/m^3$.

Table 4.6-2: list of external data sources in the models for indoor BC exposure.

4.6.4.2 External validation data and the indoor micro-environment

Data from a third party participatory campaign is available to perform an external validation (see appendix A). The used time-activity application was not capable of storing the difference between an indoor activity and an outdoor activity. Spending time at a stationary location is automatically considered an indoor activity; while in reality the activity could also be (partially) spent outdoors. This potential indoor/outdoor mismatch is however partially counteracted by the actual operational situation in the measurement campaign. Since both the μ-aethalometer and PDA required charging, the equipment was most of the time not carried while spending time at home outdoors. For the activities at home the measurement

was performed typically indoors, even if the subject spent time outdoors in the vicinity of the dwelling (garden etc.). We therefore treat the at-home activities as if they are all 'indoor activities'.

4.6.4.3 Traffic diurnal pattern

No actual traffic diurnal pattern is available for the sampled households in the external participatory campaign. Therefore, a measured diurnal pattern at a dwelling (not related to the external data) is implemented as a constant traffic profile and is presumed representative pattern for all dwellings in the external data. The local traffic is the dominant noise source during the day at the measurement location. There is a low influence of distant sources (highway at 2000 m and major road at 750 m, local connecting road at 100 m) in this diurnal pattern.

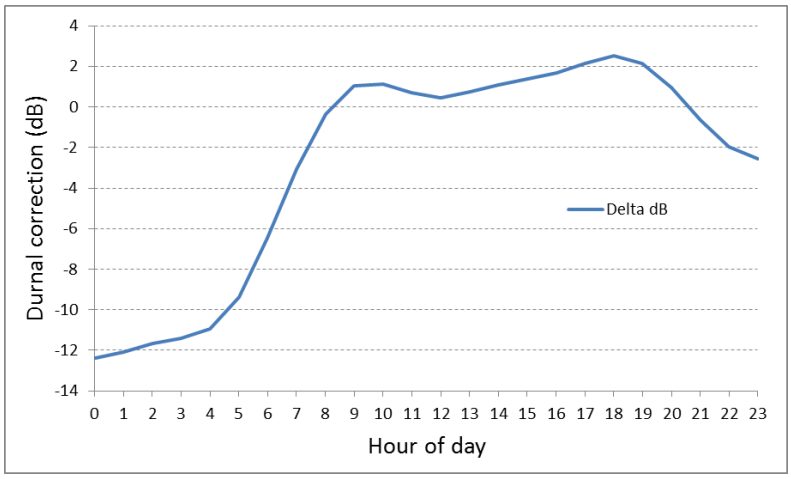

Figure 4.6.4: Measured diurnal patterns traffic pattern at a typical dwelling in Flanders.

4.6.4.4 Outdoor-indoor correction

The $BC_{loc,noisemap}$ dataset is measured outdoor (on bicycle) and the resulting estimates can therefore be interpreted as a dwelling facade estimate. Validating with indoor personal exposure measurements requires an outdoor to indoor correction factor (I/O ratio).

Many authors addressed this complicated issue and tackled the issue from different perspectives. For particulate indoor exposure, huge variability is detected. I/O ratios are highly influenced by particle size and ventilation settings. In a review, the large variability is identified as unresolved (Chen and Zhao, 2011). The main driving force is related to the ventilation properties of the dwellings but the influence of indoor sources on the I/O ratio is poorly understood. UFP and coarse particles get lower I/O ratios compared to the midrange size fraction ($PM_{2.5}$). Especially UFP shows extreme low I/O ratios, I/O ratios for particles smaller than 0.1µm are lower than 0.5 and drop to 0.2 for particles smaller than 0.01 µm (Chen and Zhao, 2011). For larger particles typical I/O ratios are found between 0.4 and 1.0. No independent references with I/O ratios for BC are available, but BC overlaps in size with $PM_{2.5}$ and UFP.

The first approach is based on the evaluations of the external participatory sensing campaign. Not only the personal exposure is assessed but a BC measurement was also performed at the dwelling facades of the participants. This data resulted in an average reduction of outdoor to indoor of 0.78 over the full campaign (Dons et al., 2011). This correction is based on a daily background adjusted average of the measured data. The reported I/O ratio of 0.78 is among the higher reported values in the literature. An I/O ratio of 0.78 is used in the $BCBA_{const}$ model.

4.6.5 Model results

Since the gam models are based on data gathered during commuting on weekdays, it is not expected that the model will be valid for activities during the weekends. In addition, a difference can be expected between the home locations and the other destinations (work, school, office, restaurants,…) etc. Therefore the basic evaluation is restricted to weekdays and at home activities.

4.6.5.1 Background adjusted models: $BCBA_{const}$ and $BCBA_{season}$

The model fitting strength is tested by evaluating the average activity prediction versus the measured BC activity exposure. The results of the $BCBA_{const}$ model are presented in Figure 4.6.5. The slope of the linear fit on the average trip exposure prediction is 0.7, with correlations of 0.65 (Pearson) and 0.64 (Spearman). When the linear fit is forced to an intercept at zero, the slope is 1.01. The median and mean relative fit for the at home activities is 1.17 and 1.38 respectively, overestimating the measured indoor levels considerably.

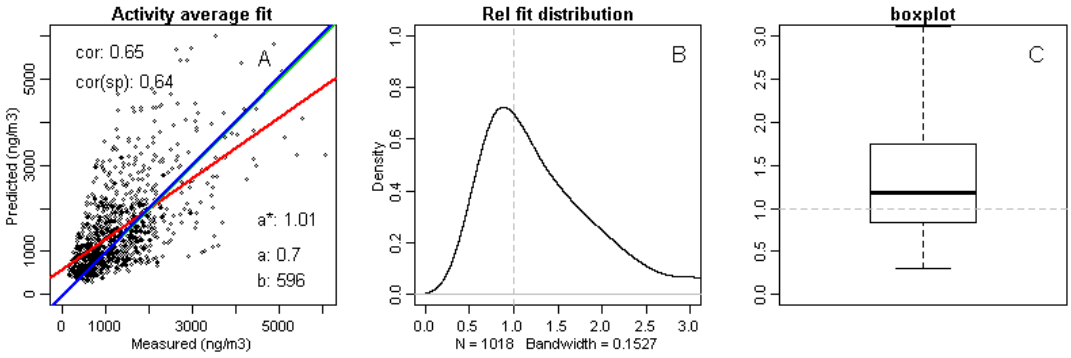

Figure 4.6.5: BCBA model, external validation, at home indoor activities during weekdays only with fixed outdoor-indoor correction. Chart A presents the average by activity, measured versus predicted. Chart B and C show the distribution as a density plot and a boxplot. The boxplot shows the median, Q1, Q3 and P95 whiskers.

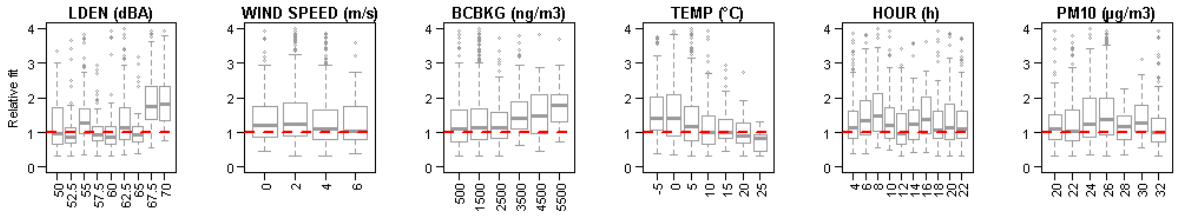

Figure 4.6.6: BCBA model: evaluation of the relative fit for six spatial and temporal covariates, at home indoor activities during weekdays only with fixed outdoor-indoor correction (noise map, wins speed, BC background concentration at the measurement location, averaged daily temperature, hour of the activity and PM_{10} value). All covariates are reported in classes matching the covariate properties.

In Figure 4.6.6 the relative fit is evaluated for the most relevant covariates. The red lines show the ideal situation. A large discrepancy is found for the high L_{DEN} values. The wind speed and PM_{10} covariates are almost constant over the full range. The background concentration and temperature express a typical seasonal component. A diurnal pattern is visible in the hour of day covariate. A linear fit is calculated for the median values of the relative fits for the daily temperature based covariate. This function is presented in Table 4.6-3 and is assumed to act as a seasonal I/O ratio.

Temperature dependent outdoor to indoor correction
$OutIn_{cor}(temperature) = 1/(1.29 - 0.018\ T_{day})\ OutIn_{const}$

Table 4.6-3: Daily temperature dependency in the BCBA model.

This function is added as a seasonal I/O ratio, replacing the fixed I/O ratio retrieved from literature. The resulting $BCBA_{season}$ model is shown in Figure 4.6.7. The evaluation of this approach will be addressed in the discussion.

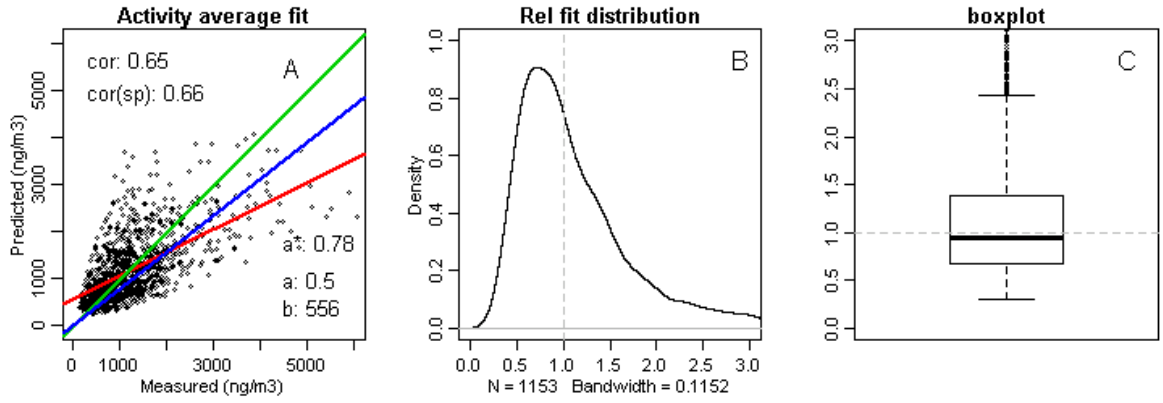

Figure 4.6.7: $BCBA_{season}$ model, external validation, at home indoor activities during weekdays only with daily temperature sensitive outdoor-indoor correction.

The slope of the linear fit on the average trip exposure prediction is 0.5, a relative large drop compared to the $BCBA_{const}$ model. The correlations are 0.65 (Pearson) and 0.66 (Spearman), small changes compared to $BCBA_{const}$. When the linear fit is forced to an intercept at

zero, the slope becomes 0.78. The median and mean relative fit for the at home activities is 0.95, closer to 1 by design, and 1.13 respectively.

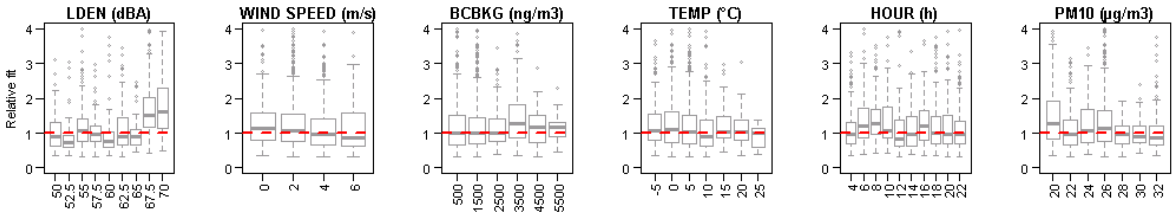

Figure 4.6.8: $BCBA_{season}$ model: evaluation of the relative fit for six spatial and temporal covariates, at home indoor activities during weekdays with daily temperature sensitive outdoor-indoor correction.

In Figure 4.6.8, the activity relative fit behavior of the $BCBA_{season}$ model is the relative fits are closer to 1 for most of the covariates and more narrow distributions of the relative fits. The temperature covariate is close to 1 by design, but the correlated background concentration is adjusted as well, reaching a flat profile. Also the diurnal pattern is improved, showing less rush hour sensitivity compared to $BCBA_{const}$.

4.6.5.2 Absolute contributions of background and local component to the Black Carbon indoor exposure

It is interesting to present external validation data and prediction in absolute BC levels for the different covariates as well. The external measurements are presented in Figure 4.6.9. The absolute predicted values for the $BCBA_{season}$ model are shown in Figure 4.6.10 for comparison.

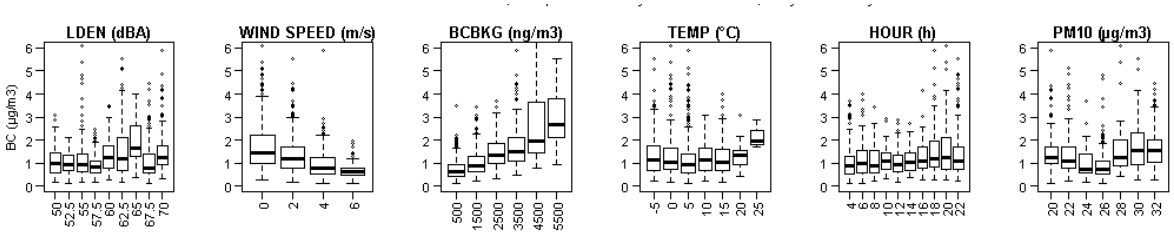

Figure 4.6.9: Evaluation of the average measured indoor exposure for six spatial and temporal covariates, at home indoor activities during weekdays with daily temperature sensitive outdoor-indoor correction.

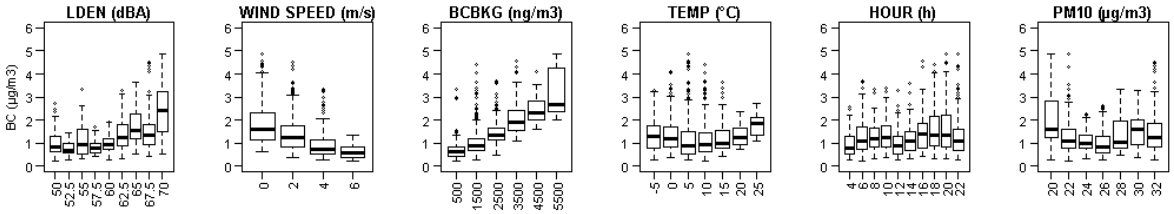

Figure 4.6.10: $BCBA_{season}$ model: evaluation of the average modeled indoor exposure for six spatial and temporal covariates, at home indoor activities during weekdays with daily temperature sensitive outdoor-indoor correction.

The pattern of the L_{DEN} covariate is similar up to 65 dBA. The measured concentration in the dwellings with noise levels higher than 65 dBA are lower compared to the measurements at dwellings with a noise levels between 60 and 65 dBA. The bad fit for the high L_{DEN} values, visible in Figure 4.6.8, is mainly the result of rather low measured concentrations for those dwellings. For the wind speed, background concentration and temperature, the patterns are very similar. In the evaluation by hour of the day, the measurements show a lower diurnal pattern compared to the model. The $BCBA_{season}$ model predicts high values for the low PM_{10} values. These features will be addressed in the discussion.

In Figure 4.6.11, the prediction is split into the two components: $BCBA_{bkg,indoor}$ and $BCBA_{loc,indoor}$. This evaluation indicates how independent both components are. The top chart for $BCBA_{bkg,indoor}$ shows the expected behavior for the wind speed and background concentration. The background contribution is almost behaving at random for the LDEN covariate. The background contribution is high for low and high temperatures; high values are expected in winter due to high background levels, high values during summer can be related to the higher I/O ratio in summer. A diurnal pattern is visible in the median values of the hour of day covariate. The behavior of the PM_{10} covariate is partially matching the expectations.

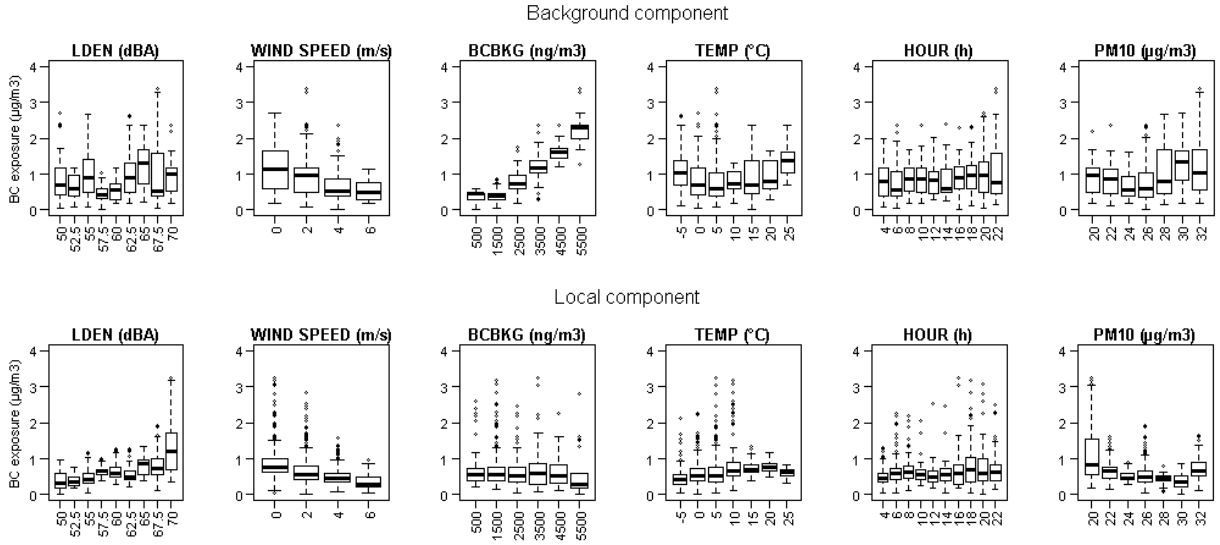

Figure 4.6.11: $BCBA_{season}$ model: evaluation of the local traffic component of the absolute indoor exposure for six spatial and temporal covariates, at home indoor activities during weekdays with daily temperature sensitive outdoor-indoor correction.

The bottom chart for $BCBA_{loc,indoor}$ shows the expected behavior for the L_{DEN}, wind speed and background concentration. In general the variation added into the model is smaller for the local component, compared to the background component. The temperature results in high values during summer are related to the higher I/O ratio in summer. A small diurnal pattern is visible in the median values of the hour of day covariate. The behavior of the PM_{10} covariate is almost constant except for the extreme high values for the low PM_{10} values. Since the same data is presented towards a different x-axis in these charts, this suggests that the measurements at the highest noise levels occurred at dwellings with low PM_{10} values.

This evaluation illustrates the logic behind the additive approach. The magnitudes and expected behavior of both local and background contributions match the expectations. The diurnal pattern in the $BCBA_{bkg,indoor}$ is unwanted. This will be explored further in the discussion.

4.6.6 Discussion

4.6.6.1 Evaluating the background adjusted approach

The most critical point in the hypothesis is the validity of splitting the instantaneous exposure in a dwelling into a local and a background component. Figure 4.6.11 illustrated that this goal is reached for a large part but some interaction remains. The most important issue is the diurnal pattern in the background BC concentration that was used. But unfortunately no alternative location was available for that episode. The external participatory campaign was performed at a time when most European countries did not yet measure Black Carbon within their basic monitoring setups (EEA Technical report, 2013). VITO and the VMM (organizer of the air pollution network) were at the forefront of current developments and technology. If compared with other more recent background measurement stations, other locations further away from cities and industry show less pronounced diurnal patterns compared to the AL01, Antwerpen-Linkeroever. A more remote background monitoring station available during the time frame of the external participatory campaign could have improved the predictive power of the background adjusted model substantially.

The local component, based on the bicycle measurements, performs above the expectations with only a single noise map based value as input. This suggests that the assumption made in the model hypothesis propagation/ dispersion of noise and BC are valid. Especially the fact that the BC concentrations result in the proper magnitude is unexpected, even before the seasonal adjustment for the I/O ratio. The diurnal pattern of the local component does not show a strong diurnal pattern, mainly due to the choice of the standard noise based traffic pattern. There is room for improvement in the attribution of traffic data at the dwellings. The underlying noise map based GAM model is by design not sensitive any more to the traffic dynamics and cannot resolve the potential effects of the dynamic emission of PM during rush hour. This leads us to a potential synergy with Section 4.3. A city wide noise map, including the traffic dynamics has the potential to add this information in the gam model. Combining the benefits of noise monitoring networks, noise map calculations and mobile noise measurements can add this information in future modeling (Can et al., 2011, Can et al., 2014, Van Renterghem et al., 2011, Dauwe et al., 2012, Wei et al., 2014).

More background measurement stations are available now; in future work the selection of the background measurements stations with local diurnal pattern influence will be an important part of the modeling process. The diurnal pattern in the prediction will drop. Improv-

ing the local traffic assessments to a level where the local traffic dynamics and the related particulate emission enter the model through the local component is a future goal. The background adjusted approach is valid and extendible with local traffic assessments.

4.6.6.2 Indoor/outdoor ratio's, infiltration and ventilation

A second crucial issue in the estimation of the indoor exposure is the relationship between outdoor and indoor particle concentrations. Applying the temperature dependent function $1/(1.29- 0.018\ T_{day})$ on the fixed correction of 0.78 results in values between 0.56 and 0.93 for temperatures between -5°C and 25°C (see Figure 4.6.12). The resulting I/O ratio is 0.010 $°C^{-1}$. Applying this slope into the $BCBA_{season}$ model results in a flat response of the inverse correlated BC background concentration (see Figure 4.6.8). This in itself is an argument for the validity of the correction but it requires external validation.

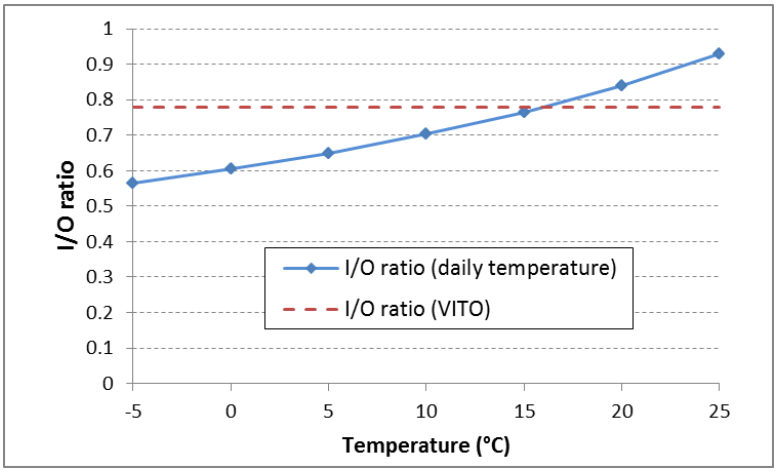

Figure 4.6.12: Temperature dependence of the I/O ratio's according to the BCBA model.

The first check focusses on other temperature effects in the model. No other explicit temperature depending parameter is available in the model. The underlying gam model potentially includes hidden temperature depending features in the $BCBA_{season}$. The background adjustment in the bicyclists' exposure data not only adjusted for the background concentration but also resolved the temperature dependency in the data (Dekoninck et al., 2013). The instantaneous model $BC_{loc,noisemap}$ gam model is insensitive to the temperature. The seasonal effect in the BC background concentration is a real phenomenon and not an actual temperature dependency in the model. It can be assumed that the daily temperature adjustment is mainly determined by the changing ventilation of the dwelling in function of the temperature.

To validate the applied correction, a comparison is made with available literature. The range of 0.56 and 0.93 is in accordance with the reported I/O ratios in other studies (Hoek et al., 2008, Hänninen et al., 2011, Chen and Zhao, 2011, Sajani et al., 2015, Meier et al., 2015). Hänninen et al. present seasonal patterns for different regions in Europe. The range found in this evaluation matches the measurements in Northern Europe better compared to Central

Europe and Southern Europe. The average temperature dependency over all the European countries was found to be 0.007°C^{-1}, about 70% of the temperature dependency found in the $BCBA_{const}$ model. The seasonal variability in the Northern European countries was however larger compared to the other regions in Europe. This information can only be deduced from a chart in the publication but was not reported separately (Hänninen et al., 2011). Larger temperature dependency in countries with colder winters is logical; the difference of 30% can match the external data. Most authors report also lower I/O ratios for UFP compared to $PM_{2.5}$, since BC tends to overlap with UFP and $PM_{2.5}$, lower I/O ratios for BC compared to $PM_{2.5}$ are plausible. The applied correction is realistic and assumed valid.

4.6.6.3 Discrepancies at high noise exposure

The presented models overestimate the indoor exposure for the high noise levels. The few dwellings in the validation dataset with high exposure levels all tend to be overestimated by the models. The dwellings with a lower noise exposure are well estimated. The number of dwellings exposed to 65 dB and more are too small to perform any statistically relevant evaluation, still several potential arguments can be provided to explain this discrepancy. Five household could be identified with extreme overestimations. Noise misclassification is possible. The underlying noise map for the region of Flanders does not include screening by buildings. Missing shielding by buildings from nearby high density roads could cause this effect but none of the five households seem shielded from the local traffic source. All dwellings could be identified as close to secondary roads or within a village near the local road. The noise level can be overestimated in the map because of a local overestimation of traffic in the external data. The underlying traffic model idealized the network and cannot account for all routing options. Traffic from multiple roads in the vicinity can occasionally accumulate on a single network link. Since the selected dwellings are positioned near the traffic links in villages, at the lowest level in the traffic network, the overestimation of the traffic in the underlying traffic sources is plausible.

Another option is the lack of spectral content in the noise map. The bicycle model showed relative strong saturation of the BC exposure at higher traffic speed (see Figure 4.2.2). This information is not included in the L_{DEN} based indoor model. Exposure to high density roads with consequently high speeds implies a relatively high contribution of rolling noise in the noise evaluation. The reduction in 'deviance explained' in $BC_{loc,noisemap}$ in comparison with the instantaneous BC model (Table 4.2-2) is partially related to that missing information. As mentioned before, combining the benefits of noise monitoring networks, noise map calculations and mobile noise measurements can add this information in the future.

The last option to explain the discrepancy is the influence of uncharted parameters. Wind direction is possible candidate.

4.6.6.4 Potential interaction between noise exposure and I/O ratios

In literature few evaluations are available with I/O ratio as a function of the outdoor traffic, but indirectly this phenomenon is visible when the slope of the I/O ratio is below 1 with increasing outdoor levels (Meier et al., 2015). At first sight, this can be the result of indoor particulate sources but reduced I/O ratios at high exposed dwelling due to changing ventilation settings also can explain this phenomenon. Sajani reported two dwellings including particle size distribution and the I/O ratio of the high exposed dwelling is much lower compared to the residential location. That effect was also stronger for smaller particles (Sajani et al., 2015). Particle size is smaller closer to the source and can also explain the discrepancy. Further evaluations on I/O ratios in respect to the local traffic exposure and particle size are necessary. Interaction between the noise exposure and the indoor air pollution is possible. Inhabitants of a dwelling highly exposed to noise will cope with the noise exposure by closing windows towards the high exposed facade. Consequently the ventilation of the dwelling will be reduced or will be organized from the low noise exposed facade. Existing data on I/O ratios could be evaluated to verify this coping effect. Coping with noise exposure by adjusting the ventilation is another plausible argument for the detected discrepancy.

4.6.6.5 Alternative modelling options

Applying this exact approach in a different setting will require a long-term mobile measurement campaign. In itself, this is a huge restriction, but the benefits of the mobile noise-BC biking are large as such. The fact that this approach works is an incentive to perform extensive mobile noise-BC measurement campaigns. City wide noise mapping results both in the required underlying dataset to build the gam models and has the potential to improve the indoor model by including the local traffic dynamics (see 4.6.6.1).

An alternative approach, replacing the underlying gam model with a direct model for local traffic assessment at the facade to indoor concentration is another option (see future work, 6.1.1). In Section 4.7, a pilot case will be evaluated. The noise levels at a high exposed facade are used to predict the outdoor BC exposure at the facade. More extended campaigns, covering multiple dwellings with various traffic situations over longer periods, including outdoor and indoor measurements for multiple air pollutants can result in an alternative direct model, including better knowledge of the spatial and temporal variability of the I/O ratios.

4.6.6.6 Limitations

The limitations can be split into three sets: fundamental unknowns, unavailable data and limitations of the validation data. The main fundamental limitation of the indoor model is the origin of the Black Carbon data to convert the noise map into a local contribution to BC at the facade of the dwellings: the bicycle data. The $1/r^2$ distance to source relation is similar for noise and air pollution but is only valid in its most basic form (see 4.6.2). The actual dis-

tance to source relation from roadside (bicyclist) to dwelling facade (outdoor at dwelling) could not be verified and identifies the second fundamental limitation. The third fundamental limitation is the extrapolation of the rush hour bicycle model to a diurnal pattern based on a standard diurnal pattern, this is also not proven.

The model suffers also from unavailable data. No dwelling specific information is included in the model, not for the traffic and not for the ventilation properties of the dwelling. The most important missing data is however a background measurement location not including a diurnal pattern. This is identified as the main data limitation.

Some of the limitations link back to the external validation set. The sample of the 31 households in the external validation set. None of the dwellings was located close the major roads (<100m) or highways (<300m) where the major road or highway is expected to have a significant impact. Extending the validation data to these spatial configurations is crucial. It is also not expected that the presented model will work in these extreme settings without modifications. Noise measurements can however distinguish between continuous noise sources and local traffic events. Splitting the $BCBA_{loc}$ component into actual local traffic in the local street and midrange influences from major sources at medium distance is a potential future development.

4.6.7 Conclusions

The indoor exposure estimation is based on a long-term bicycle exposure experiment. The in-traffic measurements are mapped to an L_{DEN} noise map and used to estimate a BC concentration with a highly improved spatial resolution. The noise map acts in this land-use regression like approach (LUR) as a distance weighted traffic assessment sensitive to the combination of exposure to local and more distant high density roads. A full continuous traffic evaluation with extreme distance to source effects emerges. The background adjusted approach is able to disassemble the exposure in two components. A background component is expressing the long-range and long-term evolution of the BC concentration, strongly determined by the meteorological effects. The local traffic component is resolved in the noise map based gam model. A seasonal adjustment of the I/O ratio is fitted and validated with external data, resolving all remaining temperature depending influence. In the provided solution, the background component includes a diurnal pattern. The components are therefore not as independent as desired. Unfortunately no alternative location for the background BC concentration with lower diurnal pattern was available. This limitation in the input data reduces the quality of this part of the exercise significantly. Despite all these restrictions, the model reaches a Spearman's correlation of 0.65 on the individual activities and a slope of 0.78.

This section is a numerical experiment based on available data only. It nevertheless illustrates the potential of the background adjusted approach. Dedicated measurements will be necessary to provide scientific validation.

4.6.8 References

Allen R.W., Adar S.D., Avol E., Cohen M., Curl C.L., et al. 2012. Modeling the Residential Infiltration of Outdoor $PM_{2.5}$ in the Multi-Ethnic Study of Atherosclerosis and Air Pollution (MESA Air). Environmental Health Perspectives, 120, 824-830.

Beelen, R., Hoek, G., Vienneau, D., Eeftens, M., Dimakopoulou, K., Pedeli, X., ... & de Hoogh, K. (2013). Development of NO 2 and NO x land use regression models for estimating air pollution exposure in 36 study areas in Europe–the ESCAPE project. Atmospheric Environment, 72, 10-23.

Can A., Van Renterghem T., Rademaker M., Dauwe S., Thomas P., et al. 2011. Sampling approaches to predict urban street noise levels using fixed and temporary microphones. Journal of Environmental Monitoring, 13, 2710-2719.

Can A., Dekoninck L. & Botteldooren D. 2014. Measurement network for urban noise assessment: Comparison of mobile measurements and spatial interpolation approaches. Applied Acoustics, 83, 32-39.

Chen C. & Zhao B. 2011. Review of relationship between indoor and outdoor particles: I/O ratio, infiltration factor and penetration factor. Atmospheric Environment, 45, 275-288.

Dauwe S., Van Renterghem T., Botteldooren D. & Dhoedt B. 2012. Multiagent-Based Data Fusion in Environmental Monitoring Networks. International Journal of Distributed Sensor Networks.

Dons E., Panis L.I., Van Poppel M., Theunis J., Willems H., et al. 2011. Impact of time-activity patterns on personal exposure to black carbon. Atmospheric Environment, 45, 3594-3602.

Dons, E., 2013. Air pollution exposure assessment through personal monitoring and activity-based modeling. PhD Thesis. Hasselt University, Diepenbeek, p. 302.

EEA Technical report No 18/2013, Status of BC monitoring in ambient air in Europe, ISSN 1725-2237

Hanninen O., Hoek G., Mallone S., Chellini E., Katsouyanni K., et al. 2011. Seasonal patterns of outdoor PM infiltration into indoor environments: review and meta-analysis of available studies from different climatological zones in Europe. Air Quality Atmosphere and Health, 4, 221-233.

Hoek G., Kos G., Harrison R.M., de Hartog J., Meliefste K., et al. 2008. Indoor-outdoor relationships of particle number and mass in four European cities. Atmospheric Environment, 42.

Meier, R., Eeftens, M., Phuleria, H. C., Ineichen, A., Corradi, E., Davey, M., ... & Künzli, N. (2015). Differences in indoor versus outdoor concentrations of ultrafine particles, PM2. 5, PMabsorbance and NO2 in Swiss homes. Journal of Exposure Science and Environmental Epidemiology.

Sajani, S. Z., Ricciardelli, I., Trentini, A., Bacco, D., Maccone, C., Castellazzi, S., ... & Harrison, R. M. (2015). Spatial and indoor/outdoor gradients in urban concentrations of ultrafine particles and PM 2.5 mass and chemical components. Atmospheric Environment, 103, 307-320.

Van Renterghem T., Thomas P., Dominguez F., Dauwe S., Touhafi A., et al. 2011. On the ability of consumer electronics microphones for environmental noise monitoring. Journal of Environmental Monitoring, 13, 544-552.

Wei W., Botteldooren D., Van Renterghem T., Hornikx M., Forssen J., et al. 2014. Urban Background Noise Mapping: The General Model. Acta Acustica United with Acustica, 100, 1098-1111.

4.7 Noise based BC exposure at a dwelling facade

4.7.1 Introduction

In the previous sections, the main focus was on matching the spatial variation of noise exposure to the spatial variation of Black Carbon exposure. In section 4.6, the indoor model, it became clear that largest part of the uncharted variability is related to the diurnal patterns of the background exposure and the local traffic. This section will investigate the temporal variation by evaluating a single location and perform an analysis of the noise-BC relation over time, focusing on the diurnal patterns of the different covariates. We explore the same type of modeling as in sections 4.2 and 4.4: correlating real-time measurements of noise with real-time pollution measurements. Ambient concentrations at a dwelling facade are sensitive to wind speed, temperature and other atmospheric conditions (Can et al., 2011). To improve the assessment, the contributions of the diurnal pattern of the background and the diurnal pattern of the traffic have to be disentangled. In this pilot, we select a dwelling in a narrow street with an expected high exposure to both noise and air pollution. The selected dwelling should express as much diurnal variation in traffic composition and traffic dynamics to contrast with the meteorological influences through the background concentration.

The basic aim of this pilot study is to explore the possibility to add value to air pollution exposure measurements at dwellings by measuring noise at the facade. This can quantify the signal of the local traffic contribution of the air pollution exposure at the dwellings on top of the obvious correlation with the background contribution. It is evident that this should be extended to more dwellings with as many air pollutants as possible. This is only possible in a larger project, joining the hardware, support and knowledge of the two disciplines.

The background adjusted approach, successful in 4.2, 4.4 and 0, will be used to investigate and disentangle the local and the background contributions. The background adjusted models will be tested for different available background measurement locations. The following research questions will be handled:

1. Which noise parameters are the best predictors of the local component of the BC exposure at the facade?
2. The different diurnal patterns in the available background measurement locations will interact with the traffic diurnal pattern. How will the properties of the background measurement locations influence the predictive quality of the noise based additive models?

4.7.2 Methodology

4.7.2.1 BC concentrations at remote, near city and in city background locations and the high exposed dwelling

Three different background locations will be compared to evaluate the diurnal patterns with the exposure at a high exposed dwelling. The BC background concentrations were retrieved from the Flemish Environmental institute (www.vmm.be) for different locations, the details are available in 4.7.2.4. The diurnal patterns are shown in Figure 4.7.4 (second row, first three charts). The first is a measurement station in a park in the city of Ghent within 1 km from the dwelling under investigation (Ghent, 'Baudelo park', ref 44R701, in-city background). The next two plots show different measurement locations, qualified by the VMM as 'background' locations. The second background location (Antwerpen-Linkeroever, ref 40AL01) is outside the city of Antwerp in an open area at a reasonable distance of major traffic sources. The third location is located 80 kilometers to the West near the coast (Houtem, ref 44N029, available since 2012, the remote background). To visualize the different properties of background measurement locations and their related diurnal patterns, the relative position of the measurement point towards local roads, city background and remote background are visualized in Figure 4.7.1.

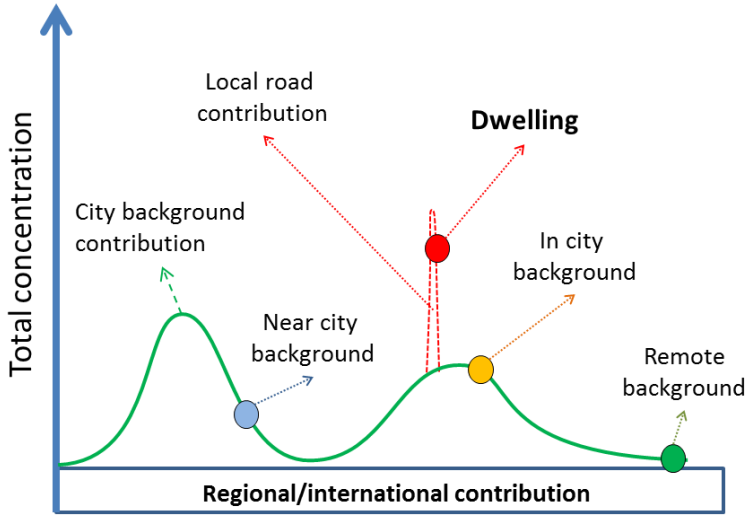

Figure 4.7.1: Abstraction of the positions of the measurement location in the Flemish region and the spatial variation of the Black Carbon concentrations (green= remote background, blue = near city background, orange=in-city background, red= dwelling at high exposure road inside the city).

The green line illustrates the impact of the cities on the background concentrations in their vicinity. Each of the points expresses a temporal variation which is the sum of all influencing factors on the Black Carbon concentrations. The local impact of the road near the dwelling (red dotted line) is shown as well. The remote background location shows no distinctive diurnal pattern, but shows higher levels during the night-time. This is related to stable atmospheric conditions, reducing the dispersion of the air pollution during the night. The

remote background location expresses the regional contribution. The outside-major-city background location already shows a distinctive diurnal pattern, related to the traffic in the wide area around the measurement location. The in-city background expresses a strong bi-modal profile, indicating the influence of large amounts traffic in the vicinity of the measurement location. Higher concentrations result in stronger diurnal patterns.

The concentrations at the high exposed dwelling are about 1.8 times the in-city-park background (see chart at top-left in Figure 4.7.4). The differences between the concentration during rush hour and night are increasing from remote to near city, in-city and dwelling exposure, expressing the impact of the traffic in the vicinity. These are the differences that will be evaluated toward the diurnal pattern of the local traffic at the dwelling, the diurnal pattern at the background locations and the long-term changes in the background due to changing meteorological conditions.

4.7.2.2 Measurement equipment, setup and location

A low-cost noise measurement setup designed by the acoustics group at the Ghent University was modified to enable automated measurements at a much lower hardware cost (Can et al., 2011a, Can et al., 2011b, Van Renterghem et al., 2011, Dauwe et al., 2012) (see Figure 4.7.2). The noise measurement module was extended with a micro-aethalometer (AE51, Aethlabs, San Francisco, CA). The person living at the dwelling was instructed on how to replace the filter and real time reporting was used to decide when the filter had to be replaced.

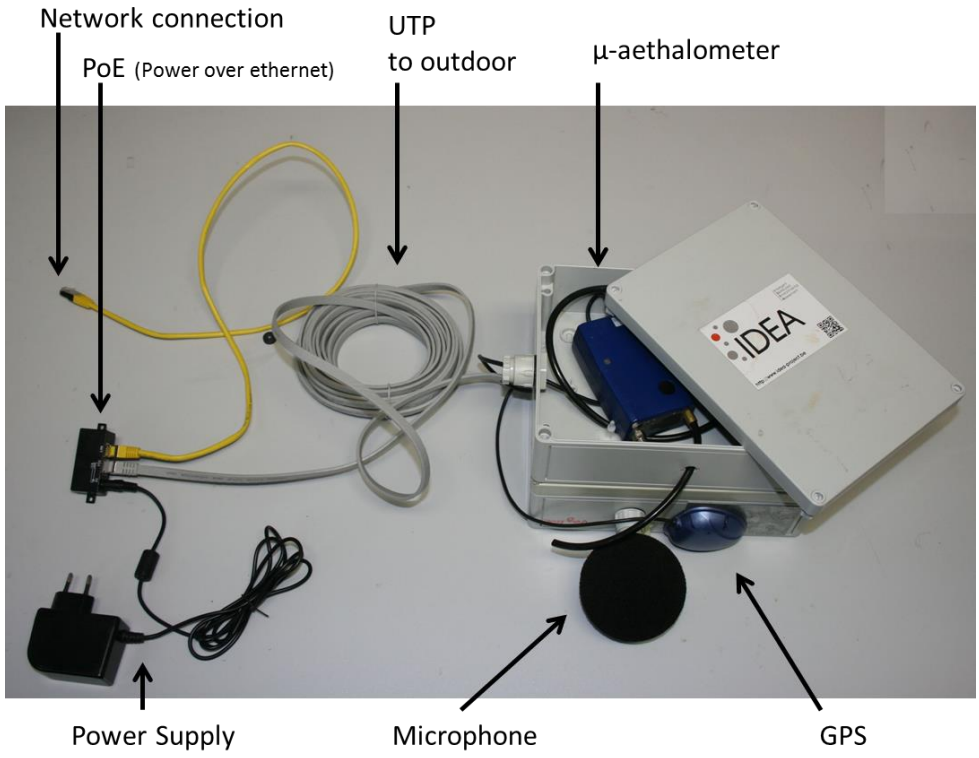

Figure 4.7.2: Inexpensive noise measurement equipment including the micro-aethalometer and GPS for continuous BC measurements.

The measurement resolution of the aethalometer was set to one minute to prevent memory overflow errors. The equipment was mounted on a windowsill at a height of 2.5 m, out of reach of passing pedestrians (Figure 4.7.3). The road has two lanes and sidewalks on each side of the road, including a parking lane but at the measurement position no parked cars can block the microphone position from the local traffic. The horizontal distance to the center of the closest traffic lane is approximately 6 m. The width of the street canyon is 16 m.

Figure 4.7.3: Measurement location at a dwelling facade on narrow busy road in the city of Ghent. The arrow shows the position of the equipment; the inset picture gives a front view of the setup.

The measurements started on March, 26th and lasted until May, 12th 2014, a period of more than six weeks. The measurement period included the Easter holiday period (two weeks in Belgium) and a holiday weekend (May 1st). Only the weekdays are included in the data analysis. This restriction is included since most activity based personal assessments focus on commuting patterns on weekdays. The influence of adding the weekends into the analysis will be briefly addressed in the results and discussion. The variability of the time-activity patterns and traffic during weekends is of a different magnitude. The meteorological data is retrieved from the closest measurement station of the national meteorological institute near the city of Ghent (www.kmi.be, measurement location Melle).

4.7.2.3 Data processing

Analyzing diurnal patterns in the local traffic requires the selection of a temporal resolution matching the exposure dynamics at the dwelling facade. The meteorological data is available by hour, the BC background concentrations at the fixed measurement locations by half hour. Most spatiotemporal models detail the temporal component by season or on long-term evolutions (Hoek et al., 2008, Beelen et al., 2011) and only recently spatiotemporal models for

BC by hour have been published (Dons et al., 2014a, Dons et al., 2014b); Since we are interested in the subtle effects of traffic jams near the dwelling and since the duration of rush hour is shorter than one hour and sensitive to the day of the week, a more detailed temporal resolution of 15 minutes is chosen. This temporal resolution should be enough to capture the changes of duration of the rush hour.

The raw noise measurements are performed in one-third octave bands, at a sampling rate of 8 measurements per second and aggregated to one second. The BC measurements have a temporal resolution of 1 minute. The data is aggregated to a temporal resolution of 15 minutes. For noise, several aggregation methods are included in the analysis. The standard A-weighted statistical noise levels are included to investigate whether instantaneous BC exposure could be predicted on the basis of well know and widely available quantities ($L_{Aeq,\ 15min}$, $L_{01,\ 15min}$, $L_{05,\ 15min}$, $L_{10,\ 15min}$, $L_{50,\ 15min}$, $L_{95,\ 15min}$). The statistical level L_N is the noise level that is exceeded for N % of the time for the chosen evaluation period. In addition the traffic-related noise parameters $L_{OLF}(t)$ and $L_{HFmLF}(t)$ are calculated at a temporal resolution of 10 seconds according to the definition in Dekoninck et al. (2013). These parameters, more successful in the bicycle models compared to L_{Aeq} evaluations, will be tested as well. The temporal evaluation of 10 seconds is chosen identically to be compatible with the bicycle model. They require aggregation to the 15 minute temporal resolution of the facade model. Two variants are tested, an arithmetic average $L_{OLF,bike,\ 15min}$ and an acoustic energy conserving equivalent noise $L_{OLFeq,\ 15min}$. $L_{OLF,bike,15min}$ will be not increase strongly when a few vehicles pass in the 15 minute interval, while $L_{OLFeq,\ 15min}$ will only result in low values with very low amounts of traffic events. The BC concentrations are averaged over the 15 minute evaluation period without applying correction functions.

4.7.2.4 Diurnal patterns of measurements and covariates

In Figure 4.7.4, boxplots for all 15 minute values of the covariates are shown by hour of the day. The top-left plot shows the diurnal pattern of the measured BC exposure at the facade. The most important feature is the high concentration and large variability during the morning rush hour. The wind speed, and temperature show a classic diurnal pattern with higher values during the day. The pressure does not show a diurnal pattern. The upper right boxplot shows the L_{Aeq} at the dwelling facade. The second row shows three background measurement locations in Flanders, presented earlier. The next two plots are the two variants of the low frequency noise evaluation: $L_{OLF\text{-}bike}$ as defined and used for the in-traffic bicycle model and $L_{OLF\text{-}eq}$, the equivalent noise evaluation of L_{OLF}, presented with identical y-axis to illustrate the mathematical difference between equivalent noise levels and arithmetic average.

The last row shows the diurnal patterns of the noise measurement in the typically use statistical levels L_{A95}, L_{A50}, L_{A10}, L_{A05} and L_{A01}, evaluated for each 15 minute interval. $L_{A95,15min}$ is the noise level that is exceeded in that time interval for 95% of the time, typically referred to as the 'background noise level'. $L_{A50,15min}$ expresses the median and $L_{A01,15min}$ is an indication

of the noise peak events, the level that is exceeded for at least 1% of the interval (e.g. 9 seconds in the 15 minute interval).

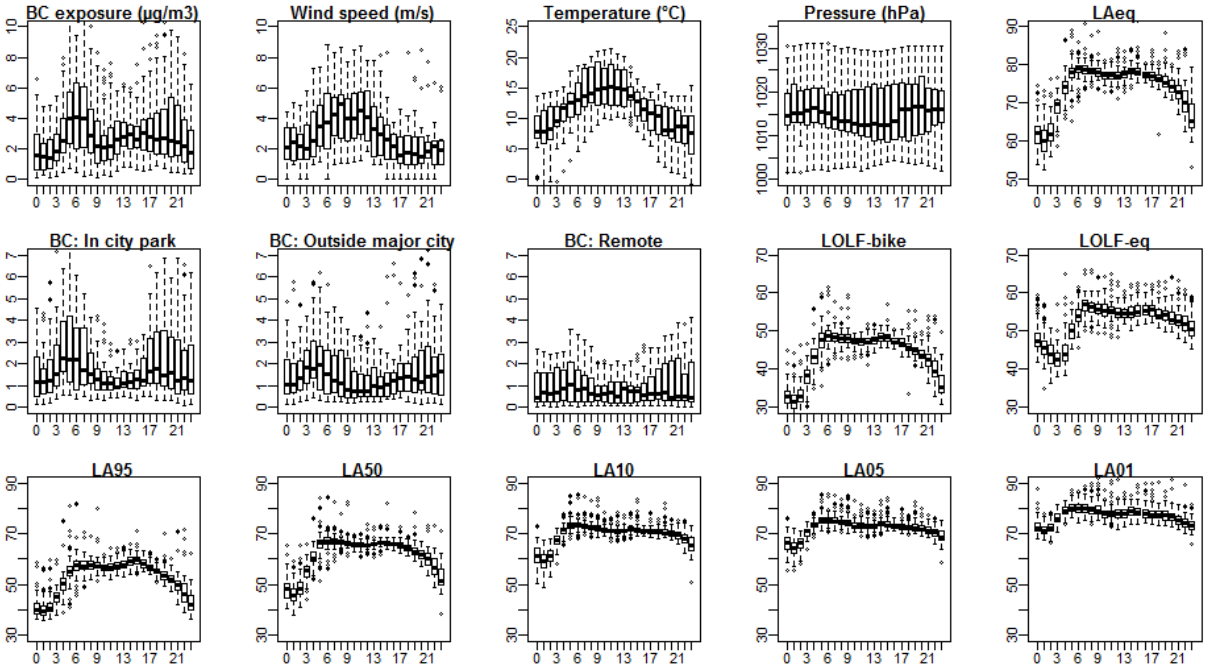

Figure 4.7.4: Diurnal patterns of the 15 minute values of the BC exposure, meteorological parameters, background measurement locations and noise parameters.

4.7.2.5 Gam models: reference and background adjusted

The diurnal patterns of the noise parameters and the background concentrations at the three background measurement locations show diurnal patterns with a different magnitude and shape. To investigate and compare the statistical strength of the possible combination for the background and the noise parameters, two sets of models are built. The models using the original data, referred to as RAW and the models with a background adjustment (referred to as LOC), similar to the bicycle model. In the instantaneous model for bicyclists the background adjustment was defined as the exposure at the background station at timestamp t minus the first quartile of the background station over the evaluation period (Dekoninck et al., 2013, see 4.2). This same approach is used again, using the yearly statistics of 2013 for all the background monitoring stations, since 2013 is the last available full year of data. The background adjustment is not applied at full for the same reasons at in the bicycle model. Instantaneous values can become negative and the background adjustment should only adjust for episodes with rather high background concentrations.

$$\mathrm{BC}_{\mathrm{excess,bkg,X}}(\mathrm{t}) = \max(0.0, (\mathrm{BC}_{\mathrm{bkg,X}}(\mathrm{t}) - \mathrm{Q1}(\mathrm{BC}_{\mathrm{bkg,X,year}}))) \quad (1)$$

$$\mathrm{BC}_{\mathrm{loc,bkg,X}} = \mathrm{BC}_{\mathrm{raw}} - \mathrm{BC}_{\mathrm{excess,bkg,X}}(\mathrm{t}) \quad (2)$$

This results in two sets of gam models with all combinations of the noise parameters and the background (eq. 3 and 4). Equation 4a includes the background concentration to evaluate the residual effects of background adjustment in 4.7.3.1and 4.7.3.2. Equations 4b does not include the background concentration and assumes that the background adjustment is valid and is used to evaluate the predictive strengths (4.7.3.3).

$$\mathrm{gamBC_{raw,bkg,X,noise_Y}} = \mathrm{gam_{raw}}\left(\mathrm{Noise_Y}, \text{Wind Speed}, \mathrm{BC_{bkg,X}}\right) \quad (3)$$

$$\mathrm{gamBC_{loc,bkg,X,noise_Y}} = \mathrm{gam_{loc}}\left(\mathrm{Noise_Y}, \text{Wind Speed}, \mathrm{BC_{bkg,X}})\right) \quad (4a)$$

$$\mathrm{gamBC^{*}_{loc,bkg,X,noise_Y}} = \mathrm{gam_{loc}}(\mathrm{Noise_Y}, \text{Wind Speed}) \quad (4b)$$

The background exposure is still added in the local models to show the strong reduction of the covariate's strength in the local models. Each noise parameter (6) is modeled for each background measurement station (3) using both the raw and the background adjusted approach (2), resulting in two sets of 18 gam models. Reconstruction of the total exposure requires the prediction of the model at timestamp t (eq. 5). For the local background adjusted model, the background adjustment at timestamp t is added to the predicted value to reconstruct the total exposure (see eq. 6)

$$\mathrm{BC_{tot,raw,bkg,X}}(t) = \mathrm{predict}(\mathrm{gamBC_{raw,bkg,X,noise_Y}}, t) \quad (5)$$

$$\mathrm{BC_{tot,loc,bkg,X}}(t) = \mathrm{predict}(\mathrm{gamBC^{*}_{loc,bkg,X,noise_Y}}, t) + \mathrm{BC_{excess,bkg,X}}(t) \quad (6)$$

Another prediction approach will be tested as well. The used background in the gam model and the added background adjustment do not necessarily have to be retrieved from the same background measurement location. The background adjustment can include a traffic related diurnal profile, competing with the diurnal profile of the noise based traffic assessment. A remote background will add knowledge into model about the atmospheric conditions without disturbing the local traffic assessment from the noise covariate. That model will not be sensitive to the accumulated BC concentrations of the traffic in the large vicinity of the investigated dwelling. Reconstructing the total exposure can therefore be based on a background adjusted gam model based on a remote location, but adjusted with a local assessment of the background capturing accumulated BC concentration in the vicinity (see eq. 7). The rationale of this approach will be addressed in detail in the discussion.

$$\mathrm{BC_{tot,loc,bkg,X,bkg_Y}}(t) = \mathrm{predict}(\mathrm{gamBC_{loc,,bkg,X,noise_Y}}, t) + \mathrm{BC_{excess,bkg,Y}}(t) \quad (7)$$

4.7.3 Results

4.7.3.1 Model fits

Table 4.7-1 shows the two sets of models (raw and local), sorted by the deviance explained. For the local models, formula (4a) is used to evaluate the residual effect of the background adjustment. The raw models show much higher deviance explained compared to the local models, the strength of the noise covariate is similar in the two sets, but it is the dominant covariate in the local models. In the raw models the variance explained by the model using the in-city park background is the strongest covariate; the variance explained by the model based on the background measured at the remote location is the lowest. This is completely inversed in the local models; there the remote background adjusted model is the strongest. The noise based traffic related covariate is the strongest, while in the raw model; the strongest component is the background station closest to the measurement point. This illustrates that the dominant component of the BC concentration at the dwelling is the background, even for a high exposed dwelling. The purpose of the background adjusted models is to overcome that obvious correlation with the background and detect the best model to predict the location specific traffic related component in the concentration at the dwelling.

The next step is determining which noise covariate is best suited to express the traffic related contribution at the dwelling. Two important trends can be observed. First $L_{OLF,bike}$ and L_{Aeq} result in similar model strengths (in deviance explained). The differences between models are not statistically significant, the best performing model will have to be selected by its power to predict the short and high traffic related episodes in the time series that is predominantly defined by the background concentrations. The strength (F-value) of the $L_{OLF,bike}$ covariate is systematic stronger than the L_{Aeq} covariate, even is the deviance explained of the corresponding models is not stronger. A similar observation was made in the bicycle model (see 4.2). The strength (F-value) of the L_{HFmLF} was low in the models and is therefore not reported in the models. Another important observation is the systematic low strength (F-value) of $L_{OLF,eq}$ throughout all model variants, both raw and local. The noise based traffic assessment is clearly not correlated with the acoustical energy in the low frequency bands. These features will be addressed in detail in the discussion.

Raw models					F-values				
Background station	Noise parameter	Deviance explained	AIC	Intercept (ng/m3)	BCbkg	Wind speed	Tempera-ture	Noise parameter	# samples
In-city park	LAeq	63.4%	3351	2116	402	30	33	84	1961
In-city park	LA50	63.3%	3355	2117	404	29	32	73	1961
In-city park	LOLF,bike	63.3%	3357	2117	406	30	31	105	1961
In-city park	LA05	63.2%	3362	2112	390	27	33	59	1961
In-city park	LA95	62.8%	3383	2117	421	28	33	51	1961
In-city park	LOLF,eq	62.5%	3400	2117	461	18	38	44	1961
Near major city	LOLF,bike	58.4%	3601	2085	283	16	25	109	1961
Near major city	LAeq	58.4%	3603	2084	276	16	28	108	1961
Near major city	LA50	58.4%	3603	2085	279	15	27	107	1961
Near major city	LA95	57.5%	3645	2082	288	15	32	90	1961
Near major city	LA05	57.3%	3651	2077	248	17	34	90	1961
Remote background	LA05	57.2%	3658	2090	240	58	55	104	1961
Remote background	LAeq	57.0%	3666	2093	243	59	57	110	1961
Remote background	LA50	56.9%	3673	2093	243	57	57	116	1961
Remote background	LOLF,bike	56.8%	3677	2092	246	59	56	143	1961
Near major city	LOLF,eq	56.2%	3703	2081	304	6	42	70	1961
Remote background	LA95	55.4%	3737	2090	241	57	66	76	1961
Remote background	LOLF,eq	53.4%	3826	2087	243	42	79	42	1961

Local models					F-values				
Background station	Noise parameter	Deviance explained	AIC	Intercept (ng/m3)	log(BCbkg)	Wind speed	Tempera-ture	Noise parameter	# samples
Remote background	LOLF,bike	28.8%	5290	1432	17	62	58	218	1961
Remote background	LAeq	28.6%	5299	1432	16	62	57	71	1961
Remote background	LA50	28.3%	5307	1432	16	60	59	72	1961
Remote background	LA05	28.2%	5310	1429	17	61	61	66	1961
Remote background	LA95	26.9%	5345	1430	18	60	64	54	1961
Near major city	LOLF,bike	26.2%	5688	1114	79	14	13	112	1961
Near major city	LA50	25.9%	5697	1114	78	14	14	109	1961
Near major city	LAeq	25.8%	5699	1113	79	15	15	108	1961
Remote background	LOLF,eq	25.1%	5393	1426	16	46	83	37	1961
Near major city	LA95	24.8%	5725	1110	77	12	17	96	1961
Near major city	LA05	23.1%	5769	1106	77	17	22	81	1961
Near major city	LOLF,eq	22.8%	5778	1110	72	4	26	78	1961
In-city park	LOLF,eq	21.2%	5359	1238	49	14	26	49	1961
In-city park	LOLF,bike	20.6%	5370	1237	56	23	20	131	1961
In-city park	LAeq	20.6%	5371	1236	56	23	23	130	1961
In-city park	LA50	20.6%	5371	1237	55	23	22	130	1961
In-city park	LA95	20.6%	5375	1238	51	21	18	43	1961
In-city park	LA05	20.0%	5389	1233	55	21	26	39	1961

Table 4.7-1: The BC_{raw} and BC_{loc} gam model summary for six noise parameters and three background measurement stations.

4.7.3.2 Model spline behavior

The $L_{OLF,bike}$ covariate describes the local traffic related component of the BC concentration better than the other noise parameters. In Figure 4.7.5, the splines of four models are shown to illustrate the behavior of the different models. The top row shows the raw model with the in-city park background concentration. The highest values at the background location do not correlate with the BC concentration at the dwelling. $L_{OLF,bike}$, wind speed behave as expected. The concentration at the dwelling slightly increases with temperature.

The spline of the background covariate in the local models based on the in-city park background and the near major city background are overadjusting for the high exposure values at the dwelling. High values at the background locations do not correlate with the highest values at the dwelling. The slope of the spline of the $L_{OLF,bike}$ covariate is increasing.

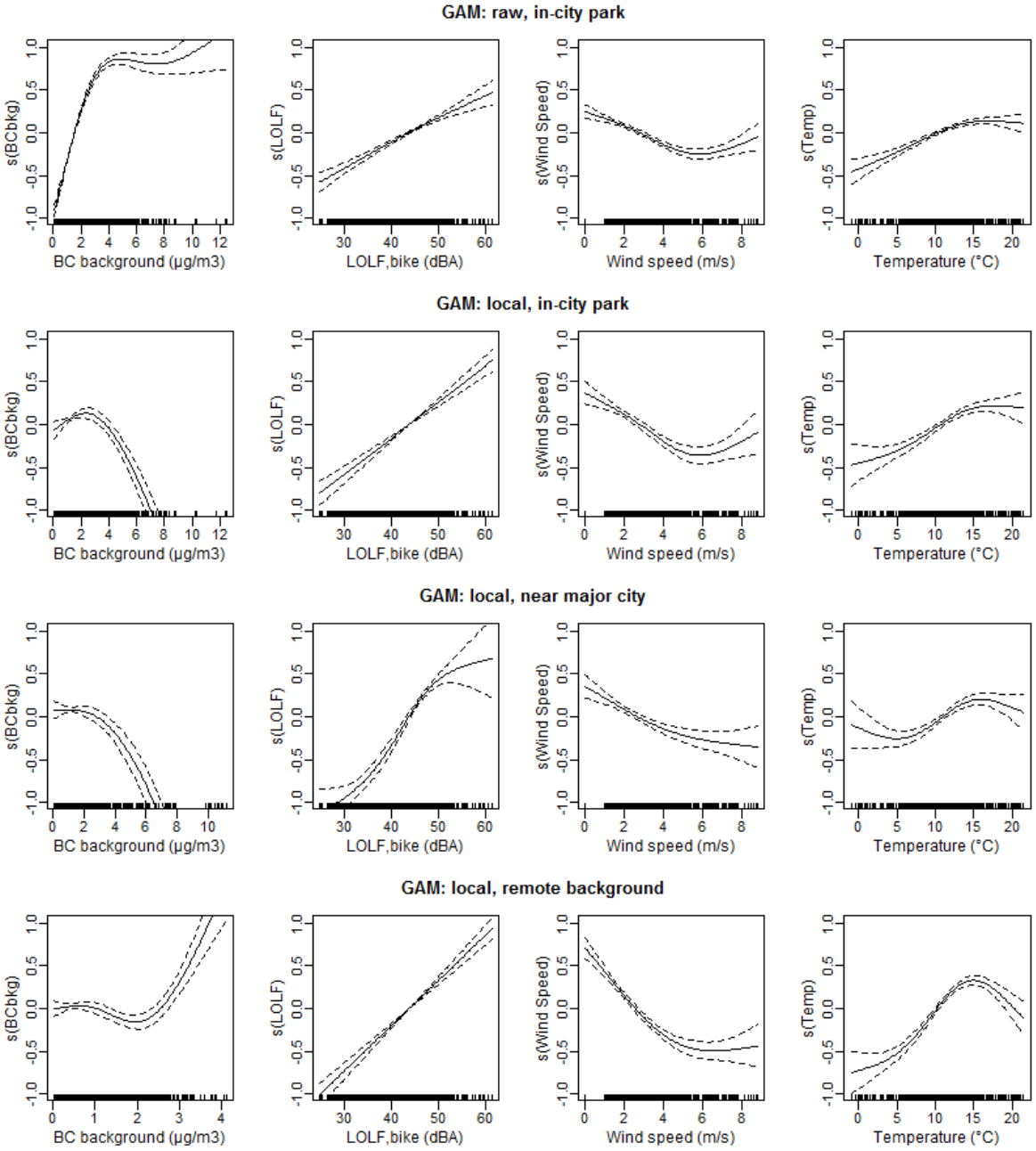

Figure 4.7.5: Splines of the $L_{OLF,bike}$ gam models for the in-city-park raw model (top row) and the three local models,. Note the different ranges of BC exposure for the different background locations.

The local model based on the remote location, results in a correct background adjustment for the low background concentrations but requires adjustments for the higher background values (up from 2.5 µg/m^3). High background concentrations at the remote background location result in extreme increased concentration at the dwelling, not explained by the remote background location. The $L_{OLF,bike}$ covariate shows the strongest slope and lowest error over all the models.

4.7.3.3 Model predictive strength

In Figure 4.7.6 the predictive strength of the models based on $L_{OLF,bike}$ are illustrated. In this case, the local gam models do not include the background covariate (see formula 4b). As mentioned before, it is not the deviance explained that defines the selection of the best model, but the potential to predict the local high concentrations. Each chart shows the estimation versus the measurement according the formulas (5), (6) and (7). The root mean square error (rmse) and mean average error (mae) are added as additional parameters to compare the predictive strength of the models.

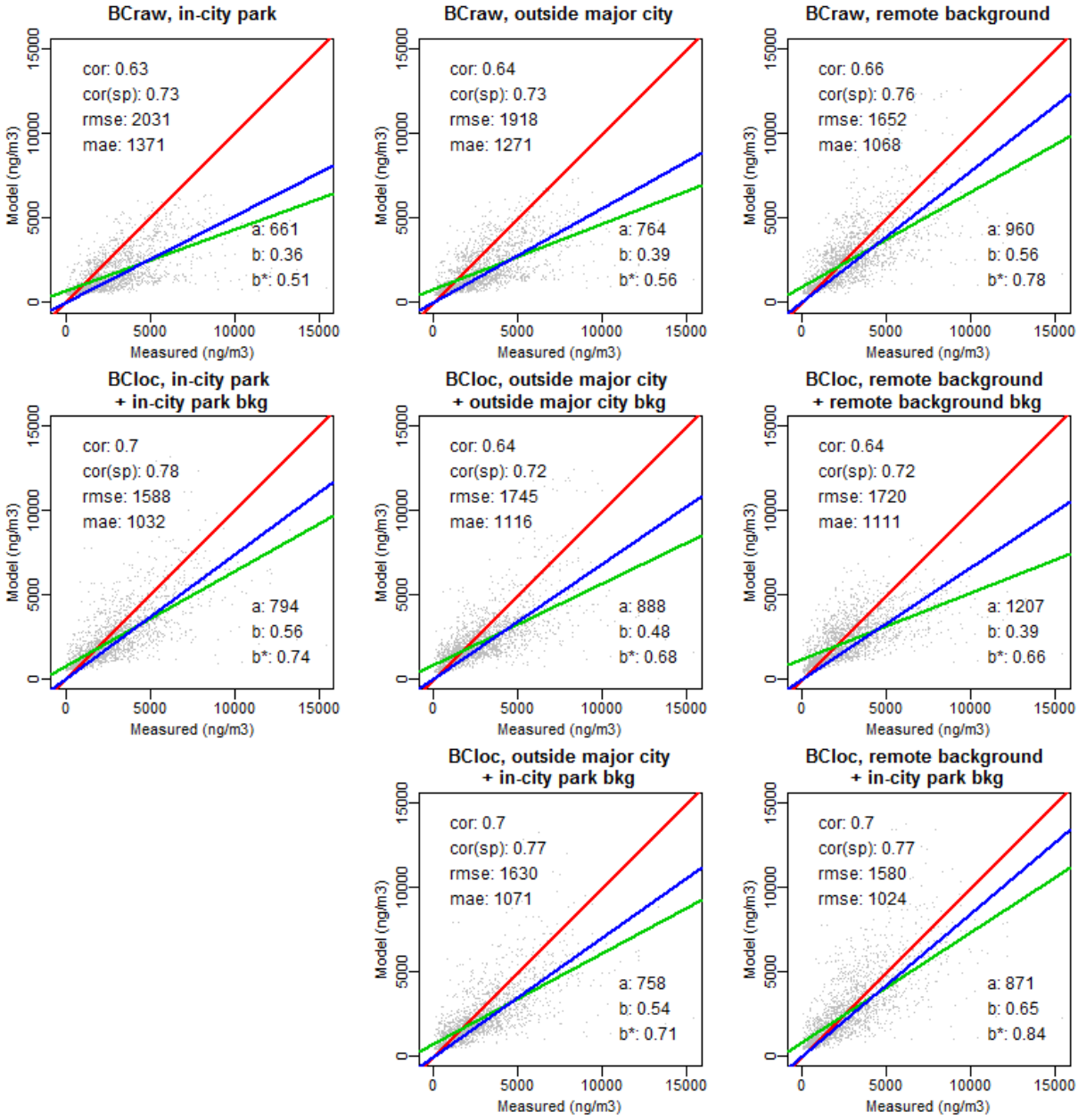

Figure 4.7.6: Model strength of the BC gam models for $L_{OLF,bike}$: the raw models for the three background locations, the three local models for the three locations. Two local models combined with the in-city background exposure complete the third row.

The first row shows the raw models for the three background locations, the next row the local models. The third row gives the local models according to equation 7, with the 'in-city park' background measurement as the background adjustment but the 'near major city' and 'remote background' as background correction in the gam model describing the local traffic component. The 'in-city park' background model is not relevant in the third row, since this combination is available in the second row. The red line is the perfect prediction; the green line is the linear fit on the estimated values. The blue line is the linear fit with the intercept forced to zero. The correlation and linear fit intercept and slope are added to the charts. A good model combines a good correlation with a slope close to one.

The raw models are not capturing the high exposure episodes at the dwelling. The slope remains well below 0.5. The highest exposure episodes cannot be predicted by the background concentrations. The local models according formula 6, are slightly improving with the model based on the in-city park background as the best option. The strongest model is by far the local model based on the remote background location, combined with the local background adjustment derived from the in-city park (formula 7). A slope of 0.65 is reached; the slope without intercept is 0.84 while the correlations are among the best in the set. The rmse and mae support the conclusions based on the correlation and slope at full.

This is further illustrated in Figure 4.7.7, comparing the estimation distributions with the measurement distribution. At the left, the raw model and local model based on the in-city park illustrate the improvement of the additive approach. In the right, the additive models for the different background stations while adding the in-city park excess background are compared. The remote background model adjusted with the local excess background outperforms all other models, matching the distribution of highest measurements.

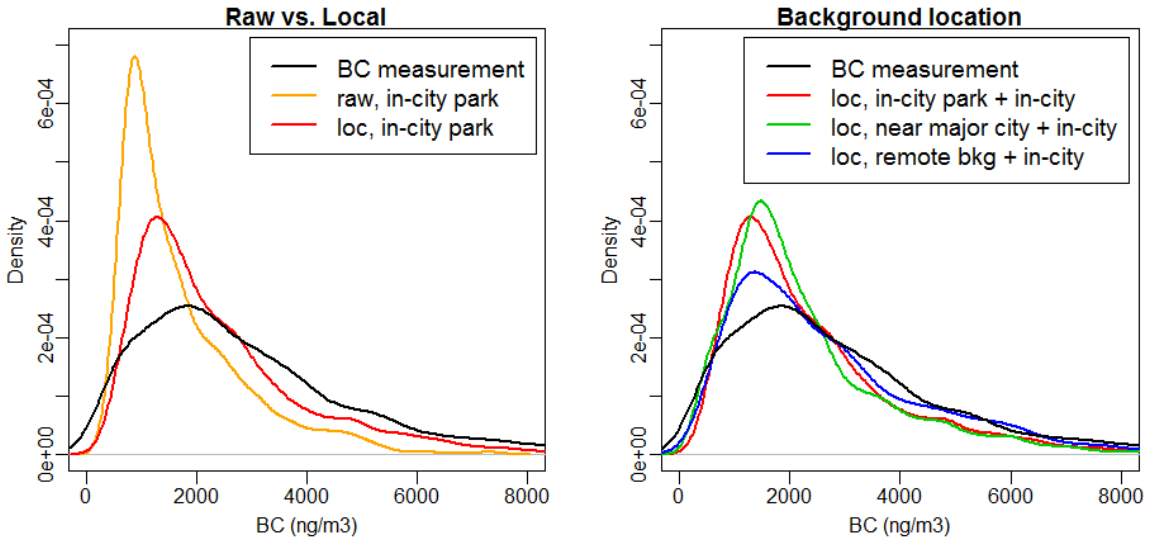

Figure 4.7.7: distributions of the prediction: difference between raw and local model for the in-city park background model (left); effect of the background for the local models (center) and the difference between $L_{OLF,bike}$ and L_{Aeq} (right).

4.7.4 Discussion

4.7.4.1 Noise parameters

The noise levels at the facade quantify the local traffic at the street level in good detail. The traffic related noise parameters is $L_{OLF,bike}$; yet L_{Aeq} is still an option. In future evaluations, in a larger set of dwellings with a wider range of traffic situations and different distance to sources, both should be evaluated and compared again. Another important feature is the failure of $L_{OLF\text{-}eq}$ as noise parameter. This was not expected and could be due to the mismatch between noise and air pollution emission due to idling vehicles while a traffic jam occurs. Under these conditions noise exposure in the low frequency is low but the exposure time if high and the $L_{OLF\text{-}eq}$ parameter will increase. In that traffic situation, vehicles are idling and the corresponding BC emissions are low.

The $L_{OLF,bike,10\ sec}$ parameter, averaged over the 15 minute interval expresses an event-like behavior. Few high $L_{OLF,bike,10\ sec}$ values will result in a low $L_{OLF,bike,15min}$ evaluation. Continuous traffic will result in many high $L_{OLF,bike,10\ sec}$ values and consequently in high $L_{OLF,bike,15min}$ values. If traffic jams result in high $L_{OLF,bike,10\ sec}$ and consequently lower BC emission can be established explicitly. Visual coverage is an option to evaluate this in the future.

The models are also evaluated including the weekends. The quality of the models is slightly reduced, mainly due to the completely different traffic profile on Sundays. This is not reported in detail.

4.7.4.2 Complexity of the dwelling exposure

Black Carbon concentrations at a dwelling are known to correlate with the concentrations at the background measurement stations. In this analysis, that phenomenon is confirmed. To increase the spatial and temporal detail in the exposure assessments we are not interested in the similarities between dwellings but in the differences. Performing the background adjustment attempts to detect the local component in the exposure. The strong reduction of the deviance explained between the raw and the local models only expresses the dominance of the background concentrations at the dwellings. A lower quality model, capable of detecting the local traffic effects, is therefore not a problem but rather the solution. The selection of a dwelling in a busy street is part of the design of the experiment. If this approach can work, it should work at least at the high exposed dwellings.

This exercise shows that even background stations close to the investigated dwelling do not cover the local variability of the exposure. The background concentration of the in-city park measurement location is the highest, but still fails to predict the local exposure peaks and for high background episodes, the background concentration can be even higher than the instantaneous exposure at the high exposed dwelling. The background adjusted approach improves the prediction a lot. The noise parameter becomes the strongest compo-

nent in the gam models after the background adjustment, but the diurnal profile of the in-city background station hampers the detection of the local traffic pattern in the gam models. When using the remote background location or near-city location; the 'deviance explained' improve. On the other hand, the exposure at the dwelling is underestimated for high background concentration episodes. The exposure at the dwelling is influenced by accumulation of traffic in the wide vicinity of the dwelling, information that is not available in the remote background location. This information is available in a generalized way in the closest background measurement station. Combining the remote background adjusted model with the in-city background location results in the strongest prediction, combining the city-wide accumulation effects with the most sensitive local traffic model.

Using the properties of two background stations in the same model may seem an odd and questionable approach, but this can be supported. The gam model covariates do not always express a direct relation between covariate and outcome. It can express correlations between the outcome and the underlying properties of the covariate. In the case of the background concentrations, the covariate expresses a combination of meteorological conditions determining the dispersion characteristics of the atmosphere at that time, including accumulations and lags of the BC emissions over time. Each background measurement locations will express a different set of influences. The remote background locations will only express general meteorological information on the stability of the atmosphere and seasonal aspects of BC emissions of all sources. The in-city background location expresses the high exposure episodes of combined traffic over a wider area and the accumulation effects of all city-wide BC sources. Each component expresses a relevant phenomenon and contributes equally to a proper prediction of the exposure of the dwelling.

4.7.4.3 Extending this approach

As mentioned in the introduction, long-term combined measurements at multiple locations, covering a wide range of local traffic situations, are necessary to actually disentangle the background contribution and the local contribution. A measurement campaign of that magnitude should also include multiple air pollutants and measure indoor concentrations as well. A detailed quantification of the traffic near the dwelling can be performed with noise measurements. It is important to cover as many changes over time for both the traffic and the meteorological conditions. Evaluations of the outdoor-indoor ratios as a function of the local traffic volume and the hour of the day can be derived and can improve the indoor model presented in the previous section (4.6). Two approaches are possible: evaluate the models at each individual dwelling and correlate the local traffic air pollution component to the local traffic evaluations and the best matching available background measurements or building a pooled model over multiple dwellings. It can be expected that more complex models with more than two contributions will be necessary.

This pilot is also complementary to other work that already investigated the potential of combining fixed noise measurements with mobile noise measurements to improve the spatial resolution of noise mapping (Can et al., 2014). The combined information on traffic, measured through noise with high temporal resolution at the fixed locations and high spatial resolution along the network with mobile city-wide coverage (see 0) is an important synergy that can improve the quality of exposure assessments for both disciplines significantly.

4.7.5 Conclusions

Capturing the spatial and temporal variability of particle concentration at facades is a daunting task but may be necessary to improve the quantification of particle matter exposure. The conclusions of this section are twofold. The in-city local background measurements results in a reasonable prediction of the facade exposure but does not result in valid predictions of the higher levels. This is due to the strong diurnal pattern included in the in-city background measurement location. In-city background measurements can be used to evaluate the exposure in the city as a whole, but will not detect the spatial variability inside the city; the main objective is not achieved. The model based on the remote background location detects the local variation of the traffic condition much better but fails to capture the BC accumulation of the city-wide emission. The combined model covers both phenomena.

The selection of suitable noise parameters is important. Few commonly used noise parameters capture the details in the traffic flow necessary for a good prediction model. The noise parameter $L_{OLF,bike}$ described in previous work for the prediction of instantaneous Black Carbon exposure is successful and reflects an event-like evaluation while focusing on the engine noise related part in the noise exposure. The equivalent noise L_{Aeq} is still an option, but this result indicates that the noise-BC relation is not straight forward. Evaluations of other authors using L_{Aeq} can fail due to these subtle effects related to engine noise and noise event sensitive evaluations. Since the dwelling is highly exposed and the dominant noise source is traffic it is possible this correlation will not be valid at dwellings located in quiet streets. This requires further investigation and extended multidisciplinary measurement campaigns.

This exercise illustrates again the potential of instantaneous noise assessments to disentangle variation in the BC concentrations into meteorological influences and local traffic influences.

4.7.6 References

Beelen R, de Hoogh K, Eeftens M, Meliefste K, Cirach M, de Nazelle A, et al. Estimating Long-term Exposure to Air Pollution in 38 Study Areas in Europe in a Harmonized Way Using Land Use Regression Modeling (ESCAPE Project). Epidemiology 2011; 22: S82-S82.

Can A, Dekoninck L, Botteldooren D. Measurement network for urban noise assessment: Comparison of mobile measurements and spatial interpolation approaches. Applied Acoustics 2014; 83: 32-39.

Can A, Dekoninck L, Rademaker M, Van Renterghem T, De Baets B, Botteldooren D. Noise measurements as proxies for traffic parameters in monitoring networks. Science of the Total Environment 2011a; 410: 198-204.

Can A, Rademaker M, Van Renterghem T, Mishra V, Van Poppel M, Touhafi A, et al. Correlation analysis of noise and ultrafine particle counts in a street canyon. Science of the Total Environment 2011b; 409: 564-572.

Dauwe S, Van Renterghem T, Botteldooren D, Dhoedt B. Multiagent-Based Data Fusion in Environmental Monitoring Networks. International Journal of Distributed Sensor Networks 2012.

Dons E, Van Poppel M, Kochan B, Wets G, Panis LI. Implementation and validation of a modeling framework to assess personal exposure to black carbon. Environment International 2014a; 62: 64-71.

Dons E, Van Poppel M, Panis LI, De Prins S, Berghmans P, Koppen G, et al. Land use regression models as a tool for short, medium and long term exposure to traffic related air pollution. Science of the Total Environment 2014b; 476: 378-386.

Hoek G, Beelen R, de Hoogh K, Vienneau D, Gulliver J, Fischer P, et al. A review of land-use regression models to assess spatial variation of outdoor air pollution. Atmospheric Environment 2008; 42: 7561-7578.

Van Renterghem T, Thomas P, Dominguez F, Dauwe S, Touhafi A, Dhoedt B, et al. On the ability of consumer electronics microphones for environmental noise monitoring. Journal of Environmental Monitoring 2011; 13: 544-552.

4.8 Summary

In this chapter, models are presented to predict exposure to Black Carbon in three different microenvironments. High background exposure reduced the quantification of the local traffic contribution at low-density roads but the pooled models based on the in-traffic noise evaluations are capable of capturing the local variability beyond the background concentration.

A methodology is presented to extrapolate a bicycle in-traffic noise assessment to yearly meteorological conditions. Four bicycle passages in similar traffic conditions already result in a yearly averaged local Black Carbon exposure estimate for the bicyclists at a specific location on the network. Random noise sampling trips can be used to build a city-wide spatiotemporal model.

In-vehicle measurements were investigated in a similar way but the noise measurements are replaced with a noise map. The in-traffic in-vehicle exposure dynamics can be fitted with a six parameter model including a general available L_{DEN} noise map. The noise map as a proxy for the traffic is performing slightly better than the parallel approach with traffic counts. Traffic counts do not explain the diurnal pattern of the in-vehicle exposure, traffic dynamics and diurnal patterns of particle dispersion and propagation seem to be stronger than the traffic counts.

An indoor model was built with the L_{DEN} noise map as a proxy for the spatial variability of the air pollution exposure. The bicyclist exposure experiment is re-evaluated on the noise map while still including the spatiotemporal aspects of wind speed, street canyon features and background exposure. An additive approach is able to disentangle the local traffic related Black Carbon exposure and the background exposure. The model could not be validated for highways and major roads due to lack of matching households in the external data. Overestimations are found for the dwellings with the highest exposure (medium roads through villages). No actual diurnal traffic patterns were available at the dwellings, resolving this lack of data should be the first actions in future work.

The issue on quality and validity of the background measurement location for the models could not be investigated with the external validation campaign since in 2010 only one measurement location could be qualified as a background estimate. In section 4.7 this is investigated in 2014 at a high exposed dwelling facade, with more options for the background measurement location. The diurnal pattern at Antwerpen-Linkeroever, close to a major city, results in similar model quality compared with a remote background near the coast (Houtem/Veurne). At the dwelling facade, the additive model approach is successful. The noise parameter with the strongest predictive power is also the L_{OLF} parameter, as identified in the first instantaneous model for the exposure of bicyclist in section 4.2. More measurements on a wide range of exposed dwellings are necessary to extend this approach. Measuring simultaneous indoor and outdoor concentration is necessary to resolve the issues on the indoor exposure.

Chapter 5 Daily exposure to Black Carbon

5.1 Introduction

In this chapter the activity specific results in 0 are merged to evaluate the personal daily exposure including all activities (5.2). A general discussion is added, covering the results of both Chapter 4 and 5.

5.2 Validating the daily BC exposure model

5.2.1 Introduction

Activity specific models (ASM) are built for in-vehicle exposure and indoor at home microenvironments (0 and 0). Now the activity specific models can be merged into a daily personal prediction, by applying the ASMs to the matching activity. All activities recorded in the diaries in the external participatory campaign (appendix A) are evaluated through the presented data workflow (see 2.3). The personal exposure participatory campaign acts as a fully independent validation set for the combined models. The resulting indicator is the instantaneous daily exposure to BC, referred to as BC_{day}. No activity specific dose corrections are included.

5.2.2 Activity based daily BC exposure model: BC_{day}

The indicator definition has to result in a daily BC exposure estimate including all activities in any microenvironment. Activity specific models are not available for all microenvironments. An approximation is proposed based on the available activity specific models.

A selection of the activity specific models (ASM) presented in the previous chapter is used to define the ASMs in the daily model. They are listed in Table 5.2-1.

Exposure in busses is assumed to be equal to exposure in cars since not enough data is available to build a specific activity specific function for busses. For the indoor activities at other destinations, the indoor model at home is applied without modifications. All other activities (walk, bike, railway, light-rail and in transit) are evaluated with an outdoor model, equal to the indoor model $BCBA_{const}$ but not including the outdoor to indoor correction. The actual outdoor activities (biking and walking) are evaluated though the noise map based bi-cycle experiment. For rail, overestimations can be expected, since the activity is not outdoor but a closed micro-environment and mostly at reasonable distances from traffic sources. The influence of the ventilation in rail vehicles is unknown. For light-rail (tram and metro), expec-tations are divers, tram might be predicted better by the in-vehicle model. Since the number of light-rail activities is low in the validation dataset, no large effects in the overall evalua-tions are expected and no statistically relevant analysis will be possible.

It is evident that the used methodology can include more details for the diverse activities or micro-environments. In this evaluation, the choice is made to not include external param-eters or corrections on specific activities from other sources or external publications. The purpose of this section is to evaluate the quality of the spatiotemporal models as such.

Micro-environment	**Activity specific model**
Car Bus	Car model BCR_LDENW_AGE_EU5 (section 4.5)
Indoor @ home Indoor @ other destination	Indoor BCBA I/O adjusted model $BCBA_{season}$ (section 4.6)
Walk Bike Railway Light Rail Transit (switching between travel modes)	outdoor model = $BCBA_{const}$ indoor model without I/O correction (section 4.6)

Table 5.2-1: Overview of the activity specific models in the diurnal Black Carbon exposure factory.

The main difference with chapter 4 is the reporting level. Results are now reported on a daily basis instead of on activity level. Every person-day results in one single result. In this project we do not aim to give a result for the average personal exposure of the individual participants since we test the instantaneous prediction of the daily exposure including all specific daily features (actual daily pattern and instantaneous exposure parameters).

5.2.3 Results

5.2.3.1 Diurnal evaluation including all activities

In Figure 5.2.1, the prediction of the daily exposure BC_{day} is presented for all person-days. The first chart shows the measurements versus the predicted values, correlations and slopes, including the slope forced through zero (a*). The green line is the ideal situation. The red line shows the linear fit in the data and the blue line the linear fit forced through zero. The second chart shows the density plot of the relative fit distribution. The red dotted line indicates the ideal situation. The third charts shows the same results with the median, Q1, Q3 and the 95% values, including the outliers. Each dot is a single person-day, including all exposure over all activities.

The comparison is based on the results of the ASMs for all time steps where a prediction could be made. Only if all required data is available along the whole data flow, the episode is included. For indoor activities, this is the five minute interval, for the in-traffic data is it the 10 second interval. In-traffic data results in a valid estimate if the GPS data is available within the start and end time of the in-traffic activity in the diary. A small set of person days (10 out of 303) of extreme values is removed from the dataset (based on a relative fit < 0.2 and relative fit > 5.0). The BC measurements can be highly disturbed, negative values or huge peaks occur and they can perturb the evaluation. The removal is performed after the daily aggregation, not on the basis of the individual activities. Large variability throughout the day can be cancelled out by the aggregation process over all activities in that day.

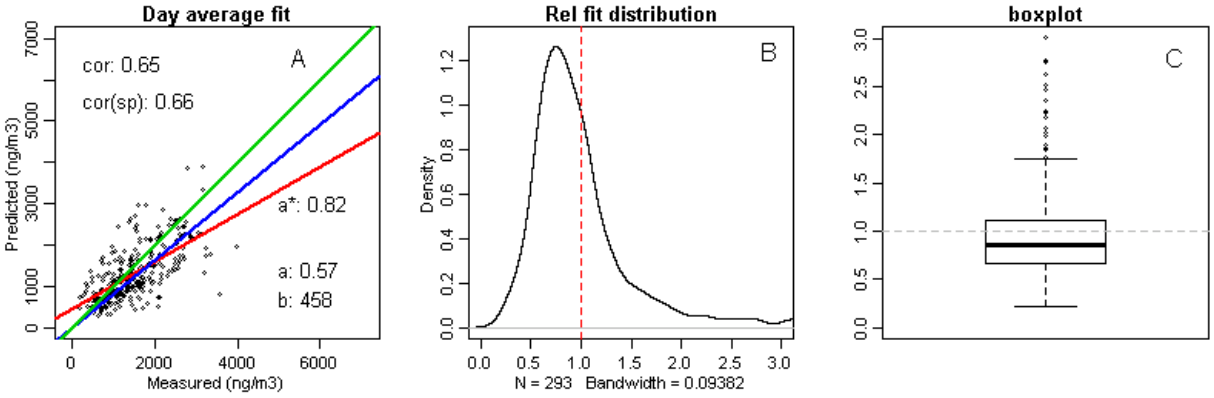

Figure 5.2.1: Evaluations of the diurnal model BC_{day}.

The slope of the linear fit on the average daily exposure prediction is 0.57, with correlations of 0.65 (Pearson) and 0.66 (Spearman). When the linear fit is forced to an intercept at zero, the slope is 0.82. The median and mean relative fit is 0.85 and 0.99 respectively, slightly underestimating the daily exposure.

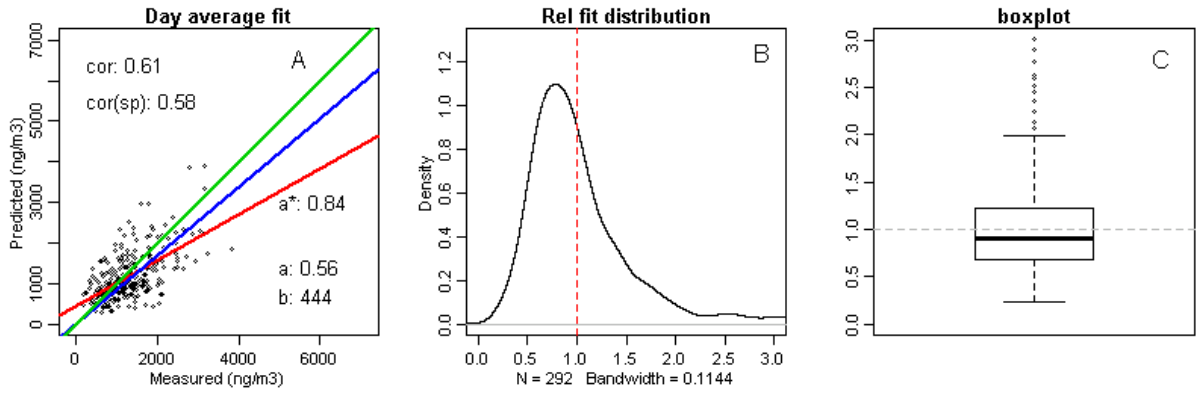

Figure 5.2.2: Evaluations of the diurnal model BC_{day}: indoor activities only.

A similar evaluation can now be performed, but with only including all indoor activities and all in-traffic activities separately (Figure 5.2.2 and Figure 5.2.3). In Table 5.2-2, the summary of the basic statistics for all three evaluations is gathered. For the indoor micro-environments, the slope of the linear fit on the average daily exposure prediction is 0.56, with correlations of 0.61 (Pearson) and 0.58 (Spearman). When the linear fit is forced to an intercept at zero, the slope is 0.84. The median and mean relative fit is 0.90 and 1.04 respectively.

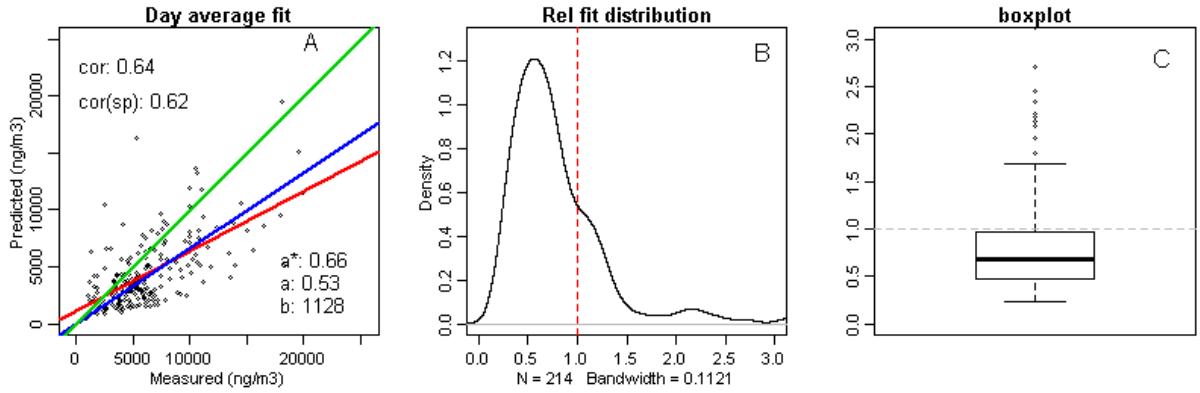

Figure 5.2.3: Evaluations of the diurnal model BC_{day}, only in-traffic activities

Percentiles	P10	Q1	Median	Mean	Q3	P90	IQR
BC24_TEMP	0.56	0.67	0.85	0.99	1.11	1.58	0.44
BC24_TEMP: all indoor	0.54	0.68	0.90	1.04	1.21	1.69	0.53
BC24_TEMP: all in-traffic	0.33	0.48	0.68	0.82	0.96	1.28	0.48

Daily average	Cor (Pearson)	Cor (spearman)	A	B	A*	band-width
BC24_TEMP	0.65	0.66	0.57	458	0.82	0.094
BC24_TEMP: all indoor	0.61	0.58	0.56	444	0.84	0.114
BC24_TEMP: all in-traffic	0.64	0.62	0.53	1128	0.66	0.112

Table 5.2-2: Overview of the prediction statistics of three evaluations: Percentiles, IQR, correlations, linear fits and bandwidth.

For the in-traffic micro-environments, the slope of the linear fit on the average daily exposure prediction is 0.53, with correlations of 0.64 (Pearson) and 0.61 (Spearman). When the linear fit is forced to an intercept at zero, the slope is 0.66. The median and mean relative fit is 0.68 and 0.82 respectively. The distribution has two components, a set with rather strong underestimations and a set near the relative fit of 1.0.

5.2.3.2 Predictive quality by micro-environment

Specific models were developed for in-vehicle and indoor exposure, but the models are applied to other micro-environments based on an expected applicability. The relative fit of the micro-environments is now investigated by micro-environment. For each person-day a value is available for each used micro-environment, a sum over all activities in that day of the person in the specific micro-environment. In Figure 5.2.4, the distributions of the relative fits are presented. The colours indicate the used activity specific model (green = indoor, red = in-vehicle, orange = outdoor).

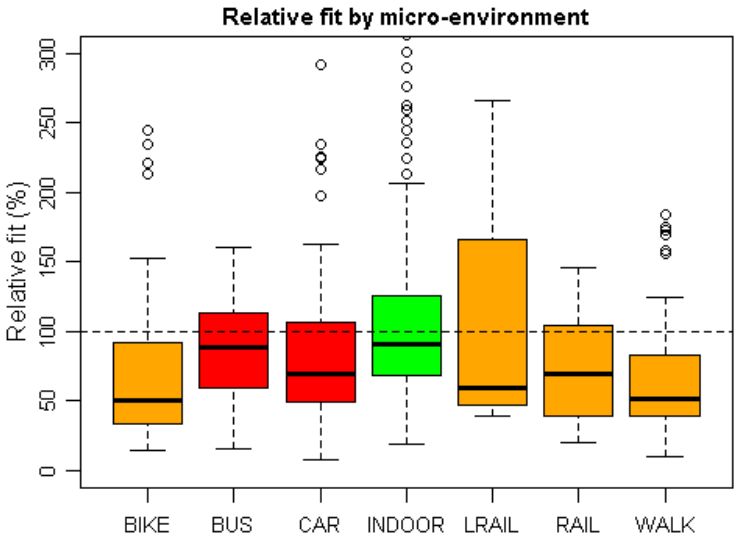

Figure 5.2.4: Boxplot of the relative fits per person-day-microenvironment. The colors indicate the used ASM. Green is indoor, red is in-vehicle, outdoor is orange.

The indoor micro-environment, now also including the indoor activities at other locations, results in a good prediction. The car micro-environment results in a large set of underestimated trips, but the underestimation of the exposure of bike, rail and walk is much larger, only predicting half of the exposure. The exposure in the busses is predicted better compared to the car micro-environment.

5.2.4 Discussion

5.2.4.1 The personal daily exposure to Black Carbon: BC_{day}

The BC_{day} model is based on activity specific models based on BC measurements performed on bicycle and in vehicles. The instantaneous model is applied on an independent participatory campaign including BC exposure measurements. Applying a model to an independent population including the personal behaviour is a basic functionality of the data workflow (2.3). A correlation of 0.65 is achieved between the daily personal exposure measurements in the external validation set and the instantaneous activity specific and route sensitive prediction with the BC_{day} model. The indoor micro-environment specific evaluation is predicting the mean, median, IQR and slope well (see Table 5.2-2). The similar evaluation for the in-traffic prediction is underestimating the exposure but the correlation is very similar and slightly higher compared to the indoor evaluation. The strong underestimations occur for walking and biking.

The external validation campaign is performed with a temporal resolution of five minutes. The prediction models are based on bicyclist and in-vehicle exposure measurements, modelled with a temporal resolution of 10 seconds and spatial resolution sensitive to meters and required aggregation to perform the validation. The activity specific models are based on a limited set of five to seven parameters for each micro-environment. None of the models include local daily traffic data. Despite these strong restrictions in the underlying ASMs, the known variability of real life BC exposure and restrictions in the external validation data (see appendix A), the validation is successful.

It is difficult to compare this result with current literature since few instantaneous daily models are published for Black Carbon at this moment. No examples are known where a fully independent validation is performed as well but in a recent publication, land-use regression models for UFP are cross-validated over different areas of the Boston area (Patton et al., 2015). The LUR models are based on mobile monitoring over periods up to 40 days and are evaluated on daily basis. The authors could not reach good cross-validation with this set of state-of-the-art land-use regression models. The direct transferability only resulted in correlations of 0.17. Local recalibration of the LUR models only resulted in correlations between 0.19 and 0.40. This publication is illustrating the difficulties in the prediction of traffic related air pollution. It puts the achieved correlation of 0.65 for the BC_{day} model into perspective. Considering that this result is reached for an instantaneous daily activity specific BC exposure including in-traffic exposure and is based on a fully independent external validation, this result becomes even stronger.

5.2.4.2 Indoor sources in the indoor micro-environments

The model only predicts the traffic related BC exposure inside the dwellings or in the buildings at the destinations. Indoor sources of BC can introduce errors in the validation. The model itself does not attempt to include indoor sources. Nevertheless, it is interesting to verify is indoor sources could improve the exposure model. This will be tested by comparing the residual errors for the indoor activities at home and at the other destinations.

The only available attribute to distinguish between indoor micro-environments is the purpose of the activity in the diary registrations. The purpose holds indirect information of the destination. Destinations linked to a similar purpose tend to have similar properties, including I/O ratios and the occurrence of non-traffic related Black Carbon sources (cooking, candles, smoking…). The exposure dynamics of the indoor activities can be different for the indoor activities at the destinations. In Figure 5.2.5, the distributions of the relative fits are presented for the indoor at home activities and the indoor activities on other locations according the BC_{day} model including the daily temperature adjusted I/O ratio.

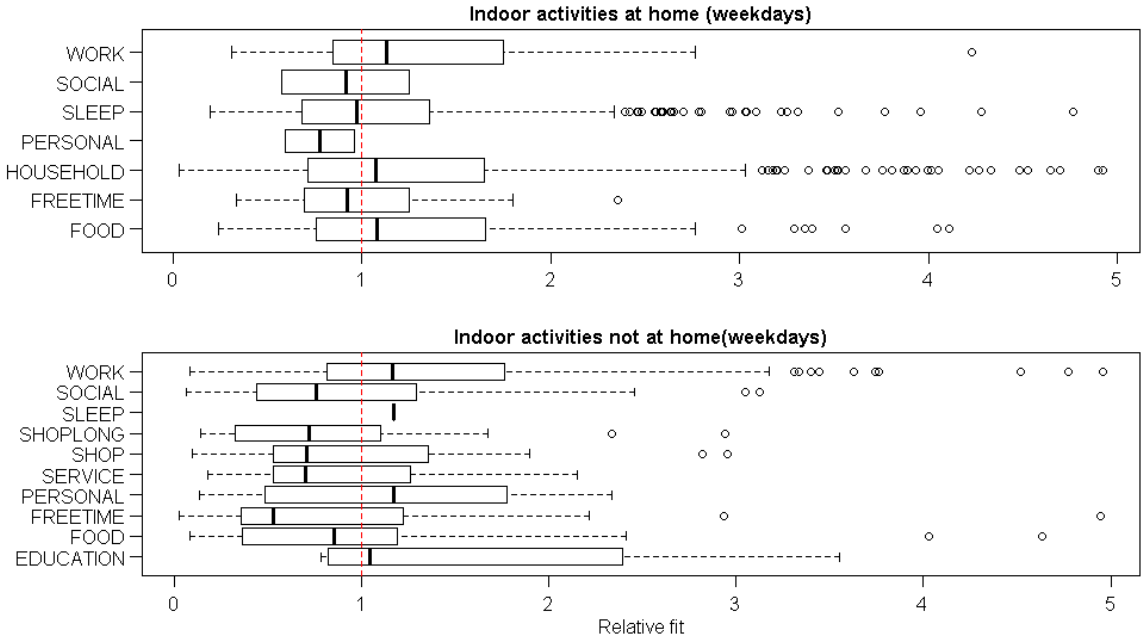

Figure 5.2.5: Relative fit distributions by activity purpose for indoor at home activities (top) and indoor at other locations (bottom), restricted to weekdays.

The at home activities reach for most of the activities median relative fits close to 1. This implies that there is no evidence that additional indoor sources are required during the at-home activities. This can be related to the fact that the households in the validation study where all non-smokers. For the activities at other destinations, the relative fits are in general much lower than 1, compared to the at home indoor activities. Only for the work, school and personal activities, the median is close to 1. Strong undershoots are visible for social activities, service, free time and shopping. The underestimation by the BC_{day} model in those activities can be related to higher risk of exposure to other or unmapped BC sources (smoking,

cooking, local traffic). Another important factor is related to a restriction of the participatory sensing diary, no distinction could be made between actual indoor and outdoor activities. Some activities were probably performed outdoor but the I/O correction was applied to all activities at fixed location. This can also account for a significant portion of the underestimations. In general, the activities linked to social interaction with other people tend to be underestimated (social not at home, shop, service and free time not at home). The mean and median values of all purposes at home and at other destinations are summarized in Table 5.2-3.

Activities at home	**Median**	**Mean**
FOOD	1.08	1.31
FREETIME	0.93	1.04
HOUSEHOLD	1.08	1.32
PERSONAL	0.78	0.78
SLEEP	0.97	1.13
SOCIAL	0.91	0.91
WORK	1.13	1.37
Activities other destinations	**Median**	**Mean**
EDUCATION	1.05	1.61
FOOD	0.85	1.01
FREETIME	0.53	0.90
PERSONAL	1.17	1.7
SERVICE	0.70	0.87
SHOP	0.71	0.96
SHOPLONG	0.72	0.84
SLEEP	1.17	1.17
SOCIAL	0.76	0.93
WORK	1.17	1.40

Table 5.2-3: Purpose related activity specific discrepancies (median value and mean value).

When the research objective requires the inclusion of indoor sources, modifications can be included into the ASMs. There are several options: modifying the I/O ratios by purpose and type of destination, adding non-traffic related BC contribution, improving the local traffic information. External data is requires to add this functionality into the models.

5.2.4.3 Discrepancies for the in-traffic micro-environments

The outdoor model, based on the bicycle measurements and extrapolated using a region wide noise map, is strongly underestimating the in-traffic activities (bike, walk) and in a lesser extent, the rail micro-environment. For biking and walking, this phenomenon was ex-

pected, but it is even stronger than anticipated. The origin of this discrepancy is simple. No traffic data is available for the local roads were most of the walking and biking activities occur. In the publication of Patton (Patton et al., 2015), this is also the key argument to explain the poor results of the cross-validation. The models require parameterization of diurnal, weekly traffic trends on the local streets, while typically only traffic data is available for the higher density roads. In this PhD, it is also shown that the local exposure is also highly sensitive to local traffic dynamics, adding another dimension of missing data to the requirements. The reduction of the sensitivity of the $BC_{outdoor}$ model towards local traffic was anticipated, this decision is purely data driven due to lack of alternatives. The potential solution for this lack of data is already presented in 0: the city-wide mobile noise mapping will be able to quantify the local traffic including the traffic dynamics over larger areas. The next challenge is to provide this improved quality of data region-wide. Once a larger mobile noise mapping data is available, a land-use regression technique can be used to extrapolate the results region-wide.

As a last point, the choice of applying the model for cars for the exposure in the bus has to be evaluated. Several authors have found that the exposure in a bus is higher compared to in-vehicle (see 1.1.5.2). This information was not included in the assumption of the BC_{day} model since not enough data is available to build an instantaneous model for the bus micro-environment. The distribution of the relative fit for the bus micro-environment is however closer to 1 compared to the car micro-environment. The model performs better for the bus trips compared to the car trips. This indicates that there is no evidence in this dataset that an upward correction for busses is required; a significant portion of differences in the exposure in busses is already captured by the underlying covariates in the model. This can be related to the fact that busses follow routes where an average, the traffic information is more accurate. Busses tend to follow the connecting roads from village to villages and the high density roads in the cities. In the underlying dataset, traffic on these roads is available and is included in the noise maps. Cars are used more on low density roads with lower quality of traffic data and/or missing traffic data. Again, the city-wide noise mapping methodology has the potential to add this missing spatial information into the in-vehicle models. The efforts required improving the exposure models for walking and biking will add value for the in-vehicle micro-environment as well.

5.2.4.4 Comparison with other methodologies

Most of the external available land-use regression models are combining traffic data, population data, building layers and distance buffers for large traffic sources (Hoek et al., 2008, Beelen et al., 2013). Most of the current LUR models address PM_{10}, $PM_{2.5}$ and NO_x, BC and UFP are scarcer (Dons, 2013, PhD). Few layers in the LURs express spatial details sensitive to meters, the relevant spatial resolution of the traffic related particulate matter concentrations. None of the methods are able to include traffic on all roads, due to lack of data. On

top of that, many of the layers express similar features. More length of roads in the vicinity, a classical LUR covariate is indeed more traffic, the layers including the amount of dwellings and population relate to also to traffic and human activities (dwelling heating etc…). Multiple layers express complex and interacting correlations with the investigated exposure. Overfitting the scarce measurement data is therefore a huge risk. In the noise map based approach, a single data layer is used incorporating all relevant traffic information. The risk of overfitting is highly reduced. The layer includes a weighted distance to source with a resolution that is not reached by the discrete distance buffers in the external LURs. The noise map is proven to be a valid and strong alternative. The most crucial limitation in the classical land-use regression models is however even more fundamental. The exposures cannot be disentangled into a background meteorological induced contribution and a local traffic contribution. The underlying gam models, capable of distinguishing between the local and the background induced variability are the reason why the noise map based extrapolation is successful.

There are publications that come close to some of the features of this approach, but mostly one or two specific properties are evaluated in the similar detail. The EPA's Stochastic Human Exposure and Dose Simulation (SHEDS-PM_{10}) approach, for example is highly detailed in the activity definitions, but used PM_{10} which does not express the spatial and temporal variability of the traffic related pollutants BC and UFP (Burke et al., 2001). The PM_{10} evaluation is also not sensitive to temporal changes. In Montréal, a detailed model is made, including route sensitive evaluation but the underlying NO_2 air pollution map does not have the same spatial resolution of BC and UFP (Hatzopoulou et al., 2013). In this particular solution, a more detailed traffic related PM layer and a more activity specific evaluation can be added. A near highway hourly model for UFP was built recently by Patton (Patton et al., 2014). A larger scale model was built by Rivera in the province of Girona based on 644 short term measurements in front of the dwellings (Rivera et al., 2012). A full overview of available LURs is assembled by Dons (Dons, 2013, PhD).

Another important effort to build a spatiotemporal land-use regressions model for BC (AB^2C model) is based on the data used for the external validation in this PhD (Dons et al., 2014). It is one of the few models that provide an hourly estimate for the indoor exposure and a road type specific exposure while being in traffic. A daily adjustment towards an annual average exposure is added to account for the seasonal changes. The model is however based on the assumption that it is unbiased for personal behaviour and the bias toward the meteorological sampling is resolved. The dataset is large, and probably the strongest dataset collected so far. It is however virtually impossible to perform unbiased participatory measurement campaigns. This is addressed in detail in 5.3.2.3. The main difference between the AB^2C model and this approach is the instantaneous modelling including the disentanglement of background and local traffic contributions.

5.2.5 Conclusions

The validated instantaneous models of the activity specific models for in-vehicle and indoor Black Carbon exposure are combined in an instantaneous daily exposure model, covering all micro-environments. The $BCBA_{season}$ indoor model with the daily temperature adjusted I/O ratio combined with the euro 5 adjusted in-vehicle model results in a prediction model reaching a correlation 0.65. The main goal of this PhD is hereby achieved. A fully independently defined set of activity specific models successfully predict the measured personal BC exposure in an external participatory sensing campaign. The spatial resolution and distance to source effect of the underlying noise maps matches the spatial resolution of the Black Carbon exposure for both indoor and in-vehicle exposure. For the active transport modes, bike and walk, the noise map based models are not accurate enough due to lack of traffic data on the local roads. This aligns with the results from the noise measurement based bicycle models. More detailed traffic assessment, including traffic dynamics was proven to be is necessary for the bicyclists. It is expected that this local data will also improve the exposure of the pedestrians. City wide traffic noise mapping will improve the noise map based BC_{day} model for the active modes and have potential for the in-vehicle exposure models as well.

Using noise as a proxy for traffic related air pollution exposure is successful. The background adjusted approaches, able to distinguish between meteorological influences and local traffic influences is crucial in this solution. The bias in the air pollution measurements due to the meteorology is largely removed. Once this is achieved the spatial details in the traffic become statistically significant.

5.3 General discussion and overall analysis

This section summarizes the lessons learned and pending issues in traffic related health and exposure science. The issues link back to the different results in this PhD without the aim to be exhaustive. Of course, the link to noise assessment is included, which does not imply that noise assessments are the solution to every problem in traffic related air pollution. The noise discipline is however, a very important component in the multidisciplinary aspects of traffic related health effect research.

5.3.1 The concept of micro land use regression (µLUR)

5.3.1.1 Background air pollution exposure: the strongest component but not the most interesting part

A constant in the presented measurements and models, is the importance of the background exposure in the total exposure. When attempting to identify differences in the personal exposure, this strong correlation with the background exposure hampers the quantification of the variability related to the individual time-activity pattern. From a health perspective, the interpersonal differences are the most important part of the exposure. Most of this PhD can be catalogued as a struggle to quantify this second order component in the total exposure related to the personal behavioural pattern in combination with local variation in traffic.

5.3.1.2 Improving traffic assessments through noise measurements

Air pollution exposure is highly variable and strongly influenced by meteorological effects. The major component of the spatial and temporal variability is however still the exposure to the local traffic sources. If traffic data is available, it is only available for the high exposure locations (highways, major roads). It is mostly only available in a highly generalized time resolution and it rarely includes traffic dynamics. When the data exists, access and lag between data and results can be significant, delaying the post-processing and evaluation. The most important problem is that the available data only covers a small portion of the road network and that most of the people live and travel along the smaller not attributed road segments. This lack of data is even more important for the active travel modes, biking and walking. Exposure scientists lack spatial and temporal resolution at the low exposure side of the distribution. Lack of resolution at the low exposure part of the distribution hampers the quantification of the health effects.

This traffic data issue does not only relate to air pollution, the same lack of data also hampers noise exposure, noise related health assessments and other mobility related as-

pects. Also in the noise discipline, for both annoyance and sleep disturbance, more measurements are needed to capture the spatial and temporal variability of the exposure. A strong synergy is possible here.

5.3.1.3 Disentangling meteorology and local traffic effects in air pollution exposure measurements

Noise measurements are capable of quantifying the local traffic and local traffic dynamics instantaneously, in a high spatial resolution by using mobile measurements and in a high temporal resolution in fixed measurements. Instantaneous traffic assessments through noise assessments enable the disentanglement of the variability in the air pollution measurements into local traffic and large scale meteorological influences. This aspect is a fundamental component of the success of the BC models presented in this PhD.

5.3.1.4 Participatory and mobile campaigns are by default biased

Personal measurement equipment is expensive and the burden for the subjects of performing the measurements for the subjects is hampering research. No present day measurement campaign can assess enough locations for a long enough periods and cover all potential variability on local traffic, distance to major roads, short-term and long-term meteorological conditions, background exposures, season, time of day, diurnal patterns and other. No campaign can truly result in an unbiased dataset. When comparing participatory sensing campaigns in different era's or between different countries the differences between the exposure levels can be linked to different environmental external parameters. Wind speed, vehicle fleet, road design, background levels and many other parameters might differ between these campaigns. Since many parameters influence the actual exposure, it can be stated that every air pollution measurement campaign is by default biased.

5.3.1.5 Resolving 'selection bias by design' in the measurements

The fundamental issue of selection bias cannot be resolved by restricting the measurements to avoid unwanted influences if those influences are not well understood or quantifiable. The solution is to embrace that variability and measure it at full.

In the bicycle measurements this was accomplished by measuring in all meteorological conditions over the range of one year, combined with random route selection and frequent changes in the routes from high to low exposure segments in the same run. All variability of traffic exposure and meteorological conditions are mixed, a model that can resolve this will be robust and can be extrapolated without (or at least with fewer) restrictions. Instantaneous traffic attribution removes the classic restriction in mobile air pollution campaigns to measure fixed trajectories.

A similar approach is taken for the in-vehicle measurements: by design ‘not design the route choices of the participants’. The participants do what they are used to do in real life in all traffic conditions, routes and meteorological situations. A ‘real life’ exposure dataset is the aim. The most difficult part is to cover the full diversity of the vehicle fleet. The uncharted potential influences of quality of the car and the personal use of the ventilation system is also an important concern. With only nine participants, the full diversity of the fleet was not reached in Section 4.5, the ventilation use was also not recorded. In an epidemiological context, the personal use of the ventilation system will probably never be included in the personal information. A model sensitive to the ventilation settings is interesting from a general scientific point of view, but will be less relevant if it cannot be applied on epidemiological databases. A model should be applicable to the investigated population. A model sensitive to the used vehicle (age, make, make, fuel, catalogue prize) is useful since this can correlate with the socio-economic aspects of the participants.

To conclude, the main objective of the experimental approach should be to gather the data in all its variability as close to real life settings and matching the potential relevant information available in the epidemiological datasets.

5.3.1.6 Increasing spatiotemporal resolution and instantaneous modelling

The previous statement implies at first sight the requirement to perform massive measurements campaigns. In a sense this is true, but it can be nuanced. Since the variability in the emission and exposure is high, the different influencing factors become visible by increasing the spatial and temporal resolution of the measurement campaigns. By increasing the spatiotemporal detail, two important features emerge. First the actual short term variability can be investigated. Secondly, the short term variability will reveal knowledge, previously hidden in the data due to the lower temporal resolution. The sampling requirements can change due to the newly detected information, so the required increase of number of measurements can be modest.

The key issue is attributing the measurements in a similar spatial and temporal resolution. The problem is reduced to finding and quantifying the external attributes explaining the variability in the measurements. In this specific case, the noise measurements act as a physical measurable proxy for the local traffic and local traffic with a temporal resolution of seconds.

In general, the solution to resolve the huge complexity of the many influencing factors on the personal exposure is building instantaneous models. Instantaneous models capture and explain the actual exposure dynamics. Increasing spatiotemporal resolution automatically results in instantaneous models.

Most air pollution exposure models in literature attempt to predict yearly averages since the potential health effects become only quantifiable on the long term. Instantaneous models can provide unbiased yearly averages by extrapolating the instantaneous exposure to yearly averaged prediction. This approach is illustrated in 0. Comparing health evaluations

based on yearly exposure models and yearly extrapolated instantaneous models might reveal the relevance of this approach in the future.

5.3.1.7 Generalized additive models

The tool, used to analyse the large and diverse sets of data is the 'generalized additive model' (Hastie and Tibshirani, 1986). The non-linear fitting properties of the technique can detect and disentangle effects in the multivariate data. The measured variability in the 'not predesigned' experiments becomes an asset rather than a drawback. The technique can handle sparse data and still disentangle the relevant effects over multiple covariates simultaneously. An implementation is available in R (Wood, 2006). It also becomes a more and more popular technique in environmental exposure and health analysis (Dominici et al., 2002). It is a data driven approach, removing the need of providing a full analytical solution of the underlying and interacting environmental, chemical and physical processes.

5.3.1.8 Microscopic and micro-environment specific spatiotemporal land-use regression models (µLUR)

Looking back on the models and the results, it is clear that the approaches used in this PhD add spatial and temporal resolution to the current LUR practice in air pollution research. It not only adds improved resolution, it is also crucial to capture the extreme variability of the particle matter exposure. Aggregation and data cleaning of the short-term measurements risk removing relevant information from the detailed measurement sequences. The only way to understand the variability is to attempt to attribute the sequences with relevant external information. In the specific case of traffic related air pollution, the relevant information is definitely the traffic and the traffic dynamics itself. In this work this information is added through noise assessments. Other methods might replace the noise approach, but the need for increased spatiotemporal resolution is fundamental. Therefor an extended form of land-use regression is introduced:

The microscopic and micro-environment specific non-linear spatiotemporal land-use regression model (µLUR)

A µLUR should at least have the following features:

1. Low aggregation level of the measurements.
2. Detailed spatial and temporal attribution of all driving forces.
3. Measurements campaign designed to capture as much of the variability over all driving forces.
4. Activity and/or micro-environment specific models
5. Non-linear modelling techniques capable of adjusting for non-linear aspects and/or saturation of the pollution indicator towards the driving forces.

Full coverage of all requirements was necessary to achieve the presented results. Designing measurement campaigns to cover all variability and attributing the results with the instantaneous traffic is absolutely crucial.

The µLUR is an exemplary case of the Activity Specific Function in the MEX data flow framework (2.3). The µLUR in the MEX workflow covers all the complexity of the exposure, dose and indicator calculations, adding a non-linear coverage of the full path of external exposure, dose corrections, internal dose corrections and effects evaluations. The only fundamental restriction is the capability of feeding the µLUR with the relevant personal data matching the requirements of the model.

5.3.2 Noise measurements and noise map specific features

5.3.2.1 Spectral noise evaluation

From an acoustic point of view, the most important aspect in this work is the inclusion of the spectral content to detect the traffic dynamics of the local traffic. For bicyclists, the instantaneous noise exposure provided two strong noise related covariates; the first and strongest covariate is related to the low frequency engine noise in the vehicle noise emission spectrum. This relation was also tested in Bangalore, India. The approach was valid under extremely different traffic and exposure conditions for air and noise pollution, despite important disturbances due to the habit of honking in the traffic jams. The instantaneous relation is valid for particle number (PN) as well for Black Carbon. The difference between low and high frequencies can be regarded as a proxy for driving speed (see Figure 5.3.1).

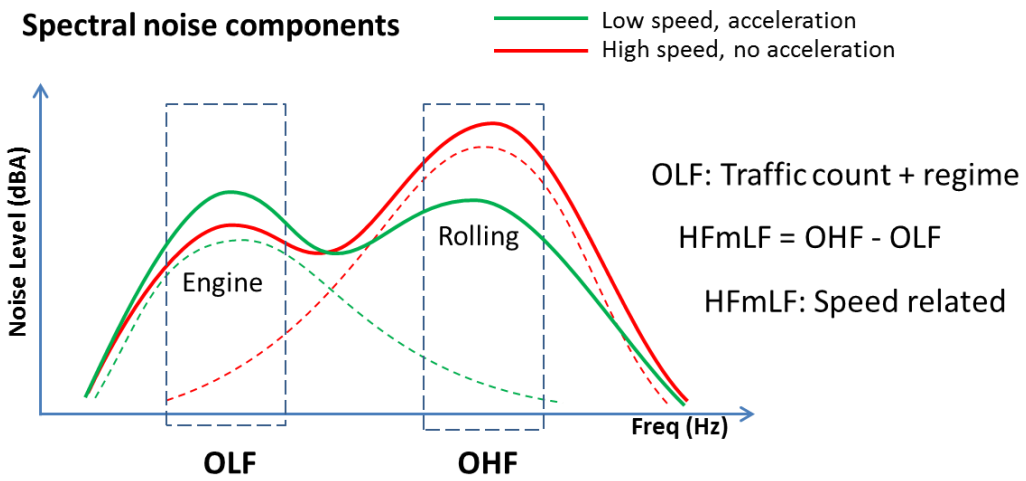

Figure 5.3.1: Visualization of the importance of the spectral evaluation on the instantaneous noise exposure in detecting the vehicle dynamics. The dotted lines show the typical spectrum of engine noise (green) and rolling noise (red) for the high speed traffic situation.

An important comment has to be made here. It is not because noise events (and the spectral content in those events in the case of mobile noise measurements) are relevant, that there is a direct relationship between air pollution and the total acoustical energy. Rather the opposite is true. The dwelling facade model is more successful with the arithmetic mean of the L_{OLF} noise parameter over the evaluation period of 15 minutes. The energy-conserving variant $L_{OLF,eq,15min}$ was even weaker than any other standard noise evaluations (L_{Aeq} and the statistical parameters). This also explains why previous attempts by other authors are less successful compared to the results in this PhD (Beelen et al., 2009, Ross et al., 2011, Gan et al., 2012). Further research into the best noise based indicator to build the noise-BC relationship near the dwellings is relevant.

5.3.2.2 Spatiotemporal models and noise: dimension reduction.

An important feature of the presented noise based spatiotemporal models is the dimension reduction in the spatial resolution of the input data sources without losing the relevant spatial resolution. Let's explain this in detail.

If a bicyclist's exposure has to be estimated with a combination of a temporal and a spatial dataset, the spatial dataset has to be sensitive to the relative position of the bicycle to the local traffic sources (with a spatial resolution of meters). The bicyclist is however bound to the relative position of the bicycle infrastructure to the street infrastructure. The relevant position of the bicyclist contains two components: the position along the road, sensitive to distance to a crossing and the distance perpendicular to the local traffic lanes. The spatial resolution along the road segments is the temporal resolution of the evaluation multiplied with the instantaneous speed, typically 18 km/h. An evaluation distance of approximately 50 m along the road segments is the automatic result. In the case of the noise based models, the noise assessments include all those aspects at once. It quantifies and characterises the amount of traffic and includes a distance to source. The models are sensitive to a resolution of meters without requiring explicit spatial models or external data with a spatial resolution of meters.

A similar effect is reached for in-vehicle exposure. The vehicle is bound to the driving lanes on the road, the speed of the vehicles is higher and the in-vehicle exposure requires smoothing due to the ventilation system. The resulting spatial resolution is between 50 and 300 m along the road network (matching instantaneous speeds of 20 and 120 km/hour). The underlying noise map has a spatial grid resolution of 20 m; more than enough to account for the resolution of changing traffic along the road segments. The position error perpendicular to the road segment is resolved by applying a map matching technique (vehicle automatically positioned on the road segment of the input data). Again, a strong reduction in the required resolution of the spatial data sources is achieved. This dimension reduction is a key feature of the success of the presented spatiotemporal models.

5.3.2.3 The noise map as a LUR input layer

Land-use regression models are common in air pollution science due to the complexity and lack of data to calculate detailed local dispersion models for larger areas. The noise maps are used here as the spatial data layer to provide the traffic data to the land-use regression approach. The noise maps act also as a distance to source weighted layer for exposure to traffic. It incorporates a detailed distance evaluation, a strong dispersion effect (order of magnitude 2) and an accumulation effect when roads join. The specific characteristics and potential issues of the used noise map in this solution are addressed in 5.3.2.4.

Land-use regression techniques only transpose the spatial features of the underlying data sources to predict the investigated indicator. It is not only the direct relationship between air and noise pollution exposure related to the simultaneous emission that is responsible for the successful prediction. It is the similar propagation characteristics of noise and BC combined with the spatial resolution of the noise map that is responsible for the successful prediction, not the simultaneous emission as such. This is the reason why using a noise map as an alternative traffic layer is a valid approach. The spatial detailed calculation methods in the acoustic field are a fundamental part of the discipline. The air pollution field can only benefit of this spatially detailed data layer covering a lot of the effort and data processing available at the adjacent discipline.

5.3.2.4 Noise map features and their potential influence on the models

The used noise map (INTEC-VMM noise map) for the Flemish region has an important drawback. It does not include the screening of buildings. The noise map is in first order a distance weighted traffic map but also includes noise specific features (road surface corrections, noise screens near the highways, aging and replacement of road surfaces, vehicle fleet evolutions and other). It is calculated for the regional environmental reporting, independently from the EU noise directive requirements. The main reason the EU noise directive maps are not used is that they focus on the high traffic roads. They include only roads with traffic above a predefined threshold and report only for the highest noise levels (EU noise directive, 2002). The second part of the EU noise directive requires full noise maps for the agglomerations which are available throughout Europe for all cities. The external validation data is however distributed over the whole Flemish area, not restricted to one of the agglomeration in Flanders. Using the EU noise maps was therefore not an option in this work.

It is unclear how this lack of screening influences the quality of the model. This could imply that using EU noise directive maps might be less effective. The other option, improvement of the models due to screening is also not impossible. It is known that Black Carbon and UFP emission can be screened by buildings and noise screens. Including screening in the noise map can relate to that and improve the correlation between noise and BC. Reverberation effects due to multiple reflections increase noise levels in narrow streets and can indi-

rectly incorporate the street canyon accumulation effects of air pollutants. Many features in the noise maps might reduce or improve the correlation between noise and traffic related particulate matter. This cannot be quantified or evaluated at this moment. The presented technique; where the gam model is based on the noise map and the same noise map is used to extrapolate the results, incorporates and/or cancels out the specific features of the used noise map by design, for the better and the worse. The features of the noise map are an interesting topic for further research.

5.3.2.5 Effects of changing fleet composition on the models

The noise based models are providing a general assessment of the noise-BC relations for the actual fleet at the time of the measurement campaign. In the city-wide noise mapping (Section 4.3), it is already advised to perform a local calibration on the underlying instantaneous model. This statement has to be extended to all micro-environments.

A frequently returning question is the potential effects of electric and/or hybrid vehicles in the fleet on the fleet. Since electric and hybrid vehicle will emit less PM, but also emit less or no engine noise, the physical link remains intact. The models are assessing a fleet as a whole. This will only affect the absolute magnitudes of the exposure. An interesting application would be to perform these measurements in different countries at the same time, which would allow the researchers to compare fleet level specific differences (fuel types, renewal rate etc.). This exercise can also be made at a local scale when significant spatial changes in the fleet can be expected, for example when low emission zones are implemented (Invernizzi et al., 2011, Cesaroni et al., 2012).

In the in-vehicle model is shown that the effect of the European Euro 5 emission legislation has a strong effect. This leads to the conclusion that the combined monitoring has to be repeated on regular basis and the model parameters should be updated frequently. These methods will assess the combined changes of the fleets and the emissions correctly, including the changes in traffic densities and dynamics due to local policy decisions.

5.3.3 Particulate matter exposure in detail

5.3.3.1 Strong traffic related gradients for other air pollutants

One of the first conclusions that could be drawn from the combined mobile noise and BC measurements was the stronger than anticipated decrease with distance to source effects. The concentration gradients in relation to the road side are summarized for different air pollutants by Karner and colleagues (Karner et al., 2010). The distance to source relation is stronger for BC and UFP compared to PM_{25} and PM_{10}. Polycyclic gaseous components show similar gradients as BC and UFP. These components cannot be assessed in the same spatial and temporal resolution yet due to technical limitations in the measurement technology. It

is very well possible that those polycyclic air pollution components are an important factor in the health effects. For traffic related health effects, exposure to BC and UFP might correlate with exposure to these carcinogenic gaseous components. BC and UFP can be a proxy for other carcinogenic gaseous components. As in all epidemiological evaluations, we should be aware that we only detect associations and not causal relations. The small particles can also be the physical path of the internal exposure, enabling the transport of the hazardous components into the body.

5.3.3.2 Background measurement location features are relevant

The results in this PhD rely strongly on the available background measurements from the Flemish Government. At the time of the external participatory campaign (Appendix A) few continues measurement stations were equipped with Black Carbon equipment. A recent overview of the EU evaluates the monitoring of Black Carbon in European countries. The Flemish region was one of the first areas implementing this technology (from 2009 onwards). The results in this PhD rely therefore strongly on the state-of-the-art quality of the measurement network in the region of Flanders. To put this into perspective, The Netherlands started their first continuous BC background measurements in 2013.

At that time, only one location was useful as a 'background measurement' (Antwerpen-Linkeroever). That location is actually quite close to the largest agglomeration in Flanders and can (from a geographically viewpoint) hardly be viewed as 'background' since it is close to one of the largest port cities in Europe. Yet due to the strong distance to source effects of Black Carbon and the proximity of the river Schelde, it did serve as a proper background measurement in the models. The upwind location to the harbour and the city are probably also reasons for the validity of this location as a background location. Only the extreme high exposure episodes are probably not representative for Flanders. Low wind speeds and cold weather typically occur with East and North East wind conditions, the downwind situation of this location for the city and the harbour. The gam models successfully captured that non-linearity of the background exposure at the measurement location.

Nevertheless, the models are sensitive to the location of the background measurement station. This was already visible and discussed in the measurement campaign in Bangalore, India (section 4.4) and for the indoor model (4.6) and the daily model (5.2.4.2). The instantaneous model at a dwelling facade in section 4.7 investigates the choice of the background location and its effect on the models (4.7.4.2). The number of measurement stations including Black Carbon that can qualify as background locations has grown fast in the past years. In the future, modelling will have to address the properties of the most representative background measurement location for each model.

5.3.3.3 Micro-aethalometer measurement corrections

The micro-aethalometer technology has been subject of extensive investigations on potential measurement errors. The most commonly used measurement correction is described by Hagler (Hagler et al, 2010) and is used in other sections (4.2, 4.4 and 4.5). In section 4.4 the noise based models were applied for Black Carbon evaluations with different correction functions. None of the correction functions improved the noise-BC models compared to a basic running average of 20 seconds on the raw BC data from the µ-aethalometer. The data set measured in Bangalore was limited to about 20 hours, so strong conclusions cannot be drawn here. The results suggest that all other available adjustment functions remove short-term variability from the measurement sequence that also contains actual physical variation in the measurements. The validity of the correction functions should be re-evaluated in the context of the µLURs.

5.4 References

Basagaña, X., Rivera, M., Aguilera, I., Agis, D., Bouso, L., Elosua, R., ... & Künzli, N. (2012). Effect of the number of measurement sites on land use regression models in estimating local air pollution. Atmospheric Environment, 54, 634-642.

Beelen, R., Hoek, G., Vienneau, D., Eeftens, M., Dimakopoulou, K., Pedeli, X., ... & de Hoogh, K. (2013). Development of NO 2 and NO x land use regression models for estimating air pollution exposure in 36 study areas in Europe–the ESCAPE project. Atmospheric Environment, 72, 10-23.

Burke, J. M., Zufall, M. J., & Ozkaynak, H. (2001). A population exposure model for particulate matter: case study results for PM2. 5 in Philadelphia, PA. Journal of Exposure Analysis and Environmental Epidemiology, 11(6), 470-489.

Cesaroni, Giulia, et al. "Health benefits of traffic-related air pollution reduction in different socioeconomic groups: the effect of low-emission zoning in Rome." Occupational and environmental medicine 69.2 (2012): 133-139.

Dominici, F., McDermott, A., Zeger, S. L., & Samet, J. M. (2002). On the use of generalized additive models in time-series studies of air pollution and health. American journal of epidemiology, 156(3), 193-203.

Dons, E., 2013. Air pollution exposure assessment through personal monitoring and activity-based modeling. PhD Thesis. Hasselt University, Diepenbeek, p. 302.

Dons, E., Van Poppel, M., Kochan, B., Wets, G., & Panis, L. I. (2014). Implementation and validation of a modeling framework to assess personal exposure to black carbon. Environment international, 62, 64-71.

EU Directive (2002). Directive 2002/49/EC of the European parliament and the Council of 25 June 2002 relating to the assessment and management of environmental noise. Official Journal of the European Communities, 189(12).

Hastie, T., & Tibshirani, R. (1986). Generalized additive models. Statistical science, 297-310.

Hatzopoulou, M., Weichenthal, S., Barreau, G., Goldberg, M., Farrell, W., Crouse, D., & Ross, N. (2013). A web-based route planning tool to reduce cyclists' exposures to traffic pollution: A case study in Montreal, Canada. Environmental research, 123, 58-61.

Hoek G, Beelen R, de Hoogh K, Vienneau D, Gulliver J, Fischer P, et al. A review of land-use regression models to assess spatial variation of outdoor air pollution. Atmospheric Environment 2008; 42: 7561-7578.

Gan WQ, Davies HW, Koehoorn M, Brauer M. Association of Long-term Exposure to Community Noise and Traffic-related Air Pollution With Coronary Heart Disease Mortality. American Journal of Epidemiology 2012; 175: 898-906.

Invernizzi, Giovanni, et al. "Measurement of black carbon concentration as an indicator of air quality benefits of traffic restriction policies within the ecopass zone in Milan, Italy." Atmospheric Environment 45.21 (2011): 3522-3527.

Karner AA, Eisinger DS, Niemeier DA. Near-Roadway Air Quality: Synthesizing the Findings from Real-World Data. Environmental Science & Technology 2010; 44: 5334-5344.

Lane, K. J., Levy, J. I., Scammell, M. K., Patton, A. P., Durant, J. L., Mwamburi, M., ... & Brugge, D. (2015). Effect of time-activity adjustment on exposure assessment for traffic-related ultrafine particles. Journal of Exposure Science and Environmental Epidemiology.

Patton, A. P., Collins, C., Naumova, E. N., Zamore, W., Brugge, D., & Durant, J. L. (2014). An hourly regression model for ultrafine particles in a near-highway urban area. Environmental science & technology, 48(6), 3272-3280.

Patton, A. P., Zamore, W., Naumova, E. N., Levy, J. I., Brugge, D., & Durant, J. L. (2015). Transferability and Generalizability of Regression Models of Ultrafine Particles in Urban Neighborhoods in the Boston Area. Environmental science & technology.

Rivera, M., Basagaña, X., Aguilera, I., Agis, D., Bouso, L., Foraster, M., ... & Hoek, G. (2012). Spatial distribution of ultrafine particles in urban settings: A land use regression model. Atmospheric Environment, 54, 657-666.

Ross, Z., Kheirbek, I., Clougherty, J. E., Ito, K., Matte, T., Markowitz, S., & Eisl, H. (2011). Noise, air pollutants and traffic: continuous measurement and correlation at a high-traffic location in New York City. Environmental research, 111(8), 1054-1063.

Wood, S. (2006). Generalized additive models: an introduction with R. CRC press.

Chapter 6 Outlook and Conclusions

6.1 Future developments and applications

6.1.1 Extending the indoor exposure model

The fact that the indoor exposure can be predicted by mapping the bicycle measurements to a noise map is very surprizing. This does not imply that this method is put forward as a solution to predict indoor exposure in the future. It is a numerical experiment that in this stage acts as an interesting option in future work. Two reasons can be put forward why this technique tends to work. The disentanglement of the short term variability of the BC exposure into a local component and a large scale background component in the underlying data for the gam model is the first reason. The gam model only covers the local component and is fed by local traffic data through the noise map. The second reason why it works is related to the unintended bias of the sampling of the dwellings in the external participatory campaign. Few dwellings were within close proximity of major roads and highways. It is not expected that the underlying bicycle ASM model will be successful for the high exposed dwellings. The real goal should be an underlying gam model specifically designed for indoor exposure based on a combination of local traffic and large scale background contributions.

In Section 4.6, only two components were included and the local component is not sensitive to midrange effects in time in the vicinity of the cities (only a simple fixed spatial correction based on the PM_{10} map is available). There is room for improvement. In Section 4.7, the real complexity of background and local contribution is already visible. In the future more complex models will be necessary. The current background component can be split in a large scale meteorological component and a midrange local component covering the influence of traffic within a few kilometres (a typical parameter in the current land-use regression models (Dons, 2013, PhD thesis)). The noise-BC relation might change dramatically near highways and other continuous traffic sources. Splitting the local contributions into a local street traffic component and a local component from large nearby highways or major roads is an option.

To achieve this, it is necessary to perform long-term combined noise-BC/UFP measurements at a wide range of dwellings, both at the facade and indoor. The noise measurements at the facade can be used to add the required local traffic data and traffic dynamics into the models. In a spatiotemporal model covering multiple dwellings, the meteorological and local traffic contribution disentangle the indoor exposure. The noise indicator to include the local traffic component in the models should be the overall best choice valid over a wide range of dwellings. This noise indicator will not be the standard L_{Aeq}, as was shown extensively in this PhD. The I/O ratios can be established for seasonal ventilation aspects, but diurnal variations in the I/O ratio are also possible and might be related to the amount of traffic near the dwelling. Assessing the actual traffic at the dwelling is crucial. Mobile city-wide noise mapping can provide a data layer to extrapolate the new established indoor model to the entire city.

6.1.2 Which traffic air pollutants require quantification?

The most fundamental issue is determining which physical and/or chemical component is the most relevant component to evaluate the health effects. Black Carbon is already source specific for traffic but it is not sensitive enough to the particle size. Particle size and number are most likely the stronger indicators for the cardiovascular health effects. The mass-based measurement technique of the µAethalometer results in a faint signal for the large amounts of small particles close to the traffic sources. Black Carbon is used because the µAethalometer is most portable measurement equipment, capable of gathering the required amount of data. For UFP measurements and particle size distributions, the available data is a lot sparser. The air pollution and the environmental epidemiological community acknowledge the importance of particle size evaluations to resolve the health effects. The presented results for Black Carbon have to be extended to particle counts, particle distributions, particle surface area and/or the loading of the particles with other chemical components.

6.1.3 MEX functionality: complex dose corrections

The activity specific models (Chapter 4) and the diurnal model BC_{day} (5.2) illustrate the functionality of the MEX data workflow extensively (2.3). Many authors reporting on activity based air pollution exposure already include activity specific dose correction related to the inhalation rate (see 1.1.2.3). The MEX frame is capable of applying any set of complex dose corrections. A hypothetical dose correction function and indicator evaluation is illustrating the flexibility of the MEX data workflow (Figure 6.1.1).

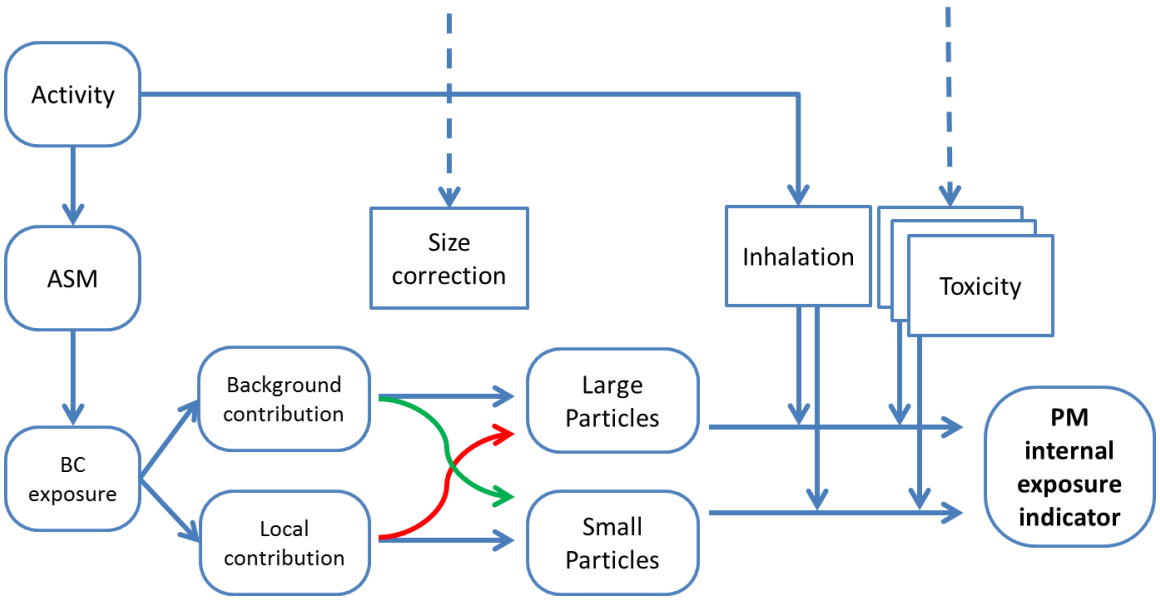

Figure 6.1.1: Example of available indicator functionality: adjusting exposure for particle size, personal and activity specific inhalation and toxicity corrections at the spatial and temporal resolution of the activity specific model (ASM).

The correction can be detailed to include individual features of the subjects if the relevant information is available through the person factory. The dose corrections can be extended to other features of the pollutant under investigation. The potential use of the background adjusted models is an option. Since particle size distributions are different for background exposure and local contributions, correction functions adjusting for the amount of the small and potentially more harmful portion of the particulate matter exposure are relevant. This theme, adjusting for the actual amount of small particles in the exposure is addressed by several authors (Anderson et al., 2012, Bell, 2012, Chang et al., 2011, Chuang et al., 2005, Kelly and Fussel, 2012, Langrish et al., 2012, Laumbach and Kipen, 2012, Lippmann et al., 2013, Liu et al., 2015, Lopez et al., 2012, Perrone et al., 2013, Steenhof et al., 2011, Strak et al., 2012). This type of corrections can be detailed by activity type and/or micro-environment in the ASMs. The size correction functions can be a function of the magnitude of the background and/or local contribution. The inhalation can be made sensitive to the activity and personal attributes. Internal dose could be adjusted to particle size (e.g. smaller particles may penetrate the lung-blood barrier or translocate to the nervous system, whereas the larger particles do not). Additional information on in-body biomedical and toxicity effect can be added. The MEX model will process the combined non-linear effects of all these corrections at the temporal and spatial resolution of the activity specific models, 10 seconds for in-traffic exposure in the presented models.

6.1.4 Noise exposure indicator definitions

Within this PhD no noise indicators are presented for noise exposure as such. Of course, the presented methodology applies for complex noise indicator definitions as well. The noise indicators are known and in short introduced in 1.1.2.3. Dose corrections, personal information, diurnal profiles for noise exposure are relevant as well in the evaluation of noise on the subjects in the study population. An epidemiological cohort can be attributed with noise surveys gathering information about annoyance and sleep disturbance from different sources (traffic, neighbours, industrial sources…). Personal and dwelling attributes can be gathered (noise sensitivity, hearing impairment, quiet facade, sleeping with open windows, insulation quality of the windows…). All of these parameters can be used to build noise indicators in as much variants as relevant for the research project at hand. The indicator can be sensitive to the diurnal pattern of the noise exposure. Sleep quality is sensitive to the period of the night (getting into sleep, awakenings in the morning due to less deep sleep status during the morning). The functions to evaluate the awakenings can be made sensitive to the sleeping pattern, combined with the diurnal profile. The 'shoulder hours' (early morning and late in the evening) are important for the sleep quality and are an increasing risk factor since the increasing traffic also intrudes this vulnerable episode in the person's sleeping pattern. Indicator definitions can be built to be sensitive for the combination of each of these corrections.

The most important feature of the MEX model emerges: all personal information, regardless the origin or purpose can affect any indicator in any research field. Correlations and secondary effects can emerge across the disciplines. The personal information has to be collected only once and is identical across disciplines. This is illustrated in the Quality of Life model (Section 2.2 and Chapter 3). If hidden and uncharted correlations are available in the personal information, the combined influences on the indicators can be investigated at full. This leads us to the underlying goal of the combined measurements of noise and air pollution: the potential mutual confounding of the health effects

6.1.5 How to disentangle the health effects of noise and air pollution?

We return to the basic question on the mutual potential confounding of the health effects due to traffic related noise and air pollution exposure (1.1.2.4). Epidemiologists use stratification to quantify the health effect of the investigated indicator. When investigating two correlated burdens, it is interesting to compare the differences of the spatial and temporal behaviour of the exposure and see if those differences can be used to stratify a population. Noise exposure is evaluated at the dwelling and is used to estimate the noise annoyance and the sleep disturbance. In questionnaires this is evaluated with a standardized question: "*To what extent are you annoyed or not annoyed in your dwelling and in the vicinity of your*

dwelling?" Sleep disturbance is evaluated at the expected location of the bedroom. Both paths are strongly bound to the dwelling.

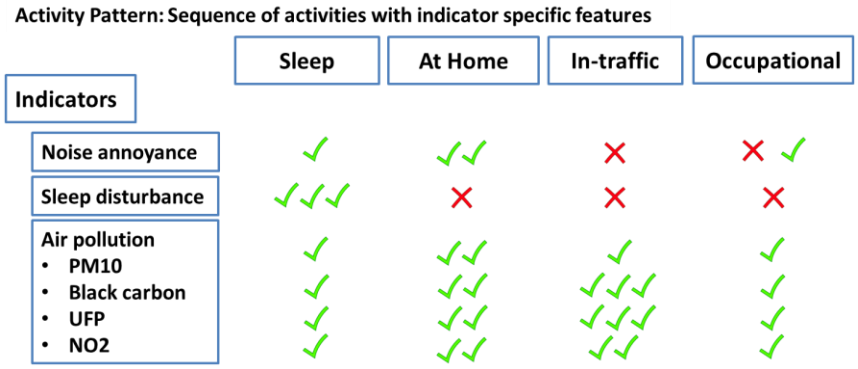

Figure 6.1.2: Differences in impact of noise and air pollution indicators over the full diurnal time activity pattern.

For air pollution, the people are exposed throughout the day. This difference in exposure pattern is the key feature of the methodology to disentangle the health effects. The difference in exposure (and expected health effects) is visualised in Figure 6.1.2. The green flags suggest potential effects, the red crosses suggest little to no effect. The number of flags or crosses gives a general potential impact and is only used for visualizing purposes; no absolute magnitude of effects is intended. The exposure (and activity related dose) to the different air pollutants is higher while in-traffic, effects are possible for the occupational exposure.

When the exposure of a population is assessed for the different burdens, the stratification process will result in clusters of individuals with different combinations of exposure for the different burdens. The clustering process is visualized in Figure 6.1.3.

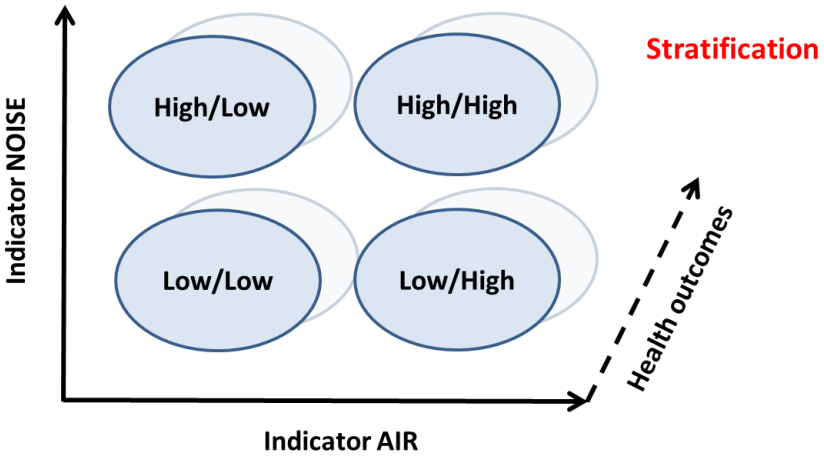

Figure 6.1.3: Visualisation of the stratification of exposure to multiple environmental burdens with a third dimension in the different health effects.

When the used air pollution indicator is evaluated at home, a strong correlation will emerge in the data. Only the 'Low/low' and 'High/High' groups will be populated. When a personal exposure indicator is used, people with time-activity patterns resulting in high in-

traffic air pollution exposure but low noise exposure at home and people with high noise exposure at home, but small in-traffic air pollution exposure will contrast with the people where the correlation for both burdens occurs. Since the health effects of air pollution and noise pollution may differ, a third dimension can be added for the different health effects. This multivariate dataset includes all information necessary to disentangle the health effects.

In Figure 6.1.4, the full workflow for applying the personal activity indicator framework (MEX) is illustrated for the case of noise and air pollution exposure. The input data is based on noise and air pollution measurements and external data. Activity specific models are created and are combined into full personal exposure models. Any relevant dose correction can be applied on any indicator. Each indicator can be applied to the same population if the relevant personal parameters are available. The red dashed line shows the range of the models presented in this work. The full workflow is operational in the MEX framework.

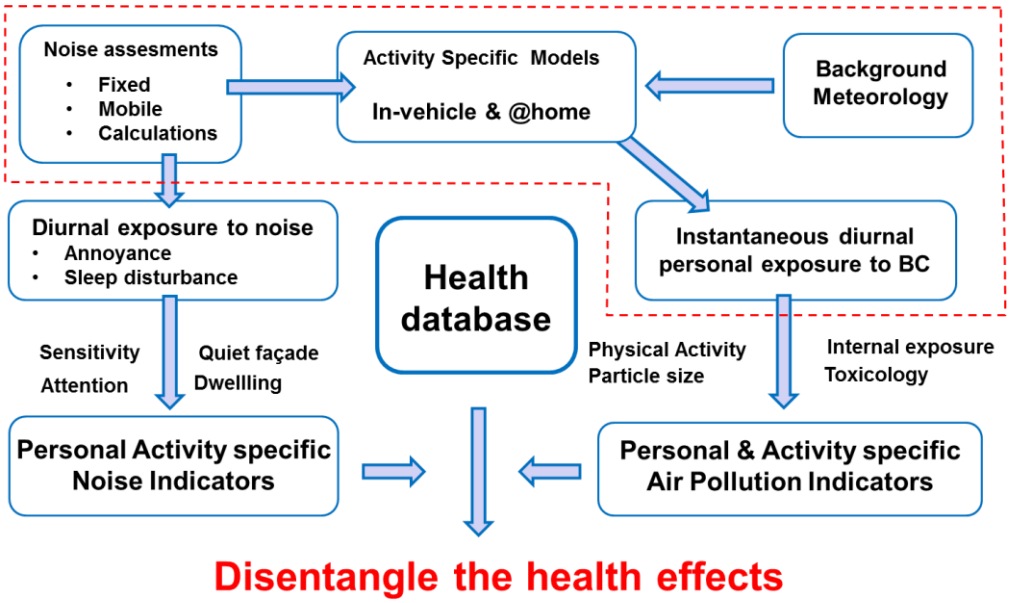

Figure 6.1.4: Full data flow of the MEX model to provide the multivariate exposure database to disentangle the health effects of noise and air pollution. The red dotted line indicates the work covered in this PhD.

6.2 Results

6.2.1 Quality of Life can be assessed through combined noise assessments at the dwelling and in the neighbourhood

The quality of Life is modelled with a multilevel indicator model including personal assessments including exposure during trips. The QoL is calibrated with a questionnaire focussing on a wide range of environmental burdens. The strongest component in the perceived quality of the environmental quality is noise, both in positive and negative sense. Not only is the

noise exposure at the dwelling important, also the noise evaluation along the roads in the vicinity add value. People assess the traffic related burdens in and around their dwelling through noise. Evaluations of indicators at the dwelling, along the travelled trajectories and at the destination are capable of capturing the personal perception of the neighbourhood.

6.2.2 Exposure of bicyclists and traffic mapping opportunities

Instantaneous noise measurement while biking predicted the instantaneous Black Carbon exposure of bicyclists. Effects of meteorological and local traffic variation on the in-traffic exposure can be disentangled. The noise measurements are less sensitive to meteorology and background exposure compared to the in-traffic air pollution exposure. Noise quantifies both the amount of traffic and the local traffic dynamics. For a specific traffic situation, only a few passages are necessary to predict Black Carbon exposure for bicyclists after adjusting for the meteorological influences and the background concentrations. Similar solutions are also achieved in a smaller setup for Ultrafine Particle Counts. The fast convergence enables extended city traffic mapping, capable of capturing traffic related features for the low exposure roads and bicycle trajectories.

6.2.3 In-vehicle and indoor exposure to Black Carbon

The results for bicyclist are extended towards in-vehicle and indoor exposure by the use of microscopic instantaneous land-use regression models. The noise measurements are replaced by noise maps. No instantaneous traffic is included but the activity specific models perform beyond expectation.

For the in-vehicle model, the measurements for the instantaneous model were performed more than three years after the external validation measurements. The external validation revealed a strong discrepancy but similar changes are detected in the continuous Black Carbon measurement locations of the VMM. This discrepancy can plausibly be related to the implementation of the European Emission Standard (Euro5). After adjusting the in-vehicle model towards the changed vehicle fleet emission, the model predicts the instantaneous exposure of the external participatory campaign a correlations above 0.5 for the average exposure during the trip and up to 0.8 when including the trip duration.

An indoor at home exposure model is based on the bicycle measurement campaign, replacing the noise measurements with a noise map. The background adjusted approach is able to disassemble the indoor BC exposure into a meteorology driven background component and a local traffic related component. The model includes a seasonal adjustment for the I/O ratio compatible with available literature. The external validation results in correlations above 0.65. This numerical experiment will require extended future work. The pilot

experiment at a single facade shows that the background adjusted approach has potential for dwellings as well.

6.2.4 Personal exposure to Black Carbon

The activity specific models are combined into an instantaneous daily exposure model covering all micro-environments. In busses, the in-vehicle model is applied. For all indoor activities the indoor at home model is applied. For bike, walk, rail and light rail, the indoor model is applied without indoor-outdoor correction. The external validations results in a correlation of 0.65. The main goal is hereby achieved.

The results by micro-environment show that the active modes (biking and walking) are poorly predicted due to the lack of traffic data on the local roads. The noise based traffic mapping (4.3) will be capable of providing the missing data to improve the personal exposure model. The main limitation is the lack of high exposed dwellings in the validation dataset. More detailed future measurement campaigns and exposure modelling will be necessary at high exposed dwellings. The combined techniques of microscopic land-use regression and the disentanglement of the variability of the traffic related air pollution exposure into a meteorological driven background component and a local traffic related component are crucial.

6.2.5 MEX, an exposome compatible data flow framework

To handle the data processing in all its potential variants in input and output required a detailed analysis of the data workflow. The MEX data workflow has proven its value. The main distinctive features are:

- High spatial and temporal resolution
- Activity specific modelling
- Route sensitive for in-traffic exposure
- External models can be implemented
- Any dose or dose-effect indicator can be implemented
- Population extrapolations enable detailed policy support
- Epidemiological databases can be attributed

Both Quality of Life and personal exposure assessments result in complex evaluations on a personal level. The goal of the thesis implies data processing of participatory sensing data, the calculation of indicators and the need to extrapolate the activity and micro-environment specific models to larger populations, matching several of the requirements listed in the vison and strategy on exposure science by Lioy and Smith (Lioy and Smith, 2013). The data

flow framework and its implementation is therefore presented as an independent result. It is not a scientific result as such but it is an important from the engineering point of view. A tool is created to combine and merge multidisciplinary knowledge and data to improve health effect assessments and policy support.

6.3 Conclusion

This PhD investigates the potential of noise exposure assessments as a proxy for traffic related Quality of Life and traffic related air pollution exposure. The personal perception of the traffic related aspects in and around the dwelling can be predicted with noise exposure at the dwelling and noise exposure along the roads in the vicinity of the dwelling. The correlation between traffic noise and traffic related air pollution is used to extend this finding to air pollution.

This was achieved for bicyclists by using combined mobile noise and Black Carbon measurements. The spectral evaluation of the vehicle noise can distinguish between engine noise and vehicle speed and adds instantaneous traffic and traffic dynamics into the model. The variability of the instantaneous exposure can be disentangled into a local traffic related component and the meteorological influences on the background concentrations. The effects of the traffic dynamics on the emission of BC and UFP are relevant to quantify the local variation in the exposure. The technique was successfully validated in extreme traffic conditions in Bangalore, India.

The technique is extended to the in-vehicle micro-environment and the indoor at home micro-environment. The noise measurements are for that purpose replaced with detailed noise maps. The indoor model is only a numerical pilot experiment based on available data. Despite the strong reduction in traffic detail, the models performed beyond expectation. In the future the underlying activity specific function has to be replaced with a model based on simultaneous air pollution measurements (indoor and outdoor) and noise measurements at the facade. The available activity specific models are combined in a daily personal exposure model including all activities. The external validation results in a correlation of 0.65. The personal exposure to Black Carbon can be modelled using noise as a proxy. The main goal of this PhD was hereby achieved. The presented methodology of mobile noise mapping can add value to the in-vehicle and indoor models in the near future.

These results were only possible due to the development of instantaneous land use regression models with highly improved spatial and temporal resolution for the different micro-environments. The underlying statistical technique (generalized additive models) is an important component in the solution since it captures and conserves the non-linear effects in the air pollution exposure. The most crucial aspect is however the possibility to disentan-

gle the exposure into a local traffic and a background component due to instantaneous noise based traffic assessments.

The data flow framework, developed to process all the data, can apply any indicator to any population to provide high quality personal assessments for use in epidemiological research and to provide advanced policy support.

6.4 References

Anderson, J. O., Thundiyil, J. G., & Stolbach, A. (2012). Clearing the air: a review of the effects of particulate matter air pollution on human health. Journal of Medical Toxicology, 8(2), 166-175.

Bell, M. L. (2012). Assessment of the health impacts of particulate matter characteristics. Research report (Health Effects Institute), (161), 5-38.

Chang, H. H., Peng, R. D., & Dominici, F. (2011). Estimating the acute health effects of coarse particulate matter accounting for exposure measurement error. Biostatistics, kxr002.

Chuang, K. J., Chan, C. C., Chen, N. T., Su, T. C., & Lin, L. Y. (2005). Effects of particle size fractions on reducing heart rate variability in cardiac and hypertensive patients. Environmental health perspectives, 1693-1697.

Kelly, F. J., & Fussell, J. C. (2012). Size, source and chemical composition as determinants of toxicity attributable to ambient particulate matter. Atmospheric Environment, 60, 504-526.

Langrish, J. P., Li, X., Wang, S., Lee, M. M., Barnes, G. D., Miller, M. R., ... & Jiang, L. (2012). Reducing personal exposure to particulate air pollution improves cardiovascular health in patients with coronary heart disease. Environmental health perspectives, 120(3), 367-372.

Laumbach, R. J., & Kipen, H. M. (2012). Respiratory health effects of air pollution: update on biomass smoke and traffic pollution. Journal of allergy and clinical immunology, 129(1), 3-11.

Lippmann, M., Chen, L. C., Gordon, T., Ito, K., & Thurston, G. D. (2013). National Particle Component Toxicity (NPACT) Initiative: integrated epidemiologic and toxicologic studies of the health effects of particulate matter components. Research report (Health Effects Institute), (177), 5-13.

Liu, X., Zhai, Y., Zhu, Y., Liu, Y., Chen, H., Li, P., ... & Zeng, G. (2015). Mass concentration and health risk assessment of heavy metals in size-segregated airborne particulate matter in Changsha. Science of The Total Environment, 517, 215-221.

López-Villarrubia, E., Iñiguez, C., Peral, N., García, M. D., & Ballester, F. (2012). Characterizing mortality effects of particulate matter size fractions in the two capital cities of the Canary Islands. Environmental research, 112, 129-138.

Perrone, M. G., Gualtieri, M., Consonni, V., Ferrero, L., Sangiorgi, G., Longhin, E., ... & Camatini, M. (2013). Particle size, chemical composition, seasons of the year and urban, rural or remote site origins as determinants of biological effects of particulate matter on pulmonary cells. Environmental Pollution, 176, 215-227.

Steenhof, M., Gosens, I., Strak, M., Godri, K. J., Hoek, G., Cassee, F. R., ... & Pieters, R. H. (2011). In vitro toxicity of particulate matter (PM) collected at different sites in the Netherlands is associated with PM composition, size fraction and oxidative potential–the RAPTES project. Part Fibre Toxicol, 8(1), 1-15.

Strak, M. M., Janssen, N. A., Godri, K. J., Gosens, I., Mudway, I. S., Cassee, F. R., ... & Hoek, G. (2012). Respiratory health effects of airborne particulate matter: the role of particle size, composition, and oxidative potential-the RAPTES project. Environmental health perspectives, 120(8), 1183-1189.

Appendices

A External validation data set

The scientific process requires external validation for the presented models. In this PhD an external participatory campaign is available through VITO. The participatory campaign is reported independently in several occasions (Dons et al., 2011, Dons et al., 2012, Dons et al., 2013, Dons et al., 2014). It contains a one-week long personal Black Carbon exposure measurements for 62 people, living in 31 different dwellings across Flanders, including a subset of 8 dwellings in the spring and summer (June and July 2010) and 23 dwellings in winter (November 2010-January 2011) . The personal exposure is measured on the two adults living in each dwelling. The activity pattern is stored with a PDA application available from the local mobility research team. It captures the activity pattern in a temporal resolution of 5 minutes. The Black Carbon measurements, performed with the AE51 µ-aethalometer are stored in 5 minute averages. A GPS recording is available for the outdoor measurements.

Some specific features of the participatory sensing campaign should be considered since they influence the measurement and the modelling. The time-activity application was not capable of storing the difference between an indoor activity and an outdoor activity. The application was originally developed for mobility research and did not cover this activity parameter. Spending time at a stationary location is automatically considered an indoor activity; while in reality the activity could also be (partially) spent outdoors. This potential indoor/outdoor mismatch is however partially counteracted by the actual operational situation in the measurement campaign. Since both the aethalometer and PDA required charging, the equipment was most of the time not carried while spending time at home. For the activities at home the measurement was performed typically indoors, even if the subject spent time outdoors in the vicinity of the dwelling (garden etc.). We therefore treat the at-home activities as if they are all ‘indoor activities’.

The measurements are performed in a temporal resolution of five minutes, the same resolution of diary application. Cross-overs of the exposure measurements from in-traffic activities into indoor activities are possible within that five minute window. Full misclassifications (short trips not correctly entered in the diary) are also possible. This results in missing data in the data processing. Technically it is possible to adjust the diaries with available GPS data, but this approach was rejected since a lot of GPS data is missing (specially at the beginning of the trips, people can already be in transport before a valid GPS position is available). Adjusting the misclassification using the GPS data might overshoot its goal. The spatial location of the dwellings and destination was manually established based on the trip ends of the GPS tracking data. The locations were manually mapped in the GPS cloud of point at the end of the trip.

Dons E, Panis LI, Van Poppel M, Theunis J, Wets G. Personal exposure to Black Carbon in transport microenvironments. Atmospheric Environment 2012; 55.

Dons E, Panis LI, Van Poppel M, Theunis J, Willems H, Torfs R, et al. Impact of time-activity patterns on personal exposure to black carbon. Atmospheric Environment 2011; 45: 3594-3602.

Dons E, Temmerman P, Van Poppel M, Bellemans T, Wets G, Panis LI. Street characteristics and traffic factors determining road users' exposure to black carbon. Science of the Total Environment 2013; 447: 72-79.

Dons, E., 2013. Air pollution exposure assessment through personal monitoring and activity-based modeling. PhD Thesis. Hasselt University, Diepenbeek, p. 302.

Dons E, Van Poppel M, Kochan B, Wets G, Panis LI. Implementation and validation of a modeling framework to assess personal exposure to black carbon. Environment International 2014; 62: 64-71.

B External modelling data

1. Open Streetmap network data

The network layer is based on a recent version of the Open StreetMap data. This dataset is used for both the traffic attribution and the position of the noise emission in the noise mapping. The basic information is downloadable from www.**geofabrik**.de. The network enabled version is a not a free service.

2. Traffic data

The traffic data is available from the Flemish Government for an extended network. More than 80,000 road links are modelled and attributed with number of passenger cars, number of heavy vehicles and their estimated speed for each hour of a full year. The most recent year available is 2012. The dataset (size > 12 Gb per year) is aggregated by day of week for each hour on each traffic link. This aggregated dataset is used as the input of the traffic co-

variate, which results in a diurnal detailed parameter. Only weekdays are aggregated in the dataset. A weighted amount of traffic is calculated using the standard approach by giving each heavy vehicle a weight of 2.

3. Noise mapping

Noise mapping is performed within a two-year cycle of environmental evaluation for the Flemish institute responsible of environmental reporting (Vlaamse Milieu Maatschappij). The noise map is built on the traffic data of 2012, described above.

The noise map is calculated with ISO 9613-2, using the emission definitions of the European Cnossos project. It is calculated for Flanders and Brussels using a spatial resolution of 10, 20 and 50 m buffers around the roads and a spatial resolution of 100 m further away from the road network. This result is interpolated to a grid with grid size of 20 m for the whole region under investigation. Screening of buildings in not included. Noise screens near highways are included

The traffic attribution of the generalized link to the actual roads is performed by local routing of the traffic links, resulting is a high spatial resolution in local communities.

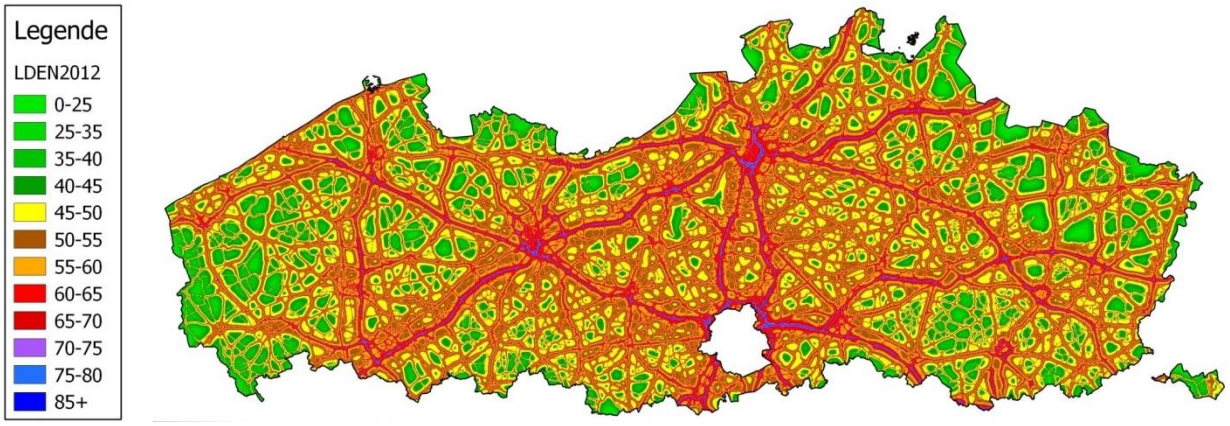

Figure A 1: L_{DEN} Noise map for Flanders for 2012.

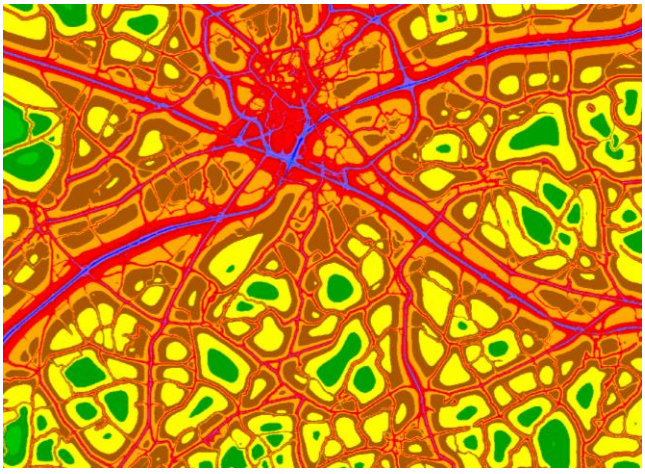

Figure A 2: Detail of the noise map showing the spatial resolution of the low-density roads (due to the traffic attribution by routing). Along the highways, the location of the noise screens is visible.

4. Meteorological data

Meteorological data is available at nine locations in Flanders, with following attributes: 'wind direction', 'wind speed', 'temp', 'temp_min', 'temp_max', 'rel_humidity', 'pressure', 'precip_quantity_1hour' (source www.kmi.be). A measurement point is mapped to the closest available meteo station.

5. Black Carbon background measurements

Background Black Carbon measurements are available from the Flemish institute responsible of all environmental reporting (Vlaamse Milieu Maatschappij, www.vmm.be, www.irceline.be). Since an external validation is included in the research setup, only the background measurements available during the first participatory campaign could be included in the evaluation. The data of Antwerpen-Linkeroever (40AL01) are used for both campaigns.

6. PM_{10} background map

A PM_{10} spatial map of Flanders is available from the website 'irceline.be', responsible for the air pollution reports towards the European government to assess the compliance of the air quality in Flanders. The map is an interpolated version of a five-kilometre grid interpolation

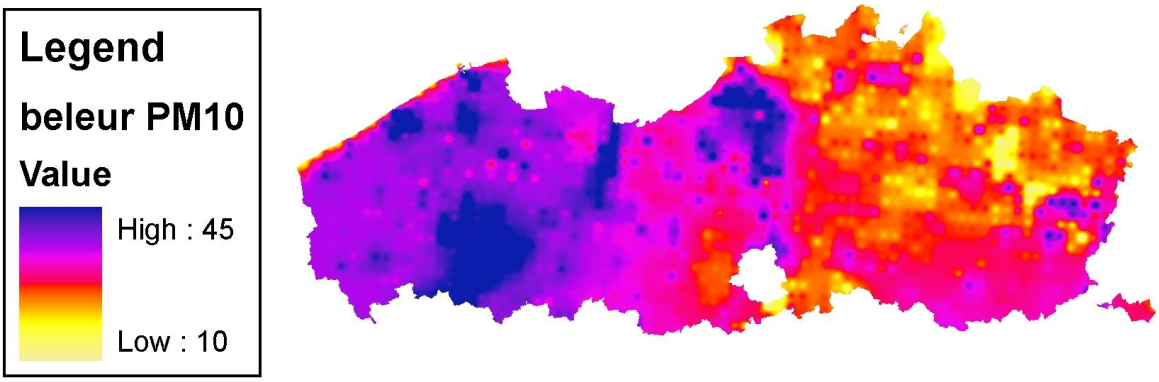

Figure A 3: PM_{10} map (Beleur, 2010 in µg/m3).

7. Street Canyon index

For the spatiotemporal model for bicyclists, a street canyon index was calculated for the area of Ghent (Supplementary data of Dekoninck et al., 2013). The same procedure is applied to the full region of Flanders, including Brussels. The street canyon index is evaluated along the road network every 50 m. The building layer for Brussels was retrieved from Open Street

Map; de building layer for Flanders is based on the CadMap (ownership database with parcels and buildings). The street canyon index is a two-dimensional numerical approximation of the free view area divided by the total area of the evaluation distance, no building height is included. Similar techniques have been reported by Steen Solvan Jensen, 1999 and many others.

$$StCan_{p_x} = 1 - \frac{\sum_{r=1}^{nRad} \theta.(\min(d_{building,r},R))^2}{\pi R^2}$$

Where $d_{building,\ r}$ is the distance from the aggregation point p_x to the closest building along radial r, nRad is the number of radials to process, θ is the opening angle (2π/nRad) and R is the maximum evaluation distance.

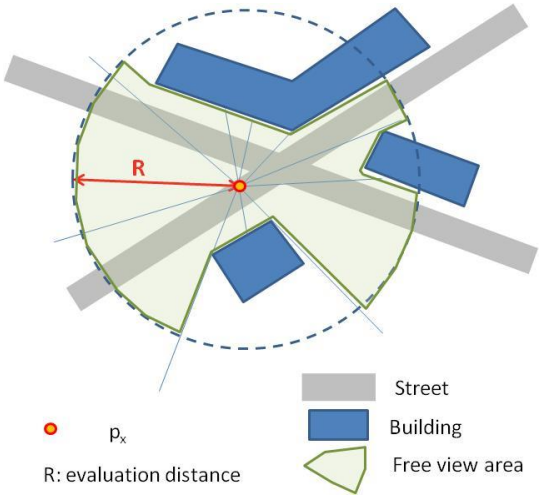

Figure A 4: Illustration of the free view area. The enumerator of equation is a numerical approximation of the surface of the free view area s_{free}.

The Street canyon index $StCan_{p_x}$ was calculated with nRad = 18 and R = 200m. High values reflect narrow streets, low values detect open areas. The street canyon index has to be seen as a 'street canyon likeliness', evaluated for each aggregation point p_x. The radius used for the evaluation of the built up area has no relation with the spatial resolution of the p_x. The street canyon index is evaluated in each p_x, which means that approximately every 50m the street canyon index is re-evaluated. If the evaluation point p_x is only partially surrounded by buildings the index drops. Only really narrow street canyon result in high street canyon indexes since in every direction (except along the street segment) the distance to the buildings is small.

8. Calculation of L_{OLF} and L_{HFmLF} (python code)

In the preprocessing of the noise measurements a smoothing is applied on the 1 second data series of de noise measurement equipment. The code of this smoothing function is added in this section. It uses the pandas library (designed for time series processing). The code results in a smoothed series of 1 second values. These data series are averaged to 10

second values to perform the modelling. The aggregation function is the arithmetic average (no energy conserving Leq).

```
# ----------------------------
def Leq(values):
       values_e = [10**(x/10.0) for x in values]
       result = 10 * math.log10(sum(values_e))
       return result


# SMOOTH THE 1 SECOND DATA
# smooth the third octave data
thirdOctaveBands   =   ['B20_Leq',   'B25_Leq','B31_5_Leq',   'B40_Leq','B50_Leq',
                     'B63_Leq',  'B80_Leq',  'B100_Leq',  'B125_Leq',  'B160_Leq',
                     'B200_Leq',  'B250_Leq',  'B315_Leq',  'B400_Leq',  'B500_Leq',
                     'B630_Leq',     'B800_Leq',     'B1000_Leq',     'B1250_Leq',
                     'B1600_Leq',     'B2000_Leq',     'B2500_Leq',     'B3150_Leq',
                     'B4000_Leq',            'B5000_Leq',            'B6300_Leq',
                     'B8000_Leq','B10000_Leq',     'B12500_Leq',     'B16000_Leq',
                     'B20000_Leq']

for fld in thirdOctaveBands:
      # Leq running average by octave band
       #similar smoothing window as BC measurements
      df[fld] = rolling_apply(df[fld].shift(-6), 11, Leq)
       # extend smooth to avoid missing data
      df[fld] = df[fld].fillna(method='pad')
      df[fld] = df[fld].fillna(method='bfill')

# CALCULATE MODEL PARAMETERS

prep_OLF = []
prep_OHF = []
prep_HFmLF = []
for row_index, row in df.iterrows():
      # OLF
      OLF_cols = ['B100_Leq', 'B125_Leq', 'B160_Leq', 'B200_Leq']
      OLF = dBsum([row[x] for x in OLF_cols])
      prep_OLF.append(OLF)
      # OHF
      OHF_cols = ['B1000_Leq', 'B1250_Leq', 'B1600_Leq', 'B2000_Leq']
      OHF = dBsum([row[x] for x in OHF_cols])
      prep_OHF.append(OHF)
      # HFmLF
      prep_HFmLF.append(OHF - OLF)
df['OLF'] = Series(prep_OLF, index = df.index)
df['OHF'] = Series(prep_OHF, index = df.index)
df['HFmLF'] = Series(prep_HFmLF, index = df.index)
```

C The influence of traffic noise on appreciation of the living quality of a neighbourhood.

Full journal paper:

Botteldooren, D., Dekoninck, L., & Gillis, D. (2011). The influence of traffic noise on appreciation of the living quality of a neighbourhood. INTERNATIONAL JOURNAL OF ENVIRONMENTAL RESEARCH AND PUBLIC HEALTH, 8(3), 777–798.[2]

1. Abstract

Traffic influences the quality of life in a neighbourhood in many different ways. Today, in many places in the world the benefits of accessibility are taken for granted and traffic is perceived as having a negative impact on the satisfaction with the neighbourhood. Negative health effects are observed in a number of studies and stimulate the negative feeling in the population exposed. The noise produced by traffic is one of the most important contributors to the appreciation of the living quality. Thus, it is useful to define a number of indicators that allow monitoring current impact of noise on the quality of life and predicting the effect of future developments. This work investigates and compares a set of indicators related to exposure at home and exposure during trips around the house. The latter require detailed modelling of trip behaviour of the population. The validity of the indicators is checked by their ability to predict the outcome of a social survey and by outlining potential causal paths between them and the outcome variables considered: general satisfaction with the quality of life in the neighbourhood, noise annoyance at home, and reported traffic density in the area.

2. Introduction

In societies where basic needs are largely fulfilled, attention for mental well-being is growing. The quality of the living environment is one of the determinants for this well-being [1]. Therefore there is also a growing interest in how the quality of a neighbourhood is to be assessed and guarded. The appreciation of the living quality of a neighbourhood is depending on various indicators, which can be grouped into personal attributes, attributes of the house

and the characteristics of the neighbourhood [2]. Early studies examine the living density of the neighbourhood as a determinant for quality of life [3,4,5]. In [2] it is shown that the type of the area where the house is located is more useful in predicting individual neighbourhood satisfaction than variables relating to the individual respondent like age, sex or economic status. Also the accommodation type (detached house, semi-detached, flat) are largely contributing to this model. Other references however [6] prove the impact of several resident types ('advantaged', 'generally satisfied', 'settled', 'withdrawn', 'indifferent', 'insecure'), each reporting different reasons to (dis)like their neighbourhood.

Traffic has a significant impact on the quality of a living environment. Traffic grants access to neighbourhood functions and the rest of the world, but this positive aspect is largely taken for granted in many places in the world. Negative impacts include safety, air pollution, smell and noise, but it is mainly noise annoyance that is perceived as a burden and threat to quality of the neighbourhood in everyday life. Also noise annoyance is determined by attributes of the person, the house and the neighbourhood. The most stable personal factor is 'subjective noise sensitivity' [7,8] which is an important predictor of noise annoyance [9,10]. In [10] it is shown that other significant indicators include person-related variables (age, years of employment, Paykel stress score, duration of stay at the apartment at day), house-related variables (windows of living room and/or bedroom oriented toward street, floor) and neighbourhood-related variables (noise levels as night-time L_{eq}, night-time L_{max}, daytime L_{eq}, traffic flow during day and during the night).

This paper presents part of an ongoing quest for models that allow assessing the impact of land use and mobility planning on quality of the living environment. It attempts to quantify the relationship between street traffic, traffic noise as an important impact of traffic, traffic noise annoyance as an important effect of traffic noise, and the quality of life in a neighbourhood. A classical methodology based on a questionnaire survey on the one hand and exposure indicators on the other, is followed. The uniqueness of the paper lies in the introduction of additional exposure indicators for noise exposure away from the dwelling. This exposure is related to trips that people living in a certain neighbourhood might make and the traffic modus they are likely to use. Special care is taken to accurately aggregate the exposure both within one trip and between trips. It will be shown that the best available indicator for noise exposure on the road significantly improves models for noise annoyance based on a more classical facade L_{Aeq}. It will also be shown that this indicator very significantly outperforms facade exposure when it comes to modelling reported quality of life in the neighbourhood. It even models perceived traffic intensity better than the number of vehicles passing in front of the dwelling.

The proposed indicators for traffic noise and pathways to the appreciation of the quality of the living environment are validated and tested on Flanders, the northern part of Belgium and – for the more detailed modelling – on Gent, a 350,000-inhabitant city in the centre of it. This context may affect some of the details of the conclusions so it is discussed in some-

what more detail. Flanders has about 6 million inhabitants living on 13500 square kilometres. About one quarter of this area is built area. The largest city in the region is Antwerp with about 470,000 inhabitants. Thus mega-city problems are not expected in the study area. Transport is attracted to several sea harbours: Antwerp, Gent, Zeebrugge, Oostende together handling about 250 million ton of goods. In addition Flanders is very close to the harbours of Rotterdam and Duinkerken. Flanders is also surrounded by several big cities: Brussels, its capital, Paris, Amsterdam … influencing strongly the amount of traffic on the major arteries.

The city of Gent has a historical centre that is now mainly a recreational and shopping area, which is largely free of car and truck traffic but has an extended tram and bus system. The surrounding areas include a ring road connecting the harbour to the main highways E17 and E40. The E17 connects Antwerp and The Netherlands to France, the E40 connects Brussels and parts of Germany to the coast, France and the channel tunnel to England. Both highways pass within 4 km from the city centre.

Thus the selected study area is heavily loaded with traffic (mainly goods transport) external to the area and thus well suited to investigate the influence of traffic on the appreciation of the living environment.

3. Method

3.1. Survey

This study relies on an existing series of surveys conducted every three years by the Department for Environment, Nature, and Energy of the Flemish Government for subjective evaluation. This written survey (Schriftelijk LeefomgevingsOnderzoek or SLO) addresses quality of the living environment in general and annoyance by noise, odour, and light in particular. Three years of surveys are considered: SLO0 conducted in 2001 with 3200 participants, SLO1 conducted in 2004 with 5000 participants and SLO2 conducted in 2008 again with 5000 participants. Response rate of the written survey was relatively high, 65%, 63%, and 56% respectively due to a telephone recruitment of participants prior to sending out the survey. Due to this high response rate only a slight bias in age, gender, education, and province was observed compared to Flemish demographics. At the Flemish level reported results were corrected for this bias. For the purpose of this paper – which is selecting new exposure indicators – representativity of the sample for the Flemish population is of lesser importance and no correction was made...

The questions of relevance for the current investigation are (English version obtained via Google translate, original in brackets):

Q1.1: How satisfied are you generally on the quality of life (safety, child friendliness, environment…) in your neighbourhood? <Hoe tevreden bent u in het algemeen over de leefkwa-

liteit (veiligheid, kindvriendelijkheid, leefmilieu, …) in uw buurt?> Five point answering scale: very satisfied, satisfied more or less satisfied, not satisfied, not at all satisfied.

Q1.2: If we only look at the quality of life in your neighbourhood, would you recommend friends and acquaintances to come here to live? <Als we enkel kijken naar de leefkwaliteit in uw buurt, zou u vrienden en kennissen aanraden om hier te komen wonen?> Two open answers: Why? Why not?

Q1.3: If you think about the past 12 months, to what extent are you annoyed or not annoyed by noise, odour or light in and around your home? <Als u denkt aan de voorbije 12 maanden, in welke mate bent u gehinderd of niet gehinderd door geluid, geur of licht in en om uw woning?> Five point answering categories for noise, odour, and light separately labelled: not at all, a little, moderately, highly, and extremely.

Q1.8: Do you live in an environment with … five answering categories: very heavy traffic, heavy traffic, normal traffic, little traffic, very little traffic? <Woont u in een omgeving met ... five categories: zeer veel verkeer, veel verkeer, normal verkeer, weinig verkeer, zeer weinig verkeer?>

Q2.1: If you think about the past 12 months, how annoyed or not annoyed are you by the noise from the following sources in and around your home? <Als u denkt aan de voorbije 12 maanden, hoe gehinderd of niet gehinderd bent u door het geluid van de volgende bronnen in en om uw woning?> Five point answering categories for each source separately, labeled: not at all, a little, moderately, highly, and extremely.

Q2.1a: street traffic

Q2.1b: rail traffic

Q2.1c: air traffic

The annoyance questions closely follow the ISO/TS 15666:2003 standard.

3.2. Estimating road traffic noise

This work surpasses prior work in the accuracy in estimating road traffic and road traffic noise exposure. For the population of Gent, a small city of roughly 350,000 inhabitants, the daily trip behaviour of inhabitants is modelled in detail. This allows us at the one hand to estimate exposure to noise – and pollutants – while on the road, and at the other hand it gives us the opportunity to obtain much more detailed traffic intensity data for the smaller roads which are generally not or poorly included in city wide traffic models.

The model proposed for obtaining all trips starts from several sets of input data: the location of dwellings (postal addresses); the location of frequent trip destinations (e.g. shops, schools, employment) and their weights; the statistical database on travel habits of Flemish people. The latter database contains individual trip information about the daily number of trips, their purpose (hence destination), travel mode and the typical distance.

A first step in the modelling consists in generating all potential trips between dwellings and potential destinations (origin-destination combinations) for all modes separately. For car

trips, the fastest route is selected, while for walking and biking the shortest route is used. To reduce computational burden, dwellings are grouped per street segment and the origin of trips is assumed at the centre of the street. Once all potential trips are thus constructed, for each of the dwellings in the model area a household is randomly selected from the database on travel habits. The travel habits of this particular Flemish family are used to simulate the trip pattern for this dwelling, including the travel modes and routes. Thus for example families with children will be assigned school trips to a randomly chosen school at a distance corresponding to the typical travel time. This information determines the trip completely.

The trips are used in different ways in the model. Firstly, aggregating all trips per road section constitutes the local traffic in a road. This is added to the through traffic from a regional traffic model to obtain more accurate estimates of traffic intensities for smaller urban streets. Secondly, the trips are used to calculate exposure to air pollution and noise during travel for the members of every family included in the sample. For exposure during trips, a minimal distance of 10 m to the source is assumed even if both the receiver and the traffic follow the same route. When using motorized vehicles neither the emission of the vehicle itself nor the sound insulation of the vehicle are considered. Thirdly, the trips determine the travel time to all essential destinations and thus give an indication of accessibility of these destinations.

Figure 1 shows as an example, a part of the city of Gent with thickness of streets corresponding to the intensity of trips made by inhabitants of the region passing on these streets. This map is based on a sample of 10% of the 350000 inhabitants of the study area. 300000 trips made by this synthetic population were selected from 24 106 potential routes that were generated in the first step.

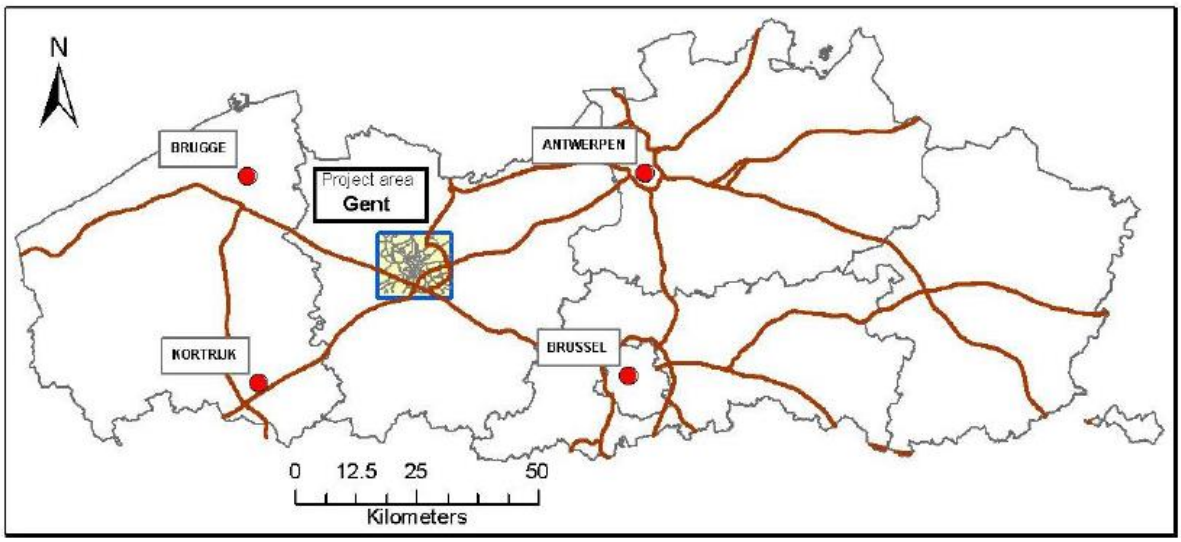

Figure 1: Regional positioning of the project area (blue) within the Flanders, showing the highways (brown) and the major surrounding cities (red).

Noise maps are constructed on the basis of the improved traffic estimates using the Harmonoise/Imagine [12] source model and ISO9613-2 propagation model taking into account the location and height of all buildings but limiting the calculation to a single reflection and diffraction to improve calculation speed. It has been shown that in particular in urban areas, these approximations may underestimate both street canyon noise levels and shielded backyard levels [13]. To reduce computational cost, short term temporal fluctuations in noise levels are ignored reducing the calculation to hourly averaged LAeq. In previous work we stressed the importance of notice events for explaining variations in reported noise annoyance [14] and illustrated the effect of temporal structure on perceived quality of open space [15, 16]. By including traffic intensity in the models that were constructed, the effect of temporal structure can to some extent be reconstructed a posteriori. Finally, the potential positive influence of masking – both energetically and perceptually – by for example natural sounds, human vocalizations or the sound produced by the traveller itself has not been taken into account [17].

Figure 2: Map of part of the city of Gent showing the intensity of trips with local origin or destination as line thickness on a background of grey dots of dwelling addresses; crosses are survey point used in Section 3.

The proposed model allows quantifying exposure while moving from one location to another. This is potentially very useful for calculating health impact of traffic related air pollution [18]. Current air pollution maps have rather coarse calculation grids. This might be sufficient for some pollutants such as PM_{10} but others such as traffic related UFP (ultrafine particles) and NOx show much stronger spatial variations. On annual scale, traffic noise levels might be a good proxy for estimating the concentration of these pollutants – and their health impact – but on a day by day basis, meteorological effects introduce significant differences [19]. It should also be kept in mind that air pollution may not have a significant direct

influence on reported quality of the living environment since persons may use proxies (like traffic intensity and traffic noise levels) anyhow while trying to judge the traffic related pollution level in their area.

3.3. Suitable exposure indicators

The enormous amount of exposure data generated by the model described in the previous section needs to be summarized in a small set of indicators for further analysis. For noise exposure at home, L_{den} at the most exposed facade is included because of its importance in European noise mapping. Since local traffic is however only obtained during the day, we will limit the indicator to daytime only in most of the analyses. Since it was shown [20] that the availability of a quiet side can reduce reported noise annoyance, the level at the least exposed facade is also included in the analysis.

For noise exposure on the road, noise maps are sampled every 25m. For one particular trip, the noise exposure needs to be spatially averaged over the route followed. Several alternatives were investigated: equivalent level over space, 10% highest levels, median level over space, or a total exposure indicator SEL=L_{eq}+10log(distance). The part of the trip included in the average was also varied. The first 300m of the trip normally takes a person just outside its own street with the typical street geometry of the city of Gent. Alternatively the average over the whole trip, until the destination, was also considered, although it is expected that this indicator will incorporate effects which are too far from home to be considered part of the neighbourhood.

When considering multiple trips, exposure also has to be aggregated over the different trips. For this the equivalent level, the median level, and the mathematical average of levels are considered. Because it is obvious that exposure to environmental noise will be masked by a person's own vehicle when motorized transport is used, an aggregation only taking into account trips on foot or on bike is also included in the pool of indicators. Table 1 summarizes the indicators for noise exposure during trips that are considered in the analysis.

			Exposure aggregation over a single trip							
			Equivalent level		10% highest		Median		Exposure	
			300m	whole trip	300m	whole trip	300m	whole trip	300m	whole trip
Agg. over different trips	All modes	Equivalent	$L^{eq}_{T,300,eq}$	$L^{eq}_{T,w,eq}$	$L^{eq}_{T,300,10}$	$L^{eq}_{T,w,10}$	$L^{eq}_{T,300,50}$	$L^{eq}_{T,w,50}$	$L^{eq}_{T,300,sel}$	$L^{eq}_{T,w,sel}$
		Median	$L^{50}_{T,300,eq}$	$L^{50}_{T,w,eq}$	$L^{50}_{T,300,10}$	$L^{50}_{T,w,10}$	$L^{50}_{T,300,50}$	$L^{50}_{T,w,50}$	$L^{50}_{T,300,sel}$	$L^{50}_{T,w,dB}$
		Linear average of dB values	$L^{dB}_{T,300,eq}$	$L^{dB}_{T,w,eq}$	$L^{dB}_{T,300,10}$	$L^{dB}_{T,w,10}$	$L^{dB}_{T,300,50}$	$L^{dB}_{T,w,50}$	$L^{dB}_{T,300,sel}$	$L^{dB}_{T,w,sel}$
	Bike and pedestrian	Equivalent	$L^{eq}_{BP,300,eq}$	$L^{eq}_{BP,w,eq}$	$L^{eq}_{BP,300,10}$	$L^{eq}_{BP,w,10}$	$L^{eq}_{BP,300,50}$	$L^{eq}_{BP,w,50}$	$L^{eq}_{BP,300,sel}$	$L^{eq}_{BP,w,sel}$
		Median	$L^{50}_{BP,300,eq}$	$L^{50}_{T,w,eq}$	$L^{50}_{T,300,10}$	$L^{50}_{T,w,10}$	$L^{50}_{T,300,50}$	$L^{50}_{T,w,50}$	$L^{50}_{T,300,sel}$	$L^{50}_{T,w,sel}$
		Linear average of dB values	$L^{dB}_{BP,300,eq}$	$L^{dB}_{BP,w,eq}$	$L^{dB}_{BP,300,10}$	$L^{dB}_{BP,w,10}$	$L^{dB}_{BP,300,50}$	$L^{dB}_{BP,w,50}$	$L^{dB}_{BP,300,sel}$	$L^{dB}_{BP,w,sel}$

Table 1: Indicators for noise exposure during trips.

4. Results and discussion

4.1. Analyses of the survey data

It is interesting to investigate first the response to the open question Q1.2 since it justifies the choice of variables included in the further analyses and modelling of exposure. In Figure 3 the words – or synonyms – are shown that are frequently used by the survey respondents while mentioning reasons to recommend to friends and acquaintances to either come to live in this neighbourhood (a) or not (b). At the positive side the availability of green and nature dominates, followed by a group of factors relating to tranquillity and absence of traffic. Many respondents nevertheless also mention accessibility to city centre and facilities as being important. The importance of green and nature was previously investigated in detail by Gidlof-Gunnarsson et al [24]. At the negative side too much traffic pops up together with several associated burdens such as traffic safety, unsafe traffic for children, too high traffic speed, traffic noise. In addition, noise in general and industry and other sources of annoyance are mentioned frequently as well as a lack of tranquillity. Traffic and traffic noise thus seem of sufficient importance to merit a specific investigation, both in the positive as in the negative sense. This finding corresponds to the work by Leslie et al. [21] that recovered traffic and traffic noise as one of the five principle component in a 17 items investigation of neighbourhood satisfaction and showed a significant relationship with mental health. O'Campo et al [22] based on concept mapping session also recover traffic and noise but with a much less prominent role. The latter study was done in Toronto, which is a completely different context that might explain these differences. It should however also be mentioned for completeness that the survey used in the underlying work was conducted by the regional government which might have urged participants to focus more on issues that are related to this level of governance and not on local urban issues.

(a)

(b)

Figure 3: (a) Tag cloud of terms mentioned while asking why the respondent would suggest friend and acquaintances to come and live in his neighbourhood; (b) same when asked why not; the size of the word corresponds to the frequency of occurrence, colours are used only to facilitate reading

To quantify these first observations and to identify potential pathways before proceeding with relating the survey to exposure indicators, relationships between answers on the survey questions are investigated. Since no exposure calculation is needed for this, the full statistical power of the region wide survey can be used.

The importance of traffic noise for the quality of life in the neighbourhood that boiled up in the open question, is confirmed by plotting the answer to the question on quality of life in the neighbourhood (Q1.1) against the answer to the question on noise annoyance at home caused by street traffic (Q2.1a) in Figure 4 and that caused by air traffic (Q2.1c) in Figure 5. People reporting to be highly or extremely annoyed by street traffic noise, are more likely to be not (or not at all) satisfied about the over-all living quality (resp. up to 30% and 50% of the people reporting highly or extremely annoyance). Only 20 to 25% of the people reporting high to extreme annoyance by street traffic noise are still satisfied about their living quality. Reporting no annoyance by street traffic noise at all, seems to be sufficient for the large majority of people to report being satisfied to very satisfied with the overall quality of life in the neighbourhood. Although the prevalence of being highly to extremely annoyed by air traffic noise is much lower (2.6%) than the prevalence of being highly to extremely annoyed by road traffic noise (11.5%), the effect on reported overall quality of the living environment is rather similar. In the categories of highly and extremely annoyed people, resp. over 20% and over 30% is not or not at all satisfied about the living quality. On the other hand, about 30% of these respondents are nevertheless satisfied or very satisfied about the living quality. It was also observed that this general trend is conserved when the population under study is limited to those living in a city or those living in smaller villages (not shown in the graphs). Both the insensitivity to the cause of noise annoyance and the insensitivity to living in a city or in a village on the countryside suggest that there is indeed a strong relationship between

reported noise annoyance and reported quality of life in the neighbourhood. The spread in the answers do not exclude - even suggest - the existence of other hidden spatially determined variables steering both noise annoyance and quality of life. Personal factors influencing sensitivity to the environment or reporting style can however not be ruled out at this point.

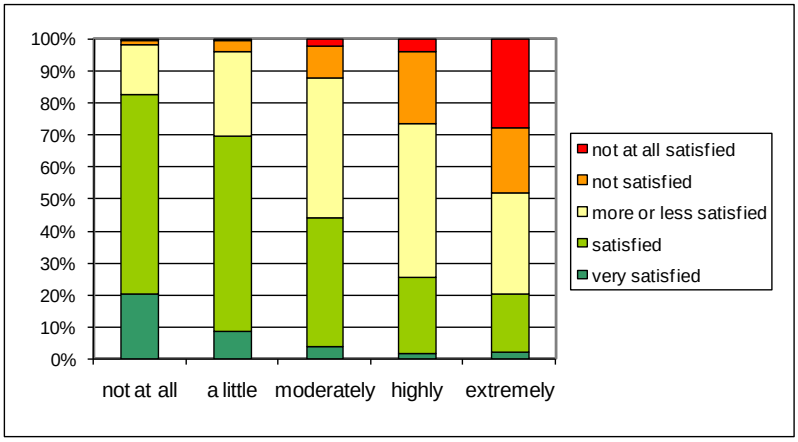

Figure 4: The influence of reported street traffic noise annoyance (Q2.1a) (horizontal) on global living quality in the neighbourhood (Q1.1) (vertical)

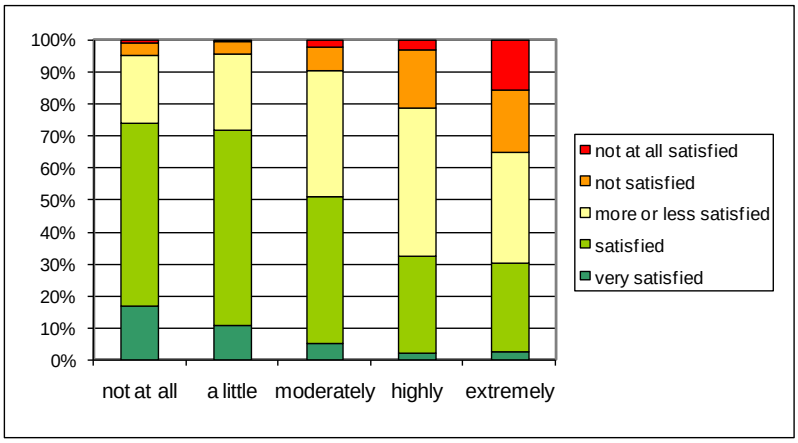

Figure 5: The influence of reported air traffic noise annoyance (Q2.1c) (horizontal) on global living quality in the neighbourhood (Q1.1) (vertical)

The reported traffic intensity in the neighbourhood (Q1.8) is related to satisfaction with the general quality of life in the neighbourhood in a similar way as noise annoyance (Figure 6) but in general the relationship is less strong. From the people who judge that there is 'very much traffic' in their neighbourhood, less than 30% is not or not all satisfied about the general living quality. In the category reporting 'a lot of traffic' in their neighbourhood, about 10% is not (or not all) satisfied about the living quality. Reporting "very little traffic" results in 30% of the people reporting also being very satisfied with the quality of the living environment. At this end of the scale, reported traffic intensity is thus a somewhat stronger predictor for quality of life in the neighbourhood than the absence of traffic noise annoyance.

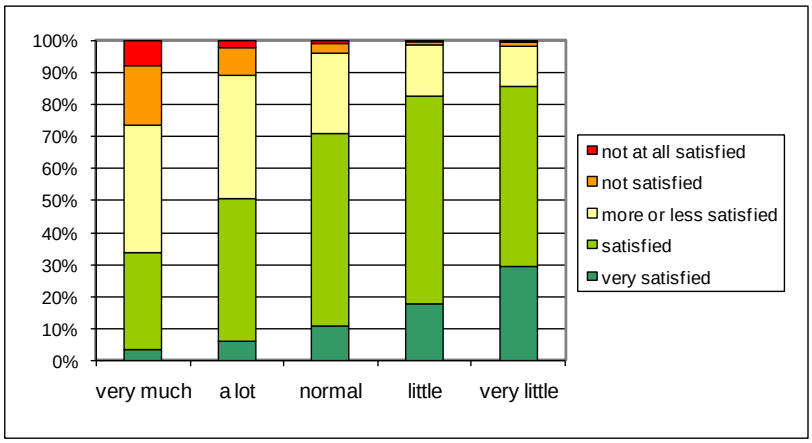

Figure 6: The effect of reported traffic intensity in the neighbourhood (Q1.8) (horizontal) on global living quality in the neighbourhood (Q1.1) (vertical)

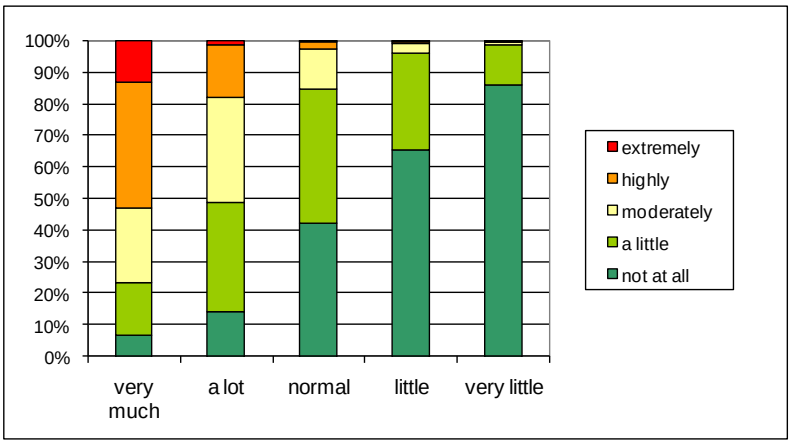

Figure 7: The effect of reported traffic intensity in the neighbourhood (Q1.8) (horizontal) on the reported annoyance by street traffic noise (Q2.1a) (vertical)

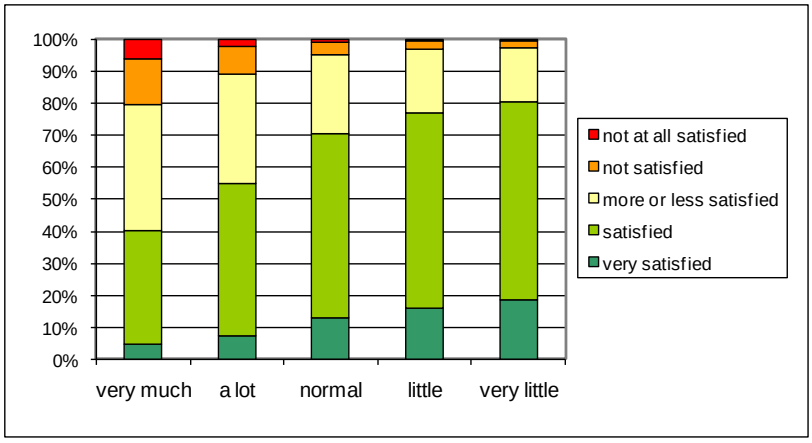

Figure 8: Probabilistic estimate of global living quality in the neighbourhood (vertical) for different traffic intensities (horizontal); to be compared with Figure 6.

The pathway between traffic intensity and quality of life in the neighbourhood could lead through street traffic noise annoyance or through other negative or positive aspects of traffic such as safety, exhaust smell, or even accessibility. The distribution of answers on the street traffic noise annoyance question (Q2.1a) for different reported traffic intensities (Q1.8) in Figure 6 reveals a rather strong relationship. Over 50% of the people that report

"very much traffic" also report high to extreme street traffic noise annoyance. Of those reporting little or very little traffic, no one reports high to extreme noise annoyance. The pathway from reported traffic intensity to quality of life in the neighbourhood through street traffic noise annoyance seems possible. To investigate its probability further, the percentages in Figure 4 and Figure 7 are interpreted as conditional probabilities $P(S_i|A_j)$ and $P(A_j|T_k)$ respectively. S_i refers to the i^{th} degree of satisfaction with quality of life in the neighbourhood; A_j refers to the j^{th} level of street traffic noise annoyance; and T_k to the k^{th} level of reported traffic intensity. $P(S_i|T_k)$ can now be calculated in a probabilistic way as $P(S_i|T_k) = \sum_j P(S_i|A_j)\, P(A_j|T_k)$. The result is shown in Figure 8. By comparing these results to Figure 6, it can be observed that the probabilistic approach slightly underestimates the percentage "not satisfied" to "not at all satisfied" in case of very much traffic and underestimates the percentage "very satisfied" in case of very little traffic, but that overall the agreement is strong. Thus the pathway through noise annoyance – that was the basic assumption for the probabilistic calculation – seems to be quite valid. The above mentioned deviations could be explained by other effects of traffic that impact the overall quality of life in both in positive (little or calm traffic in itself or child friendliness) and negative sense (traffic safety).

These conclusions form the basis for the analysis in the next paragraph, where several models are compared to explain and predict the perceived quality of life in a neighbourhood. In this further analysis exposure indicators will form the main topic of interest.

4.2. Logistic regression model for Gent data

The main outcome variable in this study is the reported general satisfaction with the quality of life in the neighbourhood (Q1.1). This question is answered using a five point bipolar scale: very satisfied, satisfied, more or less satisfied, not satisfied, not at all satisfied. This coarse granulation can hardly be approximated as a continuous answer variable. In addition, it was shown that reasons mentioned in the open question differ significantly depending on whether they relate to positive or negative evaluation. For these reasons, the outcome is quantified either as 'satisfied and very satisfied' at the one hand and as 'not satisfied and not at all satisfied' at the other hand. A logistic regression model (without interaction terms) is used to quantify the importance of indicators studied: $1/(1+\exp[-z])$, with $z=\beta 0+\beta 1x1+\beta 2x2 \ldots$

Since all indicators for exposure to noise during a trip (Table 1) are expected to be correlated (correlation coefficient reaches 0.7 in some cases), it is useful to first determine which ones are more appropriate to add to an overall logistic regression model. Therefore we first consider traffic noise annoyance in and around the house (Q2.1a). Answer categories are grouped to {moderately, highly, extremely} represented as 1 and {not at all, slightly} represented as 0 to balance the number of responses in each class. In Table 2 the p value in a chi square for each of the indicators for exposure during a trip is given when this indicator is added as an additional factor in a model based on the maximum facade exposure during the day, $L_{day,facade}$. The latter indicator is always included in the model since it is most often used

for exposure at home. $L_{day,facade}$ has very high significance in the model with a p value of 1.7 10-7. The table shows that exposure within 300m from the house taking an equivalent level over the length of each trip has the most significant effect. The method for averaging over different trips does not significantly affect this result. It should come as no surprise that an exposure level calculation over the first 300m of a trip has exactly the same significance since most trips are over 300m long. When trips are restricted to biking and walking, where exposure to external noise is expected to be more important, the influence of the parameter is largely reduced. This is mainly due to the introduction of uncertainty about the biking and walking habits of the surveyed persons.

		Exposure aggregation over a single trip							
		Equivalent level		10% highest		Median		Exposure	
		300m	whole trip	300m	whole trip	300m	whole trip	300m	whole trip
Agg. over different trips: All modes	Equivalent	0.0016**	0.09		0.02*	0.01*	0.12	0.0016**	0.22
	Median	0.0015**	0.12		0.05*	0.01*	0.15	0.0015**	0.25
	Linear average of dB values	0.0016**	0.10		0.04*	0.01*	0.13	0.0016**	0.22
Agg. over different trips: Bike and pedestrian	Equivalent	0.02*	0.20		0.78	0.11	0.19	0.02*	0.36
	Median	0.02*	0.27		0.87	0.15	0.28	0.02*	0.5
	Linear average of dB values	0.02*	0.24		0.92	0.14	0.34	0.02*	0.41

Table 2: p in chi square test for a logistic model predicting moderate, high or extreme traffic noise annoyance (Q2.1a) on the basis on Lday on the most exposed facade and the additional indicator in the table. The value of p for Lday,facade is 1.7 10-7. (* p<0.05, ** p<0.01 and *** p< 0.001).

It comes as no surprise that the first 300m of a trip are important for noise annoyance since the noise annoyance question explicitly refers to “in and around your house”. Therefore, the same exercise is repeated for the question on general satisfaction with the quality of life in the neighbourhood (Q1.1). Table 3 shows the p value for adding different indicators in a logistic model to the primary indicator $L_{day,facade}$ for predicting the answers “satisfied” and “very satisfied” while Table 4 shows the same results for predicting the answers “not satisfied” to “not at all satisfied”. Grouping positive and negative evaluation respectively assures again a balanced number of responses in each class. Before interpreting these results it should be noted that the p value for facade exposure itself is much lower than in the case of the question on annoyance (0.013 and 0.0052 respectively). For the response category “not satisfied” to “not at all satisfied”, an equivalent level outperforms other methods for aggregating over different trips. The equivalent level is the aggregator that puts most weight in the most exposed trips. Just as for traffic noise annoyance an equivalent level over the first 300m of a trip has a significant predictive effect. However, in the case of predicting “sat-

isfaction" or "high satisfaction" with the quality of life of a neighbourhood, also the exposure level during whole trips on foot or by bike pop up as highly significant.

From the above analyses it is concluded that $L^{eq}_{T,300,eq}$ is the first candidate as an indicator for exposure to noise during trips. A second candidate, especially when satisfaction with the general quality of the living environment is at stake, could be L_(BP,w,sel)^eq. Strictly speaking, a linear average over dB values for different trips has a slightly more significant effect, but for the sake of simplicity, it was decided to stick to the same aggregation procedure for both trip-related indicators.

		Exposure aggregation over a single trip							
		Equivalent level		10% highest		Median		Exposure	
		300m	whole trip	300m	whole trip	300m	whole trip	300m	whole trip
Agg. over different trips: All modes	Equivalent	0.0086**	0.081		0.81	0.16	0.19	0.0086**	0.018*
	Median	0.021*	0.055		0.91	0.23	0.13	0.021*	0.012*
	Linear average of dB values	0.031*	0.045*			0.32	0.12	0.032*	0.0081**
Agg. over different trips: Bike and pedestrian	Equivalent	0.094	0.095		0.69	0.47	0.87	0.095	0.0034**
	Median	0.18	0.091		0.41	0.73	0.93	0.18	0.0031 **
	Linear average of dB values	0.22	0.032*			0.86	0.64	0.22	0.0012**

Table 3. p in chi square test for a logistic model predicting satisfied to very satisfied with general quality of life of the neighbourhood (Q1.1) on the basis on Lday on the most exposed facade and the additional indicator in the table. The value of p for $L_{day,facade}$ is 0.013.

		Exposure aggregation over a single trip							
		Equivalent level		10% highest		Median		Exposure	
		300m	whole trip	300m	whole trip	300m	whole trip	300m	whole trip
Agg. over different trips: All modes	Equivalent	0.036*	0.49		0.096	0.15	0.23	0.036*	0.98
	Median	0.084	0.57		0.25	0.22	0.33	0.084	0.97
	Linear average of dB values	0.10	0.67			0.26	0.37	0.10	0.81
Agg. over different trips: Bike and pedestrian	Equivalent	0.33	0.21		0.31	0.53	0.06	0.33	0.85
	Median	0.54	0.28		0.60	0.73	0.12	0.54	0.94
	Linear average of dB values	0.54	0.37			0.74	0.13	0.54	0.95

Table 4: p in chi square test for a logistic model predicting not satisfied to not at all satisfied with general quality of life of the neighbourhood (Q1.1) on the basis on Lday on the most exposed facade and the additional indicator in the table. The value of p for $L_{day,facade}$ is 0.0053.

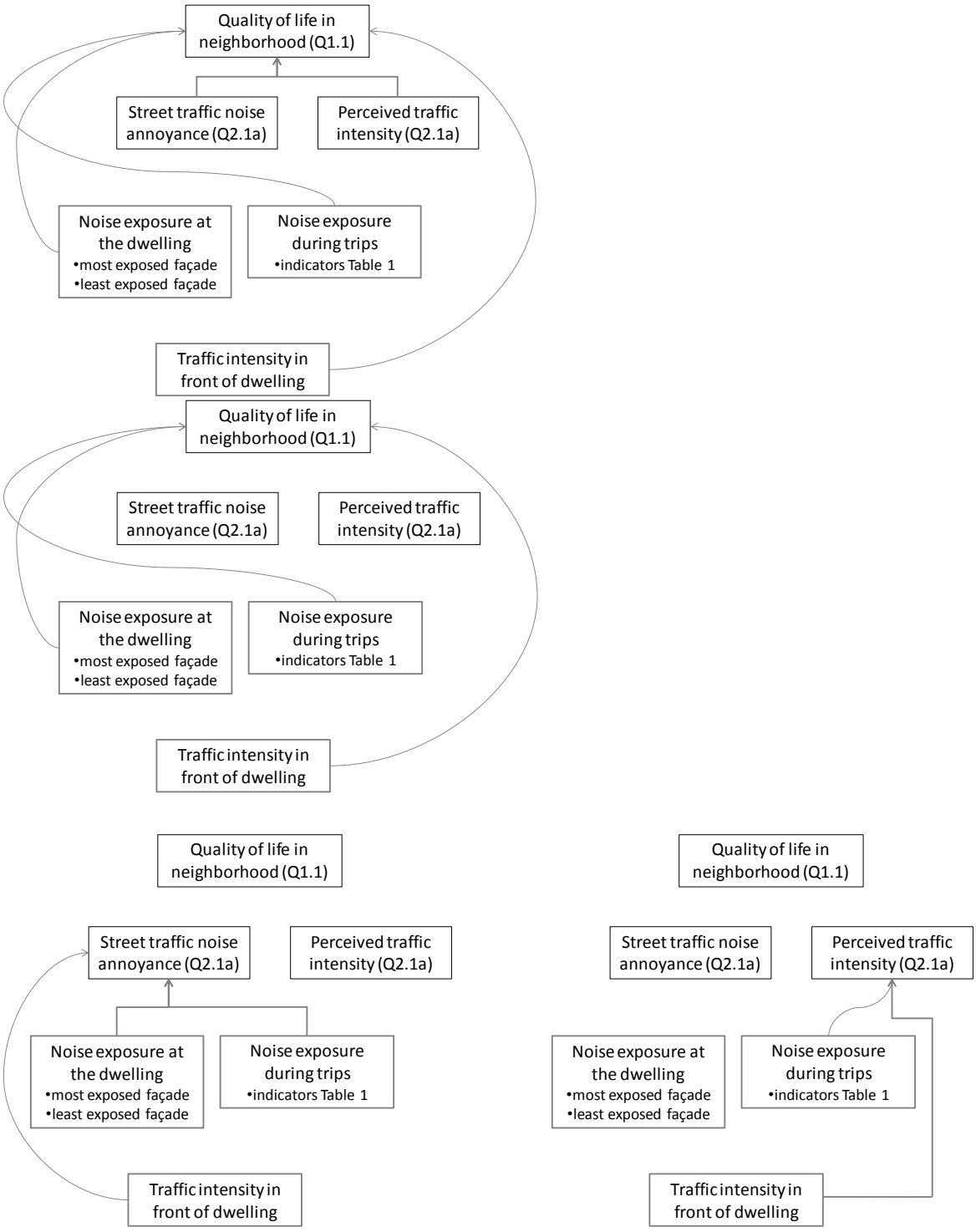

Figure 9: Models studied using logistic regression: a model for QoL including questionnaire response and data from GIS (upper left); a model for QoL including only GIS data (upper right); sub models for street traffic noise annoyance and perceived traffic intensity (lower left and right)

With the knowledge on suitable indicators for noise exposure during a trip in mind, a multiple logistic regression model for the influence of traffic noise on satisfaction with the quality of life in the neighbourhood (Figure 9) is now constructed. When constructing multiple regression models with parameters that are not orthogonal, one could either look for principle components first or account for the order in which parameters are entered. Exposure

indicators used in this study are mutually dependent but have physical relevance clearly linked to neighbourhood situations and some are commonly used in environmental noise assessment. Therefore it is preferred not to combine them in a principle component. Moreover this approach will allow finding the best indicators to add to common practice. This choice implies that all parameters will need to be entered in the models in different orders. The first model contains variables taken from the survey (Q2.1a on traffic noise annoyance and Q1.8 on traffic load of the neighbourhood) but also the noise exposure variables ($L_{day,facade}$, $L_{day,quiet}$, the traffic noise level at the quiet side of the house, $L^{eq}_{T,300,eq}$, $L^{eq}_{BP,w,sel}$) selected above and the traffic intensity on the road in front of the house (N_{street}). In the full model, the variables are added in different orders, in order to evaluate the (added) significance of each specific variable set. The variables taken from the survey have the highest significance even when added to the model last (Table 5). Survey results are indeed expected to be the best estimate of subjective evaluation of noise exposure since they account for personal factors that might influence the way the sonic environment is perceived or the way a person reports about it [23]. In addition, using reported annoyance and traffic intensity avoids potential errors in the noise exposure model or the model accounting for the behaviour of the respondents. It is interesting to investigate whether exposure to traffic noise – as measured by the proposed indicators – has an influence on reported satisfaction with the quality of life in the neighbourhood that is not captured by the question on noise annoyance at home and the question on perceived traffic intensity in the neighbourhood. Therefore the performance of a model including only these questionnaire variables is compared to the full model. The ANOVA test results in Table 6 show that there is a moderately significant improvement by adding exposure indicators for predicting satisfaction with the quality of life in the neighbourhood but not for predicting “not satisfied” to “not at all satisfied”. The availability of a quiet side, measured by $L_{day,quiet}$, and quiet walking and biking routes near the house, measured by $L^{eq}_{BP,w,sel}$, could be a proxy for the availability of tranquillity and availability of green and nature, that were mentioned in the open question as a positive factor, but less prominent as negative factors.

		$L_{day,facade}$	$L_{day,quiet}$	N_{street}	$L^{eq}_{T,300,eq}$	$L^{eq}_{BP,w,sel}$	Q1.8	Q2.1a
model 1a	order entered	1	2	3	4		5	6
	not satisfied	0.0053 **	0.47	0.14	0.061		0.0015 **	0.00060 ***
	satisfied	0.013 *	0.0056 **	0.44	0.010 *		$3.0\ 10^{-7}$ ***	$2.4\ 10^{-8}$ ***
model 1b	order entered	3	4	5	6	7	1	2
	not satisfied	0.52	0.34	0.38	0.36	0.92	$9.1\ 10^{-6}$ ***	0.00060 ***
	satisfied	0.73	0.0019 **	1.00	0.56	0.018 *	$8.6\ 10^{-10}$ ***	$4.6\ 10^{-8}$ ***
model 2a	order entered	1	2	3	4	5		
	not satisfied	0.0053 **	0.47	0.14	0.061	0.75		
	satisfied	0.013 *	0.0056 **	0.44	0.010 *	0.041 *		
model 3	order entered	2	3	4	1			
	not satisfied	0.42	0.40	0.29	0.00069 ***			
	satisfied	0.73	0.0051 **	0.78	0.00033 ***			
model 2b	order entered	3	4	5	1	2		
	not satisfied	0.42	0.36	0.31	0.00069 ***	0.90		
	satisfied	0.53	0.053	0.71	0.00033 ***	0.0048 **		

Table 5: p in chi squared test for logistic model predicting satisfaction with the quality of life in the neighbourhood (Q1.1); label "not satisfied" covers the last two response categories on the five point scale, the label "satisfied" the first two response categories.

For many practical applications, a model for quality of the living environment should not depend on questions in a survey. Hence, the response to question Q1.8 on traffic intensity and Q2.1a on road traffic noise annoyance, were removed from the model. The significance of the different factors remains the same as can be seen from Table 5. However, when $L^{eq}_{T,300,eq}$ is entered in the model first (model 2b), it becomes the most significant factor, performing even better than $L_{day,facade}$ in model 2a. Adding $L_{day,facade}$ does no longer improve the model as can be seen from the chi squared test on the comparison between models in Table 6. Adding an additional indicator for exposure during trips that is specifically targeting trips made on foot or by bike, $L^{eq}_{BP,w,sel}$, has a significant influence in the model for predicting satisfaction with the quality of life in the neighbourhood, but not for predicting dissatisfaction. A similar conclusion hold for adding the quiet side indicator, $L_{day,quiet}$, but adding both factors does not add any new value to the model. The fact that only satisfaction is predicted more accurately shows that a quiet side and quiet (and green) biking or walking routes are not missed when absent and their absence is not a negative aspect for the neighbourhood, but that their presence is perceived as an asset for the living quality. This is again confirmed by the open question results shown in Figure 3.

	Base model	Compare model	P
not satisfied	model 2a	model 1b	$1.1\ 10^{-5}$ ***
	Q1.8 and Q2.1a	model 1b	0.70
	$L_{day,facade}$	$L_{day,facade} + L^{eq}_{T,300,eq}$	0.036 *
	$L^{eq}_{T,300,eq}$	$L^{eq}_{T,300,eq} + L_{day,facade}$	0.42
	$L^{eq}_{T,300,eq}$	$L^{eq}_{T,300,eq} + L^{eq}_{BP,w,sel}$	0.89
Satisfied	model 2a	model 1b	$9.6\ 10^{-14}$ ***
	Q1.8 and Q2.1a	model 1b	0.008 **
	$L_{day,facade}$	$L_{day,facade} + L^{eq}_{T,300,eq}$	0.0086 **
	$L^{eq}_{T,300,eq}$	$L^{eq}_{T,300,eq} + L_{day,facade}$	0.73
	$L^{eq}_{T,300,eq}$	$L^{eq}_{T,300,eq} + L^{eq}_{BP,w,sel}$	0.0048 **

Table 6:. p value in ANOVA chi squared test comparing different models for predicting satisfaction with quality of life in the neighbourhood (Q1.1).

Still, the model based on exposure only, performs significantly worse than the model including noise annoyance and traffic intensity questions from the survey (Table 6). Thus it is useful to investigate whether traffic noise annoyance and reported (subjective) traffic intensity can accurately be modelled based on exposure indicators (the lower models in Figure 9). In Table 7 the significance of several exposure indicators in a logistic model for predicting street traffic noise annoyance and reported traffic intensities are shown. The indicators that come out significant in the noise annoyance model differ depending on the level of annoyance. For high to extreme annoyance, the noise level at the most exposed facade is the only significant indicator while for moderate to extreme annoyance and for "no annoyance at all", the exposure during trips should be added as an indicator. Previous work showed the importance of the noise level at the quiet side for perceived noise annoyance [20] but this effect could not be found here, probably because the noise level at the least exposed facade was not determined accurately enough.

		$L_{day,facade}$	$L_{day,quiet}$	N_{street}	$L^{eq}_{T,300,eq}$
Street traffic noise annoyance (Q2.1a)	order entered	1	2	3	4
	high to extreme	0.0034 **	0.74	0.69	0.47
	moderate to extreme	$1.7\ 10^{-7}$ ***	0.35	0.035*	0.0052 **
	not at all	$2.4\ 10^{-6}$ ***	0.55	0.51	$2.5\ 10^{-5}$ ***
Reported traffic intensity (Q1.8)	order entered	1	2	3	4
	little to very little	$6.2\ 10^{-5}$ ***	0.046 *	0.56	$2.7\ 10^{-6}$ ***
	heavy to very heavy	$3.4\ 10^{-10}$ ***	0.96	0.0089 **	$1.1\ 10^{-8}$ ***
Reported traffic intensity (Q1.8)	order entered	3	4	1	2
	little to very little	0.22	0.15	0.14	$1.3\ 10^{-9}$ ***
	heavy to very heavy	0.36	0.21	$1.4\ 10^{-4}$ ***	$3.3\ 10^{-15}$ ***

Table 7: p in chi squared test for logistic model predicting street traffic noise annoyance and reported traffic intensities

Table 8 shows that a model for moderate to extreme annoyance and a model for the absence of annoyance improve statistically significantly by adding the indicator for exposure

during the first 300m of trips: $L_{T,300,eq}^{eq}$. Adding additional factors to the model gives no significant improvement. In contrast to the model for satisfaction with the quality of life in the neighbourhood, $L_{day,facade}$ remains an important indicator. The geographical area referred to in the noise annoyance question: in and around your house, focuses attention more on the facade than the quality of life question that refers to the neighbourhood, which could explain this difference. It was nevertheless shown in previous work by Klaboe et al. [25] that the soundscape in the wider area also matters for rating noise annoyance at home, which seems to be confirmed here, at least if moderate to extreme annoyance is considered.

	Base model	Compare model	p
high to extreme	$L_{day,faccade}$	Full model of Table 7	0.85
moderate to extreme	$L_{day,faccade}$	$L_{day,facade} + L_{T,300,eq}^{eq}$	0.0017 **
	$L_{day,faccade} + L_{T,300,eq}^{eq}$	Full model of Table 7	0.20
not at all	$L_{day,facade}$	$L_{day,facade} + L_{T,300,eq}^{eq}$	$1.8\ 10^{-5}$ ***
	$L_{day,facade} + L_{T,300,eq}^{eq}$	Full model of Table 7	0.92

Table 8. p value in ANOVA chi squared test comparing different models for predicting reported street traffic noise annoyance (Q2.1a).

In the multiple logistic models for reported traffic intensity (Table 7), the number of vehicles in the street in front of the house, N_{street}, comes out rather insignificant when noise exposure indicators are added first. When N_{street} is added first, it becomes strongly significant for predicting heavy and very heavy traffic but not for predicting little traffic. In both cases noise exposure during trips is very significant. The model comparison in Table 9 confirms that adding noise exposure during the first part of trips helps very significantly in predicting both reported intensities of traffic. Thus, $L_{T,300,eq}^{eq}$ – although initially designed for predicting the quality of life in a neighbourhood – also mimics very well how persons sample traffic intensity in their neighbourhood. The most obvious explanation is that N_{street} only incorporates the traffic in the own street, while the noise indicator adds up the traffic in a larger area around the house. Another explanation might include the way people perceive traffic intensity which might include the noise level.

		$L_{day,facade}$	$L_{day,quiet}$	N_{street}	$L_{T,300,eq}^{eq}$
Street traffic noise annoyance (Q2.1a)	order entered	1	2	3	4
	high to extreme	0.0034 **	0.74	0.69	0.47
	moderate to extreme	$1.7\ 10^{-7}$ ***	0.35	0.035*	0.0052 **
	not at all	$2.4\ 10^{-6}$ ***	0.55	0.51	$2.5\ 10^{-5}$ ***
Reported traffic intensity (Q1.8)	order entered	1	2	3	4
	little to very little	$6.2\ 10^{-5}$ ***	0.046 *	0.56	$2.7\ 10^{-6}$ ***
	heavy to very heavy	$3.4\ 10^{-10}$ ***	0.96	0.0089 **	$1.1\ 10^{-8}$ ***
Reported traffic intensity (Q1.8)	order entered	3	4	1	2
	little to very little	0.22	0.15	0.14	$1.3\ 10^{-9}$ ***
	heavy to very heavy	0.36	0.21	$1.4\ 10^{-4}$ ***	$3.3\ 10^{-15}$ ***

Table 7: p in chi squared test for logistic model predicting street traffic noise annoyance and reported traffic intensities

	Base model	Compare model	p
high to extreme	$L_{day,facade}$	Full model of Table 7	0.85
moderate to extreme	$L_{day,facade}$	$L_{day,facade} + L^{eq}_{T,300,eq}$	0.0017 **
	$L_{day,facade} + L^{eq}_{T,300,eq}$	Full model of Table 7	0.20
not at all	$L_{day,facade}$	$L_{day,facade} + L^{eq}_{T,300,eq}$	$1.8\ 10^{-5}$ ***
	$L_{day,facade} + L^{eq}_{T,300,eq}$	Full model of Table 7	0.92

Table 8: p value in ANOVA chi squared test comparing different models for predicting reported street traffic noise annoyance (Q2.1a).

In the multiple logistic models for reported traffic intensity (Table 7), the number of vehicles in the street in front of the house, N_{street}, comes out rather insignificant when noise exposure indicators are added first. When N_{street} is added first, it becomes strongly significant for predicting heavy and very heavy traffic but not for predicting little traffic. In both cases noise exposure during trips is very significant. The model comparison in Table 9 confirms that adding noise exposure during the first part of trips helps very significantly in predicting both reported intensities of traffic. Thus, $L^{eq}_{T,300,eq}$- although initially designed for predicting the quality of life in a neighbourhood – also mimics very well how persons sample traffic intensity in their neighbourhood. The most obvious explanation is that N_{street} only incorporates the traffic in the own street, while the noise indicator adds up the traffic in a larger area around the house. Another explanation might include the way people perceive traffic intensity which might include the noise level.

	Base model	Compare model	P
little to very little	N_{street}	$N_{street} + L^{eq}_{T,300,eq}$	$1.3\ 10^{-9}$ ***
	$N_{street} + L^{eq}_{T,300,eq}$	Full model of Table 7	0.18
heavy to very heavy	N_{street}	$N_{street} + L^{eq}_{T,300,eq}$	$3.3\ 10^{-15}$ ***
	$N_{street} + L^{eq}_{T,300,eq}$	Full model of Table 7	0.31

Table 9: p value in ANOVA chi squared test comparing different models for predicting reported traffic intensity in the neighbourhood (Q1.8).

		$L_{day,facade}$	$L^{eq}_{T,300,eq}$	$L^{eq}_{BP,w,sel}$	N_{street}	*Constant*
Street traffic noise annoyance (Q2.1a)	High to extreme	0.046				-4.14
	Moderate to extreme	0.034	0.051			-5.33
	Not at all	-0.023	-0.075			4.55
Reported traffic intensity (Q1.8)	Little to very little		-0.11		$1.68\ 10^{-6}$	4.53
	Heavy to very heavy		0.11		$4.19\ 10^{-5}$	-6.26
Satisfaction with quality of life in neighborhood (Q1.1)	Satisfied		-0.045	0.084		-4.78
	Not satisfied		0.057			-5.14

Table 10: β coefficients in the multiple logistic regression models that were retained

To conclude and summarize, the β coefficients in the multiple linear regression models that include the minimal number of factors are given in Table 10.

5. Conclusions

The relationship between traffic noise and perceived quality of life in the neighbourhood was investigated by comparing the results of a survey with new types of exposure indicators focusing on noise exposure during trips from the house. The latter are calculated in an innovative way by sampling origins, destinations (shops, schools, etc.) and typical travel behaviour from several databases and reconstructing all possible trips leaving the dwelling.

The importance of traffic and traffic noise in reported quality of life in a neighbourhood is observed by analysing open questions on positive and negative aspects of coming to live in this neighbourhood; by analysing the relationship between the quality of life question and a standard noise annoyance question; and most importantly by obtaining multiple logistics models relating quality of life in the neighbourhood to noise exposure. The relationship between reported noise annoyance and quality of the living environment suggest that the pathway is a direct one, not relying on underlying hidden variables. Combining this analysis with a question on traffic intensity in the neighbourhood further suggests that the pathway from traffic through noise to quality of life in the neighbourhood accounts for the strongest relationship between traffic and quality of life. Other paths may contribute, but most probably to a much lesser extent.

Traffic noise exposure in the neighbourhood is assessed by estimating where people would drive their car and where they would walk close to their house while leaving for work, school, shopping or whatever other reason. In that way, the exposure indicators for noise exposure during trips account for the access routes and the location of the most important attraction poles close to the house, rather than merely considering a circular area around the house as the neighbourhood. Several ways of aggregating noise over the length of the trip and between trips are compared. Statistical analysis showed that calculating an equivalent level over the first 300m of each trip and aggregating over all trips using an equivalent level as well, $L_{T,300,eq}^{eq}$, results in the most significant improvement of models for noise annoyance at home and quality of the living environment. In addition, a restriction to trips made on foot or by bike improves the predictability of satisfaction with the quality of the living environment, but not of dissatisfaction with it. For noise annoyance at home, the level at the most exposed facade is still a dominant indicator. Adding the above mentioned indicator for noise exposure during trips improves the model for moderate to extreme annoyance and also the model for no annoyance at all. The positive effect of access to a quiet side on noise annoyance at home is not recovered probably because quiet side levels were not calculated accurately enough.

Most surprisingly at first sight, the indicator for noise exposure during trips is the most significant contributor to a model for quality of life in the neighbourhood. Adding facade

exposure to the model gives no improvement, which is a rather surprising result that is however understandable since the neighbourhood has a wider spatial meaning than just one's own dwelling. Similarly surprising is the observation that the same exposure indicator performs best in a model for perceived traffic intensity in the neighbourhood, more so than a traffic count on the street of the dwelling itself. At this point, it is only possible to propose a few hypotheses to explain this observation: traffic intensity might be judges via noise or the traffic aggregation embedded in the noise exposure indicator might be just the way to aggregate traffic intensities over an area that corresponds best to perceptive evaluation.

The logistic models obtained in this work provide an interesting step forward for building a general model for evaluating the overall impact of land use planning and mobility planning on the quality of life of a neighbourhood.

6. References and Notes

1. Guite, HF; Clark, C; Ackrill, G.,The impact of the physical and urban environment on mental well-being, in: Public health 120 (12), 2006, p. 1117-1126
2. A. Parks, A. Kearns, R. Atkinson, What makes people dissatisfied with their neighbourhoods?, in: Urban Studies, Vol. 39, No. 13, 2002, p. 2413-2438
3. L. Wirth, Urbanism as a way of life, in: American Journal of sociology 44, 1938
4. M. Baldassare, The effects of neighborhood density and social control on resident satisfaction, in: The sociologist quarterly 23, 1982
5. R.E. Adams, Is happiness a home in the suburbs? The influence of urban versus suburban neighborhoods on psychological health, in: Journal of community psychology 20, 1992
6. L Pan Ké Shon, Resident's perceptions of their neighbourhood: disentangling dissatisfaction, a French survey, in: Urban Studies, vol. 44, No. 11, October 2007, p. 2231-2268
7. N. Weinstein, Individual differences in reactions to noise: a longitudinal study in a college dormitory, in: Journal for Applied Psychology 63 (4), 1978
8. K. Zimmer, W. Ellermeer, Psychometric properties of four measures of noise sensitivity: a comparison, in: Journal of environmental psychology 19, 1999
9. K. Paunovic, B. Jakovljevic, G. Belojevic, Predictors of noise annoyance in noise and quiet urban streets in: Science of the total environment 407, 2009, p. 3707-3711
10. B. Jakovljevic, K. Paunovic, G. Belojevic, Road-traffic noise and factors influencing noise annoyance in an urban population, in: Environment international 35, 2009, p. 552-556
11. ISO/TS 15666:2003, Acoustics -- Assessment of noise annoyance by means of social and socio-acoustic surveys, 2003
12. Jonasson, H.G., Acoustical Source Modelling of Road Vehicles, in: Acta Acustica united with Acustica, Volume 93, Number 2, March/April 2007 , pp. 173-184(12)
13. Salomons, E. M., Henk Polinder, Walter J. A. Lohman, Han Zhou, Hieronymous C. Borst, and Henk M. E. Miedema, Engineering modeling of traffic noise in shielded areas in cities, in: Journal of the Acoustical Society Of America. 126, 2340, 2009
14. De Coensel B., Dick Botteldooren, Tom De Muer, Birgitta Berglund, Mats E. Nilsson, and Peter Lercher, A model for the perception of environmental sound based on notice-events, in: Journal of the Acoustical Society Of America 126, 656, 2009
15. D. Botteldooren, B. De Coensel, T. De Muer, The temporal structure of urban soundscapes, in: Journal of Sound and Vibration, Volume 292, Issues 1-2, 25 April 2006, Pages 105-123

16. De Coensel, Bert; Botteldooren, Dick, The Quiet Rural Soundscape and How to Characterize it, in: Acta Acustica united with Acustica, Volume 92, Number 6, November/December 2006 , pp. 887-897
17. Jin Yong Jeon, Pyoung Jik Lee, Jin You, and Jian Kang, Perceptual assessment of quality of urban soundscapes with combined noise sources and water sounds, in: Journal of the Acoustical Society Of America 127, 1357, 2010
18. Carolien Beckx, Luc Int Panis, Theo Arentze, Davy Janssens, Rudi Torfs, Steven Broekx, Geert Wets, A dynamic activity-based population modelling approach to evaluate exposure to air pollution: Methods and application to a Dutch urban area, in: Environmental Impact Assessment Review, Volume 29, Issue 3, April 2009, Pages 179-185
19. Ryan W. Allen, Hugh Davies, Martin A. Cohen, Gary Mallach, Joel D. Kaufman, Sara D. Adar, The spatial relationship between traffic-generated air pollution and noise in 2 US cities, in: Environmental Research, Volume 109, Issue 3, April 2009, Pages 334-342.
20. E. Ohrstrom, A. Skanberg, H. Svensson, A. Gidlof-Gunnarsson, Effects of road traffic noise and the benefit of access to quietness, in: Journal of Sound and Vibration, Volume 295, Issues 1-2, 8 August 2006, Pages 40-59.
21. Eva Leslie, Ester Cerin, Are perceptions of the local environment related to neighbourhood satisfaction and mental health in adults?, in: Preventive Medicine, Volume 47, Issue 3, September 2008, Pages 273-278.
22. O'Campo, P; Salmon, C; Burke, J. Neighbourhoods and mental well-being: What are the pathways?. In: Health & Place 15 (1), 2009, p. 56-68
23. Botteldooren D, Verkeyn A, Lercher P., Noise Annoyance Modelling using Fuzzy Rule Based Systems, in: Noise Health 4(15), 2002, p. 27-44.
24. Gidlof-Gunnarsson, A; Ohrstrom, E. , Noise and well-being in urban residential environments: The potential role of perceived availability to nearby green areas, in: Landscape and urban planning 83 (2-3), 2007, p. 115-126
25. Klaboe R, Kolbenstvedt M, Fyhri A, et al. The impact of an adverse neighbourhood soundscape on road traffic noise annoyance. in: Acta Acustica united with Acustica, 91 (6), 2005, p. 1039-1050.

D Guidelines for participatory noise sensing based on analysis of high quality mobile noise measurements

Published: Dekoninck, Luc, Dick Botteldooren, and Luc Int Panis. "Guidelines for Participatory Noise Sensing Based on Analysis of High Quality Mobile Noise Measurements." Proceedings of the 41st International Congress and Exposition on Noise Control Engineering (Inter-Noise 2012). Institute of Noise Control Engineering, 2012.

1. Introduction

Mobile noise measurements are a popular theme in noise exposure modelling. (Eisenman et al., 2009; Kanjo et al., 2010, Maissonneuve et al., 2009). They can be useful to enhance noise mapping and noise exposure modelling by adding more detailed emission parameters related to the traffic dynamic which are currently only rarely included in the noise mapping procedures. Mobile noise measurements can be done with low intrusive measurement equipment like dosimeters and the new mobile technologies. Noise is also strongly related to the traffic related air pollution exposure and might be a good proxy to model personal air pollution exposure (Can et al, 2011; Can et al, 2011b; De Coensel et al. 2007; Eisenman et al. 2009, Foraster et al., 2011).

An experiment was set up measuring both the noise and black carbon exposure on a bicycle for one year, travelling many different roads in actual commuting condition (during rush hour). From this experiment, the noise measurements are used to predict the black carbon exposure. In this paper, we focus on the noise properties that proved to be relevant in the modelling of BC. These findings are compiled in a set of guidelines and recommendations for future projects assessing mobile noise exposure measurements. If the guidelines are fulfilled the potential to use the mobile noise measurements as a proxy for air pollution related exposure will dramatically improve.

First, we will address the theoretical aspects of both noise emission and air pollution in relation to the traffic dynamics, identifying the potential correlations between the spectral content of the mobile noise measurements and the vehicle exhaust dynamics. In a second section, we will address the properties of the mobile noise measurements and present the spatial evaluations. In a third section, we will present the noise parameters with the best correlation to the black carbon and discuss the effect of the sparse sampling and its stability for both noise and black carbon. Finally, a set of guidelines are compiled to perform future mobile noise measurements.

2. Theoretical aspects of traffic noise and air pollution

Both noise level and the local component of air pollution can be attributed to traffic. By investigating theoretical emission of noise and air pollutants in typical traffic flows, noise indicators that can be used as proxies for air pollution can be identified. For this purpose, the noise emission was modelled according the Harmonoise model (Salomons et al, 2011) and the air pollution was modelled according to the Versit+ emission model (Smit et al., 2007). A realistic set of speed and acceleration data is retrieved from a traffic micro-simulation model in a major city in Flanders. For each combination of speed and acceleration the corresponding one-third octave band noise emission spectrum and the air pollution emission (CO_2, NO_x and PM_{10}) was calculated for a standard vehicle (person car type). The one-third octave bands were aggregated in four groups, each presenting a typical part of the spectrum. Base frequencies, $L_{OBFeq,1s}$, is defined as the energetic sum of bands 25 to 80 Hz, low frequency, $L_{OLFeq,1s}$ sums bands 100 to 200 Hz, mid frequency, $L_{OMFeq,1s}$ bands 400 and 500 Hz, and finally high frequency, $L_{OHFeq,1s}$, bands 1000 to 2000 Hz. In Table 1, the cross correlation between air pollutant emission per second of the vehicle stream and the noise indicators defined above, is given for the urban driving test situation. The air pollution parameters are log10 converted to match the noise evaluation.

	$L_{Aeq,1s}$	$L_{OBFeq,1s}$	$L_{OLFeq,1s}$	$L_{OMFeq,1s}$	$L_{OHFeq,1s}$	$L_{HFmLF,1s}$
Log10(CO_2)	0.358	0.913	0.665	0.522	0.305	-0.195
Log10(NO_x)	0.633	0.890	0.857	0.764	0.580	0.020
Log10(PM_{10})	-0.073	0.721	0.313	0.091	-0.120	-0.476

Table 1: Correlation table for the spectral noise parameters versus air pollution parameters.

The correlation between the low frequency noise indicators $L_{BLFeq,1s}$ and $L_{OLFeq,1s}$ and the air pollution emissions is in general higher than the correlation between L_{Aeq} and these emissions. This is not unexpected. The Harmonoise emission model relates high frequency noise emissions mainly to rolling noise and low frequency noise emission mainly to engine and drive train noise. In addition, acceleration increases engine power and thus increases the low frequency contribution. The A-weighted total noise emission is clearly determined by the higher frequencies, corresponding with the rolling noise and as such a less useful indicator for air pollutant emission. It nevertheless increases linearly with the number of vehicles, as does the overall air pollutant emission. CO_2 emission is directly related to the power produced by the engine and thus is expected to be somewhat correlated to high frequency components since they indicate high driving speed. The difference $L_{HFmLF,1s}$ between high and low frequencies is thought to be more exclusively related to rolling noise and thus correlates poorly with CO_2 emission. For particulate matter emission (PM_{10}), the correlation of the noise parameters decreases quite strongly from $L_{BLFeq,1s}$ to $L_{OLFeq,1s}$, $L_{OMFeq,1s}$, L_{Aeq} and $L_{OHFeq,1s}$. The relationship of PM_{10} emission with engine power is more difficult since PM_{10} is a product

of incomplete combustion and thus peaks during accelerating and decelerating. Accelerating increases (low-frequency) noise but decelerating does not, yet after a deceleration phase, an acceleration phase is expected.

3. Measurement setup

3.1. Measurement equipment and setup

Measurements of noise and air pollution (Black Carbon) are performed while commuting by bicycle. The experimental setup contains a basic GPS (in a HTC Desire smart phone), a Type 1 Noise Level Meter (Svantek 959) and a micro-aethalometer (Model AE51 MageeScientific, 2009) to measure Black Carbon. The measurement equipment was mounted in a bicycle bag and attached to the steering wheel. The GPS device was put on top of the bag to get the best possible gps readings. The noise equipment is calibrated on regular intervals using a Svantek SV30A Acoustic calibrator. One-third octave band spectra are measured with a time interval of 1/10 second. The very short time interval was chosen for different reasons.

- Biking in itself is noisy so the effect on the noise measurement has to be evaluated. The impact of the type and quality of road surface on the noise measurements was evaluated but was not significant.
- A short measurement also allows detecting single car passage noise events. At a time resolution of one second it would be impossible to separate and count the consecutive vehicle passages.

3.2. Location and measurement period

The measurements were performed while commuting by bicycle in suburban and urban areas in Ghent, Flanders (The third city of Belgium with a population of 250.000 and population density is 1500 people per km2). Ghent is located at the intersection of two important highways, has a major port and industrial area. The medieval inner city mainly has three storey buildings. It is surrounded by suburbs and villages where a mixture of detached houses and street canyons of two floor buildings can be found. High rise buildings are relatively rare. The commuting trips are performed from the villages to the west of the city into the city centre, covering the sparse build areas in the villages, the city centre, and open recreational areas and natural reserves in between. The majority of the measurements are performed during the morning and evening rush hour over a period of 12 months, not including public holidays (December 2010 to November 2011). Since all measurements are conducted in rush hour conditions during normal working days, the typical traffic situation is in first order constant for each observation at a given location.

The geographic scope of the trips was extended to measure a diverse mixture of traffic types (pedestrian zone, bus routes etc…), spatial layout (highways, street canyons, local ring roads, medieval city centre, etc.) and special biking facilities (dedicated cycle paths, underpasses…). A total of 209 biking trips were performed, covering a distance of 2300 kilometre, a total measurement time of 128 hours at an average speed of 18 km per hour. Over 75 km of roads were sampled at least 3 times.

3.3. Data cleaning and aggregation

Cleaning of the GPS and Black Carbon (BC) data will not be addressed in detail since this is not the main topic of this article. The contribution of local traffic to the measured BC concentration is of main interest so the background level measured by an official measurement station in the neighbourhood is subtracted from the measurement. The local contribution BC_{loc} for a location *i* and a time *j*, can be written as:

$$BC_{loc,i,j} = BC_{i,j} - BC_{j,background}$$

The noise measurements are pre-processed to a one second resolution at the one hand by calculating the one-second equivalent level, $L_{Aeq,1s}$, at the other hand by selecting the lowest 100 ms, $L_{Amin,1s}$. In addition, the frequency band sums defined in Section 2 are calculated. The measurements are mapped to the traffic network by using aggregation points, p_x, along the network with an interspatial distance of 50 m. The gps-locations are matched to the nearest aggregation point on the network, including restrictions on driving direction and bicycles' accessibility. For each specific passage, $trip_j$, at a specific aggregation point the arithmetic average of all one second measurements is calculated and this for all indicators defined above. For example for L_{Aeq}:

$$L_{Aeq,trip_j,p_x} = \frac{1}{n}\sum_{i=1}^{n} L_{Aeq,1s}\left(t_i, trip_j, p_x\right)$$

With *n* the number of samples for *trip j* at p_x and $L_{Aeq,1s}\left(t_i, trip_j, p_x\right)$ the samples for *trip j* at p_x. Note that the number of samples will be influenced by the cycling speed during a trip at a location. At the typical speed of 18 km/h the distance of 50 m between the aggregation points is covered in 10 seconds so *n* will be 10. Finally the arithmetic average (Avg), standard deviation (sd), and error on the mean (sderror) over the different trips is calculated for all parameters.

4. Analysis of sparse NOISE measurements

4.1. Spatial variation of noise parameters

Figure 1 presents $Avg(L_{Aeq})_{p_x}$ and $Avg(L_{OLF})_{p_x}$ for the aggregation points with at least three bicycle passages. The engine related noise $Avg(L_{OLF})_{p_x}$ is potentially and important indicator for predicting air pollution as derived in Section 2. In both figures, high density roads are clearly visible.

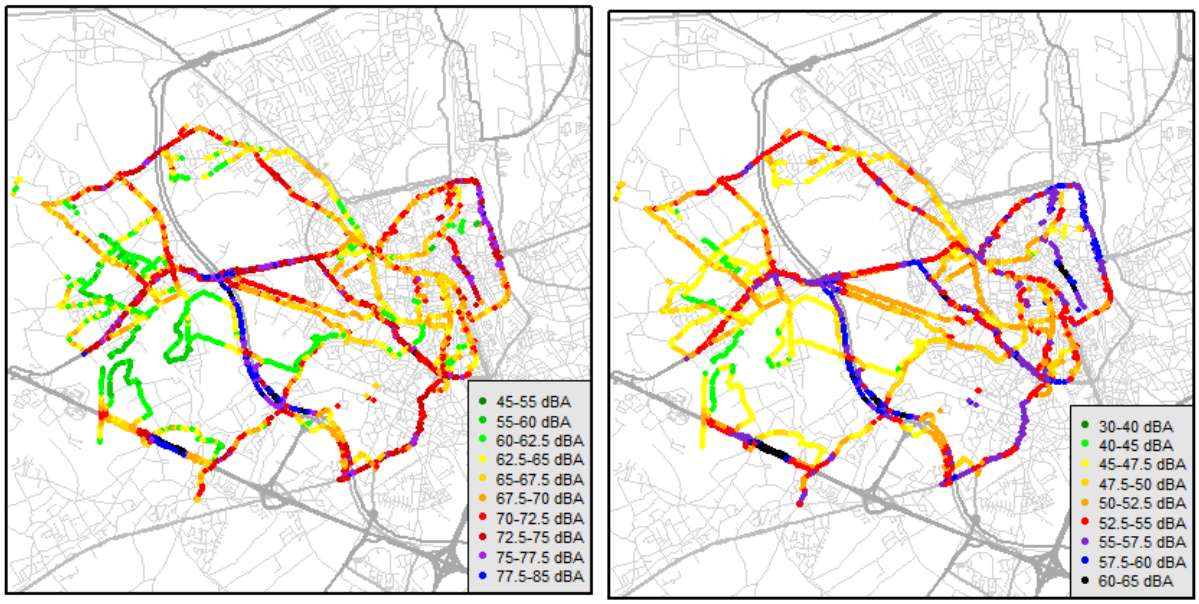

Figure 1: $Avg(L_{Aeq})_{p_x}$ (upper) and $Avg(L_{OLF})_{p_x}$ (lower) in the aggregation points along the network.

It is important to notice the spatial smoothness of $\mathrm{Avg(L_{OLF})_{p_x}}$ compared to $Avg(L_{Aeq})_{p_x}$. Thus in addition to potentially being a better indicator for air pollution, the low frequency component of the noise also seems less sensitive to errors introduced by the sparse sampling probably because of lower sensitivity to disturbing sounds. Important in this spatial evaluation is the emergence of the dynamic traffic conditions in the vicinity of traffic lights where vehicles accelerate. The local noise propagation situation is also influencing the results, for example near the highway bank and noise screen. Three different sections are visible: one part with the highway on a bank, the middle part at the same level of the highway and a third section behind a noise barrier (from North to South). When a bicycle path near a major road is diverging from the traffic lanes, $Avg(L_{OLF})_{p_x}$ is showing an immediate drop, showing detailed spatial effects. The biking trips also sampled on two roads parallel to the highway.

4.2. Statistical analysis of the effect of sparse sampling

Mobile measurements are sparsely sampled databases. The potential use of a parameter depends on its sensitivity to errors introduced by the sparse sampling since less sensitive

parameters require less measurement trips. Moreover they will result in more reliable indicators for air pollution as well. The statistics (mean, percentile intervals, and outliers) of the standard deviations $sd(L_{OLF})_{p_x}$ and $sd(L_{Aeq})_{p_x}$ over all locations p_x, are shown in Figure 2 as a function of value classes. The mean and upper percentiles of $sd(L_{OLF})_{p_x}$ are lower than the corresponding values of $sd(L_{Aeq})_{p_x}$ indicating indeed that $Avg(L_{OLF})_{p_x}$ is less sensitive to sparse sampling than $Avg(L_{Aeq})_{p_x}$. It is also important to note the strong dependence of $sd(L_{Aeq})_{p_x}$ on the parameter value. This results from the event-like time series of $L_{Aeq,1s}$ in the aggregation points: low levels correspond to cycling routes free of traffic so only the slowly varying background contributes while very high values are caused by roads carrying so much traffic that the sparse sampling again does not result in high variability.

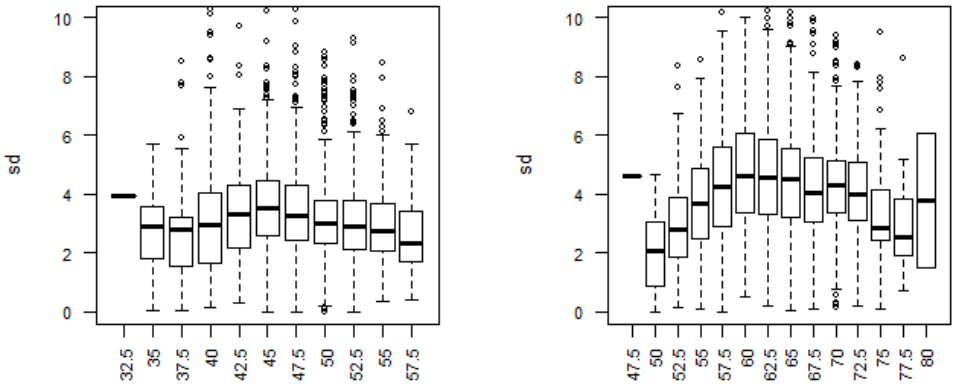

Figure 2: Statistics (median, percentile intervals, outliers) over locations p_x of the standard deviation $sd(L_{OLF})_{p_x}$(left) and $sd(L_{Aeq})_{p_x}$ (right) as a function of 2.5 dB value classes of $Avg(L_{Aeq})_{p_x}$.

The relation between the standard error on the average and the number of passages is shown in Figure 3. The median over all observation points, p_x, of the standard error of $Avg(L_{OLF})_{p_x}$ drops below 1 dB if 4 or more passages are available. Similar results are found for $Avg(L_{OMF})_{p_x}$ and $Avg(L_{HFmLF})_{p_x}$. $Avg(L_{OHF})_{p_x}$, $Avg(L_{OHF})_{p_x}$ and $Avg(L_{Aeq})_{p_x}$ show higher standard errors, with median dropping below 1dB only when more than 10 passages are available.

The standard deviation as a function of the number of passages is also shown in Figure 3. The values are more or less constant for categories with more than 4 passages, which is the hypothesis underlying the analysis of the standard error.

A theoretical evaluation to predict the effects of sparse sampling was performed by Makarewicz (Makarewicz, 2006). His model predicted the error of approximation on simulated data to be 1.3 dB when using 10 samples. In our measurements, we found a median value of the standard error for $Avg(L_{Aeq})_{p_x}$ of 1.5 dB, which leads to the conclusion that the theoretical model slightly under predicts the measurement error. The standard error of $Avg(L_{Aeq})_{p_x}$ exceeds 2 dB for a significant part of the distribution.

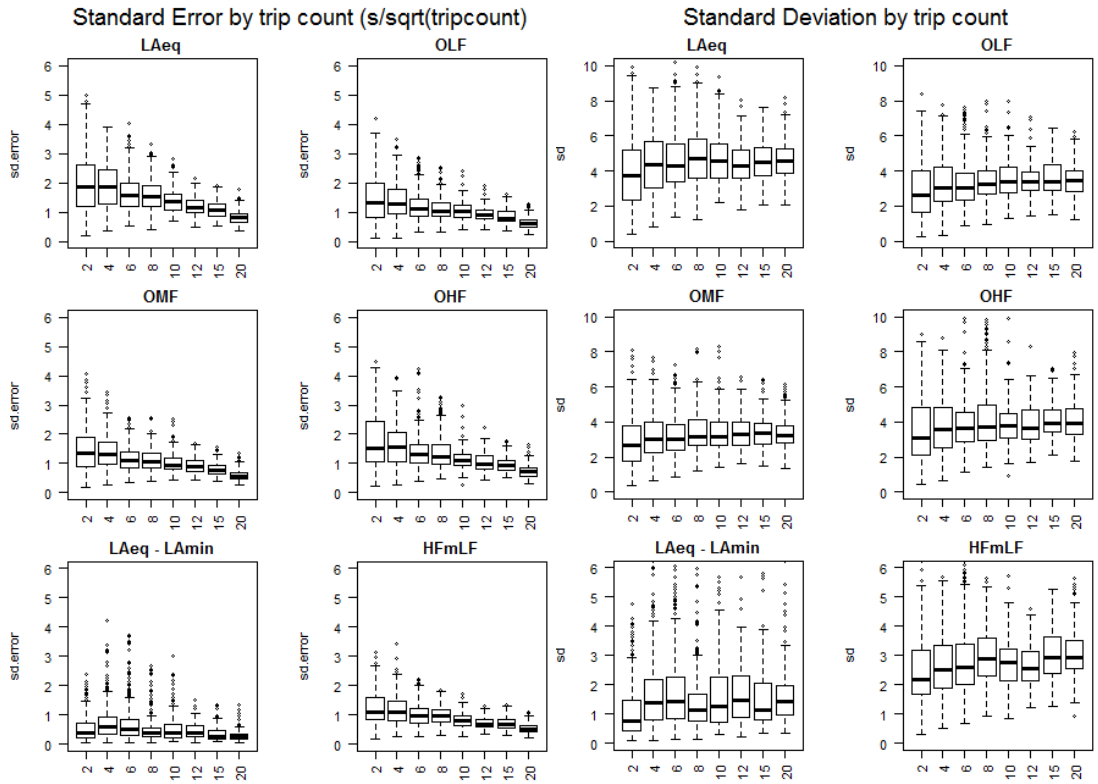

Figure 3: Statistics (median, percentile intervals, outliers) over locations p_x of the standard error (left) and standard deviation (right) as a function of the number of passages.

4.3. Principal component analysis of the mobile noise measurements

A principal component analysis over all measurement locations was performed on the noise parameters. The results are shown in Table 2. In the first component which explains 70% of variance,$Avg(L_{Aeq})_{p_x}$,$Avg(L_{OBF})_{p_x}$, $Avg(L_{OLF})_{p_x}$, $Avg(L_{OMF})_{p_x}$.and $Avg(L_{OHF})_{p_x}$ have a similar strength. It can be expected that this component is mainly related to traffic intensity since this affects all of the above mentioned parameters in a similar way. The second and the third component explain 14% and 13 % of the variance, respectively. The second component is almost completely defined by $Avg(L_{Aeq} - L_{Amin})_{p_x}$, related to the short term noise dynamics. The third component is mainly explained by $Avg(HFmLF)_{p_x}$, the spectral content of the noise immission. The orthogonality of the spectral content and the noise temporal dynamics is relevant since they describe different traffic conditions. This supports the use of partial spectral evaluations and confirms the added value of $Avg(L_{Aeq} - L_{Amin})_{p_x}$. and $Avg(HFmLF)_{p_x}$ in the mobile noise evaluation.

Importance of components:				
	Comp.1	Comp.2	Comp.3	Comp.4
Standard deviation	2.219	0.998	0.942	0.339
Proportion of Variance	0.704	0.142	0.126	0.016
Cumulative Proportion	0.704	0.846	0.973	0.989
Loadings				
$Avg(L_{Aeq})_{p_x}$.	0.430	-0.219		-0.121
$Avg(L_{Aeq-Amin})_{p_x}$.	-0.118	-0.964		0.171
$Avg(OBF)_{p_x}$.	0.398		-0.392	0.807
$Avg(OLF)_{p_x}$.	0.424		-0.323	-0.257
$Avg(OMF)_{p_x}$.	0.438			-0.410
$Avg(OHF)_{p_x}$.	0.443		0.165	
$Avg(HFmLF)_{p_x}$.	0.272		0.838	0.256

Table 6.4-1: Principal Component Analysis of the aggregation points along the network.

4.4. Correlation with Black Carbon measurements

The correlation between the log-transformed averaged local component of black carbon concentration $\mathrm{Log10}(Avg(BC_{local}))_{p_x}$ in the aggregation points and the different noise parameters is calculated restricted to aggregation points with a minimum of five passages (Table 3). Restricting the aggregation points to a minimum of five passages corresponds with a third quartile of standard error of $Avg(L_{Aeq})_{p_x}$ below 2 dB and a third quartile of the standard error of $Avg(L_{OLF})_{p_x}$below 1.5 dB. The strongest correlation is found for $Avg(OLF)_{p_x}$, $Avg(OMF)_{p_x}$, both for the Pearson and Spearman correlation.

The correlation of $Avg(L_{Aeq})_{p_x}$. is slightly lower than the correlation of these partial spectral evaluations. The difference is not as prominent as theoretically predicted in Section 2 because traffic intensity is not taken into account in Section 2 and it was found that this factor explains a large amount of the variance in the data. More importantly, the correlation of $Avg(L_{Aeq}-L_{Amin})_{p_x}$. and $Avg(HFmLF)_{p_x}$ with $\mathrm{Log10}(Avg(BC_{local}))_{p_x}$ is low or negative.

In Figure 4 the relation of $10.\mathrm{Log10}(Avg(BC_{local}))_{p_x}$ is plotted versus $Avg(L_{Aeq})_{p_x}$, $Avg(OLF)_{p_x}$, $Avg(L_{Aeq}-L_{Amin})_{p_x}$ and $Avg(HFmLF)_{p_x}$ for the aggragation points with at least 5 passages. The stronger correlation of BC with $Avg(OLF)_{p_x}$ compared to $Avg(L_{Aeq})_{p_x}$ is clearly visible. $Avg(HFmLF)_{p_x}$ shows a non linear relationship with the black carbon exposure.

	Minimum 5 passages	
Noise Parameter	Pearson	Spearman
$Avg(L_{Aeq})_{p_x}$.	0.593	0.601
$Avg(L_{Aeq} - L_{Amin})_{p_x}$	-0.246	-0.296
$Avg(OBF)_{p_x}$.	0.614	0.624
$Avg(OLF)_{p_x}$.	0.652	0.664
$Avg(OMF)_{p_x}$.	0.656	0.667
$Avg(OHF)_{p_x}$.	0.590	0.598
$Avg(HFmLF)_{p_x}$.	0.320	0.341

Table 3: Pearson and Spearman correlation between$Log10(Avg(HFmLF))_{p_x}$. and the different noise parameters for aggregation points with a minimum of five passages.

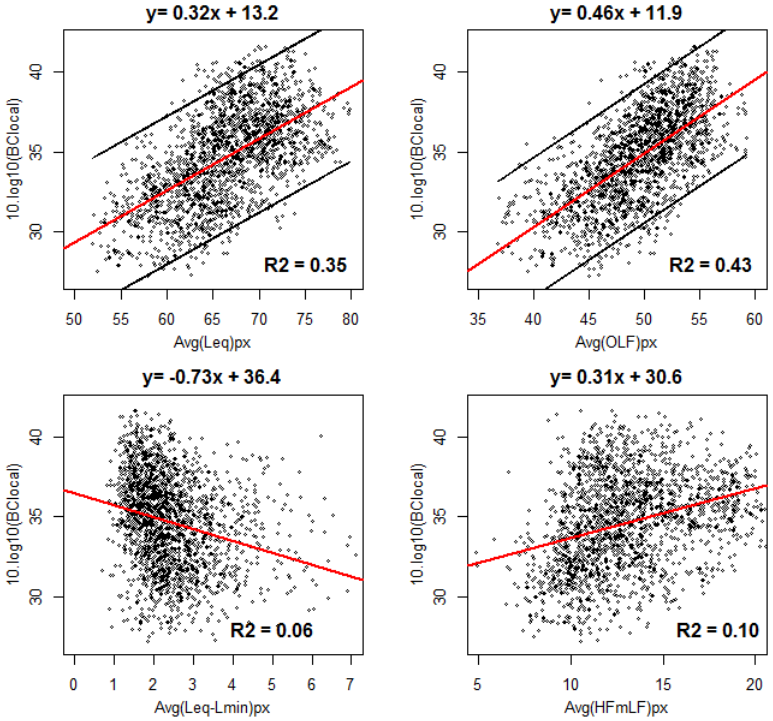

Figure 4: Linear model of Black Carbon $(\mathbf{10}.\boldsymbol{Log10}(\boldsymbol{Avg}(\boldsymbol{BC_{local}}))_{p_x})$ with $\boldsymbol{Avg}(\boldsymbol{L_{Aeq}})_{p_x}$., $\boldsymbol{Avg}(\boldsymbol{OLF})_{p_x}$. $\boldsymbol{Avg}(\boldsymbol{L_{Aeq}} - \boldsymbol{L_{Amin}})_{p_x}$ and $\boldsymbol{Avg}(\boldsymbol{HFmLF})_{p_x}$. Prediction intervals 95%) are included for $\boldsymbol{Avg}(\boldsymbol{L_{Aeq}})_{p_x}$. and $\boldsymbol{Avg}(\boldsymbol{OLF})_{p_x}$.

The overall correlation of the noise parameters with the Black Carbon is good, but not as strong as expected on the basis of theoretical considerations on emission. This is caused by the strong disturbances of the Black Carbon exposure by local dispersion parameters such as street canyon effects. Modelling air pollution based on noise exposure will therefore have to include local dispersion properties of air pollution to result in a useful model.

5. Discussion and guidelines for mobile noise measurements

Based on a one year mobile measurement campaign for noise and black carbon, insight was gained on (1) the use of sparse measurement for traffic noise exposure mapping purposes; (2) the use of noise as a proxy for black carbon exposure assessment.

The standard error on L_{Aeq} is comparable to earlier theoretical work. For this typical European city and suburb, the variability in the standard error on the sparse measurement over locations is important yet not disastrous. With 10 observations of about 10 seconds – the duration of cycling the 50m measurement grid cell – for example, the standard error on the L_{Aeq} is below 1.5 dBA for half of the locations while it is below 2.5 dBA for 95% of the locations. The measurement error depends on L_{Aeq} with standard deviations between measurements at a given location peaking between 57.5 and 72.5 dBA. At higher and lower noise levels standard deviations drop and the number of measurements can be reduced with up to a factor of 2 while keeping the measurement error similar. This is also in line with earlier findings.

In view of the use of noise as a proxy for assessing exposure to black carbon, it was theoretically expected that the low frequency part of the noise, L_{OLF} would be of importance because it has a higher theoretical correlation with air pollution emission. This component shows some interesting characteristics. Investigating the effect of the standard deviation as a function of the number of passages shows a median standard deviation of the L_{OLF} between 2.5 and 3.5 over the full range of passages, and a median standard error of 4 to 5 dB for the L_{Aeq} evaluation. The low frequencies are more stable than the L_{Aeq} evaluation and have therefore a stronger potential to result in stable models for black carbon exposure. A similar effect is visible for the standard error. The median standard error of L_{OLF} reaches 1.5 dB starting from 5 passages, a level that is not even met with 10 passages for the L_{Aeq}. The spatial difference between the L_{Aeq} and L_{OLF} is also showing some interesting features related to the local traffic noise emission. Near crossings, traffic lights and roads with dense and congested traffic the L_{OLF} results in relatively higher levels than L_{Aeq}. This indicates a stronger contribution of the engine noise in the overall noise level at these areas and potentially higher emission of air pollutants.

Additional noise indicators that could be useful proxies for black carbon were investigated. Principle component analysis shows that the L_{Aeq} and all spectral indicators match an underlying factor explaining most of the variance, probably straight forward traffic intensity. As expected on the basis of theoretical emissions, L_{OLF} correlates best with BC exposure measurements amongst the single indicators in this factor. A second principle component relates to the difference between one second L_{Aeq} and minimum value. This could be an indicator of continuous traffic flow or larger distance between the cyclist and the motorized road traffic. The third component relates to the spectral content, the amount of high frequencies compared to low frequencies. Although their correlation with BC concentration is

weaker than the correlation with the first component, these two additional orthogonal indicators could prove useful in modelling BC exposure on the basis of noise monitoring.

When there is an interest in analysing traffic noise for example for predicting air pollution it is therefore recommended to measure at least one-third octave band spectra and repeat measurements at least every second but preferably ten times per second. A statistical evaluation (min/max) within the sampled second might be an alternative to the sub second time sampling.

6. Conclusions

Mobile noise measurements (bicycle, on foot) have the potential to improve the noise mapping by introducing local noise characteristics currently not including in the noise mapping. In this paper it was shown on the basis of an extensive measurement campaign that accurate results can be obtained with as few as ten to twenty passages at every grid location.

Spectral and temporal information can give insight in traffic dynamics and related perception of the sonic environment. These traffic dynamics might be even more important when it comes to predicting exposure to air pollution caused by local traffic sources. To ensure the extended use of the mobile noise measurements, a good temporal resolution and a detailed spectral evaluation in third octave bands is recommended.

7. References

Can, A. and D. Botteldooren (2011). "Towards Traffic Situation Noise Emission Models." Acta Acustica United with Acustica 97(5): 900-903.

Can, A., L. Dekoninck, et al. (2011). "Noise measurements as proxies for traffic parameters in monitoring networks." Science of the Total Environment 410: 198-204.

Can, A., L. Leclercq, et al. (2010). "Traffic noise spectrum analysis: Dynamic modeling vs. experimental observations." Applied Acoustics 71(8): 764-770.

De Coensel, B., D. Botteldooren, et al. (2007). "Microsimulation based corrections on the road traffic noise emission near intersections." Acta Acustica United with Acustica 93(2): 241-252.

Eisenman, S. B., E. Miluzzo, et al. (2009). "BikeNet: A Mobile Sensing System for Cyclist Experience Mapping." Acm Transactions on Sensor Networks 6(1).

Foraster, M., A. Deltell, et al. (2011). "Local determinants of road traffic noise levels versus determinants of air pollution levels in a Mediterranean city." Environmental Research 111(1): 177-183.

Kanjo, E. (2010). "NoiseSPY: A Real-Time Mobile Phone Platform for Urban Noise Monitoring and Mapping." Mobile Networks & Applications 15(4): 562-574.

Maisonneuve, N., M. Stevens, et al. (2009). "NoiseTube: Measuring and mapping noise pollution with mobile phones." Information Technologies in Environmental Engineering: 215-228.

Makarewicz, R. and R. Golebiewski (2006). "Estimation of the A-weighted long term average sound level." Acta Acustica United with Acustica 92(4): 574-577.

Salomons, E., D. van Maercke, et al. (2011). "The Harmonoise Sound Propagation Model." Acta Acustica United with Acustica 97(1): 62-74.

Smit, R., R. Smokers, et al. (2007). "A new modelling approach for road traffic emissions: VERSIT+." Transportation Research Part D-Transport and Environment 12(6): 414-422.

E In-vehicle Black Carbon exposure: Supplementary data.

1. Data preparation and covariates

1.1. Measurements data processing

1.1.1. Manual trip preparation

The participants had a choice to start and stop the equipment before and after every trip, but since the sales representatives found this too difficult, the equipment ran all day on the passenger seat. In the post, processing phase the quality of the measurements was evaluated and the start and the end of the trips was defined to clip all stops from the data series. The low quality GPS measurements were also removed.

1.1.2. Map matching the GPS data

GPS data is known to express certain spatial errors. A map matching procedure is developed to move the measured GPS point to the most likely road segment. This procedure is performed for both measurement campaigns. This was the trip assessment matched the centre of the roads and the noise evaluation always results in the maximum value at the position of the road.

1.1.3. Spatial and temporal attribution

The car trip data is merged at a one-second resolution with a 20 seconds running average function for the GPS and BC readings. This one-second data series is aggregated to 10 seconds to build the dataset used in the modelling process. In this set, the necessary lag operations are added.

1.1.4. Diurnal correction of L_{DEN} noise map

The diurnal correction is based on the average diurnal traffic pattern over all segments in the external traffic dataset (year 2012), see appendix B. The correction is converted into dB and referenced to the L_{DEN} value of the averaged diurnal pattern (see Table 1).

hour	0	1	2	3	4	5	6	7	8	9	10	11
diurnal_dl	-14.8	-7.3	-9.5	-11.2	-11.6	-10.1	-6.5	-2.9	0.2	1.6	1.3	0.5
hour	12	13	14	15	16	17	18	19	20	21	22	23
diurnal_dl	0.3	0.6	1.3	1.3	1.5	2.2	2.7	2.4	1.0	-0.8	-2.1	-3.1

Table 1: Diurnal correction of the L_{DEN} map in dB.

1.2. Covariates description

Speed and acceleration: The speed and acceleration are calculated based on the sequence of position resulting from the GPS evaluations (on a 10-second basis for speed and the instantaneous and next position for the acceleration).
Relative speed: The speed limit of the road is retrieved from the traffic database (set to the maximum of the speed over the 24 hours of the day). De speed in that dataset is sensitive to the actual traffic situation. By using the maximum, the speed limit is retrieved.
Meteo: External data is available at a temporal resolution of 30 minutes. No additional smoothing is applied.
L_{DEN} noise mapping: map matched data point is matched to the 20 m grid.
Lday conversion: A fixed correction for all roads is applied based on the average diurnal pattern for the traffic dataset over a full year. No sensitivity to road type included.
Traffic counts (hourly): measurement hour and actual road link back to the traffic dataset (weekdays only). Heavy vehicles count as two.
Traffic counts (AAWT): Actual road link back to the traffic dataset. Sum all traffic for the actual road, weight of heavy vehicles is two.
PM_{10} map: mapped to grid of spatial resolution 100 m.
Street Canyon Index: Find closest street canyon evaluation.

2. Intermediate results

2.1. In-vehicle exposure lag and weighting of the data

Ventilation settings and influence of the speed of the vehicle on the ventilation is addressed by Hudda et al., 2011, Knibbs et al., 2010, Fruin et al., 2011). The strongest effects are found when the ventilation is set to in-vehicle recirculation, a condition were the in-vehicle air is only renewed at a very low pace, mainly through leakage of the cabin (Hudda et al., 2012). An experiment while measuring both the outside and inside concentrations at a location with very constant outdoor UFP levels showed a drop of the in-vehicle concentrations of more than 80% compared to the outside concentration for in-vehicle recirculation. The authors also mention that this condition will only occur for long trips since this equilibrium condition is only reached after 15-20 minutes. When the ventilation is set to outside airflow the levels drop with 20% compared to the outside air at low airflow exchange rates and with 40% at high air exchange rate. These equilibrium conditions are reached in 5-10 minutes with constant outdoor UFP concentrations. Another interesting finding in other experiments is the strong increase of the in-vehicle CO_2 concentration while driving at recirculation settings, easily reaching 5000 ppm. CO_2 is known to cause headaches, rapid long ventilation, dizziness, sweating and increased lung ventilation. Since the recirculation has direct effects on the personal well-being, the long time before the equilibrium situation is reached and the

known high spatial and temporal variability along the trajectories, the authors conclude that these conditions will not be abundant in a real life personal in-vehicle exposure sample (Hudda et al., 2011). Knibss examined air exchange rates while driving through a long tunnel with five different passenger cars, measuring UFP. Outdoor and indoor concentrations were often similar but important effect of airflow rate, vehicle type and age were found (Knibbs et al., 2009). A more extensive study by Fruin builds a model to predict the airflow rate based on age, mileage, speed of the car and a manufacture specific adjustment (Fruin et al., 2011) While the fan setting was not significant. Within the mentioned references, the authors attempted to avoid changing concentrations along the routes. When investigating the effect of ventilation settings, several authors estimated the lag between outdoor and indoor concentrations changes. At 'outdoor air ventilation' settings lags as low as 30 to 60 seconds were found. Outdoor changes can therefore be registered very quickly inside the vehicle.

The lag between indoor and outdoor concentration tested in the PSC dataset by comparing model variants with different temporal smoothing. The traffic related covariates are evaluated on a 10-second resolution and the smoothing of the BC exposure inside the cabin is instantaneous for the zero lag model (LAG0) and to the average exposure over the next 60 and 120 seconds for the LAG60 and LAG120 model. The results are reported in Table 2. The model with LAG60 is significantly stronger than the LAG0 model, the LAG120 model is not significantly stronger than the LAG60 model and reduced the influence of the local traffic related covariates and is therefore rejected. All following models are based on the LAG60 evaluation of the in-vehicle exposure. This choice is compatible with the findings of other authors.

		F-values of covariates														
	Intercept (ng/m3)	Wind speed	Temperature	Humidity	BCbkg	Traffic count	LDEN	Hour Of Day	Speedrel	Speed act	Accel	PM10	StCan	# samples	Deviance explained	AIC
Investigating LAG and weight																
BC_LAG0	3479	1360	621	129	1059	718	856	128	280	187	34*	14*	90	77960	36.9%	195899
BC_LAG60	3685	1427	924	154	1281	808	1090	142	257	198	41	13*	192	79158	39.1%	188584
BC_LAG120	3592	1535	778	135	1159	817	1019	141	275	142	46	16*	147	79158	38.9%	190696
BC_LAG60_WBC	4029	1938	1023	240	957	845	1171	241	360	195	61	43	175	79158	46.9%	252213

Table 2: Results of the gam models to investigate the lag and the weighting of the in-vehicle exposure in relation to the local traffic dynamics, meteorology and traffic attribution. The F-values of the acceleration marked with * express a p-value higher than 2.0 e^{-16}.

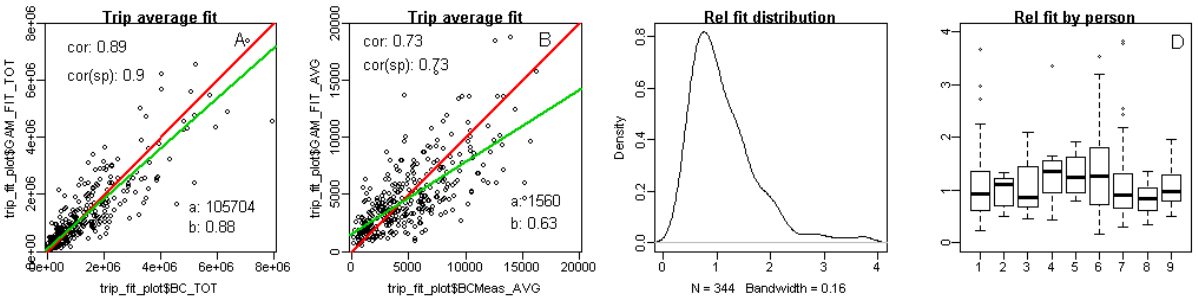

Figure 2: Trip fitting evaluation of the model BC_LAG60_WBC: Total trip fit versus measurement (A), average trip fit versus measurement (B), relative trip fit distribution (C) and relative trip fit distribution by person.

The measurement data has an abundance of low exposure values compared to the high levels. Higher BC exposure should get a higher weighting in the model to enable the models to predict the total trip exposure. A weighting function adjusts for the exposure level, increasing the weight for the high exposure values to correctly predict the distribution of the exposure for all possible conditions. The weighting function is fitted to the data to achieve a good trip prediction. The gam evaluation is available in the Table 2.

2.2. Comparing the traffic covariates and diurnal patterns

In this section the splines are available of four important models. The differences in the diurnal adjustment expressed in the HourOfDay covariate between the BCR_LDENWH and BCR_LDAYWH illustrate the higher hourly adjustment needed when using an hourly adjusted traffic covariate (Figure 3 and Figure 4).

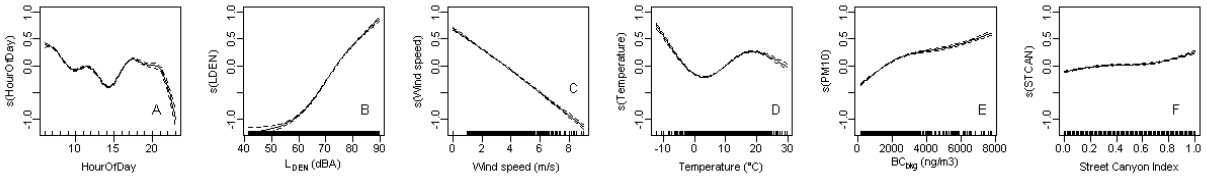

Figure 3: Splines of the BCR_LDENWH gam model.

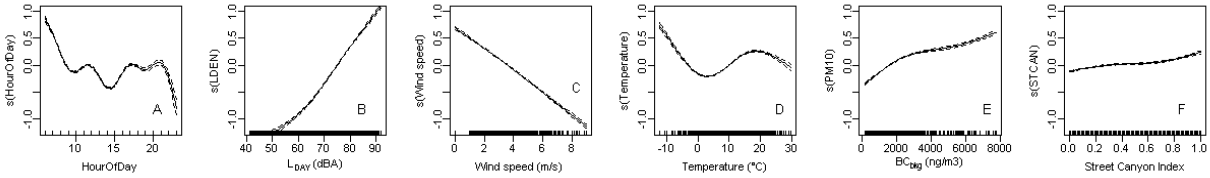

Figure 4: Splines of the BCR_LDAYWH gam model.

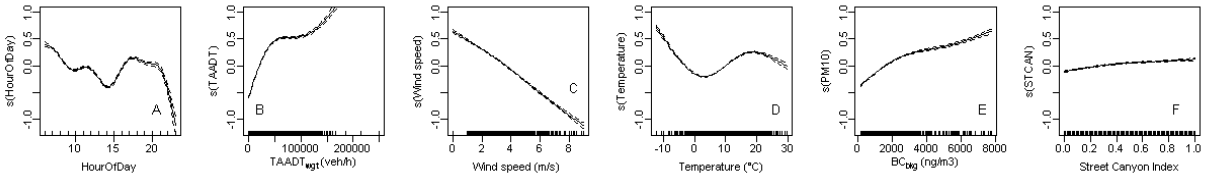

Figure 5: Splines of the BCR_TRAFWAADTH gam model.

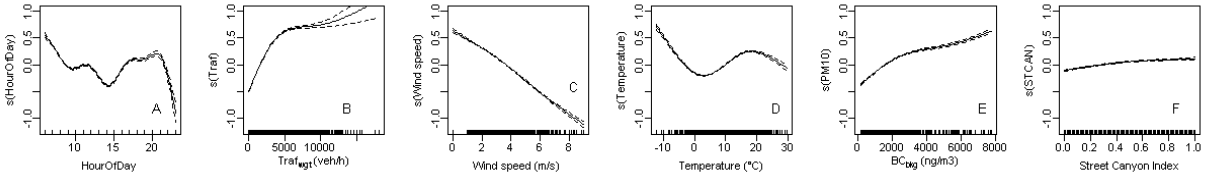

Figure 6: Splines of the BCR_TRAFWH gam model.

In table 2 of the main article this is expressed by the higher F-value of the HourOfDay covariate in the BCR_LDAYWH model compared to the BCR_LDENWH model. The same behaviour is visible for the BCR_ TRAFWAADTH and BCR_ TRAFWH models (Figure 5 and Figure 6).

2.3. Sales representatives' measurements: new vehicles

Due to the strong differences between the exposure of the participants and especially the atypical behaviour of the sales persons the influence of the sales person on the dataset is investigated. The model is evaluated while removing the two sales persons. This reduces the available data points from 80,000 to 42,000. The quality of the prediction (Figure 7) is much lower due to a strong increase of the width of the distribution (0.084 to 0.13), indicating that the dataset excluding the sales persons does not cover enough variation in certain covariates.

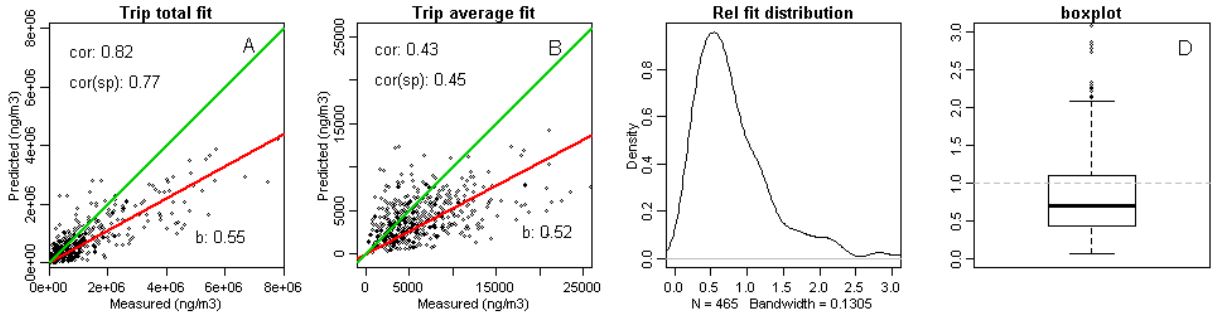

Figure 7: External validation based on BCR_LDENWH excluding the sales persons: Total trip fit versus measurement (A), average trip fit versus measurement (B), relative trip fit distribution (C) and relative trip fit distribution (D).

The median only increases with from 67% to 70%, the mean increases from 74% to 95%. Correlations drop a little, but the trip fit distribution is widened strongly. The IQR increases to 65%.

2.4. Vehicle age and vehicle quality related adjustments.

A new covariate is built in the PSC to express the year of assembly of the vehicle: "car_yearbuild". The age of the cars is known, but for a few of the participants, it is known that not all measurements were performed with the same vehicle. Since only nine participants are included in the PSC, no detail on the make or catalogue prize is added in this exercise. In Figure 8, the splines of the model are available.

```
Family: gaussian
Link function: identity
Formula:
bclog_field ~ +s(car_yearbuild, k = 3) + s(wind_speed, k = 4) +
  s(temp, k = 4) + s(BCbkg, k = 4) + s(CAP.hour, k = 9) + s(LDEN_OSMtot,
  k = 4) + s(stcan_index_20, k = 4)
Parametric coefficients:
      Estimate Std. Error t value Pr(>|t|)
(Intercept) 8.281153   0.003297   2512   <2e-16 ***
---
Signif. codes: 0 '***' 0.001 '**' 0.01 '*' 0.05 '.' 0.1 ' ' 1
Approximate significance of smooth terms:
          edf Ref.df     F p-value
s(car_yearbuild) 1.995 2.000 3296.15 <2e-16 ***
s(wind_speed)    2.896 2.992 1341.36 <2e-16 ***
```

```
s(temp)       2.998 3.000 1209.85 <2e-16 ***
s(BCbkg)      2.993 3.000 1075.19 <2e-16 ***
s(CAP.hour)    7.949 7.999 339.06 <2e-16 ***
s(LDEN_OSMtot)  2.987 3.000 3335.31 <2e-16 ***
s(stcan_index_20) 2.956 2.998  67.23 <2e-16 ***
---
Signif. codes: 0 '***' 0.001 '**' 0.01 '*' 0.05 '.' 0.1 ' ' 1

R-sq.(adj) = 0.463  Deviance explained = 46.6%
REML score = 1.2635e+05 Scale est. = 4.9686  n = 79158
```

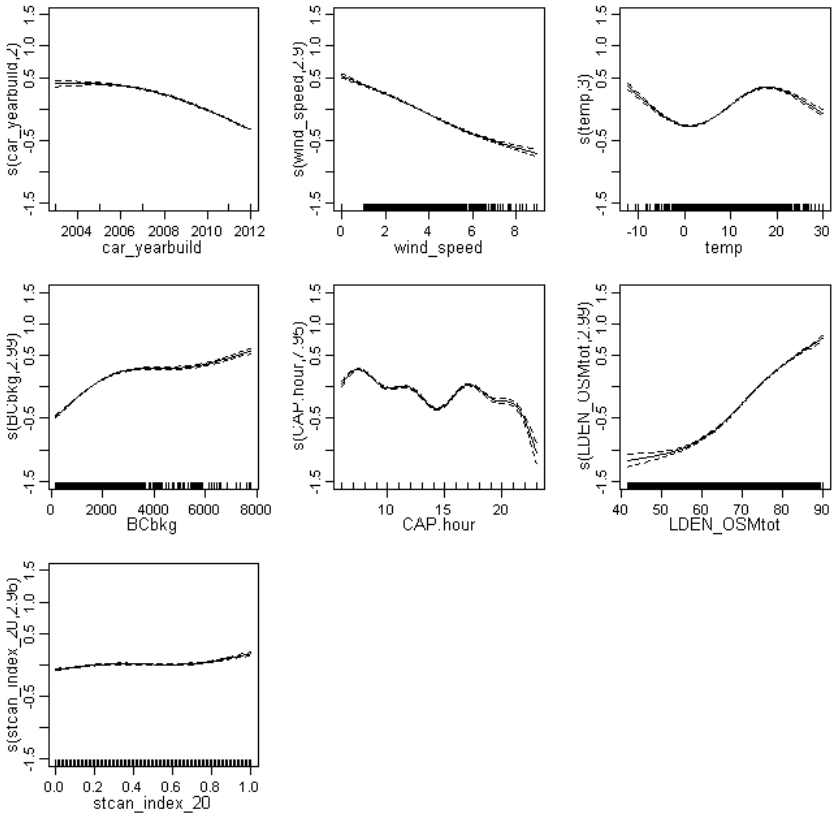

Figure 8: Splines of the vehicle age adjusted BCR_LDENWH_AGE gam model.

For the EX_PSC only the number of vehicles available to the household, the fuel types and an indirect reference (old vs new) to the age is available. All 'old' cars are set to 2007 and 'new' cars to 2010. The resulting model BCR_LDENWH_AGE trip fit is presented in Figure 9. The external validation is available in Figure 10.

The Q1, median, mean and Q3 of the relative trip fit are increasing from 32% to 38%, 49% to 50%, 68% to 74% and 75% to 81% compared to the BCR_LDENWH validation. The correlation of the trip average exposure fit increased from 0.47 to 0.5 (Spearman) and is equal for Pearson's correlation. Despite the poor vehicle age attribution in both campaigns, the external validation slightly improves. This is an indication that age and/or quality of the vehicle is part of the discrepancy in the validation. When comparing the vehicle age adjusted model with the model excluding the sales persons, it is clear that the vehicle age adjusted model is qualitative higher. Especially the very wide relative fit distribution of the model excluding the

sales persons is indicating the reduce quality. The improvement of the average trip exposure is mainly related to the widening of this distribution, not due to improved model fit.

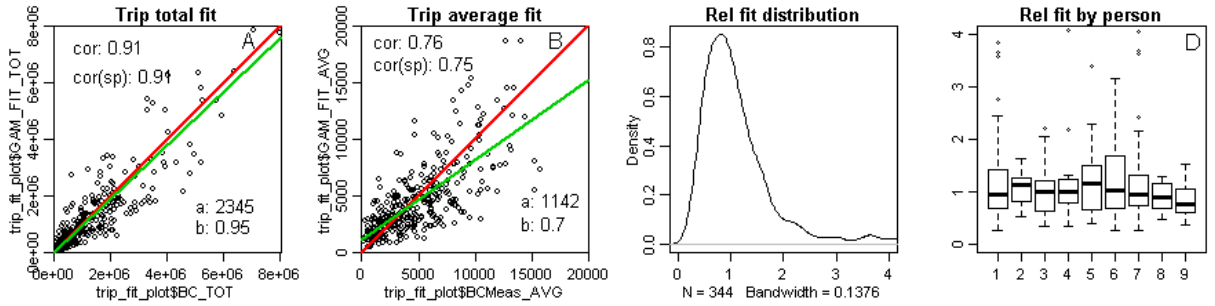

Figure 9: Trip fitting evaluation of the model BCR_LDENH_AGE: Total trip fit versus measurement (A), average trip fit versus measurement (B), relative trip fit distribution (C) and relative trip fit distribution by person.

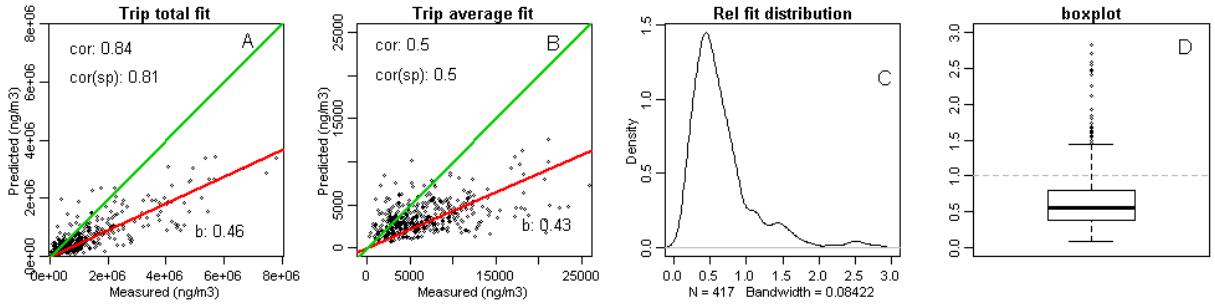

Figure 10: External validation based on BCR_LDENWH_AGE: Total trip fit versus measurement (A), average trip fit versus measurement (B), relative trip fit distribution (C) and relative trip fit distribution (D).

3. Vehicle fleet evolution

3.1. Estimating the changes in the vehicle fleet

In Table 3, the average PM emission is calculated for the vehicle fleet of passenger cars. The data is available at the website of the automobile organization of Belgium (www.febiac.be).

Year of appliance		2010*	2011	2013	PM limit (g/km)	Fleet 2010	Fleet 2011	Fleet 2013	
	Euro 0	5.6%	5.6%	4.7%		0.0079	0.0079	0.0066	
1992	**Euro 1**	4.4%	4.4%	2.2%	0.140	0.0062	0.0062	0.0031	
1996	**Euro 2**	14.5%	14.5%	9.0%	0.080	0.0116	0.0116	0.0072	
2000	**Euro 3**	34.9%	19.9%	15.1%	0.050	0.0174	0.0100	0.0075	
2005	**Euro 4**	40.6%	45.6%	38.6%	0.025	0.0101	0.0114	0.0096	
2009/2011	**Euro 5**		9.9%	30.0%	0.005	0.0000	0.0005	0.0015	
2014	**Euro 6**		0.0%	0.3%	0.005	0.0000	0.0000	0.0000	
		100.0%	100.0%	100.0%					
		* simulated composition			**Average fleet emission**	**0.0076**	**0.0068**	**0.0051**	(g/km)
					Reduction of the PM emission			33%	

Table 3: Evolution of the PM fleet emission for passenger cars.

This data, estimating the vehicle composition by environmental class is only available since 2011. The vehicle distribution is estimated for 2010. The estimated average PM emission drops with 33% between 2010 and 2013.

3.2. External evidence for Euro5 diesel related emission reduction.

In 2009 more stringent EU-legislation (euro 5) reduced particulate matter emission from diesel vehicles. The average age of the vehicle fleet in Belgium is 8 years (www.febiac.be). Over 60% of the vehicles in Belgium are diesel and diesel vehicles perform an even larger part of the total vehicle-kilometres. Over 40% of the vehicles in Belgium are employer owned and are typically replaced every 4 to 5 years. In 2013 about half of the diesel fleet (and kilometres travelled) complies with Euro 5. The effect of this legislation could be already visible in the PSC campaign in 2013 and explain the contrast in the external validation. The EU limits for PM exhaust is reduced from 0.025 g/km to 0.005 g/km for Euro 4 to Euro 5. If half of the fleet emits 80% less particulate matter, an emission reduction of 40% is possible. The in-vehicle exposure samples the emission of the preceding vehicles close to the source as possible for the entire active fleet, is influenced by the ventilation settings in an almost random way but should be able to detect these emission changes inside the vehicles. If this magnitude of the PM reduction of the euro5 legislation is real in practice, it should already be visible in the Black Carbon background exposure levels.

	Off-peak			Rush hour		
	2010	2013	Reduction	2010	2013	Reduction
Background (AL01)	1100	900	-22%	1800	1400	-29%
Roadside (R801)	1600	1200	-33%	3500	2600	-35%
Industrial (R815)	1200	1000	-20%	2400	1700	-41%

Table 2: reduction of the background Black carbon concentrations in Flanders, Belgium between 2010 and 2013.

The technology to measure BC is relatively recent. In Belgium the first long term measurements were set up during 2009. The diurnal patterns in three measurement points are compared for 2010 and 2013 in Figure 11. The blue lines match the lower median values in the diurnal patterns. These levels drop with 20 to 33% between 2010 and 2013, with the highest values for the near road location. The median value during the rush hour drops with 29% in the remote location and with up to 40% near industrial sites and near major roads inside the city of Antwerp (not at the on actual road side). This suggests the background reduction is related to an emission reduction of the traffic related emission since near the source the effect is higher during the rush hour. This external and fully independent data

source results in similar reductions as estimated on the vehicle fleet composition and the potential effect of the Euro5 legislation.

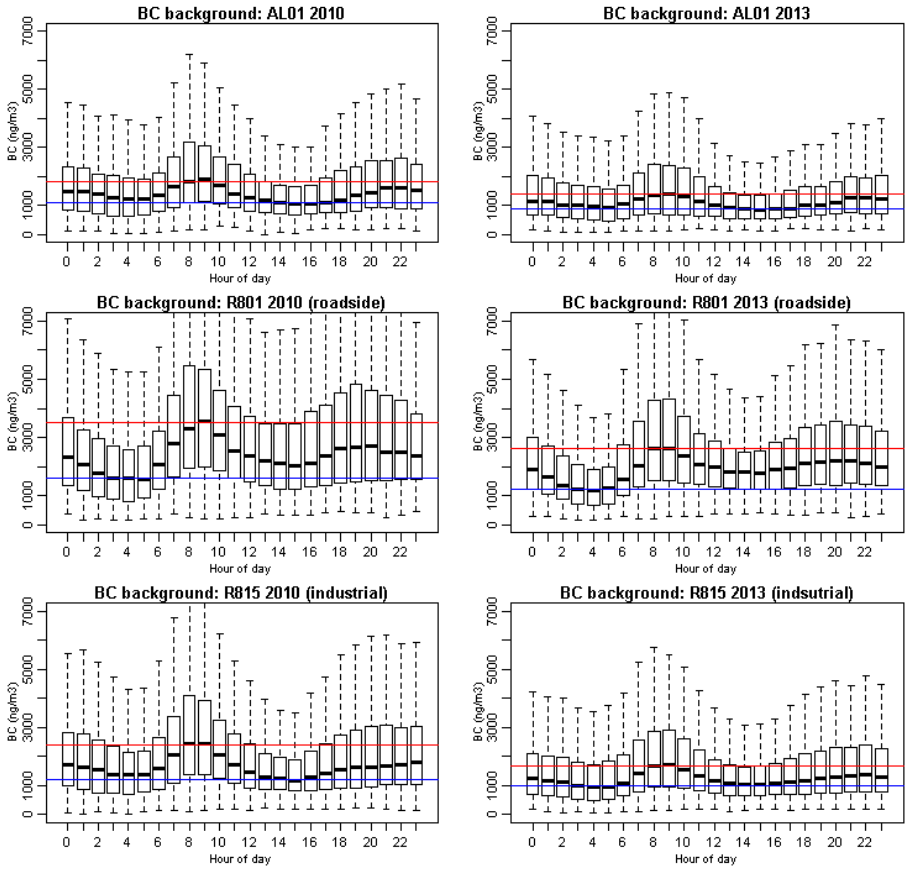

Figure 11: Diurnal patterns of background exposure in three measurement stations, red lines indicate the median values during rush hour, the blue lines the median during off-peak/night.

4. Adjusted model for vehicle age and Euro5 emission reduction.

In the PSC dataset the euro 5 EU emission standards was active for four years. The vehicle air inlets are sampling the traffic related emission sources. A potential reduction of 30 to 40% is found when evaluating the background measurements. It is however delicate to decide how this adjustment can be superimposed on the existing models. It can be expected that the reduction is not a constant over all driving conditions, but will more effective in driving conditions with higher PM emission. Therefore a non-linear relation is defined to adjust the predicted more with increasing exposure levels. A function is defined to reduce the highest exposure episodes with 80% and 20% reduction at low exposure conditions (see Figure 12).

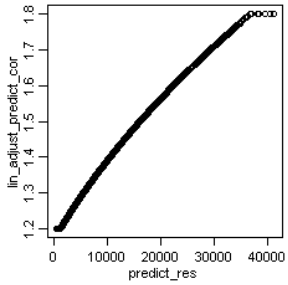

Figure 12: Non-linear function to adjust the BCR_LDENWH_AGE model to the emission situation in 2010. Each predicted values is adjusted with a factor between 1.2 and 1.8.

The external validation performed after adjusting the BCR_LDENWH_AGE with the non-linear adjustment as presented in Figure 13.

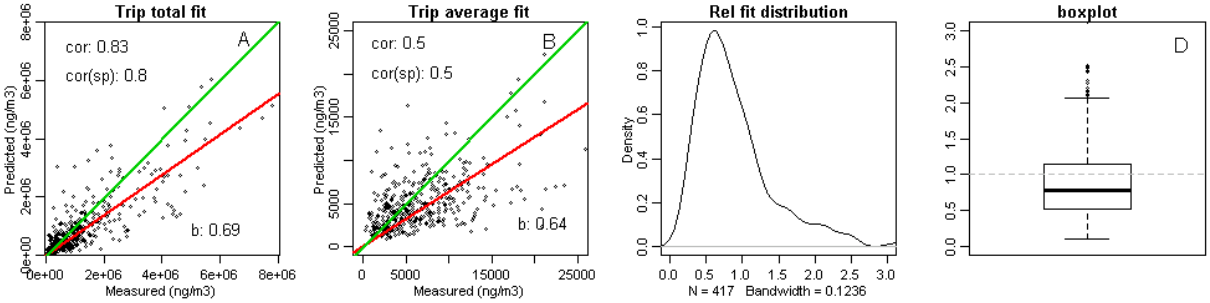

Figure 13: External validation based on BCR_LDENWH, vehicle age adjusted and adjusted for the EU euro5 legislation: Total trip fit versus measurement (A), average trip fit versus measurement (B), relative trip fit distribution (C) and relative trip fit distribution (D).

The Q1, median, mean and Q3 of the relative trip fit are increasing from 38% to 53%, 50% to 79%, 74% to 104% and 81% to 114% compared to the BCR_LDENWH_AGE validation. The correlation of the trip average exposure remains the same, the total trip correlations increase slightly. The average is increased with 30%, similar to the increase at the near road-side long-term measurement location.

5. References

Fruin S.A., Hudda N., Sioutas C. & Defino R.J. 2011. Predictive Model for Vehicle Air Exchange Rates Based on a Large, Representative Sample. Environmental Science & Technology, 45, 3569-3575.

Hudda N., Eckel S.R., Knibbs L.D., Sioutas C., Delfino R.J., et al. 2012. Linking in-vehicle ultrafine particle exposures to on-road concentrations. Atmospheric Environment, 59, 578-586.

Knibbs L.D., de Dear R.J. & Morawska L. 2010. Effect of Cabin Ventilation Rate on Ultrafine Particle Exposure Inside Automobiles. Environmental Science & Technology, 44, 3546-3551.

Li L.F., Wu J., Hudda N., Sioutas C., Fruin S.A., et al. 2013. Modeling the Concentrations of On-Road Air Pollutants in Southern California. Environmental Science & Technology, 47, 9291-9299.

Xu B., Wu Y., Lin Z. & Chen Z. 2014. Investigation of Air Humidity Affecting Filtration Efficiency and Pressure Drop of Vehicle Cabin Air Filters. Aerosol and Air Quality Research, 14, 1066-1073.